Three-Dimensional Intravascular Ultrasound Assessment of Coronary Lumen and Atherosclerotic Plaque Dimensions

ISBN 90-73235-66-9

Printed by Optima Grafische Communicatie, Rotterdam.

Cover illustration: the upper panel shows an automated 3D contour detection analysis of a diseased left anterior descending coronary artery [reprinted with permission from von Birgelen et al., Circulation 1997;96:2944-2952]. The lower panels display an automated 3D contour detection analysis and a spatial 3D reconstruction of coronary lesions with inadequate compensatory vascular enlargement [reprinted with permission from von Birgelen et al., Heart 1998;79:137-143 (left) and Am Heart J 1996;132:694-696 (right)].

THREE-DIMENSIONAL INTRAVASCULAR ULTRASOUND ASSESSMENT OF CORONARY LUMEN AND ATHEROSCLEROTIC PLAQUE DIMENSIONS

Drie-dimensioneele intravasculaire ultrageluid analyse van de dimensies van coronaire lumen en atherosclerotische plaque

Proefschrift

Ter verkrijging van de graad van doctor
aan de Erasmus Universiteit Rotterdam
op gezag van de Rector Magnificus
Prof. dr P.W.C. Akkermans M.A.
en volgens besluit van het College voor Promoties.

De openbare verdediging zal plaatsvinden
op woensdag 16 december 1998 om 15.45 uur

door

Clemens von Birgelen

geboren te Aken

Promotiecommissie

Promotor:	Prof. dr P.W. Serruys
Overige leden:	Prof. dr J.R.T.C. Roelandt
	Prof. dr Ir. N. Bom
	Prof. dr R. Erbel
Co-promotor:	Dr P.J. de Feyter

Financial support by the Netherlands Heart Foundation and the Interuniversity Cardiology Institute of the Netherlands for the publication of this thesis is gratefully acknowledged.

Support by a Fellowship of the German Research Society is gratefully acknowledged (Bi 553/1-1).

to my parents

and

to Gabriëlle and Carl Vincent

Contents

INTRODUCTION AND OUTLINE OF THE THESIS

Introduction and Outline of the Thesis

Since the introduction of coronary balloon angioplasty in the clinical arena, percutaneous catheter-based interventions are performed with coronary angiographic guidance, depicting the lumen of an entire coronary artery in certain angiographic views.

Subsequently, quantitative coronary angiography was developed as an instrument for off-line quantitative analysis of the acute and long-term effects of catheter-based and pharmacological approaches on atherosclerotic lesions and on lesion recurrence following angioplasty. Despite some inherent limitations, this analysis method became generally accepted for on-line guidance of balloon angioplasty and alternative catheter-based techniques.

Thereafter, intravascular ultrasound (IVUS) was introduced as a new imaging method that provided deeper insights into the pathology of coronary artery disease by defining vessel wall geometry and the major components of the atherosclerotic plaque. Although invasive, IVUS is safe and allows in vivo a more comprehensive assessment of the plaque than the 'luminal silhouette' furnished by coronary angiography, as it provides transmural cross-sectional imaging of coronary arteries and allows diameter and area measurements of both lumen and atherosclerotic plaque. These measurements can be used for guidance of interventional procedures and for research purposes.

Nevertheless, conventional IVUS is a planar technique, which displays only a single site of the coronary vessel at a time. However, three-dimensional (3D) reconstruction of sequences of IVUS images, acquired with defined sample spacing, allows to overcome this limitation.

The 3D IVUS systems were initially used *visually* to assess the configuration of plaques, dissections, and stents and to perform basic measurements. Comparable with the progress in quantitative angiographic methods, which started with manual caliper assessment and finally reached computerized detection of the opacified lumen, 3D IVUS systems have recently included approaches for automated *quantitative analysis* of the entire stack of images. Such 3D analysis tools reduce the subjectivity of manual boundary tracing, as they apply computer algorithms to detect the vascular structures.

At the catheterization laboratory of the Thoraxcenter Rotterdam two quantitative 3D IVUS systems were clinically applied: first, an *acoustic quantification system*, which allows the detection of the lumen based on statistical pattern recognition, and secondly, a *contour detection system*. The latter was developed at the Thoraxcenter and Erasmus University Rotterdam and detects both luminal and external vascular boundaries based on the application of a minimum cost algorithm. The present thesis sheds a light on numerous aspects of quantitative 3D IVUS.

The subject of the *first part* of this thesis is the validation of the Thoraxcenter contour detection system, both in vitro and in vivo. Histomorphometric measurements were performed to validate computerized 3D IVUS cross-sectional and volumetric measurements of lumen and plaque in human atherosclerotic coronary artery specimen (*Chapter 1*). In *Chapter 2*, the contour detection algorithm was tested in tubular phantoms. This section also reports the feasibility and reproducibility of analyzing clinical 3D image sets, acquired during continuous motorized transducer pullbacks.

As the systolic-diastolic changes in vascular dimensions and the movement of the IVUS cathe-

ter relative to the vessel wall may cause cyclic imaging artifacts, a dedicated ECG-triggered pullback device with a stepping motor was developed at the Thoraxcenter. A work station for 3D image acquisition, previously used for 3D reconstruction of cardiac ultrasound, was utilized to steer the pullback device and to perform an electrocardiogram-gated acquisition of a 3D image set. The feasibility of ECG-gated IVUS image acquisition in humans and the reproducibility of 3D analyses with this methodology are reported in *Chapter 3*. The work presented in *Chapter 4* evaluates the impact of different sample spacings (distance along the vessel's axis between two images) on volumetric data, calculated by the application of Simpson's rule.

The *second part* of the thesis reports on the clinical experience with quantitative 3D IVUS and on the practice, potential, and limitations of this approach in clinical research. The first chapters of this part focus on the application of the acoustic quantification system (Chapters 5 and 6) and the 3D contour detection system (Chapters 7 and 8) in the context of coronary stenting.

Chapter 5 provides a comparison of 3D IVUS (acoustic quantification system) with conventional IVUS and quantitative angiographic techniques in measuring the minimal stent cross-sectional area. Insights with IVUS into the acute result of coronary stenting showed evidence of significant differences between the IVUS results after implantation of the short, balloon-expandable Palmaz-Schatz stents and long, self-expandable Wallstents (*Chapter 6*).

In combination with the ECG-gated image acquisition method, the Thoraxcenter 3D IVUS system can be used online. *Chapter 7* addresses the feasibility of analyzing the luminal dimensions along an entire stented segment with 3D IVUS and evaluates the reliability and reproducibility of this approach.

In *Chapter 8*, neointima formation in self-expandable Wallstents was quantified with 3D IVUS at follow-up. In addition, the relation between the amount of neointima and late post-procedural expansion of the stent as well as other details of the intervention was assessed.

Chapter 9 reports on the first 3D IVUS examination of a lesion with inadequate compensatory enlargement (i.e. "reverse Glagovian modeling" or paradoxical arterial wall shrinkage) ever published. In a series of 35 patients, treated by catheter-based coronary interventions, plaque and vessel volumes of lesions with inadequate compensatory enlargement were compared with those of lesions without inadequacy of adaptive remodeling (*Chapter 10*).

Whether differences in the remodeling state have implications on the long-term success of catheter-based interventions was unknown. Accordingly, in *Chapter 11* the extent of angiographic lumen renarrowing after successful directional atherectomy was evaluated for both, lesions with and without inadequate vascular enlargement prior to the intervention.

Chapter 12 discusses the limitations of angiographic measures for the assessment of structural changes of the atherosclerotic vessel wall during progression/regression of coronary atherosclerosis and reviews the potential of 3D IVUS in this context.

Chapter 13 reviews the main technical aspects of the 3D IVUS systems applied in this thesis. In addition, the limitations of these methods and the potential of future technical refinements and developments are discussed.

Finally, in some settings 3D IVUS may not be required or may be even useless. *Chapter 14* gives an example of a study, in which conventional planar IVUS was sufficient to gain novel insights into vascular remodeling in response to atherosclerotic plaque accumulation in left main coronary arteries.

PART I

VALIDATION STUDIES

Chapter 1

Computerized assessment of coronary lumen and atherosclerotic plaque dimensions in three-dimensional intravascular ultrasound correlated with histomorphometry

C von Birgelen, A van der Lugt, A Nicosia, GS Mintz,
EJ Gussenhoven, E de Vrey, MT Mallus,
JRTC Roelandt, PW Serruys,
PJ de Feyter

Reprinted with permission from *Am J Cardiol* 1996;78:1202-1209

Computerized Assessment of Coronary Lumen and Atherosclerotic Plaque Dimensions in Three-Dimensional Intravascular Ultrasound Correlated With Histomorphometry

Clemens von Birgelen, MD, Aad van der Lugt, MD, Antonino Nicosia, MD, Gary S. Mintz, MD, Elma J. Gussenhoven, PhD, Evelyn de Vrey, MD, Maria Teresa Mallus, MD, Jos R.T.C. Roelandt, PhD, Patrick W. Serruys, PhD, and Pim J. de Feyter, PhD

Intravascular ultrasound (IVUS), which depicts both lumen and plaque, offers the potential to improve on the limitations of angiography for the assessment of the natural history of atherosclerosis and progression or regression of the disease. To facilitate measurements and increase the reproducibility of quantitative IVUS analyses, a computerized contour detection system was developed that detects both the luminal and external vessel boundaries in 3-dimensional sets of IVUS images. To validate this system, atherosclerotic human coronary segments (n = 13) with an area obstruction ≥40% (40% to 61%) were studied in vitro by IVUS. The computerized IVUS measurements (areas and volumes) of the lumen, total vessel, plaque-media complex, and percent obstruction were compared with findings by manual tracing of the IVUS images and of the corresponding histologic cross sections obtained at 2-mm increments (n = 100). Both area and volume measurements by the contour detection system agreed well with the results obtained by manual tracing, showing low mean between-method differences (−3.7% to 0.3%) with SDs not exceeding 6% and high correlation coefficients (r = 0.97 to 0.99). Measurements of the lumen, total vessel, plaque-media complex, and percent obstruction by the contour detection system correlated well with histomorphometry of areas (r = 0.94, 0.88, 0.80, and 0.88) and volumes (r = 0.98, 0.91, 0.83, and 0.91). Systematic differences between the results by the contour detection system and histomorphometry (29%, 13%, −9%, and −22%, respectively) were found, most likely resulting from shrinkage during tissue fixation. The results of this study indicate that this computerized IVUS analysis system is reliable for the assessment of coronary atherosclerosis in vivo. *©1996 by Excerpta Medica, Inc.*

(Am J Cardiol 1996;78:1202–1209)

The natural history and progression or regression of coronary atherosclerosis after pharmacologic and nonpharmacologic interventions have most often been assessed by quantitative coronary angiography.[1–3] However, the quantitative angiographic approach permits only the assessment of the luminal silhouette[4] and indirect estimation of plaque burden. As a result of vessel remodeling, early atherosclerosis remains angiographically undetected until luminal encroachment starts and plaque occupies approximately 40% of the internal elastic membrane area.[5] Intravascular ultrasound (IVUS) depicts both coronary lumen and vessel wall; measurements can be obtained by manually tracing the luminal and external vascular boundaries.[6–8] To reduce the time and subjectivity of manual tracing,[9] automated systems for quantitative analysis in 3-dimensional IVUS image sets have been developed.[10–14] As the available systems detect only the lumen, we developed a contour detection algorithm that detects both the luminal and external vascular boundaries of atherosclerotic coronary arteries in 3-dimensional IVUS image sets.[15,16] This approach allows the quantification of all IVUS images and permits even volumetric assessment which has recently been advocated as a valuable concept in research and clinical practice.[17–20] To validate this contour detection algorithm, atherosclerotic human coronary explants obtained postmortem or from heart transplant recipients at transplantation were studied with IVUS. Results by the IVUS contour detection system were compared with measurements obtained from manual tracing of the IVUS images and of the corresponding histologic sections.

From the Thoraxcenter, University Hospital Rotterdam-Dijkzigt, Erasmus University Rotterdam, and the Interuniversity Cardiology Institute, Rotterdam, The Netherlands; and the Washington Hospital Center, Washington, DC. This project was partly supported by the Dutch Heart Foundation (Grants 94.016 and 94.006). Dr. von Birgelen was supported by a fellowship of the German Research Society (Bonn, Germany). Manuscript received March 21, 1996; revised manuscript received and accepted June 14, 1996.

Address for reprints: Pim J. de Feyter, MD, PhD, Department of Coronary Imaging and Intervention, Thoraxcenter, Bd 381, P.O. Box 1738, University Hospital Rotterdam-Dijkzigt, 3000 DR Rotterdam, The Netherlands.

METHODS

Human coronary specimens: Thirteen coronary arteries (6 right coronary [RCA], 6 left anterior descending [LAD], and 1 left circumflex [LCX]) with segments of mild to moderate atherosclerosis were

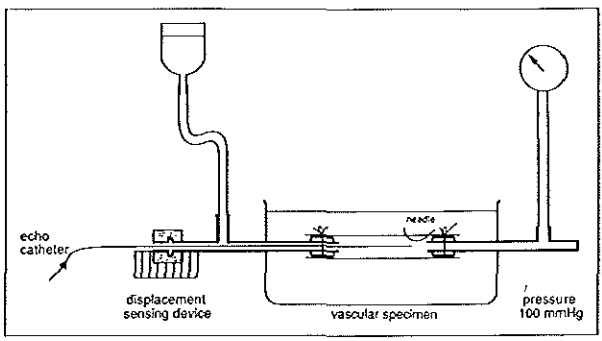

FIGURE 1. The in vitro setup. The ultrasound catheter is advanced through the catheter displacement-sensing device toward the pressurized coronary specimen. A needle attached distally to the artery is used as a reference. The position of the catheter tip in relation to the needle is measured (step size 0.1 mm).

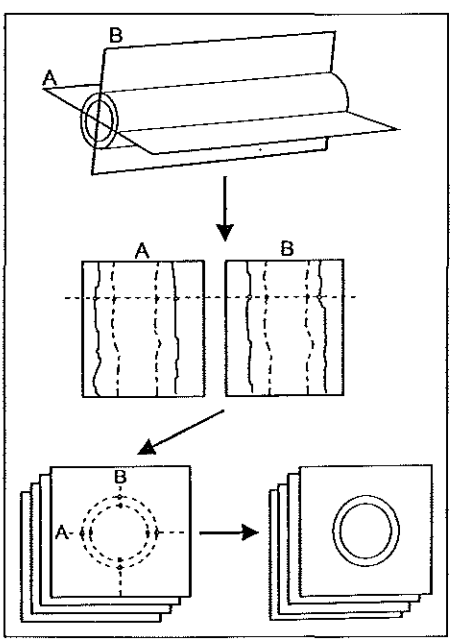

FIGURE 2. Computerized intravascular ultrasound (IVUS) contour detection. Two perpendicular planes running longitudinally along the axis of the artery are used to reconstruct 2 longitudinal sections from the entire sequence of digitized IVUS images. The position and rotation angle of the 2 cut planes can be interactively changed to obtain an optimal representation of the coronary segment. Consecutively, the longitudinal contours are automatically detected in these 2 sections and, if required, interactive corrections may be performed. The longitudinal contours intersecting the planes of the transverse images are represented as edge points, guiding the final automated contour detection in the cross-sectional IVUS images by defining the center and the range of the boundary-searching process.

explanted postmortem (n = 6) and post-transplantation (n = 4) from the hearts of 10 patients (7 men, 3 women) with a median age of 51 years (range 39 to 55). Segments with ≤1 major side branch were included in the study. The investigation was approved by the Local Council on Human Research.

In vitro study protocol: For in vitro studies the side branches of the coronary specimen were ligated and the proximal and distal ends were connected to sheaths fixed in a waterbath at 20°C. A distal reference segment was indicated using a needle. The arteries were pressurized at 100 mm Hg by a water reservoir connected to the sidearm of the proximal sheath (Figure 1). The IVUS examination of the pressurized specimen was performed with a mechanical 30-MHz imaging system (Du-MED, Rotterdam, The Netherlands). The IVUS catheter displacement-sensing device of the Thoraxcenter Rotterdam, which was previously described and applied,[21] was used to monitor the displacement of the ultrasound catheter tip in steps of 0.1 mm, using the distal needle as the reference. Distance information and IVUS images were automatically mixed and recorded on videotape. This was used as the source for further analyses by the IVUS contour detection system and by manual tracing.

Histologic preparation: The coronary arteries were fixed under pressure (100 mm Hg) in 10% buffered formalin for 2 hours and subsequently decalcified in a standard RDO solution (Apex Inc., Plainfield, Illinois) for 5 hours. The arteries were then processed for routine paraffin embedding. The site of the reference needle was marked using india ink. The 5-μm-thick transverse sections were cut at 2-mm intervals perpendicular to the long axis of each specimen, resulting in a total of 100 histologic sections. Staining of the histologic sections was performed with the elastic van Gieson technique. Matching between the IVUS images and the histologic sections was achieved by use of the distance information provided by the displacement-sensing device. Anatomic markers such as side branches or spots of calcium were used to confirm precise matching.

Computerized intravascular ultrasound contour detection system: The analysis program uses the Microsoft Windows operating system on a Pentium (60 MHz) personal computer with 16 Mbytes of internal RAM. A frame-grabber (DT-3852; resolution: 800 × 600 × 8 bits) digitizes a user-defined region of interest from a maximum of 200 IVUS images. While a version for clinical application makes use of a motorized pull-back device and digitizes the IVUS images automatically,[16] selection and digitization of the present in vitro IVUS images was performed by manually choosing the appropriate

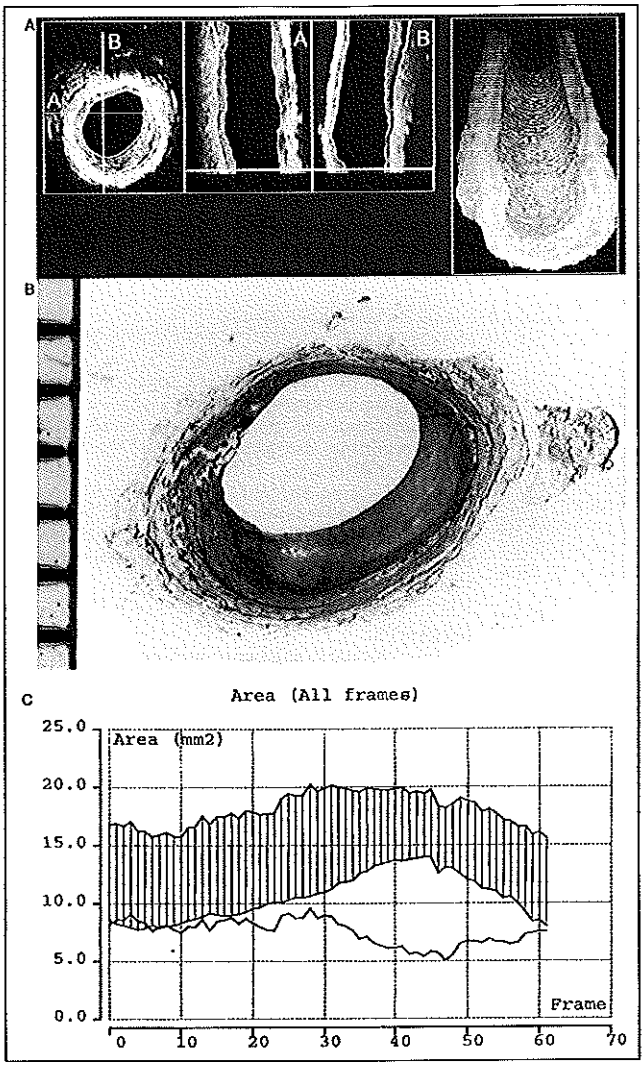

FIGURE 3. Example of the computerized intravascular ultrasound (IVUS) contour detection in vitro. A horizontal cursor can be moved through the perpendicular longitudinal IVUS sections A and B *(A, midpanels)* to check the quality of the boundary detection on the cross-sectional IVUS images *(left panel)*. A spatial display of the coronary specimen can be obtained *(A, right panel)*; however, this is not required to quantify the vascular dimensions. A histologic section *(B)*, showing eccentric plaque formation, corresponds with the IVUS image displayed in the cross-sectional view *(A, left panel)*. The measurements are displayed in an illustrative way *(C)*: The area values of the lumen *(lower line)* and total vessel *(upper line)* form the boundaries of a *hatched zone*, which represents the plaque–media complex, and a *single line* below this zone depicts the absolute area value of the plaque–media complex.

images using the distance information provided by the catheter displacement-sensing device. Images were selected and digitized every 0.2 mm. The algorithm is based on the concept that longitudinal contours facilitate the automated contour detection on the cross-sectional IVUS images by defining the center and the range of the boundary-searching process (Figure 2). The position of an individual cross-sectional IVUS image in the longitudinal sections is indicated by a horizontal cursor line which can be used to scroll through the entire series of transverse IVUS images. The detected contours are checked by the analyst, and corrections can be performed by simply pointing with the computer mouse on the correct site and redetecting the contours, using this additional edge information. Corrections are required particularly in images of lower quality and in rapid contour transitions. Whenever the contour of a single slice has been corrected and redetected, the entire data set is updated. As the analysis is performed in a 3-dimensional image set, coronary segments can be displayed in a cylindrical format (Figure 3), although this option is not required for the purpose of quantification.

MINIMUM-COST ALGORITHM: Detection of the intimal leading edge and external boundary of the vessel within each image slice is accomplished with the application of a minimum-cost algorithm, previously applied[22] to single cross-sectional IVUS images. With this approach the digitized IVUS images are resampled according to a radial image reconstruction (64 radii in the cross-sectional images). A cost matrix that represents the edge strength is calculated from the image data. For contour detection of the boundary between lumen and plaque, the cost value is defined by the spatial first derivative. To detect the external boundary contour of the vessel, a pattern matching process by cross correlation is adopted for the cost calculations. Through the cost matrixes a path with the smallest accumulated value is determined by dynamic programming techniques.[15]

VOLUME CALCULATION: Volumes of lumen, total vessel, and plaque–media complex were calculated as:

TABLE I Measurements and Between-Method Differences*

	IVUS (CD)	IVUS (MA)	HISTO	Δ (CD-MA)	Δ (CD-HISTO)
Area					
Lumen (mm^2)	13.4 ± 3.6	13.4 ± 3.7	10.0 ± 2.4†	0.1 ± 0.3 (0.3 ± 2.5%)	3.4 ± 1.6 (28.6 ± 9.5%)
Total vessel (mm^2)	21.0 ± 4.6	21.3 ± 4.7†	18.2 ± 3.0†	−0.3 ± 0.4 (−1.1 ± 2.0%)	2.8 ± 2.4 (13.5 ± 10.2%)
Plaque–media (mm^2)	7.6 ± 2.0	7.9 ± 2.1†	8.2 ± 1.9†	−0.4 ± 0.5 (−3.1 ± 6.2%)	−0.6 ± 1.2 (−8.6 ± 18.0%)
% area obstruction	36.8 ± 7.6	37.6 ± 8.0†	45.3 ± 8.1†	−0.8 ± 1.8 (−2.0 ± 4.8%)	−8.5 ± 4.1 (−22.1 ± 12.5%)
Volume					
Lumen (mm^3)	205.9 ± 70.4	205.5 ± 69.6	153.1 ± 46.7†	0.5 ± 1.9 (0.2 ± 0.9%)	52.8 ± 26.2 (28.3 ± 7.2%)
Total vessel (mm^3)	322.8 ± 92.4	327.5 ± 94.8†	279.2 ± 71.8†	−4.8 ± 5.8 (−1.4 ± 1.5%)	43.5 ± 35.5 (13.7 ± 9.2%)
Plaque–media (mm^3)	116.8 ± 28.8	122.1 ± 33.3†	126.1 ± 34.1	−5.3 ± 6.5 (−3.7 ± 4.3%)	−9.3 ± 14.2 (−6.8 ± 14.2%)
% volume obstruction	36.9 ± 6.4	37.8 ± 6.7†	45.3 ± 7.4†	−0.9 ± 1.1 (−2.4 ± 2.9%)	−8.4 ± 3.1 (−20.5 ± 7.6%)

* All values are mean values ± SD.
† $p < 0.05$; ‡ $p < 0.0001$, for comparison with the results obtained by CD.
CD = contour detection; HISTO = histology; IVUS = intravascular ultrasound; MA = manual; Δ = between-method difference.

$$V = \sum_{i=1}^{n} A_i \cdot H$$

where V = volume; A = area of lumen, total vessel, or plaque in a certain digitized cross-sectional ultrasound image; H = thickness of the coronary artery slice represented by this digital cross-sectional IVUS image; and n = number of digitized cross-sectional IVUS images encompassing the volume to be measured.

Manual intravascular ultrasound analysis: On the cross-sectional IVUS images that correspond to the histologic sections, a manual tracing of the lumen and the external vessel borders was performed by another independent investigator. This individual was experienced in the manual IVUS analysis, but did not have knowledge of the results of the computerized analysis. Volumetric data were obtained by Simpson's rule.

Histomorphometric analysis: The histomorphometry was performed with an IBAS 2000 image analysis system (Kontron, Eching, Germany) that allowed manual contour tracing of the luminal contour and the external elastic membrane on digitized microscopic images (magnification ×12.5; pixel size: 0.8262×10^{-2} mm) and provided area measurements. Volumetric data were obtained using Simpson's rule.

Data analysis: The quantitative results by all 3 methods included:

- Cross-sectional area of the lumen (mm^2)
- Cross-sectional area of the total vessel (mm^2)
- Cross-sectional area of the plaque–media complex (total vessel area − lumen area) (mm^2)
- Percent area obstruction (plaque–media complex area ÷ total vessel area) (%)
- Volume of the lumen (mm^3)
- Volume of the total vessel (mm^3)
- Volume of the plaque–media complex (total vessel volume − lumen volume) (mm^3)
- Percent volume obstruction (plaque–media complex volume ÷ total vessel volume) (%).

Statistical analysis: Results are given as mean ± 1 SD. According to Bland and Altman,[23] the agreement between the computerized IVUS contour detection and the manual IVUS measurements and between the computerized IVUS analysis and the histomorphometric measurements were assessed by determining the mean ± SD of the between-method differences. Differences were analyzed with the 2-tailed Student t test for paired data analysis. Linear regression analysis was performed to assess the strength of the relation between the methods. p values <0.05 were considered statistically significant.

RESULTS

The coronary segments included in the study were 15.4 ± 2.8 mm long (14 to 22 mm) and all specimens had a maximum percent area obstruction >40% (47% ± 7%; range 40% to 61%) as measured by the computerized IVUS analysis system. The minimum percent area obstruction was 29% ± 5% (range 21% to 35%). Complete volumetric analysis by the computerized contour detection system (77 ± 14 images) required significantly less time compared with pure manual contour tracing (19 ± 4 minutes vs 121 ± 26 minutes; $p < 0.0001$). The results of the computerized IVUS contour detection, manual tracing on the IVUS images, and histomorphometry are presented in Table I.

Contour detection versus manual tracing: The measurements of the lumen, total vessel, plaque–media complex, and percent obstruction by the computerized IVUS contour detection system differed little from the results obtained by manual tracing: The between-method differences (contour detection–manual tracing) were 0.3% ± 2.5%, −1.1% ± 2.0%, −3.1% ± 6.2%, and −2.0% ± 4.8% for the area measurements, and 0.2% ± 0.85%, −1.4% ± 1.5%, −3.7% ± 4.3%, and −2.4% ± 2.9% for the volume measurements, respectively. Correlations between the area (r = 0.97 to 0.99) and volume (r = 0.99) measurements obtained by both methods were high (Figures 4 and 5).

Contour detection versus histomorphometry: Measurements of the plaque–media complex and percent obstruction by the contour detection system were lower ($p < 0.0001$) than by histomorphometry (Table I), whereas the measurements of the lumen and total

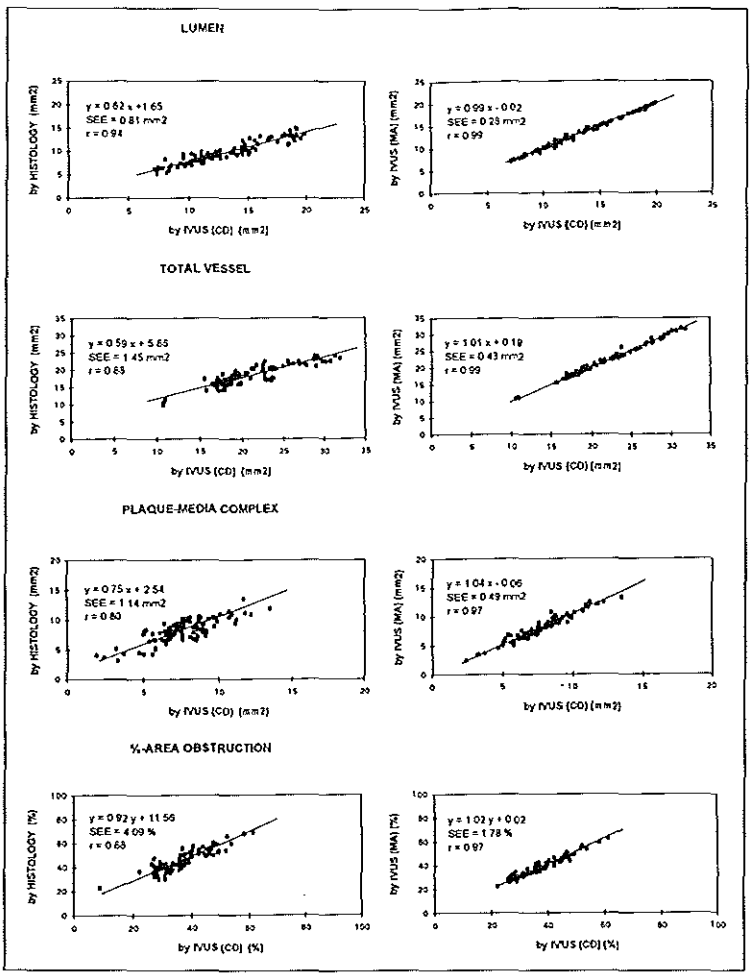

FIGURE 4. Correlations between the area measurements. The results of linear regression analyses are displayed, comparing the measurements of the lumen, total vessel, plaque–media complex, and percent area obstruction provided by the computerized intravascular ultrasound (IVUS) contour detection (CD) method and manual tracing (MA) on the IVUS images *(right panels)*, and morphometry on the histologic sections *(left panels)*.

vessel dimensions by the IVUS contour detection system were significantly higher than the histomorphometric results ($p < 0.0001$). The between-method differences (contour detection vs histomorphometry) of the lumen, total vessel, plaque–media complex, and percent obstruction were 29% ± 10%, 14% ± 10%, −9% ± 18%, and −22% ± 13% for area measurements, and 28% ± 7%, 14% ± 9%, −7% ± 14%, and −21% ± 8% for volumetric measurements, respectively. High correlations (Figures 4 and 5) were found for the area ($r = 0.80$ to 0.94) and volume ($r = 0.83$ to 0.98) measurements by both methods.

DISCUSSION

In the present study histomorphometric validation of a computerized IVUS analysis system was performed by comparing the results obtained by the computerized IVUS analysis system both with the measurements made by manual contour tracing of the IVUS images and with the corresponding histomorphometric results. The key findings of this study are that (1) the computerized IVUS measurements of areas and volumes are in excellent agreement with the measurements obtained by manual tracing on the IVUS images, and (2) there is a good correlation betweeen measurements obtained from the computerized IVUS analysis and histomorphometry. The good correlation between the results provided by the IVUS contour analysis system and histomorphometry demonstrates the reliability of the computerized approach in performing both area and volume measurements.

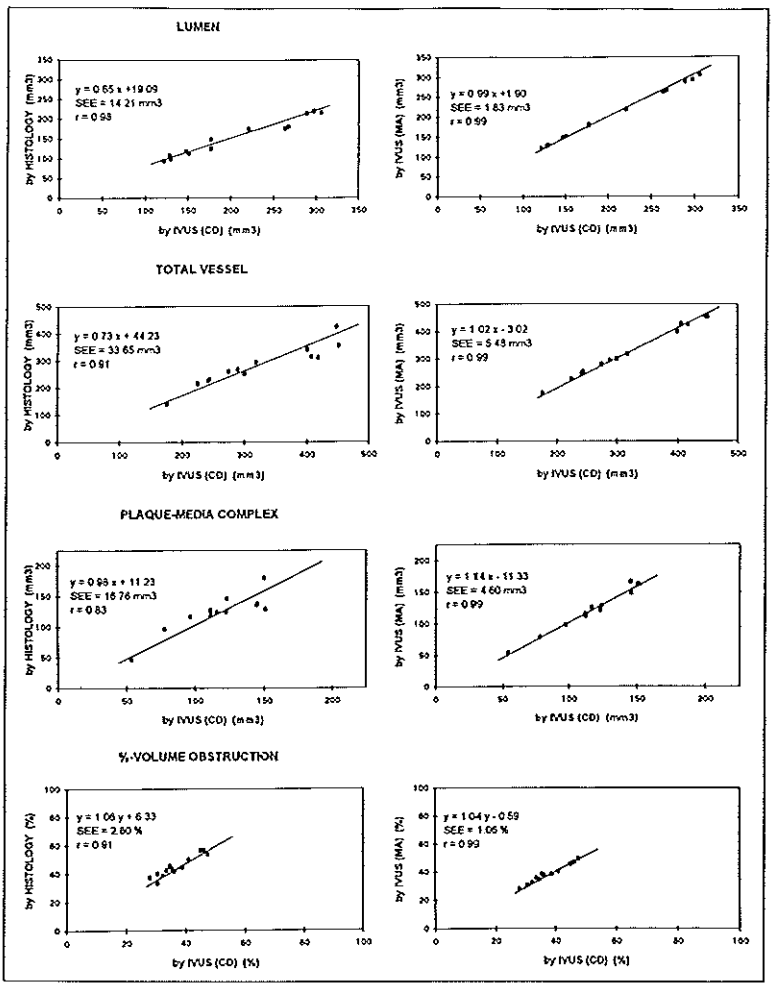

FIGURE 5. Correlations between the volumetric measurements. The results of linear regression analyses are displayed, comparing the measurements of the lumen, total vessel, plaque–media complex, and percent volume obstruction provided by the computerized contour detection (CD) method and manual tracing (MA) on the intravascular ultrasound (IVUS) images *(right panels)*, and morphometry on the histologic sections *(left panels)*.

Previous studies: The high correlations between measurements on the cross-sectional IVUS images and the corresponding histologic sections observed in the present study are in concordance with previous observations of Potkin et al,[24] who found correlation coefficients of 0.94, 0.85, and 0.84 for total vessel area, lumen area, and percent area obstruction. The measurements by IVUS were smaller for the lumen and larger for the total vessel area.[24] The effect of tissue shrinkage[25] and different modalities of tissue fixation and pressurization may account for the differences from previous observations[6,19] which showed a larger lumen area by IVUS than by histomorphometry. To date only 1 study comparing true volumetric IVUS measurements and histomorphometry has been reported.[26] Excellent correlations between the computerized threshold-based IVUS analysis of the lumen volume in vivo and measurements based on both manual tracing and histomorphometry were found ($r = 0.97$ for both), confirming the results of the present study ($r = 0.99$ and 0.98, respectively). Comparable data on the total vessel and plaque–media volume were not available, as this threshold-based method was able to detect only the lumen.

Sonka et al[27] devised an alternative approach of contour detection that performs a computerized detection of both the intimal leading edge and the external vessel boundary in IVUS image sequences. In contrast to our analysis system, the automated contour detection on the cross-sectional images is performed without guidance from the additional information provided by contour detection on longitudinally reconstructed IVUS images.[15] In their study, the correlation between automatic and manual contour tracing on the IVUS images in vitro was good[27] ($r = 0.91$ and 0.83 for lumen and plaque area, respectively), but slightly lower than the correlation observed in our study.

Study limitations: On IVUS images the external vessel boundary cannot be detected behind calcium owing to acoustic shadowing. The IVUS contour analysis system, however, allows better interpolation of the vessel boundary behind calcium and thus may be more reliable than conventional manual tracing of a single cross-sectional IVUS image. Finally, because there are differences in the velocities of ultrasound in water and blood, the use of water instead of blood in our experimental setup may partly account for an overestimation of the vascular dimensions by IVUS.

Clinical implications: The examination of the coronary arteries by IVUS allows the assessment of atherosclerotic changes[6,7,28] and the quantification of the progression or regression of atherosclerosis.[17] To determine the latter, anatomic landmarks such as side branches or spots of calcium can be used to define corresponding IVUS images in serial studies. Our automated approach using the spatial information of the IVUS images acquired during defined transducer pull-back facilitates this process and permits the volumetric assessment of lumen and/or plaque without need for laborious manual analyses.[15,16] The proposed quantitative IVUS analysis system allows the reproducible[16] and reliable identification of both the luminal and external vessel boundaries and may thus be used for the routine analysis of IVUS studies, although wedging of the IVUS catheter may slightly increase the variability of preintervention analyses. Cyclic artifacts can be avoided by electrocardiographic-gated image acquisition,[29,30] which is a prerequisite for on-line application of this analysis system, currently performed in our catheterization laboratory.

1. de Feyter PJ, Serruys PW, Davies MJ, Richardson P, Lubsen J, Oliver MF. Quantitative coronary angiography to measure progression and regression of coronary atherosclerosis: value, limitations, and implications for clinical trials. *Circulation* 1991;84:412–423.

2. Waters D, Lesperance J, Craven TE, Hudson G, Gillam LD. Advantages and limitations of serial coronary arteriography for the assessment of progression and regression of coronary atherosclerosis. Implications for clinical trials. *Circulation* 1993;87:II-38–II-47.

3. Fuster V, Badimon L, Badimon JJ, Chesebro JH. The pathogenesis of coronary artery disease and the acute coronary syndromes. *N Engl J Med* 1992;326:242–250.

4. von Birgelen C, Umans V, Di Mario C, Keane D, Gil R, Prati F, de Feyter PJ, Serruys PW. Mechanism of high-speed rotational atherectomy and adjunctive balloon angioplasty revisited by quantitative coronary angiography: edge detection versus videodensitometry. *Am Heart J* 1995; 130:405–412.

5. Stiel GM, Stiel LSG, Schofer J, Donath K, Mathey DG. Impact of compensatory enlargement of atherosclerotic coronary arteries on angiographic assessment of coronary artery disease. *Circulation* 1989;80:1603–1609.

6. Gussenhoven EJ, Essed CE, Lancee CT, Mastik F, Frietman P, van Egmond FC, Reiber J, Bosch H, van Urk, Roelandt J, Bom N. Arterial wall characteristics determined by intravascular ultrasound imaging: an in-vitro study. *J Am Coll Cardiol* 1989;14:947–952.

7. Ge J, Erbel R, Gerber T, Gorge G, Koch L, Haude M, Meyer J. Intravascular ultrasound imaging in angiographically normal coronary arteries: a prospective study in vivo. *Br Heart J* 1994;71:572–578.

8. Mintz GS, Painter JA, Pichard AD, Kent KM, Satler LF, Popma JJ, Chuang YC, Bucher TA, Sokolowicz LE, Leon MB. Atherosclerosis in angiographically "normal" coronary artery reference segments: an intravascular ultrasound study with clinical correlations. *J Am Coll Cardiol* 1995;25:1479–1485.

9. Hausmann D, Lundkvist AJS, Friedrich GJ, Mullen WL, Fitzgerald PJ, Yock PG. Intracoronary ultrasound imaging: intraobserver and interobserver variability of morphometric measurements. *Am Heart J* 1994;128:674–680.

10. Rosenfield K, Losordo DW, Ramaswamy K, Pastore JO, Langevin RE, Razvi S, Kosowsky BD, Isner JM. Three-dimensional reconstruction of human coronary and peripheral arteries from images recorded during two-dimensional intravascular ultrasound examination. *Circulation* 1991;84:1938–1956.

11. Roelandt JRTC, Di Mario C, Pandian NG, Wenguang Li, Keane D, Slager CJ, de Feyter PJ, Serruys PW. Three-dimensional reconstruction of intracoronary ultrasound images: Rationale, approaches, problems, and directions. *Circulation* 1994;90:1044–1055.

12. von Birgelen C, Kutryk MJB, Gil R, Ozaki Y, Di Mario C, Roelandt JRTC, de Feyter PJ, Serruys PW. Quantification of the minimal luminal cross-sectional area after coronary stenting by two-dimensional and three-dimensional intravascular ultrasound versus edge detection and videodensitometry. *Am J Cardiol* 1996;78:520–525.

13. Gil R, von Birgelen C, Prati F, Di Mario C, Ligthart J, Serruys PW. Usefulness of Three-dimensional reconstruction for interpretation and quantitative analysis of intracoronary ultrasound during stent deployment. *Am J Cardiol* 1996;77:761–764.

14. von Birgelen C, Gil R, Ruygrok P, Prati F, Di Mario C, van der Giessen WJ, de Feyter PJ, Serruys PW. Optimized expansion of the Wallstent compared to the Palmaz-Schatz stent: on-line observations with two- and three-dimensional intracoronary ultrasound after angiographic guidance. *Am Heart J* 1996;131:1067–1075.

15. Li W, von Birgelen C, Di Mario C, Boersma E, Gussenhoven EJ, van der Putten N, Bom N. Semi-automatic contour detection for volumetric quantification of intracoronary ultrasound. In: Computers in Cardiology 1994. Los Alamitos, California: IEEE Computer Society Press, 1994:277–280.

16. von Birgelen C, Di Mario C, Li W, Schuurbiers JCH, Slager CJ, de Feyter PJ, Roelandt JRTC, Serruys PW. Morphometric analysis in three-dimensional intracoronary ultrasound: an in-vitro and in-vivo study using a novel system for the contour detection of lumen and plaque. *Am Heart J* (in press).

17. von Birgelen C, Slager CJ, Di Mario C, de Feyter PJ, Serruys PW. Volumetric intracoronary ultrasound: a new maximum confidence approach for the quantitative assessment of progression-regression of atherosclerosis? *Atherosclerosis* 1996;118(suppl):S103–S113.

18. Hong MK, Mintz GS, Popma JJ, Kent KM, Pichard AD, Satler LF, Leon MB. Limitations of angiography for analyzing coronary atherosclerosis progression or regression. *Ann Intern Med* 1994;121:348–354.

19. Matar FA, Mintz GS, Farb A, Douek P, Pichard AD, Kent KM, Satler LF, Popma JJ, Keller MB, Pinnow E, Merriu AJ, Lindsay J Jr, Leon MB. The contribution of tissue removal to lumen improvement after directional coronary atherectomy. *Am J Cardiol* 1994;74:647–650.

20. Dussaillant GR, Mintz GS, Pichard AD, Kent KM, Satler LF, Popma JJ, Wong SC, Leon MB. Small stent size and intimal hyperplasia contribute to restenosis: a volumetric intravascular ultrasound analysis. *J Am Coll Cardiol* 1995;26:720–724.

21. van der Lugt A, Gussenhoven EJ, Stijnen T, van Strijen M, van Driel E, van Egmond FC, van Suylen RJ, van Urk H. Comparison of intravascular ultrasonic findings after coronary balloon angioplasty evaluated in vitro with histology. *Am J Cardiol* 1995;76:661–666.

22. Di Mario C, The SHK, Madretsma S, van Suylen RJ, Wilson RA, Bom N, Serruys PW, Gussenhoven EJ, Roelandt JRTC. Detection and characterization of vascular lesions by intravascular ultrasound: an in vitro study correlated with histology. *J Am Soc Echocardiogr* 1992;5:135–146.

23. Bland JM, Altman DG. Statistical methods for assessing agreement between two methods of clinical measurement. *Lancet* 1986;2:307–310.

24. Potkin NN, Bartorelli AL, Gessert JM, Neville RF, Almagor Y, Roberts WC, Leon MB. Coronary artery imaging with intravascular high-frequency ultrasound. *Circulation* 1990;81:1575–1585.

25. Siegel RJ, Swan K, Edwards G, Fishbein MC. Limitations of postmortem assessment of human coronary artery size and luminal narrowing: differential

effects of tissue fixation and processing on vessels with different degrees of atherosclerosis. *J Am Coll Cardiol* 1985;75:452–460.
26. Matar FA, Mintz GS, Douek P, Farb A, Virmani R, Saturnino PJ, Popma JJ, Pichard AD, Kent KM, Satler LF, Keller M, Leon MB. Coronary artery lumen volume measurement using three-dimensional intravascular ultrasound: validation of a new technique. *Cathet Cardiovasc Diagn* 1994;33: 214–220.
27. Sonka M, Zhang X, Siebes M, DeJong S, McKay CR, Collins SM. Automated segmentation of coronary wall and plaque from intravascular ultrasound image sequences. In: *Computers in Cardiology 1994*. Los Alamitos: IEEE Computer Society Press, 1994:281–284.
28. Ge J, Erbel R, Zamorano J, Koch L, Kearney P, Gorge G, Gerber T, Meyer J. Coronary artery remodeling in atherosclerotic disease: an intravascular ultrasonic study in vivo. *Coron Artery Dis* 1993;4:981–986.
29. Dhawale PJ, Wilson DL, Hodgson JM. Optimal data acquisition for volumetric intracoronary ultrasound. *Cathet Cardiovasc Diagn* 1994;32:288–299.
30. Bruining N, von Birgelen C, Di Mario C, Prati F, Li W, Den Hood W, Patijn M, de Feyter PJ, Serruys PW, Roelandt JRTC. Dynamic three-dimensional reconstruction of ICUS images based on an ECG-gated pull-back device. In: *Computers in Cardiology 1995*. Los Alamitos, CA: IEEE Computer Society Press, 1995:633–636.

Chapter 2

Morphometric analysis in three-dimensional intracoronary ultrasound: An in-vitro and in-vivo study using a novel system for the contour detection of lumen and plaque

C von Birgelen, C Di Mario, W Li, JHC Schuurbiers,
CJ Slager, PJ de Feyter, JRTC Roelandt,
PW Serruys

Reprinted with permission from *Am Heart J* 1996;132:516-527

Morphometric analysis in three-dimensional intracoronary ultrasound: An in vitro and in vivo study performed with a novel system for the contour detection of lumen and plaque

Clemens von Birgelen, MD, Carlo Di Mario, MD, PhD, Wenguang Li, MSc, Johan C.H. Schuurbiers, BSc, Cornelis J. Slager, MSc, Pim J. de Feyter, MD, PhD, Jos R.T.C. Roelandt, MD, PhD, and Patrick W. Serruys, MD, PhD *Rotterdam, The Netherlands*

Currently, automated systems for quantitative analysis by intracoronary ultrasound (ICUS) are restricted to the detection of the lumen. The aim of this study was to determine the accuracy and reproducibility of a new semiautomated contour detection method, providing off-line identification of the intimal leading edge and external contour of the vessel in three-dimensional ICUS. The system allows cross-sectional and volumetric quantification of lumen and of plaque. It applies a minimum-cost algorithm and the concept that edge points derived from previously detected longitudinal contours guide and facilitate the contour detection in the cross-sectional images. A tubular phantom with segments of various luminal dimensions was examined in vitro during five catheter pull-backs (1 mm/sec), and subsequently 20 diseased human coronary arteries were studied in vivo with 2.9F 30 MHz mechanical ultrasound catheters (200 images per 20 mm segment). The ICUS measurements of phantom lumen area and volume revealed a high correlation with the true phantom areas and volumes ($r = 0.99$); relative mean differences were −0.65% to 3.86% for the areas and 0.25% to 1.72% for the volumes of the various segments. Intraobserver and interobserver comparisons showed high correlations ($r = 0.95$ to 0.98 for area and $r = 0.99$ for volume) and small mean relative differences (−0.87% to 1.08%), with SD of lumen, plaque, and total vessel measurements not exceeding 7.28%, 10.81%, and 4.44% (area) and 2.66%, 2.81%, and 0.67% (volume), respectively. Thus the proposed analysis system provided accurate measurements of phantom dimensions and can be used to perform highly reproducible area and volume measurements in three-dimensional ICUS in vivo. (Am Heart J 1996;132:516-27.)

From the Thoraxcenter, Division of Cardiology, University Hospital Rotterdam, Dijkzigt, Erasmus University, The Netherlands.

Received for publication November 27, 1995; accepted January 4, 1996.

Reprint requests: Patrick W. Serruys, MD, PhD, Thoraxcenter, Interventional Cardiology, P.O. Box 1738, University Hospital Rotterdam, Dijkzigt, 3000 DR Rotterdam, The Netherlands.

0002-8703/96/$5.00 + 0 4/1/73663

Intracoronary ultrasound (ICUS) provides arterial cross-sectional images and allows diameter and area measurements of coronary lumen and plaque.[1,2] These measurements have usually been limited to manual contour tracing of cross-sectional images at the site of the reference segment and the target stenosis. In parallel with the progress in quantitative angiography techniques, which started with manual caliper assessment and finally reached computer-assisted methods,[3,4] fully automated methods of quantitative analysis of ICUS have been developed to reduce the time of analysis and the subjectivity of manual tracing.[5] These automated systems can be rapidly applied on-line and provide a survey of vascular structure for clinical decision-making.[6,7,8]

Because the automated quantitative analysis of these programs is restricted to the detection of the lumen and because their success rate frequently is limited,[9] a semiautomated system for off-line ICUS analysis of atherosclerotic coronary segments was developed to detect the intimal leading edge and the external vessel contour on all of the individual cross-sectional images, with use of the complete three-dimensional data set obtained during a motorized pull-back of the ICUS transducer.[10] This method permits volumetric quantification of vessel dimensions by compiling information obtained from the individual cross-sectional images.

The present study was performed to determine the accuracy of this contour detection method in tubular phantoms of known dimensions in vitro and to evaluate intraobserver and interobserver variabilities of area and volume measurements in diseased human coronary arteries in vivo.

Table I. Characteristics of patients and coronary artery segments

Patients *(n)*	20
Age (yr)	52 ± 9.4
Men *(n)*	16 (80%)
Vessels *(n)*	
LAD	15 (75%)
LCX	1 (5%)
RCA	4 (20%)
Segments *(n)*	
Proximal	11 (55%)
Middle	8 (40%)
Distal	1 (5%)
Intervention status *(n)*	
Before intervention	3 (15%)
Control after HTX	1 (5%)
After PTCA	2 (10%)
Follow-up PTCA	3 (15%)
After DCA	3 (15%)
Follow-up DCA	5 (25%)
After stenting	3 (15%)

DCA, Directional coronary atherectomy; *HTX*, heart transplantation; *LAD*, left anterior descending coronary artery; *LCX*, left circumflex coronary artery; *PTCA*, percutaneous transluminal coronary angioplasty; *RCA*, right coronary artery.

METHODS

Phantom study in vitro. A tubular paraffin phantom was constructed and fixed inside an acrylate tube. The phantom has a circular lumen with a stepwise increase in diameter (2, 3, 4, and 5 mm) defining four segments (S2, S3, S4, and S5, respectively) each 5 mm in length (Fig. 1). A paraffin phantom was used because its properties with regard to the reflection and absorption of ultrasound are similar to those of vessel tissue. An optical calibration was performed with a calibrated stereomicroscope with 40-fold magnification for the 2 mm segment and sixteenfold magnification for all of the remaining segments. The mean difference between measurements and the true lumen diameter was −15 ± 41 μm at 20° C, the temperature at which the experiments were performed. Temperature dependency of the paraffin phantom was assessed by comparing measurements obtained at 2° and 37° C (range 35° C). This temperature increment resulted in an increase in luminal dimensions of 2%.

Five motorized uniform pull-backs (1 mm/sec) of the ultrasound imaging transducer through the paraffin phantom were performed in water (20° C) and recorded on videotape. A mechanical rotating ICUS catheter (Microview, Cardiovascular Imaging Systems, Inc., Sunnyvale, Calif.) with a distal external diameter of 2.9F was used for both in vitro and in vivo studies. This ICUS imaging catheter is equipped with a distal transparent sleeve that covers the rotating imaging core. With a motorized pull-back system the imaging core is withdrawn inside this sleeve. The design of the catheter and pull-back system minimizes the risk of catheter rotation and facilitates several pull-backs of the echo transducer without increasing the risk of vessel damage, because the echo-transparent distal sleeve prevents the ICUS transducer from coming into direct contact with the vessel wall.

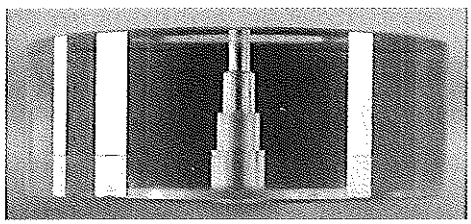

Fig. 1. Model of paraffin phantom used in in vitro study. Phantom has circular lumen and consists of four segments with stepwise increase in diameter (2, 3, 4, and 5 mm).

Study in vivo. Intraobserver and interobserver variabilities of the quantification method were studied in 20 ICUS examinations of diseased, nonwedged human coronary segments in vivo. Segments with short calcifications or single major side branches were included in the study; ICUS studies with excessive systolic-diastolic movement were not considered for analysis. The maximum and average cross-sectional area obstructions were 65.6% ± 8.8% (range 83% to 49%) and 49.2% ± 6.6% (range 83% to 17%), respectively. The composition of the study population reflects the current clinical application of ICUS imaging in our center. Characteristics of the patients and analyzed coronary artery segments are shown in Table I.

ICUS imaging was performed during motorized pull-backs (1 mm/sec) of a 2.9F ICUS catheter. Because the imaging core is straightened during the first seconds of withdrawal, care was taken to start the pull-back 1 cm distal to the segment analyzed. The ICUS examinations were recorded on videotape, and analysis was performed off-line by a new quantitative ultrasound analysis system set at a digitization frame rate of 10 images/sec. Thus 20 mm–long coronary artery segments were reconstructed and measured using the system's maximum memory capacity, which is currently 200 images.

The quantitative ICUS analysis system. The analysis program uses the Microsoft (Redmond, Wash.) Windows operating system on a Pentium (Intel)-based 60 MHz personal computer with 16 Mb internal random-access memory. A frame-grabber is installed (DT-3852, Data Translation, Inc., Malboro, Mass.; resolution 800 × 600 × 8 bits), digitizing a user-defined region of interest from the video images. A maximum of 200 ICUS images can be digitized at a user-defined digitization frame rate (maximum 20 images/sec). The reconstructed segment length is thus defined by the speed of the motorized pull-back during the basic image acquisition and by the digitization frame rate. In the present study a pull-back speed of 1.0 mm/sec and a digitization frame rate of 8 images/sec (in vitro) and 10 images/sec (in vivo) were used, resulting in reconstructed segment lengths of 25 and 20 mm, respectively. The pixel size, which depends on the magnification applied by the basic ICUS imaging system, ranged from 26 to 36 μm.

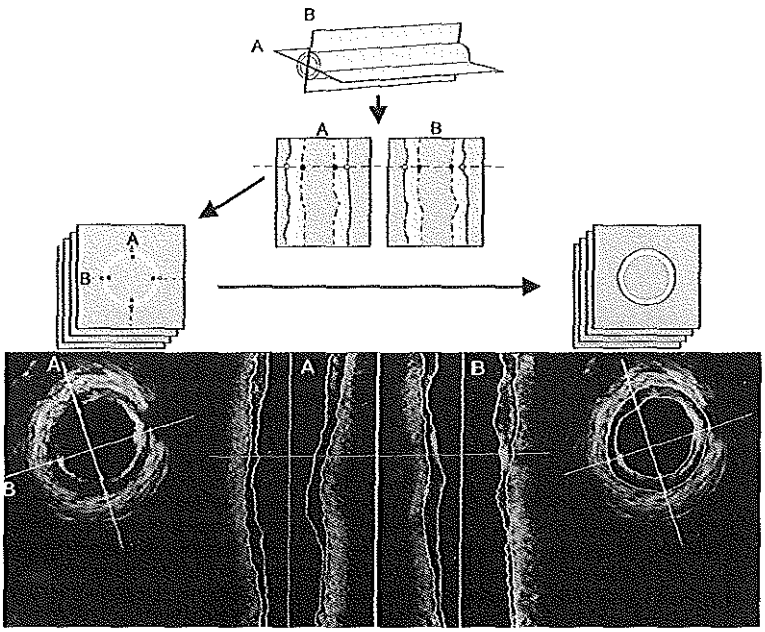

Fig. 2. Morphometric analysis by contour detection in three-dimensional ICUS. With this method, edge points derived from longitudinal contours previously detected on two longitudinally reconstructed images guide and facilitate final contour detection on transverse ICUS images. ICUS images, obtained during motorized pull-back, are stored in voxel space. Two perpendicular cut planes (*A* and *B*) that are placed interactively are used to reconstruct two longitudinal sections from ICUS image data located at intersections. Automated contour detection is performed in these longitudinal sections on basis of application of minimum-cost algorithm. User then is free to set some markers on longitudinal images to force contours to pass through these sites, and optimal path is redefined by dynamic programming techniques. Longitudinal contours are updated during entire interactive procedure and are represented as individual edge points in transverse images; these points guide contour detection on basis of application of minimum-cost algorithm. Position of an individual transverse plane in longitudinal sections is indicated by horizontal cursor line, which can be used to scroll through whole series of transverse images. Finally, detected contours are checked in all of transverse images, and manual correction of contours can be performed.

Minimum-cost algorithm. The contour detection of the intimal leading edge and the external boundary of the total vessel applies a minimum-cost algorithm, previously applied[11] and described[12] in cross-sectional ICUS images. By this approach the digitized ICUS images are resampled according to a radial image reconstruction (64 radii in the cross-sectional images; 200 rows in the longitudinal sections). A cost matrix that represents the edge strength is calculated from the image data. For the detection of the boundary between lumen and plaque, the cost value is defined by the spatial first derivative. To detect the external boundary of the total vessel a pattern-matching process by cross correlation is adopted for the cost calculations. Through the cost matrixes a path with the smallest accumulated value is determined by dynamic programming techniques.[11]

Automated contour detection. For contour detection of the intimal leading edge and the external boundary of the total vessel, three steps must be performed because, in this system, edge points, derived from previously detected longitudinal contours, guide and facilitate the final contour detection in the cross-sectional ICUS images.

First, a sequence of digitized ICUS images obtained from the motorized pull-back of the ultrasound transducer is stored in a voxel space.[13] Ringdown artifacts around the ICUS catheter, potentially interfering with the contour detection step, can be removed from all of the ICUS images with an automated function. Two perpendicular cut planes

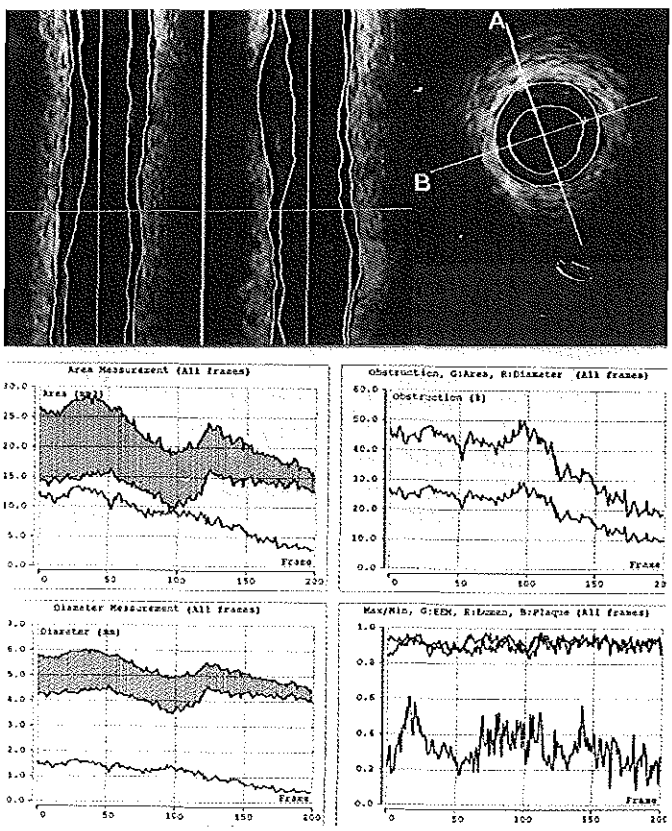

Fig. 3. Standard display of results. This clinical example shows results of quantitative analysis performed at 6-month follow-up after directional coronary atherectomy performed in proximal left anterior descending coronary artery. The intimal leading edge and external vessel contours are shown in two longitudinally reconstructed sections (*A* and *B*, *left* and *mid top*), which stand perpendicular to each other as demonstrated in the transverse image *(right top)*. *Left middle* and *left bottom*, Area and mean diameter measurements of lumen, total vessel, and plaque. *Gray areas* represent coronary plaque, and site of maximal plaque burden can thus be easily identified. Upper and lower boundaries of gray zone correspond to dimensions of coronary lumen and total vessel. Absolute value of plaque dimension is given as single function in display of area and in diameter measurements. *Right middle*, Functions of relative diameter obstruction and area obstruction. *Right bottom*, Symmetry ratios of both contours and plaque eccentricity ratio.

running along the long axis of the artery are used to reconstruct two longitudinal sections (Fig. 2). This longitudinal reconstruction uses the ICUS image data, located at the intersection of the cut planes with the voxel space. The position and the rotation angle of the two cut planes can be changed interactively by the user to obtain an optimal representation of the reconstructed coronary segment in the longitudinal sections.

Second, the longitudinal contours are detected in these two longitudinal images. A first boundary detection is performed automatically on the basis of the application of the minimum-cost algorithm. Then the user is free to set some markers in the longitudinal images and to force the contours to pass through these sites. This step is achieved by setting the cost matrix of the manually defined sites at a very low value. By applying dynamic programming techniques, the optimal path is then redefined for the modified cost matrix. During the entire user-interactive procedure

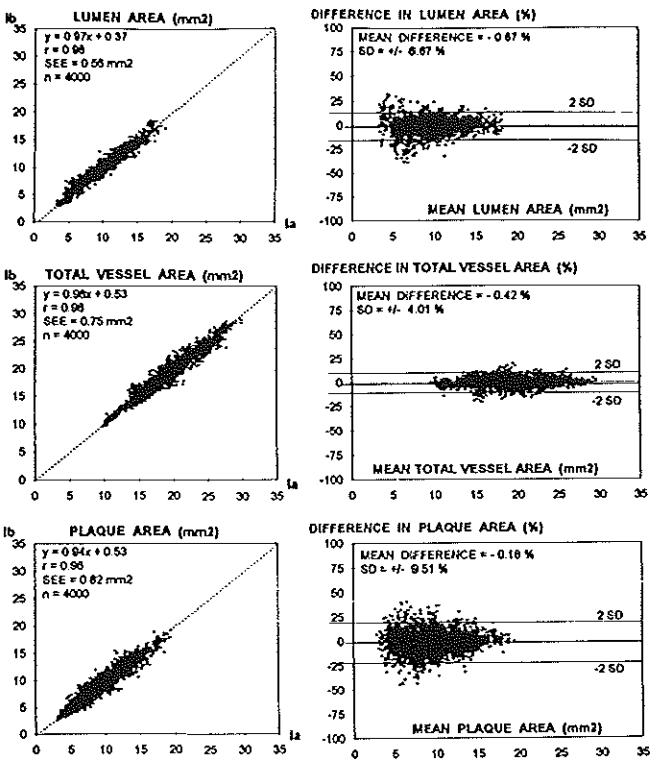

Fig. 4. Intraobserver variability of area measurements in vivo. *Left*, Results of linear regression analyses, comparing lumen, total vessel, and plaque measurements by first (Ia) and second (Ib) observations. *Right*, Relative intraobserver differences plotted against mean of two measurements. *Continuous lines*, Relative mean signed difference and 2 SD; *dotted line*, line of identity.

the longitudinal contours are visible and updated in the longitudinal sections. In the transverse images the longitudinal contours intersecting this plane are represented as points.

These individual edge points guide the third step, which is the final contour detection in the transverse images, by defining the center and range of the boundary searching process on the basis of the application of the minimum-cost algorithm. The position of an individual transverse plane in the longitudinal sections is indicated by a horizontal cursor line, which can be used to scroll through the whole series of transverse images. The detected contours are checked by the analyst in all of the transverse images, and manual correction of the contours can be performed.

Calculation and display of results. The quantitative results, including diameter and area measurements of lumen, total vessel, and plaque; percentage diameter obstruction; and percentage area obstruction are displayed (Fig. 3). Plaque area is calculated by subtracting the lumen area from the total vessel area, thus representing the plaque–media complex. Volumes of lumen, total vessel, or plaque are calculated as

$$V = \sum_{i=1}^{n} A_i \cdot H$$

where V = volume; A = area of lumen, total vessel, or plaque in a given digitized cross-sectional ultrasound image; H = the thickness of the coronary artery slice, which is represented by this digital cross-sectional ICUS image; and n = the number of digitized cross-sectional images encompassing the volume to be measured.

Mean values, SDs, and minimum and maximum values of area and volume measurements are presented. The data of the current transverse image are constantly displayed

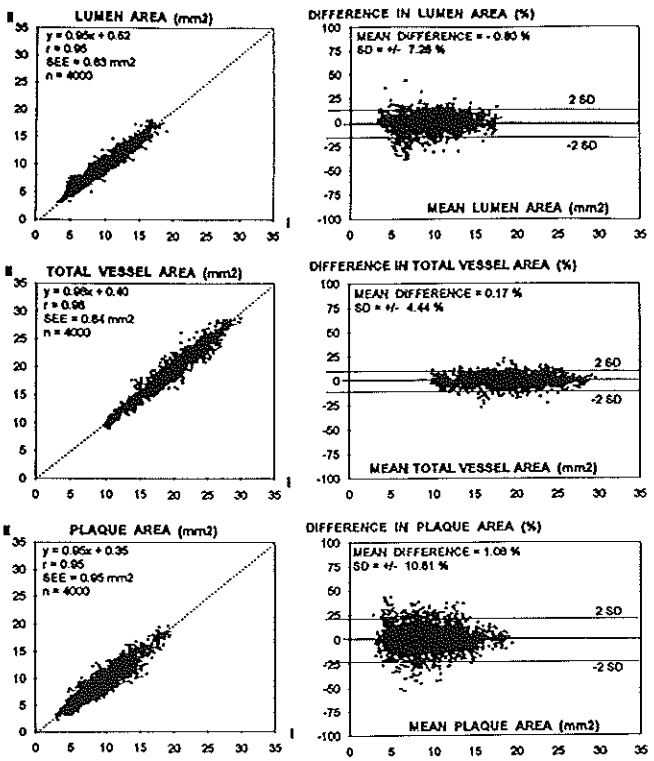

Fig. 5. Interobserver variability of area measurements in vivo. *Left*, results of linear regression analyses, comparing lumen, total vessel, and plaque measurements by first (Ia) and second (II) observers. *Right*, Relative interobserver differences plotted against mean of two measurements. *Continuous lines*, Relative mean signed difference and 2 SD; *dotted line*, line of identity.

and serially updated if manual corrections of the contours are performed. The analyzed artery segment can be displayed in a three-dimensional, cylindrical format; however, this format is not required for the quantification process that uses the three-dimensional data set (see Discussion section).

Data analysis. At the transition between two phantom segments the circular contours of the two adjacent segments are simultaneously visualized by ICUS because of the limited out-of-plane resolution of the current ultrasound transducers.[14] In this study, when the ultrasound transducer was withdrawn from the segment with the smaller dimension to the segment with the larger dimension, the transition to the larger segment was defined as the first image in which the contour of the larger segment expressed a higher intensity than the contour of the smaller segment. This definition was used to calculate the volumes of the phantom segments. For validation of the area measurements, images from the mid-portion of each segment were used.

ICUS imaging systems are calibrated for application in blood, but the in vitro experiments of the present study were performed in water. Accordingly, a correction factor (0.953) determined on the basis of the differing velocities of ultrasound in blood (1570 m/sec) and water (1497 m/sec)[15] was applied.

The same digitized in vivo ICUS images were analyzed off-line by two independent observers, who had had common training in the use of the semiautomated contour detection system. After 2 to 3 weeks the analysis was repeated by the blind, first observer. The measurements by two independent observers (Ia and II) and the repeated

Table II. Coronary artery lumen, total vessel, and plaque volume in vivo: Results of the intraobserver and interobserver studies

	Lumen (mm^3)			*Total vessel (mm^3)*			*Plaque (mm^3)*		
Patient	*Ia*	*Ib*	*II*	*Ia*	*Ib*	*II*	*Ia*	*Ib*	*II*
1	158.3	159.0	157.8	338.9	336.0	332.6	180.6	177.0	174.8
2	185.5	193.4	197.6	427.9	430.7	430.6	242.4	237.3	233.0
3	159.5	163.4	160.1	335.3	337.4	337.1	175.8	174.0	177.0
4	208.4	203.0	207.7	439.9	439.0	441.3	231.5	236.0	233.6
5	207.8	214.1	200.3	400.5	407.9	400.6	192.7	193.8	200.3
6	202.0	199.2	206.0	446.2	447.2	445.4	244.2	248.0	239.4
7	204.8	211.3	204.3	404.9	411.8	406.1	200.1	200.5	201.8
8	216.6	214.2	204.9	375.8	376.0	372.1	159.2	161.8	167.2
9	231.1	233.5	231.7	431.6	431.8	427.7	200.5	198.2	196.0
10	262.7	261.0	261.0	456.3	454.8	452.9	193.6	193.7	191.9
11	145.2	153.5	154.1	292.8	294.6	290.3	147.6	141.2	136.2
12	168.7	168.6	172.4	341.0	342.2	343.2	172.3	173.6	170.8
13	129.0	131.8	132.9	271.1	272.6	270.4	142.1	140.8	137.5
14	130.8	129.3	130.3	360.5	362.3	360.5	229.7	233.0	230.2
15	107.6	105.8	109.6	215.4	216.2	214.8	107.8	110.4	105.2
16	211.2	213.4	214.4	444.0	447.2	443.8	232.8	233.8	229.4
17	190.2	191.8	190.4	419.2	421.8	422.8	229.0	230.0	232.8
18	204.4	205.2	205.0	363.8	366.6	362.2	159.4	161.4	157.2
19	193.0	193.4	193.6	293.2	292.8	292.8	100.2	99.4	99.2
20	275.2	275.2	276.2	443.6	445.6	442.6	168.4	170.4	166.4
Mean	189.6	191.0	190.5	375.1	376.7	374.5	185.5	185.7	184.0
SD	42.9	42.6	41.7	68.4	68.8	68.7	42.3	42.9	42.8

I, First observer (*a*, first observation; *b*, second observation); *II*, second observer.

measurements by the same observer (Ia and Ib) were studied to obtain information on the intraobserver and interobserver variabilities of the new analysis method.

Statistics. Results are given as mean ± SD. The mean difference and SD of the differences were calculated for each phantom segment (ICUS measurements minus true phantom dimensions) and for repeated measurements by the same observer and for measurements by two observers.[16] Analysis of variance and linear regression analysis were performed to compare the results of the intraobserver study and the results of the interobserver study.

RESULTS

Phantom study in vitro. The lumen area measurements were compared with the true values by linear regression analysis. The measurements ($n = 600$) and true phantom values showed a high correlation ($r = 0.99$; $y = 0.99x + 0.11$; SEE = 0.12 mm^2). The mean difference between measurements and true phantom areas ranged from −0.65% to 1.24% with the exception of the smallest segment, in which a small overestimation (3.86%) was found. Correlation between the volume measurements ($n = 20$) and the true phantom volumes was high ($r = 0.99$; $y = 1.02x - 0.42$; SEE = 1.17 mm^3). The measured volumes showed a slight overestimation; the mean difference ranged from 0.25% to 1.72%. A decrease in phantom dimensions was associated with a slight increase in the relative SD of the difference of area and volume measurements (0.56%, 0.95%, 0.95%, and 2.55% for area and 1.40%, 2.69%, 2.78%, and 3.75% for volume measurements in the segments with lumen diameters of 5, 4, 3, and 2 mm, respectively).

Area measurement in vivo. The time required for the complete analysis was 1.15 ± 0.31 hours. The correlation of repeated area measurements of coronary lumen, total vessel, and plaque was high, with correlation coefficients of 0.98, 0.98, and 0.96 respectively (Fig. 4, left). The mean relative differences between repeated area measurements by the same observer were <1% for lumen, total vessel, and plaque areas (Fig. 4, right). The SD of the differences was higher for the plaque area than for lumen and total vessel areas (9.51% vs 6.67% and 4.01%, respectively). The interobserver correlation coefficients were high ($r = 0.95$, 0.98, and 0.95 for lumen, total vessel, and plaque, respectively) (Fig. 5, left), but for lumen and plaque area measurements they were slightly lower than the corresponding intraobserver correlation coefficients. The interobserver SEEs of lumen, total vessel, and plaque areas (0.63, 0.84, and 0.95 mm^2, respectively) also were higher than the

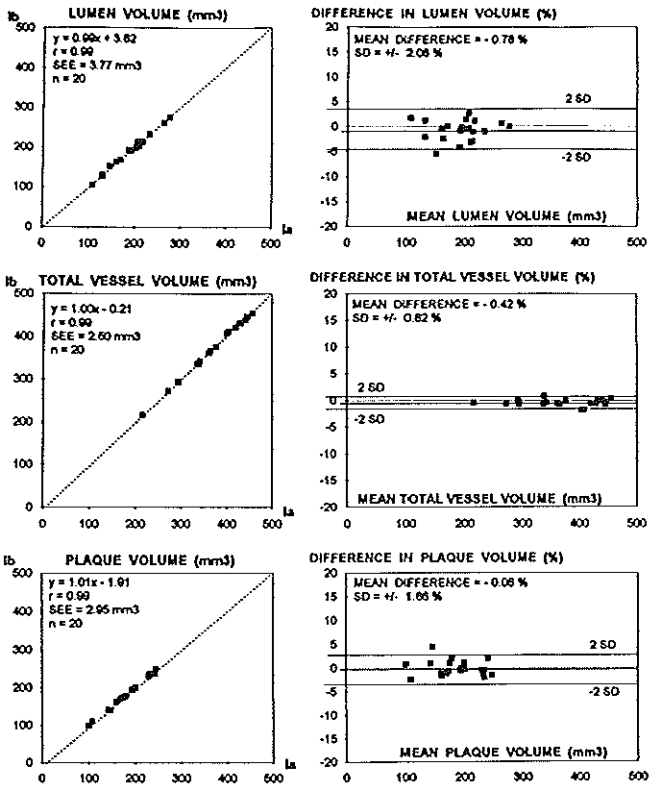

Fig. 6. Intraobserver variability of volume measurements in vivo. *Left*, Results of linear regression analyses, comparing lumen, total vessel, and plaque measurements of first (Ia) and second (Ib) observations. *Right*, Relative intraobserver differences plotted against mean of two measurements. *Continuous lines*, Relative mean signed difference and 2 SD; *dotted line*, line of identity.

corresponding intraobserver SEEs. The SD of the relative differences were slightly higher for interobserver differences (Fig. 5, right) than for intraobserver differences. The data points for smaller dimensions of lumen and plaque areas showed a larger relative dispersion.

Volume measurement in vivo. The results of the lumen, total vessel, and plaque volume measurements are shown in Table II. A high correlation between the intraobserver measurements was found, with a correlation coefficient of 0.99 for coronary lumen, total vessel, and plaque (Fig. 6, left). The correlation coefficients also were high for the comparison of the measurements by two independent observers ($r = 0.99$ for lumen, total vessel, and plaque volumes) (Fig. 7, left). The SEE and the SD of the differences were higher for the interobserver than for the intraobserver comparison (Figs. 6, right, and 7, right).

DISCUSSION

The application of high-frequency ICUS permits assessment of catheter-based interventions[17-20] and visualization (Fig. 8) and quantification of coronary artery atherosclerosis.[21-24] Serial ICUS studies also permit assessment of the progression or regression of atherosclerosis and of the mechanisms of coronary restenosis.[25]

The main limitation in the comparison of serial ultrasound studies is the virtual impossibility of examining exactly the same ultrasonic cross section in

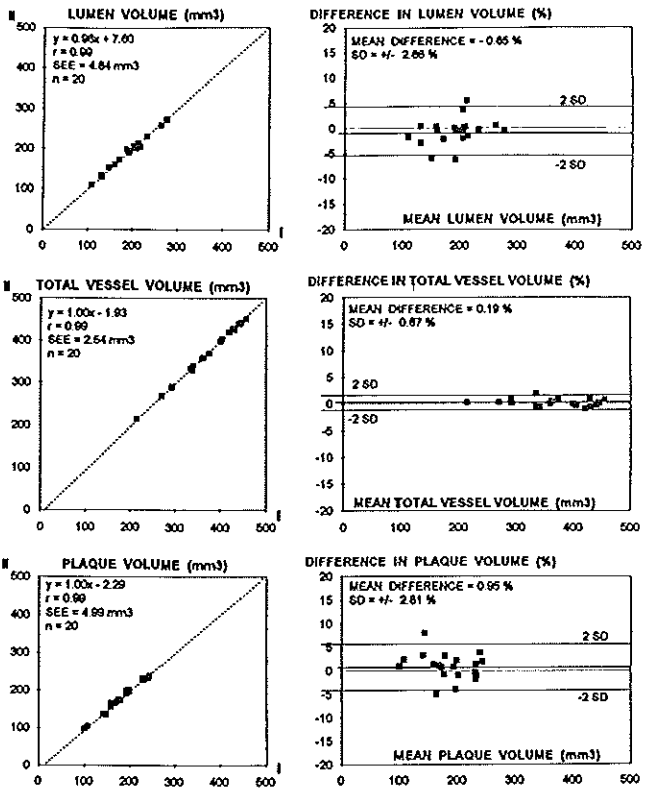

Fig. 7. Interobserver variability of volume measurements in vivo. *Left*, Results of linear regression analyses, comparing lumen, total vessel, and plaque measurements of first (Ia) and second (II) observers. *Right*, Relative interobserver differences plotted against mean of two measurements. *Continuous lines*, Relative mean signed difference and 2 SD; *dotted line*, line of identity.

each study. In previous studies, anatomic landmarks such as side branches or deep calcifications were used to define corresponding images in serial studies. The application of the proposed analysis system offers a more reliable solution to this problem, because a long arterial segment can be examined. Minimal differences in the start and end points of repeated studies are unlikely to impair the accuracy of the changes in lumen and plaque volume measurements, assessed for an entire arterial segment. Because the aim of this study was to determine the accuracy and reproducibility of the analysis method, the same set of digitized images from a single pullback per patient was used for repeated analysis.

The results of the in vitro study suggest that the automated analysis system operates accurately, and the in vivo study demonstrates high reproducibility. The SDs of the intraobserver and interobserver differences in detecting the total vessel contours were particularly low, reflecting the regular shape of the external boundary of the total vessel. The lumen contours, however, demonstrated slightly higher variability, which can be explained by irregularities in the shape of the lumen area, especially after coronary interventions. The larger variability of plaque area measurements, derived from measurements of lumen and total vessel contours, reflect the combined variability of these two contours. The volumetric

measurements in vivo showed a lower SD of the differences than did the area measurements, reflecting an averaging of the differences of the area measurements.

The ability to display the cross-sectional plus two longitudinal views simultaneously facilitates the detection of the boundary of the vessel. The reason for first performing contour detection on the longitudinal images is that the edge information obtained from this step is subsequently used to guide the final contour detection on the transverse images.

Previous studies. A different approach to contour detection, providing automated tracking of the coronary wall and lumen in ICUS image sequences, has been developed by Sonka et al.[26] The border tracking is performed only in the cross-sectional images, without the assistance of an additional contour detection step in longitudinally reconstructed images. The feasibility of this system in analyzing in vivo examinations remains to be confirmed because the movement of the ICUS catheter or the poor depiction of the plaque in single ICUS images may impair the application of this algorithm, but the first results in vascular specimen in vitro are promising.

Data on the variability and reproducibility of ICUS measurements are limited to the assessment of selected individual cross sections in in vitro and in vivo studies and, in general, address different questions. A recent systematic study[5] on the variability of measurements in 120 cross-sectional ICUS images in vivo demonstrated relatively high variability of the manual contour tracing.[27] In agreement with the present study, the SD of the differences was higher for plaque than for vessel lumen or total area measurement. However, the variability of repeated manual contour tracing[5] was indeed higher than the variability of the proposed analysis system in the present study. This difference may be explained in part by the use of larger ultrasound catheters in the previous study[27], which show strut artifacts, obscuring a portion of the vessel wall, and the use of single digitized frames without the option of scrolling the videotape back or forth.

Information about the reproducibility of volumetric measurements is limited, and it is difficult to compare results provided by different quantitative analysis systems. Matar et al.[28] recently reported an intraobserver study that yielded a correlation coefficient of 0.98 for automated threshold-based measurement of lumen volume in vivo, a result confirmed by the high reproducibility of volumetric measurement observed in the present study.

Approaches toward volumetric quantification. Three-dimensional ICUS was first used clinically to assess visually the spatial configuration of plaques.[29] The morphologic features of dissections[30,31] and stents[32,33] were examined, and their length or diameter was measured. However, the three-dimensional data set can also be processed by various technical approaches to quantify lumen or plaque volumes. These systems differ in terms of image segmentation, which is the algorithm for identification of the structures of interest in the digitized ICUS images. Distinction between vessel lumen and wall can be achieved by various (semi)automated systems on-line with binary threshold-based algorithms,[28,29] voxel-based segmentation algorithms,[34] or algorithms for statistical pattern recognition.[6-8] The applicability of these approaches depends considerably on image quality and is restricted to the automated detection of the lumen. The proposed quantitative analysis system, however, combines automatic con-

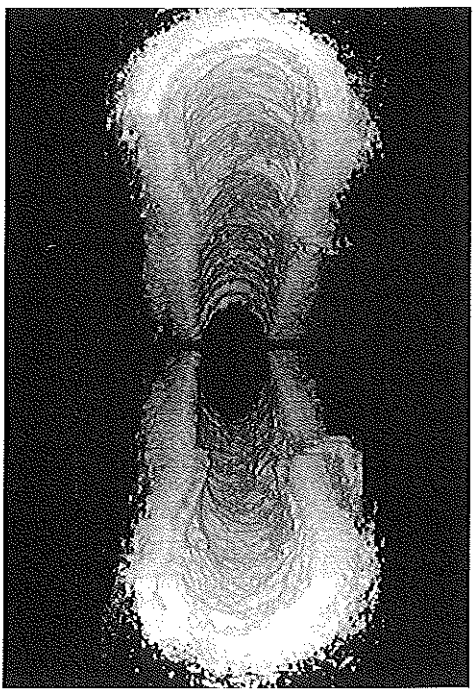

Fig. 8. Three-dimensional display of coronary segment at follow-up after directional coronary atherectomy. This display uses cylindrical format; it is not required for quantification from three-dimensional data set. Nevertheless, it may provide additional insight into plaque geometric features.

tour detection and user interaction and is therefore able partly to compensate for limitations in ICUS image quality. The system is capable of identifying the intimal leading edge and the external contour of the vessel, thus permitting automated quantification of plaque volume.

The possibility of examining the vascular segment at the same time in a transverse and two longitudinal views and the concept of applying an automated contour detection in the cross-sectional ICUS images, guided by edge points derived from previously detected longitudinal contours, are the key factors explaining the high reproducibility of this ICUS analysis method in vivo.

Contradictory results have been observed in previous progression–regression trials using quantitative coronary angiography. ICUS directly visualizes the vessel wall and therefore may better reflect the changes of the plaque, but in progression–regression studies small changes can be expected despite the long study period, and a high reproducibility of measurements is important. On the basis of the results of the present study, which demonstrates high reproducibility of the volumetric ICUS measurement, volumetric ICUS measures may be considered.[35]

Limitations. Behind deposits of calcium the external vessel boundary cannot be traced. In addition, depending on the type of stent, the metallic struts may occasionally render the external contour detection difficult. The proposed analysis system, however, allows reliable interpolation between preceding and following images on the longitudinal sections. The edge information finally permits reproducible interpolated contour tracing on the cross-sectional ICUS images. Artifacts in the longitudinally reconstructed views, caused by the movement of the ultrasound catheter during the cardiac cycle and systolic–diastolic changes in vessel dimensions,[6,9] may in the future be avoided by electrocardiographically (ECG) gated[36,37] ICUS image acquisition or even the combination of ECG-gated ICUS and angiographic data.[38,39] Application of these combined approaches is still restricted, but the analysis system used in the present study is now used clinically for on-line and off-line analyses, and evaluation of tape-recorded ultrasound studies from multicenter trials has recently been started.

Conclusion. The proposed analysis system provides accurate measurements of phantom dimensions and can be used to perform highly reproducible area and volume measurements in three-dimensional ICUS in vivo.

We thank Ellie van de Leur, Bart van der Zalm, and Jurgen Ligthart for technical support.

REFERENCES

1. Yock PG, Linker DT. Intravascular ultrasound: looking below the surface of vascular disease. Circulation 1990;81:1715-8.
2. Nissen SE, Gurley JC, Grines CL, Booth DC, McClure R, Berk M, et al. Intravascular ultrasound assessment of lumen size and wall morphology in normal subjects and patients with coronary artery disease. Circulation 1991;84:1087-99.
3. Keane D, Serruys PW. Quantitative coronary angiography: an integral component of interventional cardiology. In: Topol EJ, Serruys PW, eds. Current review of interventional cardiology. 2nd ed. Philadelphia: Current Medicine, 1995:205-33.
4. von Birgelen C, Umans V, Di Mario C, Keane D, Gil R, Prati F, et al. Mechanism of high-speed rotational atherectomy and adjunctive balloon angioplasty revisited by quantitative coronary angiography: edge detection versus videodensitometry. Am Heart J 1995;130:405-12.
5. Hausmann D, Lundkvist AJS, Friedrich GJ, Mullen WL, Fitzgerald PJ, Yock PG. Intracoronary ultrasound imaging: intraobserver and interobserver variability of morphometric measurements. Am Heart J 1994; 128:674-80.
6. Di Mario C, von Birgelen C, Prati F, Soni B, Li W, Bruining N, et al. Three-dimensional reconstruction of two-dimensional intracoronary ultrasound: clinical or research tool? Br Heart J 1995;73(suppl 2):26-32.
7. von Birgelen C, Gil R, Ruygrok P, Prati F, Di Mario C, van der Giessen WJ, et al. Optimized expansion of the Wallstent compared to the Palmaz-Schatz stent: on-line observations with intracoronary ultrasound after angiographic guidance. Am Heart J 1996;131:1067-75.
8. von Birgelen C, Kutryk MJB, Gil R, Ozaki Y, Di Mario C, Roelandt JRTC, et al. Quantification of the minimal luminal cross-sectional area after coronary stenting by two-dimensional and three-dimensional intravascular ultrasound versus edge detection and videodensitometry. Am J Cardiol [In press].
9. Roelandt JRTC, Di Mario C, Pandian NG, Wenguang Li, Keane D, Slager CJ, et al. Three-dimensional reconstruction of intracoronary ultrasound images: rationale, approaches, problems, and directions. Circulation 1994;90:1044-55.
10. Li W, von Birgelen C, Di Mario C, Boersma E, Gussenhoven EJ, van der Putten N, et al. Semi-automatic contour detection for volumetric quantification of intracoronary ultrasound. In: Computers in cardiology 1994. Los Alamitos, Calif.: IEEE Computer Society Press, 1994:277-80.
11. Di Mario C, The SHK, Madretsma S, van Suylen RJ, Wilson RA, Bom N, et al. Detection and characterization of vascular lesions by intravascular ultrasound: an in vitro study correlated with histology. J Am Soc Echocardiogr 1992;5:135-46.
12. Li W, Bosch JG, Zhong Y, van Urk H, Gussenhoven EJ, Mastik F, et al. Image segmentation and 3D reconstruction of intravascular ultrasound images. In: Wei Y, Gu B, eds. Acoustical imaging. Vol. 20. New York: Plenum Press, 1993:489-96.
13. Kitney RI, Moura L, Straughan K. 3-D visualization of arterial structures using ultrasound and voxel modelling. Int J Cardiac Imaging 1989;4:135-43.
14. Benkeser PJ, Churchwell AL, Lee C, Aboulnasr DM. Resolution limitations in intravascular ultrasound imaging. J Am Soc Echocardiogr 1993;6:168-65.
15. Hertz H. Principles of ultrasound in medical diagnosis. In: Bom N, ed. Echocardiography with Doppler applications and real time imaging. The Hague: Martinus Nijhoff Medical Division, 1977:7-14.
16. Bland JM, Altman DG. Statistical methods for assessing agreement between two methods of clinical measurement. Lancet 1986;2:307-10.
17. Ge J, Erbel R, Gerber T, Gorge G, Koch L, Haude M, et al. Intravascular ultrasound imaging in angiographically normal coronary arteries: a prospective study in vivo. Br Heart J 1994;71:572-8.
18. Hodgson JM, Reddy KG, Suneja R, Nair RN, Lesnefsky EJ, Sheehan HM. Intracoronary ultrasound imaging: correlation of plaque morphology with angiography, clinical syndrome and procedural results in patients undergoing coronary angioplasty. J Am Coll Cardiol 1993;21:35-44.
19. Losordo DW, Rosenfield K, Kaufman J, Pieczek A, Isner JM. Focal compensatory enlargement of human arteries in response to progressive atherosclerosis: in vivo documentation using intravascular ultrasound. Circulation 1994;89:2570-7.

20. St. Goar FG, Pinto FJ, Alderman EL, Valantine HA, Schroeder JS, Gao SZ, et al. Intracoronary ultrasound in cardiac transplant recipients: in vivo evidence of 'angiographically silent' intimal thickening. Circulation 1992;85:979-87.
21. Mintz GS, Potkin BN, Keren G, Satler LF, Pichard AD, Kent KM, et al. Intravascular ultrasound evaluation of the effect of rotational atherectomy in obstructive atherosclerotic coronary artery disease. Circulation 1992;86:1383-93.
22. Nakamura S, Colombo A, Gaglione A, Almagor Y, Goldberg SL, Maiello L, et al. Intracoronary ultrasound observations during stent implantation. Circulation 1994;89:2026-34.
23. Tenaglia AN, Buller CE, Kisslo KB, Stack RS, Davidson CJ. Mechanisms of balloon angioplasty and directional coronary atherectomy as assessed by intracoronary ultrasound. J Am Coll Cardiol 1992;20:685-91.
24. Tobis JM, Mallery JA, Gessert J, Griffith J, Mahon D, Bessen M, et al. Intravascular ultrasound cross-sectional arterial imaging before and after balloon angioplasty in vitro. Circulation 1989;80:873-82.
25. Di Mario C, Gil R, Camenzind E, Ozaki Y, von Birgelen C, Umans V, et al. Quantitative assessment with intracoronary ultrasound of the mechanisms of restenosis after percutaneous transluminal coronary angioplasty and directional coronary atherectomy. Am J Cardiol 1995; 75:772-7.
26. Sonka M, Zhang X, Siebes M, DeJong S, McKay CR, Collins SM. Automated segmentation of coronary wall and plaque from intravascular ultrasound image sequences. In: Computers in cardiology 1994. Los Alamitos, Calif.: IEEE Computer Society Press, 1994:281-4.
27. Haase J, Ozaki Y, Di Mario C, Escaned J, De Feyter PJ, Roelandt JRTC, et al. Can intracoronary ultrasound correctly assess the luminal dimensions of coronary artery lesions? A comparison with quantitative angiography. Eur Heart J 1995;16:112-119.
28. Matar FA, Mintz GS, Douek P, Farb A, Virmani R, Saturnino PJ, et al. Coronary artery lumen volume measurement using three-dimensional intravascular ultrasound: validation of a new technique. Cathet Cardiovasc Diagn 1994;33:214-20.
29. Rosenfield K, Losordo DW, Ramaswamy K, Pastore JO, Langevin RE, Razvi S, et al. Three-dimensional reconstruction of human coronary and peripheral arteries from images recorded during two-dimensional intravascular ultrasound examination. Circulation 1991;84:1938-56.
30. Cavaye DM, White RA, Lerman RD, Kopchok GE, Tabbara MR, Cornier F, et al. Usefulness of intravascular ultrasound imaging for detecting experimentally induced aortic dissection in dogs and for determining the effectiveness of endoluminal stenting. Am J Cardiol 1992; 69:705-7.
31. Coy KM, Park JC, Fishbein MC, Laas T, Diamond GA, Adler L, et al. In vitro validation of three-dimensional intravascular ultrasound for the evaluation of arterial injury after balloon angioplasty. J Am Coll Cardiol 1992;20:692-700.
32. Mintz GS, Pichard AD, Satler LF, Popma JJ, Kent KM, Leon MB. Three-dimensional intravascular ultrasonography: reconstruction of endovascular stents in vitro and in vivo. J Clin Ultrasound 1993;21:609-15.
33. Schryver TE, Popma JJ, Kent KM, Leon MB, Eldredge S, Mintz GS. Use of intracoronary ultrasound to identify the 'true' coronary lumen in chronic coronary dissection treated with intracoronary stenting. Am J Cardiol 1992;69:1107-8.
34. Chandrasekaran K, Sehgal CM, Hsu TL, Young NA, D'Adamo AJ, Robb RA, et al. Three-dimensional volumetric ultrasound imaging of arterial pathology from two-dimensional intravascular ultrasound: an in vitro study. Angiology 1994;45:253-64.
35. von Birgelen C, Slager CJ, Di Mario C, de Feyter PJ, Serruys PW. Volumetric intracoronary ultrasound: a new maximum confidence approach for the quantitative assessment of progression-regression of atherosclerosis? Atherosclerosis 1995;118(Suppl):S103-13.
36. Dhawale PJ, Wilson DL, Hodgson JM. Optimal data acquisition for volumetric intracoronary ultrasound. Cathet Cardiovasc Diagn 1994;32:288-99.
37. Bruining N, von Birgelen C, Di Mario C, Prati F, Li W, Den Hood W, et al. Dynamic three-dimensional reconstruction of ICUS images based on an ECG-gated pull-back device. In: Computers in cardiology 1995. Los Alamitos, Calif.: IEEE Computer Society Press, 1995:633-6.
38. Slager CJ, Laban M, von Birgelen C, Krams R, Oomen JAF, den Boer A, et al. ANGUS: a new approach to three-dimensional reconstruction of geometry and orientation of coronary lumen and plaque by combined use of coronary angiography and IVUS [Abstract]. J Am Coll Cardiol 1995;25(suppl):144A.
39. Koch L, Kearney P, Erbel R, Roth T, Ge J, Brennecke R, et al. Three dimensional reconstruction of intracoronary ultrasound images: road-mapping with simultaneous digitised coronary angiograms. In: Computers in cardiology 1993. Los Alamitos, Calif.: IEEE Computer Society Press, 1993:89-91.

Chapter 3

ECG-gated three-dimensional intravascular ultrasound: Feasibility and reproducibility of an automated analysis of coronary lumen and atherosclerotic plaque dimensions in humans

C von Birgelen, EA de Vrey, GS Mintz, A Nicosia, N Bruining, W Li, CJ Slager, JRTC Roelandt, PW Serruys, PJ de Feyter

Reprinted with permission from *Circulation* 1997;96:2944-2952

ECG-Gated Three-dimensional Intravascular Ultrasound

Feasibility and Reproducibility of the Automated Analysis of Coronary Lumen and Atherosclerotic Plaque Dimensions in Humans

Clemens von Birgelen, MD; Evelyn A. de Vrey, MD; Gary S. Mintz, MD; Antonino Nicosia, MD; Nico Bruining, BSc; Wenguang Li, MSc; Cornelis J. Slager, MSc; Jos R.T.C. Roelandt, MD, PhD; Patrick W. Serruys, MD, PhD; Pim J. de Feyter, MD, PhD

Background Automated systems for the quantitative analysis of three-dimensional (3D) sets of intravascular ultrasound (IVUS) images have been developed to reduce the time required to perform volumetric analyses; however, 3D image reconstruction by these nongated systems is frequently hampered by cyclic artifacts.

Methods and Results We used an ECG-gated 3D IVUS image acquisition workstation and a dedicated pullback device in atherosclerotic coronary segments of 30 patients to evaluate (1) the feasibility of this approach of image acquisition, (2) the reproducibility of an automated contour detection algorithm in measuring lumen, external elastic membrane, and plaque+media cross-sectional areas (CSAs) and volumes and the cross-sectional and volumetric plaque+media burden, and (3) the agreement between the automated area measurements and the results of manual tracing. The gated image acquisition took 3.9±1.5 minutes. The length of the segments analyzed was 9.6 to 40.0 mm, with 2.3±1.5 side branches per segment. The minimum lumen CSA measured 6.4±1.7 mm^2, and the maximum and average CSA plaque+media burden measured 60.5±10.2% and 46.5±9.9%, respectively. The automated contour-detection required 34.3±7.3 minutes per segment. The differences between these measurements and manual tracing did not exceed 1.6% (SD<6.8%). Intraobserver and interobserver differences in area measurements (n=3421; r=.97 to.99) were <1.6% (SD<7.2%); intraobserver and interobserver differences in volumetric measurements (n=30; r=.99) were <0.4% (SD<3.2%).

Conclusions ECG-gated acquisition of 3D IVUS image sets is feasible and permits the application of automated contour detection to provide reproducible measurements of the lumen and atherosclerotic plaque CSA and volume in a relatively short analysis time. (*Circulation.* 1997;96:2944-2952.)

Key Words • ultrasonics • coronary disease • imaging

Intravascular ultrasound allows transmural, tomographic imaging of coronary arteries in humans in vivo and provides insights into the pathology of coronary artery disease by defining vessel wall geometry and the major components of the atherosclerotic plaque.[1-7] Although invasive, IVUS is safe[8,9] and allows a more comprehensive assessment of the atherosclerotic plaque than the "luminal silhouette" furnished by coronary angiography.[10-14] Nevertheless, conventional IVUS analysis is a planar technique. Volumetric analysis of conventionally obtained IVUS images using Simpson's rule and planar analysis of multiple image slices is possible and may yield additional information, although it is time-consuming. To reduce the time for volumetric analysis[15] of IVUS images, automated 3D image reconstruction systems have been developed.[16-27] However, these systems have limitations, including (1) an inconsistent ability to detect the external arterial boundary and (2) imaging artifacts produced by cyclic changes in vascular dimensions and by movement of the IVUS catheter relative to the vessel.[20,22,24]

As a consequence, we have developed an analysis system that (1) uses 3D IVUS image sets acquired with an ECG-gated image acquisition workstation and pullback device to limit cyclic artifacts[28] and (2) detects both the luminal and external vascular boundaries of atherosclerotic coronary arteries to permit plaque volume measurement.[10,29-31] We report the feasibility of IVUS image acquisition and the reproducibility of analysis with this methodology.

Received January 8, 1997; revision received May 8, 1997; accepted May 28, 1997.

From the Thoraxcenter, Division of Cardiology, University Hospital Rotterdam-Dijkzigt and Erasmus University, Rotterdam (C. von B., E. de V., A.N., N.B., W.L., C.J.S., J.R.T.C.R., P.W.S., P.J. de F.), and the Interuniversity Cardiology Institute (W.L., P.W.S.), Netherlands; and the Washington (DC) Hospital Center (G.S.M.). Dr von Birgelen is now at the Department of Cardiology, University Hospital Essen, Germany.

Correspondence to Pim J. de Feyter, MD, PhD, Thoraxcenter, Bd 381, PO Box 1738, 3000 DR Rotterdam, Netherlands.

Methods

Patient Population

Between August 1, 1995, and February 29, 1996, we examined 28 patients with ECG-gated 3D IVUS, which represented a consecutive series of patients investigated with this approach. There were 23 men and 5 women who ranged in age from 38 to 72 years (mean, 55.3±8.9 years). All but 3 of them, studied at routine follow-up after previous catheter-based interventions, were symptomatic and/or had revealed signs of myocardial ischemia during noninvasive functional testing. Reasons for cardiac catheterization were either for diagnostic evaluation

Selected Abbreviations and Acronyms
CSA = CSA
3D = three-dimensional
EEM = external elastic membrane
IVUS = intravascular ultrasound

(n=20) or for follow-up study after a previous angioplasty procedure (n=8). Of the 20 patients examined during diagnostic catheterizations, 6 had one-vessel, 8 had two-vessel, and 1 had three-vessel disease. All patients with one- and two-vessel disease subsequently underwent successful catheter-based interventions (balloon angioplasty, n=3; directional atherectomy, n=2; stenting, n=9). Bypass surgery was performed in the patient with three-vessel disease. Of the 8 patients investigated at follow-up after previous interventions (after balloon angioplasty, n=5; directional atherectomy, n=3), 3 patients showed a significant restenosis and were successfully treated by repeat balloon angioplasty.

Thirty atherosclerotic coronary segments located in the left anterior descending coronary artery (n=15), right coronary artery (n=12), and left circumflex coronary artery (n=3) were analyzed; 13 segments were proximal, 15 mid, and 2 distal. As a condition for inclusion, segments had to be angiographically relatively straight (in at least two angiographic views from opposite projections). An exclusion criterion was calcification encompassing >180° of the arterial circumference over a ≥5-mm-long axial segment. This study was approved by the Local Council on Human Research. All patients signed a written informed consent form approved by the Medical Ethical Committee of the University Hospital Rotterdam-Dijkzigt.

IVUS Imaging

All patients received 250 mg aspirin and 10 000 U heparin IV. If the duration of the entire catheterization procedure exceeded 1 hour, the activated clotting time was measured, and intravenous heparin was administered to maintain an activated clotting time of >300 seconds. After intracoronary injection of 0.2 mg nitroglycerin, the atherosclerotic coronary segment to be reconstructed was examined with a mechanical IVUS system (ClearView, CardioVascular Imaging Systems Inc) and a sheath-based IVUS catheter incorporating a 30-MHz beveled, single-element transducer rotating at 1800 rpm (MicroView, CardioVascular Imaging Systems Inc). This catheter is equipped with a 2.9F 15-cm-long sonolucent distal sheath with a common lumen that alternatively houses the guidewire (during catheter introduction) or the transducer (during imaging after the guidewire has been pulled back), but not both. This design avoids direct contact of the IVUS imaging core with the vessel wall. The IVUS transducer was withdrawn through the stationary imaging sheath by an ECG-triggered pullback device with a stepping motor developed at the Thoraxcenter Rotterdam.[28]

ECG-Gated 3D IVUS Image Acquisition

The ECG-gated image acquisition and image digitization was performed by a workstation initially designed for the 3D reconstruction of echocardiographic images[28] (Echoscan, TomTec). This workstation received input from the IVUS machine (video) and the patient (ECG signal) and on the other hand, controlled the motorized transducer pullback device.

The steering logic of the workstation considered the heart rate variability and checked for the presence of extrasystoles during image acquisition and digitization (Fig 1). First, the RR intervals were measured over a 2-minute period to define the upper and lower limits of the range of acceptable RR intervals (mean value±50 ms). IVUS images were acquired 40 ms after the peak of the R wave. When the length of the RR interval met the preset range, the IVUS image was stored in the computer memory. Consecutively, the IVUS transducer was withdrawn 200 μm to acquire the next image. Although the longitudinal resolution available with this technical setup is 100 μm,[28] in the present study only one IVUS image per 200 μm axial arterial length was acquired. Thus, an average of 114 images per segment were digitized and analyzed (range, 48 to 200 images per segment; corresponding segment length, 9.6 to 40.0 mm).

IVUS Analysis Protocol

Each set of digitized IVUS images was analyzed off-line by two independent observers using an automated, computerized contour detection algorithm.[29-31] These measurements (Ia and II) were compared to study the interobserver variability. Blinded analyses were repeated by the first observer after an

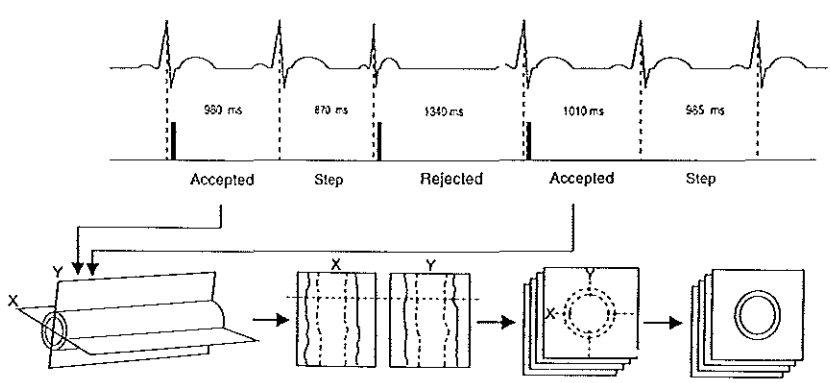

Fig 1. IVUS images were acquired 40 ms after peak of R wave and stored (accepted) in computer memory only if RR intervals met predefined range (top). Consecutively, transducer was withdrawn 200 μm to adjacent acquisition site (step) to acquire next image. If an RR interval did not meet range, image was not stored (rejected), and transducer was kept at that site until an image was acquired. Image acquisition and motorized pullback were controlled by steering logic of image acquisition workstation. Automated detection of intimal and medial boundaries was first performed on two perpendicular longitudinal sections (X, Y) reconstructed from image data of entire 3D stack of images (bottom); edge information of these longitudinal contours was represented as points on planar images, defining there the center and range of final automated contour detection process.

interval of at least 6 weeks. These measurements (Ia and Ib) were compared to study the intraobserver variability.

Two hundred planar images were randomly selected for "manual" analysis by a third investigator (MA-III) who was experienced in IVUS image analysis but blinded to the (above) automated contour detection results. This analyst could review the videotape to ensure a maximum accuracy of contour tracing, performed within an average of 4.1 minutes per image. Validation of manual CSA measurements by IVUS has been reported previously.[32-34] These measurements were compared with the automated contour detection analysis made by observer I.

Data Analysis

The CSA measurements included the lumen and EEM CSA. Plaque+media CSA was calculated as EEM minus lumen CSA, and the CSA plaque+media burden was calculated as plaque+media CSA divided by EEM CSA. The EEM CSA (which represents the area within the border between the hypoechoic media and the echoreflective adventitia) has been shown to be a reproducible measure of the total arterial CSA. As in many previous studies using IVUS, plaque+media CSA was used as a measure of atherosclerotic plaque, because ultrasound cannot measure media thickness accurately.[35] Lumen, EEM, and plaque+media volumes were calculated as

$$\text{Volume} = \sum_{i=1}^{n} \text{CSA}_i \times H$$

where H is the thickness of a coronary artery slice, represented by a single tomographic IVUS image, and n is the number of IVUS images in the 3D data set. The volumetric plaque+media burden was calculated as plaque+media volume divided by EEM volume.

Plaque composition was assessed visually to identify lesion calcium. Calcium produced bright echoes (brighter than the reference adventitia), with acoustic shadowing of deeper arterial structures. The largest arc(s) of target lesion calcium was identified and measured in degrees with a protractor centered on the lumen. The overall length (in mm) of lesion calcium was measured by use of the length measurements provided by the 3D reconstruction.

Computerized Contour Detection in ECG-Gated 3D IVUS

Steps Involved in Image Analysis

Two longitudinal sections were constructed, and contours corresponding to the lumen-tissue and media-adventitia interfaces were automatically identified (Fig 1). The necessity to manually edit these contours was significantly reduced, because cyclic "saw-shaped" image artifacts that can hamper the automated detection in nongated image sets were virtually abolished (Fig 2). The sufficiency of the contour detection was visually checked, requiring an average of 5 minutes. If necessary, these longitudinal contours were edited with computer assistance (see below) within <1 minute. The longitudinal contours were transformed to individual edge points on the planar images, defining center and range of the automated boundary search on the planar images.

Subsequently, contour detection of the planar images was performed. The axial location of an individual planar image was indicated by a cursor, which was used to scroll through the entire set of planar images while the detected contours were visually checked. Correct detection of the longitudinal contours minimized the need for computer-assisted editing of the cross-sectional contours. Careful checking and editing of the contours of the planar images was performed within an average of 25 minutes. Finally, the contour data of the planar images were used for the computation of the results.

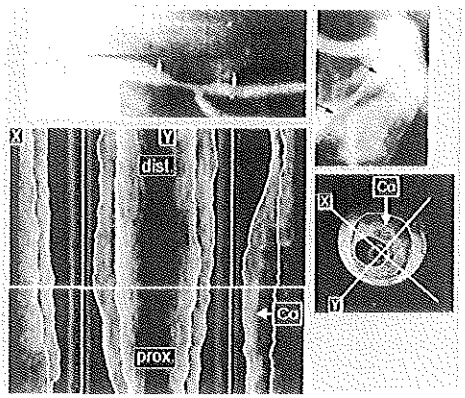

FIG 2. Example of automated 3D contour detection analysis in diseased left anterior descending coronary artery. Range of 14.6-mm-long IVUS reconstruction and analysis is indicated by arrowheads in angiograms (top) taken from opposite angiographic projections. Cut planes of two reconstructed longitudinal sections (X, Y; lower left) are indicated on planar IVUS image (lower right), depicting calcification (Ca) of atherosclerotic plaque. Horizontal cursor on longitudinal sections can be used to scroll from distal (dist.) to proximal (prox.) through planar images. Thickness of that cursor is artificially increased to improve visibility (true thickness=half a scan line). 3D approach permitted interpretation in longitudinal dimension and facilitated tracing of estimated external vascular contour in acoustic shadowing behind calcium. Angiograms (top) and radiographic image of ultrasound catheter during image acquisition (insert, top left) illustrate that analyzed arterial segment was relatively straight and showed no more than mild vessel curvatures. As linear 3D analysis systems do not account for vascular curvatures, this premise was important because it limits curve distortion–induced deviation of volumetric measurements.

Minimum-Cost Algorithm and Computer-Assisted Contour Editing

A minimum-cost algorithm was used to detect the luminal and external vessel boundaries.[29] Each digitized IVUS image was resampled in a radial format (64 radii per image); a cost matrix representing the edge strength was calculated from the image data. For the boundary between lumen and plaque, the cost value was defined by the spatial first derivative.[36] For the external vessel boundary, a cross-correlation pattern matching process was used for the cost calculations. The path with the smallest accumulated value was determined by dynamic programming techniques.[29] The computer-assisted editing differed considerably from conventional manual contour tracing. The computer mouse was pointed on the correct boundary to give that site a very low value in the cost matrix, and subsequently the automated detection of the minimum cost path was updated within <1 second. Editing the contour of a single slice caused the entire data set to be updated (dynamic programming).

Handling of Side Branches and Calcification

Side branches with a relatively small ostium were generally ignored by the algorithm as a result of its robustness, which means that the automated contour detection did not follow every abrupt change in the cost path. However, in branches with a large ostium, the contour did follow the lumen and vessel boundaries of the side branch. This was corrected by displaying the side branch in one of the longitudinal sections and interpolating the longitudinal vessel contours as straight

TABLE 1. Feasibility and Processing Time

Seg	ECG Gating	Image Quality	Images/ Seg, n	Acquisition Time/Seg, min	Acquisition Time/Image, s	Analysis Time/Seg, min	Analysis Time/Image, min
1	+++	++	123	4.2	2.0	34.6	0.3
2	+++	++	66	2.1	1.9	22.4	0.3
3	+++	+++	146	4.7	1.9	36.9	0.3
4	+++	+++	200	6.9	2.1	42.3	0.2
5	+++	+	71	2.7	2.3	38.2	0.5
6	+++	++	194	6.8	2.1	47.8	0.3
7	+++	+++	84	2.9	2.0	28.6	0.3
8	+++	++	74	2.7	2.2	29.7	0.4
9	+++	+++	150	4.7	1.9	37.3	0.3
10	+++	++	94	3.1	2.0	31.7	0.3
11	+++	++	48	1.5	1.9	21.3	0.4
12	++	+	129	4.9	2.3	48.4	0.4
13	+++	++	127	4.3	2.0	35.0	0.3
14	+++	+	147	5.7	2.3	46.4	0.3
15	+++	++	194	6.6	2.0	39.4	0.2
16	+++	++	106	3.5	2.0	36.9	0.4
17	+++	++	129	4.6	2.2	44.8	0.4
18	+++	++	150	5.4	2.2	37.3	0.3
19	+++	+++	148	4.5	1.8	37.1	0.3
20	+++	+++	152	5.2	2.0	37.5	0.3
21	+++	++	88	2.9	2.0	31.1	0.4
22	+++	++	110	3.1	1.7	33.3	0.3
23	+++	++	94	3.4	2.2	31.7	0.3
24	+++	++	100	3.5	2.1	33.1	0.3
25	+++	++	75	2.6	2.0	29.8	0.4
26	+++	+++	126	4.2	2.0	34.9	0.3
27	+++	+++	79	2.7	2.0	27.1	0.3
28	+++	+++	69	2.4	2.1	23.8	0.3
29	+++	+++	75	2.4	1.9	25.8	0.3
30	+++	+++	73	2.5	2.0	24.4	0.3
Mean	...	...	114.0	3.9	2.0	34.3	0.3
SD	...	...	41.1	1.5	0.1	7.3	0.1
n	...	...	30	30	30	30	30

Seg indicates segment. ECG gating: +++, easy performance without image artifacts; ++, easy performance with a few cyclic image artifacts. Image quality: +++, excellent; ++, good; +, mediocre.

lines. As a result, the side branch was outside the region of interest on the planar images. Similarly, small calcific portions of the plaque did not affect the detection of the external vessel boundary because of the robustness of the algorithm. In case of marked vessel wall calcification, the automated approach fails to detect the external vessel boundary. However, the 3D approach of the analysis system allowed interpretation of the external vessel boundary in the longitudinal dimension and facilitated tracing of a straight contour line behind the calcium.

Previous Validation In Vitro and In Vivo

In vitro, the algorithm has been validated in a tubular phantom consisting of several segments. The automated measurements revealed a high correlation with the true phantom areas and volumes (r=.99); mean differences were −0.7% to 3.9% (SD<2.6%) for the areas and 0.3% to 1.7% (SD<3.8%) for the volumes of the various segments.[30] A comparison between automated 3D IVUS measurements in 13 atherosclerotic coronary specimen (area plaque+media burden <40%) in vitro and morphometric measurements on the corresponding histological sections revealed good correlations for measurements of lumen, EEM, plaque+media, and plaque+media burden (r=.94,.88,.80, and.88 for areas and.98,.91,.83, and.91 for volumes).[31] In vitro, both area and volume measurements by the automated system agreed well with results obtained by manual tracing of IVUS images, showing low (−3.7% to 0.3%) mean between-method differences with SD <6% and high correlation coefficients (r≥.97 for areas and r=.99 for volumes).[31] In vivo, using 3D IVUS image sets acquired during nongated continuous pullbacks through 20 diseased coronary segments, intraobserver and interobserver comparisons revealed high correlations (r=.95 to.98 for area and r=.99 for volume)[30] and small mean differences (−0.9% to 1.1%), with SD of lumen, EEM, and plaque+media not exceeding 7.3%, 4.5%, and 10.9% for areas and 2.7%, 0.7%, and 2.8% for volumes. The time of (automated) analysis in that study was 69±19 minutes. Importantly, that study did not include segments with more than focal calcification, more than one side branch, or extensive systolic-diastolic movement artifacts in the longitudinally constructed images.

Statistical Analysis

Quantitative data were given as mean±SD; qualitative data were presented as frequencies. According to Bland and Altman,[37] the intraobserver and interobserver agreement (reproducibility) of the contour detection method was assessed by determining the mean and SD of the between-observation and between-observer differences, respectively. The results of the repeated contour analyses (Ia versus Ib), the independent contour detection analyses (Ia versus II), and the manual versus the contour analyses (III-MA versus Ia) were compared by the two-tailed Student's t test for paired data analysis and linear regression analysis; values of P<.05 were considered statistically significant.

Results

Feasibility and Acquisition and Processing Time

The gated IVUS image acquisition required 3.9±1.5 minutes (1.5 to 6.9 minutes) per coronary segment,

TABLE 2. Characteristics of Coronary Segments

Seg	Vessel	MLCSA, mm²	CSA P+M Burden, %		Side Branches, n	Calcium		
			Max	Mean		Presence	Max Arc, °	Length, mm
1	Prox LAD	6.6	54.2	47.0	2	Multiple	60	<1
2	Mid LAD	6.4	44.8	36.6	3	...	...	...
3	Prox LCx	7.4	71.4	65.9	1	Single	180	1.6
4	Distal RCA	5.7	72.1	61.1	5	...	...	...
5	Prox LCx	8.1	31.7	22.8	0	...	...	...
6	Prox LCx	6.2	62.1	51.3	1	...	...	...
7	Mid LAD	6.8	43.5	28.8	4	...	...	...
8	Mid LAD	8.5	51.9	40.1	1	Single	95	<1
9	Mid RCA	4.1	69.5	44.6	3	...	...	...
10	Prox LAD	5.5	66.0	50.6	4	Single	180	1.6
11	Prox LAD	9.6	60.2	48.1	1	Single	100	4.4
12	Prox RCA	4.3	66.4	49.3	1	Multiple	180	1.4
13	Mid RCA	4.7	77.7	58.6	2	Multiple	190	<1
14	Mid RCA	4.2	65.4	50.8	1	Multiple	180	<1
15	Mid RCA	6.4	68.4	58.9	1	Multiple	125	<1
16	Prox LAD	4.3	60.4	36.0	2	...	...	...
17	Prox LAD	5.3	64.8	51.1	1	...	...	...
18	Mid RCA	5.7	65.3	54.2	3	Multiple	50	<1
19	Mid RCA	6.4	66.7	47.9	6	...	...	...
20	Mid RCA	7.2	68.1	53.0	3	...	...	...
21	Prox RCA	9.7	56.9	33.2	0	Single	60	<1
22	Prox LAD	3.5	67.3	49.6	1	...	...	...
23	Prox LAD	6.8	59.1	51.0	2	Single	70	4.6
24	Distal LAD	7.1	50.0	36.6	5	Multiple	100	<1
25	Mid LAD	7.0	57.0	39.6	2	Single	95	<1
26	Mid RCA	5.4	51.9	38.1	4	Single	90	<1
27	Mid RCA	5.9	49.3	39.2	3	...	...	...
28	Prox LAD	9.7	59.4	45.6	2	Single	85	<1
29	Mid LAD	8.0	57.9	46.1	4	...	...	...
30	Mid LAD	5.8	75.6	58.9	2	Single	95	4.8
Mean	...	6.4	60.5	46.5	2.3	...	113.8	...
SD	...	1.7	10.2	9.9	1.5	...	48.8	...
n	...	30	30	30	30	...	17	...

Seg indicates segment; MLCSA, minimal luminal CSA; P+M, plaque+media; Prox, proximal; LAD, left anterior descending coronary artery; LCx, left circumflex coronary artery; and RCA, right coronary artery.

which corresponds to 2.0±0.1 seconds (1.7 to 2.3 seconds) per image (Table 1). All segments could be analyzed by the computerized contour detection system during an analysis time of 34.3±7.3 minutes per segment (21.3 to 48.4 minutes), corresponding to 0.3±0.1 minutes (0.2 to 0.5 minutes) per computerized IVUS image analysis.

IVUS Segment Characteristics

All but two of the segments (93%) contained at least one side branch (Table 2). The average number of side branches per segment was 2.3±1.5 (range, 0 to 6). Calcification was present in 17 segments (57%), 11 (37%) showed a single calcium deposit, and 6 (20%) contained multiple calcium deposits. The maximum arc of calcium was 114±49° (50° to 190°); in 6 segments, the length of the calcified portion exceeded 1 mm.

The minimal lumen CSA as measured by the contour detection system was 6.4±1.7 mm² (3.5 to 9.7 mm²). The maximum and average CSA plaque+media burden were 60.5±10.2% (31.7% to 77.7%) and 46.5±9.9% (22.8% to 65.9%).

Manual Tracing Versus Automated Contour Detection

In the 200 randomly selected image slices, the measurements of the lumen, EEM, and plaque+media CSAs and the CSA plaque+media burden obtained with the automated contour detection system (9.37±3.09 mm², 18.33±6.70 mm², 8.95±5.16 mm², and 46.03±13.46%, respectively) were similar to the results obtained by manual tracing (9.35±3.18 mm², 18.37±6.62 mm², 9.02±5.08 mm², and 46.53±13.41%; n=200). Between-method differences were 0.4±4.3%, −0.4±3.6%, −1.6±9.1%, and −1.2±6.8%, respectively (all P=NS). The correlations between the measurements provided by both methods were high ($r \geq .98$; Fig 3).

Reproducibility of the Contour Detection Analysis

For measurements of lumen, EEM, and plaque+media CSA and the CSA plaque+media burden (n=3421), both intraobserver (−0.4±2.7%, −0.4±1.8%, −0.4±5.1%, and −0.0±4.2%) and interobserver (0.4±5.2%, −0.9±2.7%, −1.5±7.2%, and −1.5±6.9%; all $P<.001$) differences were low. Correlation coefficients were high for repeated measurements by the same observer ($r=.99$) and measurements by the two observers ($r \geq .97$; Fig 4). For the corresponding volumetric measurements (n=30), the intraobserver (−0.4±1.1%, −0.4±0.6%, −0.3±1.0%, and 0.0±0.4%) and interobserver (0.6±2.9%, −0.8±1.0%, −2.5±3.2%, and 0.8±1.5%; $P<.05$) differences were also low, and high correlations were found for both intraobserver and interobserver comparisons ($r=.99$; Fig 5).

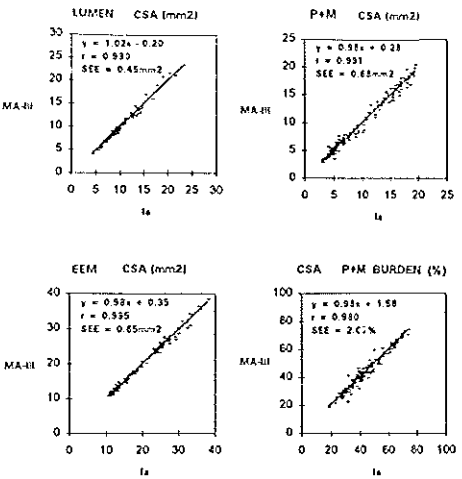

FIG 3. Correlation between results of measurements of lumen, EEM, and plaque+media (P+M) CSA and CSA P+M burden by automated contour detection (Ia) and conventional manual tracing (MA-III).

Discussion

The present study demonstrates that (1) ECG-gated acquisition of 3D IVUS images is feasible, (2) there is a good agreement between the results provided by the automated contour detection method and manual border tracing, and (3) the automated contour detection analysis can be performed in a relatively short analysis time with a high degree of reproducibility.

3D reconstruction of IVUS images was first used to visually assess the spatial configuration of plaques, dissections, and stents and to perform basic measurements.[16,17,19] More recently, the 3D reconstruction systems have included algorithms for automated quantification of lumen dimensions.[16-21,25-27] The contour detection system used in the present study can be used for the detection of both the tissue-lumen boundary and the media-adventitia (EEM) boundary, and therefore plaque volume can be measured.

Feasibility

Non–ECG-gated image acquisition is frequently marred by cardiac cycle–linked coronary artery vasomotion and IVUS catheter motion, which produce sawtooth artifacts in the reconstructed 3D images that can interfere with automated contour detection (both the ease of use and, presumably, reproducibility). Conversely, in the present ECG-gated image sets, the longitudinal contours were smooth and without such artifacts. Therefore, there was much less need to manually edit the automatically detected longitudinal contours. Moreover, the accuracy of the derived edge information improved the performance of the second automated contour detection step on the planar IVUS images. This reduction in manual editing time on both longitudinal and planar images accounts for the low time of analysis compared with a previous study using nongated image acquisition[30]

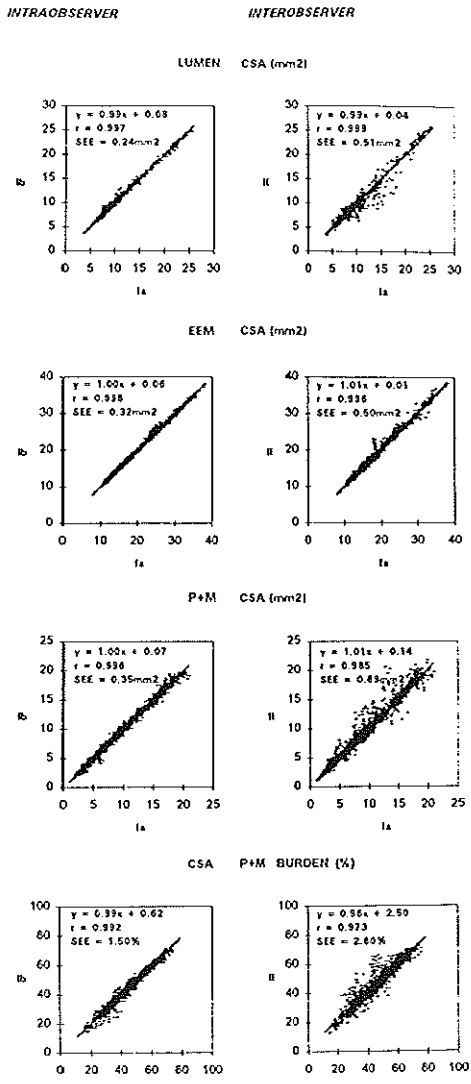

FIG 4. Intraobserver variability (left; first [Ia] vs second [Ib] observation) and interobserver variability (right; first [Ia] vs second [II] observer) of measurements of lumen, EEM, and plaque+media (P+M) CSA and CSA P+M burden by automated contour detection analysis system.

(34 minutes and 69 minutes, respectively). Indeed, this represents a significant reduction in analysis time and as a consequence reduces the cost of the analysis. However, the ECG-gated 3D IVUS acquisition in the present study required a longer acquisition time than conventional motorized pullback (eg, non–ECG-triggered pull-

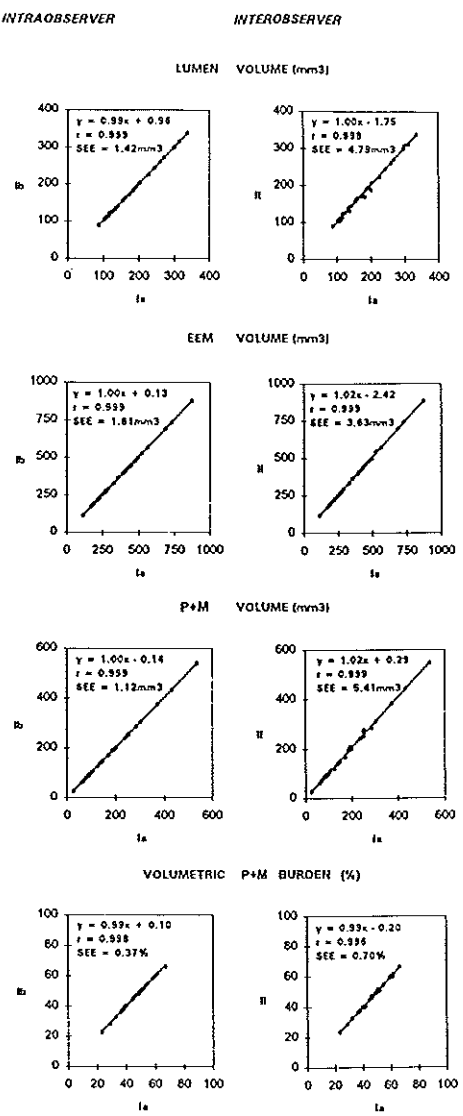

FIG 5. Intraobserver variability (left; first [Ia] vs second [Ib] observation) and interobserver variability (right; first [Ia] vs second [II] observer) of measurements of lumen, EEM, and plaque+media (P+M) volume and volumetric P+M burden by automated contour detection analysis system.

back at 0.5 mm/s). On average, only a 6-mm-long coronary segment could be imaged in 1 minute.

Reproducibility of the Contour Detection

In the present study, the measurement of the lumen, EEM, and plaque+media CSA differed little from the results obtained by manual contour tracing of these borders; there were only small interobserver and intraobserver differences in both the planar and volumetric analyses. However, the reproducibility of the plaque+media measurements was lower than for the other measures, which may reflect the combined variability of both the luminal and the EEM contours, confirming previous in vitro[31] and in vivo data (nongated patient data)[30] and findings of others.[38] The reproducibility of the volumetric measurements was higher than for the CSA measurements, which may be a result of an averaging of the differences between the individual CSA measurements.

Although the segments in this ECG-gated contour detection study were nonselected and included calcified segments with some side branches, the reproducibility of the CSA measurements was consistently better than observed in a previous study using nongated contour detection.[30] We believe that the key factors explaining the overall high reproducibility of automated contour detection observed in this study are (1) the integrated analyses of the conventional cross-sectional image slices with two longitudinal sections and (2) the facilitated and improved detection as a result of the smoothness of the contours on the ECG-gated longitudinal IVUS sections.

Reproducibility of Alternative Methods of Quantitative 3D IVUS

There is very little information on the reproducibility of 3D IVUS measurements using other measurement systems and algorithms. Matar and colleagues[21] reported a Pearson's correlation coefficient of .98 for an intraobserver study of lumen volume measurement by an automated threshold-based IVUS analysis system, confirming the low variability of the volumetric measurements observed in the present study. Another acoustic quantification system[25] performs measurements of lumen CSA and volume, based on the automated detection of the blood pool in single IVUS images acquired at random during the cardiac cycle.[21,25] Because the measurements are based on single-frame analysis, ECG-gated image acquisition may not influence the reproducibility of such systems.

Conversely, 3D contour detection–based analysis approaches benefit from an ECG-gated image acquisition.[20] Sonka and associates[39,40] developed an alternative 3D contour detection system that performs computerized detection of the luminal and external vascular boundaries in 3D sets of planar IVUS images without the additional information provided by the longitudinal contours. In their study,[39] the correlation between automated and manually traced CSA measurements was quite good (r=.91 and.83 for lumen and plaque CSA, respectively). Using ECG-gated 3D IVUS, they found significantly improved results (r=.98 and.94 for lumen and plaque+media CSA, respectively),[40] underlining the significance of ECG-gated IVUS image acquisition. Most likely, other promising contour detection algorithms[41,42] for 3D analyses may also benefit from an ECG-gated image acquisition.

Potential Sources of Error and Study Limitations

Problems related to IVUS in general[43] and to 3D reconstruction in particular[22,23] may influence the contour detection process. The quality of the basic IVUS

images is crucial to both planar and 3D image analysis.[22] Incomplete visualization of the vessel wall, for example as caused by acoustic shadowing[6] from lesion-associated calcium, hampers conventional planar IVUS analyses; however, 3D IVUS allows interpretation in the axial dimension and estimated contour tracing of the external vascular boundary. Image distortion caused by nonuniform transducer rotation or noncoaxial IVUS catheter position in the lumen may create artifacts both in planar images and in 3D reconstruction.[22]

Vessel curvatures may cause differences between the movement of the distal transducer tip and the proximal part of the catheter (although the use of sheath-based IVUS catheters reduces the latter problem) and a significant distortion of the 3D image reconstruction.

Most importantly, linear 3D systems such as used in this study can provide only approximate values of the volumetric parameters[44] because they do not account for vascular curvatures and the real spatial geometry. In curved vascular segments, this results in an overestimation of plaque volume at the inner side (expansion) and an underestimation of plaque volume at the outer side (compression) of the curve.[22] Approaches combining data obtained from angiography and IVUS[45-48] can provide information on the real spatial geometry of the vessel. Unquestionably, the combined approaches have a unique potential, but currently these sophisticated techniques are still laborious, restricted to research applications, and not yet useful for routine off-line analysis of clinical IVUS examinations. In the present study, only relatively straight coronary segments, showing no more than mild vessel curvatures, were included. We felt that this premise was important to limit curve distortion–induced deviation of volumetric measurement,[44] because linear 3D analysis systems do not account for vascular curvatures.

Compared with conventional motorized transducer pullback at a uniform speed, ECG-gated image acquisition takes longer, which may limit its use before intervention, especially in patients with very severe coronary stenoses. Therefore, we currently perform ECG-gated IVUS examinations during diagnostic or follow-up catheterizations and at the presumed end point of coronary interventions.

Clinical Implications

The examination of coronary arteries by IVUS permits the comprehensive assessment of atherosclerosis[1-3,6,7,10,11] and the evaluation of the instantaneous[27,49] and long-term effects of catheter-based interventions on the coronary lumen and plaque. To quantify these changes, anatomic landmarks such as side branches or spots of calcium can be used to define specific anatomic image slices for comparative analysis in serial studies.

The proposed 3D IVUS method, which permits reproducible and reliable contour detection of both lumen and plaque, may facilitate volumetric measurements[10,30,31] and obviate the need for laborious analyses based on Simpson's rule.[15] Furthermore, the use of ECG-gated image acquisition[28] increases the applicability of the contour detection algorithm by shortening the analysis time[49] and increasing the reproducibility of the method. These advantages may be most significant in studies that are expected to show only small changes in plaque and/or lumen over time (eg, in trials evaluating the progression or regression of atherosclerosis during pharmacological therapy[10]). In addition, because the time from the peak of the R wave to image acquisition can be varied, this method can be used to study the cyclic (systole versus diastole) changes in vessel dimensions.

Conclusions

ECG-gated acquisition of 3D IVUS image sets is feasible and permits the application of automated contour detection to provide reproducible measurements of the lumen and atherosclerotic plaque CSA and volume in a relatively short analysis time.

Acknowledgment

Dr von Birgelen is the recipient of a fellowship of the German Research Society (DFG, Bonn, Germany).

References

1. Yock PG, Linker DT. Intravascular ultrasound: looking below the surface of vascular disease. *Circulation*. 1990;81:1715-1718.
2. Nissen SE, Gurley JC, Grines CL, Booth DC, McClure R, Berk M, Fischer C, DeMaria AN. Intravascular ultrasound assessment of lumen size and wall morphology in normal subjects and patients with coronary artery disease. *Circulation*. 1991;84:1087-1099.
3. Fitzgerald PJ, St Goar FG, Connolly AJ, Pinto FJ, Billingham ME, Popp RL, Yock PG. Intravascular ultrasound imaging of coronary arteries: is three layers the norm? *Circulation*. 1992;86:154-158.
4. Ge J, Erbel R, Rupprecht HJ, Koch L, Kearney P, Görge G, Haude M, Meyer J. Comparison of intravascular ultrasound and angiography in the assessment of myocardial bridging. *Circulation*. 1994;89:1725-1732.
5. Lee DY, Eigler N, Nishioka T, Tabak SW, Forrester JS, Siegel RJ. Effect of intracoronary ultrasound imaging on clinical decision making. *Am Heart J*. 1995;129:1084-1093.
6. Mintz GS, Painter JA, Pichard AD, Kent KM, Satler LF, Popma JJ, Chuang YC, Bucher TA, Sokolowicz LE, Leon MB. Atherosclerosis in angiographically 'normal' coronary artery reference segments: an intravascular ultrasound study with clinical correlations. *J Am Coll Cardiol*. 1995;25:1479-1485.
7. Erbel R, Ge J, Bockisch A, Kearney P, Görge G, Haude M, Schürmann D, Zamorano J, Rupprecht HJ, Meyer J. Value of intracoronary ultrasound and Doppler in the differentiation of angiographically normal coronary arteries: a prospective study in patients with angina pectoris. *Eur Heart J*. 1996;17:880-889.
8. Pinto FJ, St Goar FG, Gao SZ, Chenzbraun A, Fischell TA, Alderman EL, Schroeder JS, Popp RL. Immediate and one-year safety of intracoronary ultrasonic imaging: evaluation with serial quantitative angiography. *Circulation*. 1993;88:1709-1714.
9. Hausmann D, Erbel R, Alibelli-Chemarin MJ, Alibelli-Chemarin MJ, Boksch W, Caracciolo E, Cohn JM, Culp SC, Daniel WG, De Scherder I, Di Mario C, Ferguson JJ III, Fitzgerald PJ, Friedrich G, Ge J, Görge G, Hanrath P, Hodgson J McB, Isner JM, Jain S, Maier-Rudolph W, Mooney M, Moses JW, Mudra H, Pinto FJ, Smalling RW, Talley JD, Tobis JM, Walter PD, Weidinger F, Werner GS, Yeung AC, Yock PG. The safety of intracoronary ultrasound: a multicenter survey of 2207 examinations. *Circulation*. 1995;91:623-630.
10. von Birgelen C, Slager CJ, Di Mario C, de Feyter PJ, Serruys PW. Volumetric intracoronary ultrasound: a new maximum confidence approach for the quantitative assessment of progression-regression of atherosclerosis? *Atherosclerosis*. 1995;118(suppl):S103-S113.
11. Mintz GS, Popma JJ, Pichard AD, Kent KM, Satler LF, Chuang YC, DeFalco RA, Leon MB. Limitations of angiography in the assessment of plaque distribution in coronary artery disease: a systematic study of target lesion eccentricity in 1446 lesions. *Circulation*. 1996;93:924-931.
12. de Feyter PJ, Serruys PW, Davies MJ, Richardson P, Lubsen J, Oliver MF. Quantitative coronary angiography to measure progression and regression of coronary atherosclerosis: value, limitations, and implications for clinical trials. *Circulation*. 1991;84:412-423.
13. Serruys PW, de Jaegere P, Kiemeneij F, Macaya C, Rutsch W, Heyndrickx G, Emanuelsson H, Marco J, Legrand V, Materne P, Belardi J, Sigwart U, Colombo A, Goy JJ, van der Heuvel P, Delcan J, Morel AA, for the Benestent Study Group. A comparison of balloon expandable stent implantation with balloon angioplasty in patients with coronary artery disease. *N Engl J Med*. 1994;331:489-495.

14. von Birgelen C, Umans V, Di Mario C, Keane D, Gil R, Prati F, de Feyter PJ, Serruys PW. Mechanism of high-speed rotational atherectomy and adjunctive balloon angioplasty revisited by quantitative coronary angiography: edge detection versus videodensitometry. *Am Heart J.* 1995;130:405-412.
15. Dussaillant GR, Mintz GS, Pichard AD, Kent KM, Satler LF, Popma JJ, Wong SC, Leon MB. Small stent size and intimal hyperplasia contribute to restenosis: a volumetric intravascular ultrasound analysis. *J Am Coll Cardiol.* 1995;26:720-724.
16. Rosenfield K, Losordo DW, Ramaswamy K, Pastore JO, Langevin RE, Razvi S, Kosowsky BD, Isner JM. Three-dimensional reconstruction of human coronary and peripheral arteries from images recorded during two-dimensional intravascular ultrasound examination. *Circulation.* 1991;84:1938-1956.
17. Coy KM, Park JC, Fishbein MC, Laas T, Diamond GA, Adler L, Maurer G, Siegel RJ. In vitro validation of three-dimensional intravascular ultrasound for the evaluation of arterial injury after balloon angioplasty. *J Am Coll Cardiol.* 1992;20:692-700.
18. Rosenfield K, Kaufman J, Pieczek A, Langevin RE, Razvi S, Ilsner JM. Real-time three-dimensional reconstruction of intravascular ultrasound images of iliac arteries. *Am J Cardiol.* 1992;70:412-415.
19. Mintz GS, Pichard AD, Satler LF, Popma JJ, Kent KM, Leon MB. Three-dimensional intravascular ultrasonography: reconstruction of endovascular stents in vitro and in vivo. *Clin Ultrasound.* 1993; 21:609-615.
20. Dhawale PJ, Wilson DL, Hodgson J McB. Optimal data acquisition for volumetric intracoronary ultrasound. *Cathet Cardiovasc Diagn.* 1994;32:288-299.
21. Matar FA, Mintz GS, Douek P, Farb A, Virmani R, Saturnino PJ, Popma JJ, Pichard AD, Kent KM, Satler LF, Keller M, Leon MB. Coronary artery lumen volume measurement using three-dimensional intravascular ultrasound: validation of a new technique. *Cathet Cardiovasc Diagn.* 1994;33:214-220.
22. Roelandt JRTC, Di Mario C, Pandian NG, Li W, Keane D, Slager CJ, de Feyter PJ, Serruys PW. Three-dimensional reconstruction of intracoronary ultrasound images: rationale, approaches, problems, and directions. *Circulation.* 1994;90:1044-1055.
23. Di Mario C, von Birgelen C, Prati F, Soni B, Li W, Bruining N, de Jaegere PJ, de Feyter PJ, Serruys PW, Roelandt JRTC. Three-dimensional reconstruction of two-dimensional intracoronary ultrasound: clinical or research tool? *Br Heart J.* 1995;73(suppl 2):26-32.
24. von Birgelen C, Di Mario C, Serruys PW. Structural and functional characterization of an intermediate stenosis with intracoronary ultrasound: a case of 'reverse glagovian modeling.' *Am Heart J.* 1996;132:694-696.
25. von Birgelen C, Kutryk MJB, Gil R, Ozaki Y, Di Mario C, Roelandt JRTC, de Feyter PJ, Serruys PW. Quantification of the minimal luminal cross-sectional area after coronary stenting by two- and three-dimensional intravascular ultrasound versus edge detection and videodensitometry. *Am J Cardiol.* 1996;78:520-525.
26. Gil R, von Birgelen C, Prati F, Di Mario C, Ligthart J, Serruys PW. Usefulness of three-dimensional reconstruction for interpretation and quantitative analysis of intracoronary ultrasound during stent deployment. *Am J Cardiol.* 1996;77:761-764.
27. von Birgelen C, Gil R, Ruygrok P, Prati F, Di Mario C, van der Giessen WJ, de Feyter PJ, Serruys PW. Optimized expansion of the Wallstent compared with the Palmaz-Schatz stent: online observations with two- and three-dimensional intracoronary ultrasound after angiographic guidance. *Am Heart J.* 1996;131:1067-1075.
28. Bruining N, von Birgelen C, Di Mario C, Prati F, Li W, Den Hood W, Patijn M, de Feyter PJ, Serruys PW, Roelandt JRTC. Dynamic three-dimensional reconstruction of ICUS images based on an ECG-gated pull-back device. In: *Computers in Cardiology 1995.* Los Alamitos, Calif: IEEE Computer Society Press; 1995:633-636.
29. Li W, von Birgelen C, Di Mario C, Boersma E, Gussenhoven EJ, van der Putten N, Bom N. Semi-automatic contour detection for volumetric quantification of intracoronary ultrasound. In: *Computers in Cardiology 1994.* Los Alamitos, Calif: IEEE Computer Society Press; 1994:277-280.
30. von Birgelen C, Di Mario C, Li W, Schuurbiers JCH, Slager CJ, de Feyter PJ, Roelandt JRTC, Serruys PW. Morphometric analysis in three-dimensional intracoronary ultrasound: an in-vitro and in-vivo study using a novel system for the contour detection of lumen and plaque. *Am Heart J.* 1996;132:516-527.
31. von Birgelen C, van der Lugt A, Nicosia A, Mintz GS, Gussenhoven EJ, de Vrey E, Mallus MT, Roelandt JRTC, Serruys PW, de Feyter PJ. Computerized assessment of coronary lumen and atherosclerotic plaque dimensions in three-dimensional intravascular ultrasound correlated with histomorphometry. *Am J Cardiol.* 1996; 78:1202-1209.
32. Hodgson J McB, Graham SP, Sarakus AD, Dame SG, Stephens DN, Dhillon PS, Brands D, Sheehan H, Eberle MJ. Clinical percutaneous imaging of coronary anatomy using an over-the-wire ultrasound catheter system. *Int J Card Imaging.* 1989;4:186-193.
33. Tobis JM, Mallery JA, Gerrett J, Griffith J, Mahon D, Bessen M, Moriuchi M, McLeay L, McRae M, Henry WL. Intravascular ultrasound cross-sectional arterial imaging before and after balloon angioplasty in vitro. *Circulation.* 1989;80:873-882.
34. Nishimura RA, Edwards WD, Warnes CA, Reeder GS, Holmes DR Jr, Tajik AJ, Yock PG. Intravascular ultrasound imaging: in vitro validation and pathologic correlation. *J Am Coll Cardiol.* 1990; 16:145-154.
35. Mallery JA, Tobis JM, Griffith J, Gessert J, McRae M, Moussabeck O, Bessen M, Moriuchi M, Henry WL. Assessment of normal and atherosclerotic arterial wall thickness with an intravascular ultrasound imaging catheter. *Am Heart J.* 1990;119:1392-1400.
36. Li W, Bosch JG, Zhong Y, van Urk H, Gussenhoven EJ, Mastik F, van Egmond F, Rijsterborgh H, Reiber JHC, Bom N. Image segmentation and 3D reconstruction of intravascular ultrasound images. In: Wei Y, Gu B, eds. *Acoustical Imaging, Vol 20.* New York, NY: Plenum Press; 1993:489-496.
37. Bland JM, Altman DG. Statistical methods for assessing agreement between two methods of clinical measurement. *Lancet.* 1986;2: 307-310.
38. Hausmann D, Lundkvist AJS, Friedrich GJ, Mullen WL, Fitzgerald PJ, Yock PG. Intracoronary ultrasound imaging: intraobserver and interobserver variability of morphometric measurements. *Am Heart J.* 1994;128:674-680.
39. Sonka M, Zhang X, Siebes M, DeJong S, McKay CR, Collins SM. Automated segmentation of coronary wall and plaque from intravascular ultrasound image sequences. In: *Computers in Cardiology 1994.* Los Alamitos, Calif: IEEE Computer Society Press; 1994: 281-284.
40. Sonka M, Liang W, Zhang X, De Jong S, Collins SM, McKay CR. Three-dimensional automated segmentation of coronary wall and plaque from intravascular ultrasound pullback sequences. In: *Computers in Cardiology 1995.* Los Alamitos, Calif: IEEE Computer Society Press; 1995:637-640.
41. Frank RJ, McPherson DD, Chandran KB, Dove EL. Optimal surface detection in intravascular ultrasound using multi-dimensional graph search. In: *Computers in Cardiology 1996.* Los Alamitos, Calif: IEEE Computer Society Press; 1996:45-48.
42. Brathwaite PA, Chandran KB, McPherson DD, Dove EL. Lumen detection in human IVUS images using region-growing. In: *Computers in Cardiology 1996.* Los Alamitos, Calif: IEEE Computer Society Press; 1996:37-40.
43. ten Hoff H, Gussenhoven EJ, Korbijn A, Mastik F, Lancee CT, Bom N. Mechanical scanning in intravascular ultrasound: artifacts and driving mechanisms. *Eur J Ultrasound.* 1995;2:227-237.
44. Waligora MJ, Vonesh MJ, Wiet SP, McPherson DD. Effect of vascular curvatures on three-dimensional reconstruction of intravascular ultrasound images *Circulation.* 1994;90(suppl I):I-227. Abstract.
45. Klein HM, Günther RW, Verlande M, Schneider W, Vorwerk D, Kelch J, Hamm M. 3D-surface reconstruction of intravascular ultrasound images using personal computer hardware and a motorized catheter control. *Cardiovasc Intervent Radiol.* 1992;15:97-101.
46. Koch L, Kearney P, Erbel R, Roth T, Ge J, Brennecke R, Meyer J. Three dimensional reconstruction of intracoronary ultrasound images: roadmapping with simultaneously digitised coronary angiograms. In: *Computers in Cardiology 1993.* Los Alamitos, Calif: IEEE Computer Society Press; 1993:89-91.
47. Laban M, Oomen JA, Slager CJ, Wentzel JJ, Krams R, Schuurbiers JCH, den Boer A, von Birgelen C, Serruys PW, de Feyter PJ. ANGUS: a new approach to three-dimensional reconstruction of coronary vessels by combined use of angiography and intravascular ultrasound. In: *Computers in Cardiology 1995.* Los Alamitos, Calif: IEEE Computer Society Press; 1995:325-328.
48. Evans JL, Ng KH, Wiet SG, Vonesh MJ, Burns WB, Radvany MG, Kane BJ, Davidson CJ, Roth SI, Kramer BL, Meyers SN, McPherson DD. Accurate three-dimensional reconstruction of intravascular ultrasound data: spatially correct three-dimensional reconstructions. *Circulation.* 1996;93:567-576.
49. von Birgelen C, Mintz GS, Nicosia A, Foley DP, van der Giessen WJ, Bruining N, Airiian SG, Roelandt JRTC, de Feyter PJ, Serruys PW. Electrocardiogram-gated intravascular ultrasound image acquisition after coronary stent deployment facilitates on-line three-dimensional reconstruction and automated lumen quantification. *J Am Coll Cardiol.* 1997;30:436-443.

Chapter 4

Simpson's rule for the volumetric ultrasound assessment of atherosclerotic coronary arteries: A study with ECG-gated three-dimensional intravascular ultrasound

C von Birgelen, PJ de Feyter, EA de Vrey, W Li,
N Bruining, A Nicosia, JRTC Roelandt,
PW Serruys

Reprinted with permission from *Coron Artery Dis* 1997;8:363-369

Simpson's rule for the volumetric ultrasound assessment of atherosclerotic coronary arteries: a study with ECG-gated three-dimensional intravascular ultrasound

Clemens von Birgelen*, Pim J. de Feyter, Evelyn A. de Vrey, Wenguang Li, Nico Bruining, Antonino Nicosia, Jos R.T.C. Roelandt and Patrick W. Serruys

Background Volumetric intravascular ultrasound (IVUS) assessment provides complementary information on atherosclerotic plaques. The volumes can be calculated by applying Simpson's rule to cross-sectional area data of multiple IVUS images, acquired with a fixed sample spacing, which is the distance (along the vessel's axis) between two images.

Objective To evaluate the effect of different sample spacings on the results of volumetric IVUS measurements.

Methods A stepwise electrocardiographically gated IVUS image-acquisition and automated three-dimensional analysis approach was applied to 26 patients. Twenty-eight coronary segments with mild-to-moderate coronary atherosclerosis were examined. Volumetric measurements of five images per mm (i.e. sample spacing 0.2 mm), representing a complete scanning of the coronary segment, were considered the optimal standard, against which volumetric measurements of three, one, and one-half images per mm (i.e. larger sample spacings) were compared.

Results The lumen, total vessel, and plaque volumes obtained with five images per mm were 183.3 ± 2.8, 350.6 ± 141.6, and 167.3 ± 89.2 mm^3. There was an excellent correlation ($r = 0.99$, $P < 0.001$) between these data and volumetric measurements with larger sample spacings. The volumetric measurements with larger sample spacings differed on average only by a little (< 0.7%) from the optimal standard measurements. However, a relatively small, but significant, increase in SD of these differences was associated with the wider sample spacings (< 3.6%, $P < 0.05$).

Conclusions The width of the sample spacing has a relatively small but significant impact on the variability of volumetric intravascular ultrasound measurements. This should be considered when designing future volumetric studies. The electrocardiographically gated acquisition of five IVUS images per mm axial length during a stepwise transducer pull-back is an ideal approach, particularly when addressing with IVUS volumetric changes that are assumed small, such as those expected in studies of the progression and regression of atherosclerosis.

Coronary Artery Disease 1997, 8:363–369

Keywords: Intravascular ultrasound, three-dimensional reconstruction, volumetric measurement, Simpson's rule, ultrasonics, ECG-gating, coronary disease

From the Thoraxcenter, Cardiology Division, University Hospital, Rotterdam-Dijkzigt, Erasmus University Rotterdam, The Netherlands.

*Present address: Department of Cardiology, University Hospital Essen, Hufelandstr. 55, 45122 Essen, Germany.

Requests for reprints to Professor Patrick W. Serruys, Thorax Center, Erasmus University Rotterdam, Cardiac Catheterization and Coronary Imaging Laboratory, P.O. Box 1738, 3000 DR Rotterdam, The Netherlands.

Received 14 February 1997 Revised 20 May 1997
Accepted 2 June 1997

 ISSN 0954-6928

Introduction

Intravascular ultrasound (IVUS) imaging depicts the coronary lumen and vessel wall, and permits the evaluation of atherosclerosis *in vivo* [1–5]. Volumetric data can be obtained with the use of motorized devices for controlled pull-back of the IVUS transducer [6], and allow a more comprehensive assessment of the distribution and therapy of coronary plaques [7–10]. The pioneers of volumetric IVUS assessment performed the volume calculation by applying Simpson's rule to the results of laborious manual analyses of cross-sectional IVUS images (one image per mm), acquired during a uniform transducer pull-back [8–10].

Three-dimensional IVUS and automated analysis systems have recently been developed [11–20]. Such approaches permit the automated analysis of a larger number of images. Accordingly, volumetric measurements can be performed on a larger number of IVUS images, acquired at a smaller sample spacing, which is the distance (along the vessel's axis) between two IVUS images used for volume calculation. However, the effect of different sample spacings on the results of volumetric IVUS measurements was not known. In the present study we evaluated this problem, using three-dimensional sets of IVUS images acquired with an electrocardiographically gated approach [21–23] for 28 atherosclerotic coronary segments of 26 patients. Volumetric measurements of five

images per mm (i.e. sample spacing 0.2 mm), acquired at the same phase of the cardiac cycle, were considered the optimal standard, insofar as they represented a complete scanning of the coronary segment. The purpose of this study was to evaluate the difference between the volumetric measurements obtained using the optimal standard method (five images per mm) and those with three, one, and one-half images per mm.

Methods

Study population

We examined 26 patients [of whom 21 (81%) were men] aged 54.9 ± 9.1 years during diagnostic (n = 19; 73%) and follow-up catheterization procedures after previous catheter-based interventions (n = 7; 27%) with IVUS, using an electrocardiographically gated three-dimensional image-acquisition station and a dedicated pull-back device [21–23]. In total 28 atherosclerotic coronary segments with mild-to-moderate atherosclerosis were studied. These segments were relatively straight on at least two angiograms from opposite angiographic projections. Segments with severe calcification were excluded from the study. The investigation was approved by the Medical Ethics Committee of the University Hospital Dijkzigt. All of the patients gave their written informed consent to participate in the study.

IVUS image acquisition

The coronary segments were examined with a mechanical IVUS system (ClearView; CardioVascular Imaging Systems Inc., Sunnyvale, California, USA) after standard intravenous premedication with 10 000 U heparin and 250 mg aspirin, and intracoronary administration of nitrates. Sheath-based IVUS catheters with 30 MHz single-element transducers (MicroView; CardioVascular Imaging Systems Inc.) were used. This catheter design is equipped with a 2.9Fr 15 cm long transparent distal sheath, which has a common distal lumen that houses the guide wire during catheter introduction and the transducer during imaging when the guide wire has been pulled back [24]. Electrocardiographically gated image acquisition was performed by using a three-dimensional image-acquisition station (EchoScan; TomTec, Munich, Germany), which also steered the dedicated pull-back device (stepping motor) to withdraw the IVUS transducer through the stationary imaging sheath [21]. After each 0.2 mm step, one IVUS image was acquired 40 ms after the peak of the R wave, assuring a complete scanning of the vascular segment. If the length of the R–R interval fell within the preset range, which was checked retrospectively by the acquisition station, the image was stored in the computer memory of the IVUS image-acquisition station. After an image had been stored, the following cardiac cycle was used to automatically move the transducer to the adjacent image-acquisition site, where the same procedure was repeated.

Automated contour analysis

The gated three-dimensional IVUS acquisition technique allowed measurements without systolic and diastolic artifacts and thus without gaps and overlaps between adjacent images. The IVUS analysis was performed off-line using a computerized contour-detection system [18,19,21,23,25] that permits the digitization of a maximum of 200 IVUS images and the automated detection of the luminal and external vascular boundaries (Fig. 1). It operates on the basis of the concept that longitudinal contours facilitate automated contour detection on the tomographic cross-sectional IVUS images by defining the center and the range of the boundary-detection process (Fig. 2). An analyst checked each detected contour and performed corrections, when this was required. The algorithm (the minimum-cost algorithm) has previously been described, and both its validation and its reproducibility have been reported [18,19,21,22,25].

In the present study, the entire contour-detection process (aiming at maximum accuracy) required 25 ± 5 min for five image samples per mm; at this sampling of five images per mm the 'interactive' component accounted for approximately 20 min of the overall analysis time. The different sample spacings did not affect the analysis time required for the automatic steps, but they did affect the time required for editing and visual checking of the contours. By increasing the sample spacing, the latter component could gradually be reduced to approximately 5 min (at one-half image per mm); the detection of the longitudinal contours appeared less feasible with a very large sample spacing (one-half image per mm). We experienced no adverse effects of the plaque morphology (e.g. calcium) on the computerized analysis, using wider sample spacings.

Comparisons between volumetric measurements in three-dimensional IVUS *in vitro* and measurements on the

Fig. 1

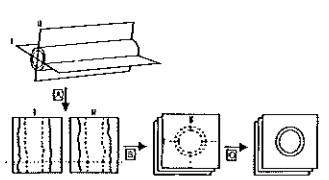

Principle of the intravascular ultrasound (IVUS) analysis system used. The stack of cross-sectional IVUS images is stored in the computer memory and sliced to provide two perpendicular longitudinal sections (I and II). Automated detection both of the luminal and of the external vascular contours is performed on these sections (A). The longitudinal contours are represented as individual edge points on the entire stack of cross-sectional IVUS images (B). They define the center and range of the final automatic contour-detection step, which is then performed on the cross-sectional IVUS images (C).

Fig. 2

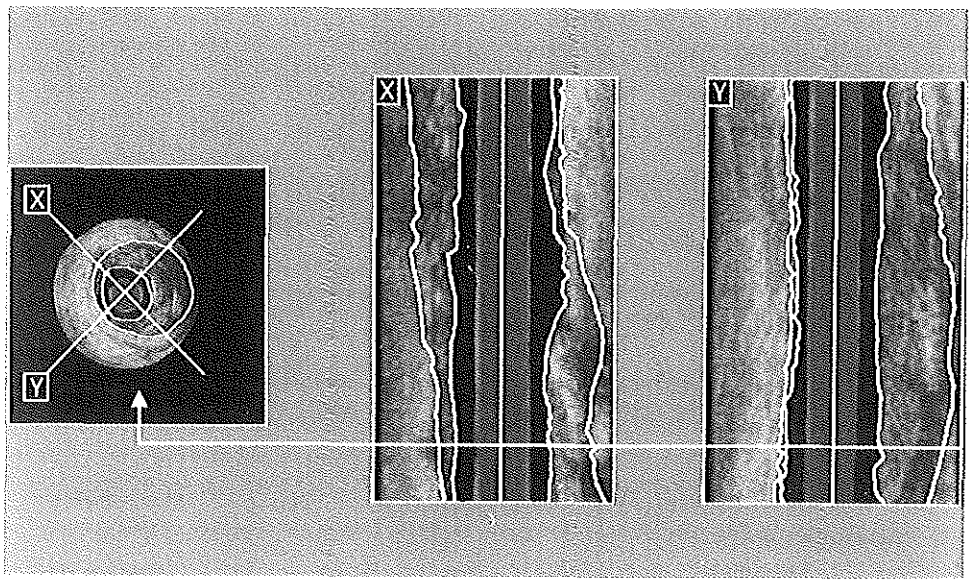

Example of a coronary segment analyzed by the automated intravascular ultrasound analysis system. The arrowhead indicates the position of the cross-sectional intravascular ultrasound image (left-hand panel) on the perpendicular longitudinal sections (X and Y).

corresponding histologic sections revealed high correlations (r = 0.83–0.98) [18], and the intra- and inter-observer differences of volumetric measurements *in vivo* were less than 1% with SD not exceeding 3.2% [21].

Data analysis

The lumen and total vessel cross-sectional areas were measured by the automated analysis system on each digital planar IVUS image. The area within the border between hypoechoic media and echoreflective adventitia has been shown to be a reproducible measure of the total cross-sectional area of the vessel. Because ultrasound cannot measure media thicknesses accurately [26], the plaque plus media dimensions were used as measures of the plaque burden, just like in many previous studies using IVUS. The plaque cross-sectional area was calculated as the total cross-sectional area of the vessel minus the cross-sectional area of the lumen. Lumen, total vessel, and plaque volumes were calculated by integrating all of the cross-sectional area measurements multiplied by the slice thickness (Simpson's rule), using the cross-sectional area measurements of five, three, one, and one-half images per mm (i.e. sample spacings of 0.2, 0.33, 1.0, and 2.0 mm). Volumetric measurements of five images per mm (i.e. a sample spacing of 0.2 mm), representing a complete scanning of the vascular segment, were used as the optimal standard against which to evaluate the effect of larger sample spacings on the results of volumetric IVUS measurements.

Statistics

Values are expressed as means ± SD; qualitative data as prevalences. The volumetric measurements of five images per mm were compared with measurements using three, one, and one-half images per mm, using Student's paired t test. According to the method of Bland and Altman [27], the agreement between these volumetric measurements was assessed by determining the mean and SD of the between-measurement differences. The variances of these differences were tested against each other with Pitman's test [28]. Linear regression analysis was performed to evaluate the strength of the relation between the volumetric measurements of five images per mm and measurements with fewer images per mm. $P < 0.05$ was considered statistically significant.

Results

IVUS segment characteristics

The coronary segments examined with three-dimensional IVUS measurements were located in the left anterior

descending (n = 15), right circumflex (n = 11), and left circumflex coronary arteries (n = 2); they were on average 21.2 ± 7.3 mm long. The SD per segment of the lumen, total vessel, and plaque cross-sectional area measurements were on average 1.52 ± 0.98, 2.03 ± 1.46, and 1.81 ± 1.06 mm^2, and 5.56 ± 3.04 mm^2; the corresponding ranges per segment (maximum minus minimum values) were 5.56 ± 3.04, 7.45 ± 4.46, and 6.94 ± 3.58 mm^2, respectively. All of the segments exhibited mild-to-moderate atherosclerotic lesions and the minimum cross-sectional area of the lumen was on average 6.7 ± 2.5mm^2. The percentage of the total vessel cross-sectional area that was covered with plaque (the percentage cross-sectional area plaque burden) varied by 30 ± 10% along individual coronary segments; at the minimum lumen site the percentage cross-sectional area plaque burden was 56 ± 11%.

Volumetric data and results of linear regression analyses

The lumen, total vessel, and plaque volumes of five IVUS images/mm (the optimal standard) were 183.3 ± 62.8, 350.6 ± 141.6, and 167.3 ± 89.2 mm^3. Volumetric measurements of fewer images per mm (i.e. larger sample spacings) correlated excellently with these optimal standard measurements: values of 0.99 for Pearson's correlation coefficient were found for the lumen, total vessel, and plaque volumes of each sample spacing compared (slopes: 0.99 for all; intercepts: between −0.1 and 1.5 mm^3). However, the increase in sample spacing was often associated with an increase in the standard error of the estimate (lumen 0.7, 2.6, and 3.6 mm^3; total vessel 1.2, 3.0, and 4.6 mm^3; plaque 0.9, 3.2, and 4.1 mm^3).

Agreement between volume measurements using different sample spacings

The agreement between volumes of three, one, and one-half images per mm and the optimal standard volumes (five images per mm) is shown in Figure 3. The volumetric measurements of the larger sample spacings differed on average only by a little (< 0.7%) from the

Fig. 3

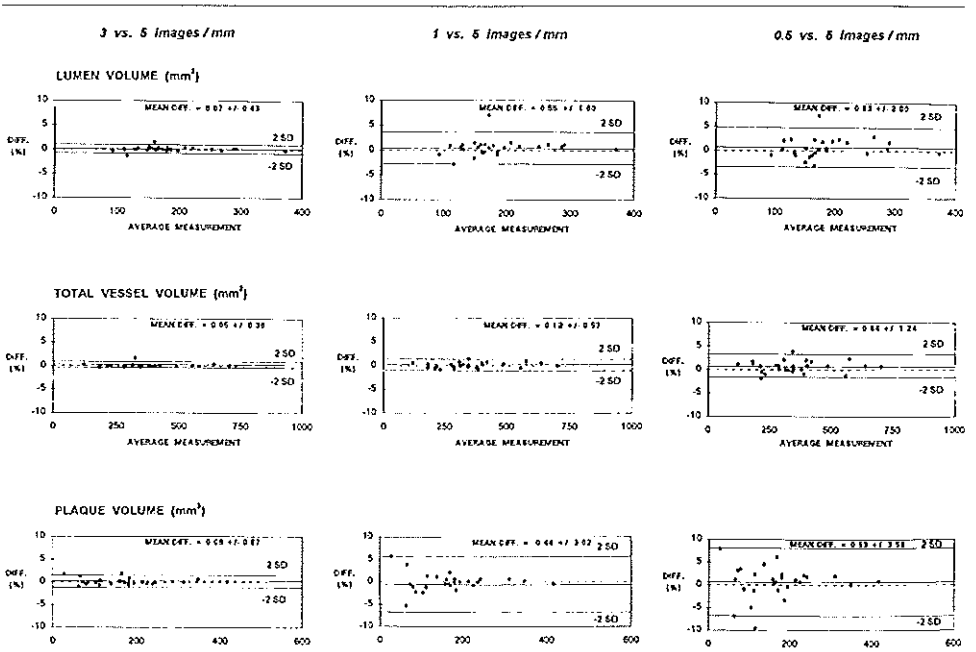

Volumetric measurements of three, one, and one-half images per mm compared with the optimal standard of five images per mm. The between-measurement differences (DIFF) were plotted against the averages of corresponding measurements, obtained at different sample spacings. Unbroken lines indicate the mean between-difference and the range ±2SD. Mean values of the between-measurement differences ±SD are given.

Fig. 4

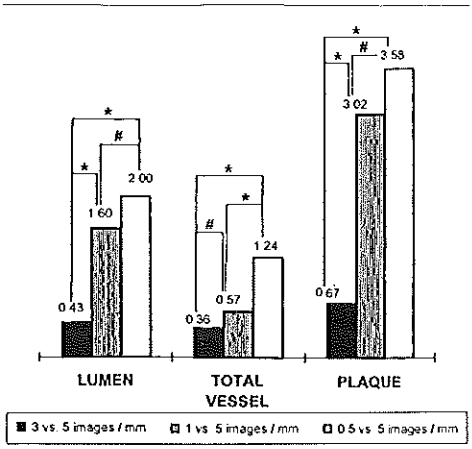

SD (%) of the between-measurement differences (five images per mm as the optimal standard versus three, one, and one-half images per mm). The SD were relatively low, but increased significantly (#$P<0.05$, *$P<0.01$) coincident with the increase in sample spacing (i.e. decrease in number of images per mm), which indicated that there was a larger variability of the agreement with the optimal standard measurements.

optimal standard. However, a relatively small but significant increase in SD of these between-measurement differences (< 3.6%, $P < 0.05$) was associated with the increased width of the sample spacing (Fig. 4).

Discussion

Although quantitative angiographic techniques permit only the interpolated measurement of the diameter stenosis and plaque dimensions [29], direct cross-sectional visualization and measurement of the coronary lumen and plaque can be obtained from IVUS assessment [1–5]. Initially, most IVUS studies were restricted to the measurement of diameters and cross-sectional areas, but accumulated evidence has shown that volumetric IVUS measurements provide important complementary information [7–10,16,18,19,21].

Volumetric data can be obtained by applying Simpson's rule to the cross-sectional area data of multiple IVUS images, acquired at a fixed sample spacing, which is the distance (along the vessel's axis) between two image samples. Sampling of a huge number of image samples would theoretically be ideal, but currently it is not realistic, for such an approach is limited by the large computer memory and increased analysis time required. The present study was the first to quantify the consequences of different sample spacings on volumetric three-dimensional IVUS measurements *in vivo*. An electrocardiographically gated stepwise image-acquisition approach [20] permitted the acquisition of a reliable standard for the volume measurements: five images per mm (i.e. a sample spacing of 0.2 mm), acquired during the same phase of the cardiac cycle, represented a complete scanning of the arterial segment because the mean width of the IVUS beam in the long vessel axis (out-of-plane resolution) was known to be 0.2 mm [30].

Our data demonstrate that the width of the sample spacing has a significant impact on the variability of volumetric IVUS measurements, even for lesions with mild-to-moderate atherosclerotic disease. An increased sample spacing width was associated with a higher variability of the agreement between these volume measurements and the optimal standard results. Although this effect remained relatively small, it should be considered when designing future volumetric IVUS studies, particularly when addressing volumetric changes that are assumed small, such as those expected, for instance, in studies evaluating the progression and regression of atherosclerosis.

Previous volumetric IVUS studies

The first clinical volumetric IVUS studies of Matar *et al.* [8] and Weissman *et al.* [9] addressed the mechanisms of the improvement of the lumen after directional coronary atherectomy, whereas Dussaillant *et al.* [10] investigated plaque ablation by rotational atherectomy of noncalcified coronary lesions. In these IVUS studies, interesting mechanistic and pathophysiologic insights were gained by computing volumes from the cross-sectional area information of one end-diastolic image per mm, acquired during continuous motorized pull-backs (at 0.5 and 1.0 mm/s) [8–10]. The application of dedicated algorithms for automated boundary detection in three-dimensional IVUS image sets allowed volume measurements using a much higher number of IVUS images. A validation of lumen volume measurements by a threshold-based three-dimensional IVUS system has been reported by Matar *et al.* [16]. Our group has validated a contour-detection-based three-dimensional IVUS analysis system that permits the measurement of lumen and vessel volumes [18,19]. As performed in the present study, the latter analysis system can be used in combination with a stepwise electrocardiographically gated image-acquisition approach [21,22]. The electrocardiographic gating improved the performance of the algorithm for automated contour detection, the efficacy of which had also been demonstrated by Sonka *et al.* [17] and Dhawale *et al.* [31,32].

Limitations and potential sources of error

Curvatures of the transducer pull-back trajectory, as seen in curved vessel segments, may cause errors in volumetric

IVUS measurements. Therefore, IVUS volume measurements from linear approaches (by manual as well as automated methods) actually represent estimates of the true volumes. To minimize the curve-induced error, we studied only segments that were straight on angiograms obtained from at least two opposite projections. Consequently, our data can not simply be transferred to lesions in significantly curved vascular segments. Combined processing of IVUS and biplane angiographic data [33] has the potential to overcome this problem in the future, but these approaches are still very laborious and only limited data are available [24]. Nevertheless, the combined approaches are beneficial, insofar as they may permit one to determine the curve-induced error in volumetric measurements. This problem is practically interesting and should be addressed in another study, using such combined methods. The data of this study were obtained for atherosclerotic lesions with mild-to-moderate disease (a 'progression–regression study population'); the use of larger sample spacings for more stenotic lesions (e.g. pre-intervention) could result in even more significant increases in measurement variability.

Implications for clinical trials

The present study demonstrated the effect of different sample spacings on the results of volumetric IVUS measurements, but no 'blanket' recommendation, valid for any volumetric IVUS study, can be given. The choice of sample spacing must be considered in the light of the study population examined and the analysis technique used. The additional variability introduced by the use of larger sample spacings might be negligible if a study addresses volumetric differences that are assumed large, or uses an analysis approach with a relatively high measurement variability, or both.

The coronary segments evaluated in this study exhibited mild-to-moderate coronary artery disease, of a degree typical of that in progression–regression studies. In such studies, potentially small changes in plaque or lumen volume may occur [7]. Therefore we may consider the use of automated analysis systems that permit both a rapid analysis of a large number of IVUS images at inherently low measurement variability, and volumetric measurements at a very low sample spacing. The acquisition of five images per mm axial length during electrocardiographically gated image acquisition and electrocardiographically triggered stepwise transducer pull-backs is ideal, and allows complete scanning of an entire arterial segment without any 'gap' or 'blind spot'. When other, nongated methods are used, complete scanning of the vessel segment cannot be guaranteed with five images per mm (and even with more images per mm). It was not the objective of this study to address the complex problems arising from nongated image acquisition, but it has been our experience that at least 10 images per mm (ideally even more) should then be acquired.

In conclusion, the width of the sample spacing has a relatively small but significant impact on the variability of volumetric intravascular ultrasound measurements. This should be considered when designing future volumetric studies. The electrocardiographically gated acquisition of five IVUS images per mm axial length during a stepwise transducer pull-back is an ideal approach, particularly when addressing with IVUS volumetric changes that are assumed small, such as those expected in studies of the progression and regression of atherosclerosis.

References

1 Ge J, Erbel R, Zamorano J, Koch L, Kearney P, Gorge G, *et al.*: Coronary artery remodeling in atherosclerotic disease: an intravascular ultrasonic study *in vivo*. *Coron Artery Dis* 1993, 4:981–986.

2 Pinto FJ, Chenzbraun A, Botas J, Valantine HA, St Goar FG, Alderman EL, *et al.*: Feasibility of serial intracoronary ultrasound imaging for assessment of progression of intimal proliferation in cardiac transplant recipients. *Circulation* 1994, 90:2348–2355.

3 Mintz GS, Painter JA, Pichard AD, Kent KM, Satler LF, Popma JJ, *et al.*: Atherosclerosis in angiographically "normal" coronary artery reference segments: an intravascular ultrasound study with clinical correlations. *J Am Coll Cardiol* 1995, 25:1479–1485.

4 Erbel R, Ge J, Bockisch A, Kearney P, Görge G, Haude M, *et al.*: Value of intracoronary ultrasound and Doppler in the differentiation of angiographically normal coronary arteries: a prospective study in patients with angina pectoris. *Eur Heart J* 1996, 17:880–889.

5 Alfonso F, Macaya C, Goicolea J, Hernandez R, Segovia J, Zamorano J, *et al.*: Determinants of coronary compliance in patients with coronary artery disease: an intravascular ultrasound study. *J Am Coll Cardiol* 1994, 23:879–884.

6 Fuessl RT, Mintz GS, Pichard AD, Kent KM, Satler LF, Popma JJ, *et al.*: *In vivo* validation of intravascular ultrasound length measurements using a motorized transducer pullback system. *Am J Cardiol* 1996, 77:1116–1118.

7 von Birgelen C, Slager CJ, Di Mario C, de Feyter PJ, Serruys PW: Volumetric intracoronary ultrasound: a new maximum confidence approach for the quantitative assessment of progression–regression of atherosclerosis? *Atherosclerosis* 1995, 118 (suppl):S103–S113.

8 Matar FA, Mintz GS, Farb A, Douek P, Pichard AD, Kent KM, *et al.*: The contribution of tissue removal to lumen improvement after directional coronary atherectomy. *Am J Cardiol* 1994, 74:647–650.

9 Weissman NJ, Palacios IF, Nidorf SM, Dinsmore RE, Weyman AE: Three-dimensional intravascular ultrasound assessment of plaque volume after successful atherectomy. *Am Heart J* 1995, 130:413–419.

10 Dussaillant GR, Mintz GS, Pichard AD, Kent KM, Satler LF, Popma JJ, *et al.*: Effect of rotational atherectomy in noncalcified atherosclerotic plaque: a volumetric intravascular ultrasound study. *J Am Coll Cardiol* 1996, 28:856–860.

11 Rosenfield K, Losordo DW, Ramaswamy K, Pastore JO, Langevin RE, Razvi S, *et al.*: Three-dimensional reconstruction of human coronary and peripheral arteries from images recorded during two-dimensional intravascular ultrasound examination. *Circulation* 1991, 84:1938–1956.

12 Coy KM, Park JC, Fishbein MC, Laas T, Diamond GA, Adler L, *et al.*: *In vitro* validation of three-dimensional intravascular ultrasound for the evaluation of arterial injury after balloon angioplasty. *J Am Coll Cardiol* 1992, 20:692–700.

13 Mintz GS, Pichard AD, Satler LF, Popma JJ, Kent KM, Leon MB: Three-dimensional intravascular ultrasonography: reconstruction of endovascular stents *in vitro* and *in vivo*. *Clin Ultrasound* 1993, 21:609–615.

14 Evans JL, Ng KH, Wiet SG, Vonesh MJ, Burns WB, Radvany MG, *et al.*: Accurate three-dimensional reconstruction of intravascular ultrasound data: spatially correct three-dimensional reconstructions. *Circulation* 1996, 93:567–576.

15 von Birgelen C, Kutryk MJB, Gil R, Ozaki Y, Di Mario C, Roelandt JRTC, *et al.*: Quantification of the minimal luminal cross-sectional area after coronary stenting by two- and three-dimensional intravascular ultrasound versus edge detection and videodensitometry. *Am J Cardiol* 1996, 78:520–525.

16 Matar FA, Mintz GS, Douek P, Farb A, Virmani R, Saturnino PJ, *et al.*: Coronary artery lumen volume measurement using three-dimensional intravascular ultrasound: validation of a new technique. *Cathet Cardiovasc Diagn* 1994, 33:214–220.

17 Sonka M, Liang W, Zhang X, De Jong S, Collins SM, McKay CR: Three-dimensional automated segmentation of coronary wall and plaque from intravascular ultrasound pullback sequences. In *Computers in Cardiology 1995*. Los Alamitos: IEEE Computer Society Press; 1995:637–640.

18 von Birgelen C, van der Lugt A, Nicosia A, Mintz GS, Gussenhoven EJ, de Vrey E, *et al.*: Computerized assessment of coronary lumen and atherosclerotic plaque dimensions in three-dimensional intravascular ultrasound correlated with histomorphometry. *Am J Cardiol* 1996, 78:1202–1209.

19 von Birgelen C, Di Mario C, Li W, Schuurbiers JCH, Slager CJ, de Feyter PJ, *et al.*: Morphometric analysis in three-dimensional intracoronary ultrasound: an in-vitro and in-vivo study using a novel system for the contour detection of lumen and plaque. *Am Heart J* 1996, 132:516–527.

20 Roelandt JRTC, Di Mario C, Pandian NG, Li W, Keane D, Slager CJ, *et al.*: Three-dimensional reconstruction of intracoronary ultrasound images: Rationale, approaches, problems, and directions. *Circulation* 1994, 90:1044–1055.

21 von Birgelen C, de Vrey EA, Mintz GS, Nicosia A, Bruining N, Li W, *et al.*: ECG-gated three-dimensional intravascular ultrasound: feasibility and reproducibility of the automated analysis of coronary lumen and atherosclerotic plaque dimensions in humans. *Circulation* (in press).

22 von Birgelen C, Mintz GS, Nicosia A, Foley DP, van der Giessen WJ, Bruining N, *et al.*: Electrocardiogram-gated intravascular ultrasound image acquisition after coronary stent deployment facilitates on-line three-dimensional reconstruction and automated lumen quantification. *J Am Coll Cardiol* 1997, 30:436–443.

23 Bruining N, von Birgelen C, Di Mario C, Prati F, Li W, Den Hood W, *et al.*: Dynamic three-dimensional reconstruction of ICUS images based on an ECG-gated pull-back device. In *Computers in Cardiology 1995*. Los Alamitos: IEEE Computer Society Press; 1995:633–636.

24 von Birgelen C, Mintz GS, de Feyter PJ, Bruining N, Nicosia A, Di Mario C, *et al.*: Reconstruction and quantification with three-dimensional intracoronary ultrasound: an update on techniques, challenges, and future directions. *Eur Heart J* 1997, 18:1056–1067.

25 Li W, von Birgelen C, Di Mario C, Boersma E, Gussenhoven EJ, van der Putten N, *et al.*: Semi-automatic contour detection for volumetric quantification of intracoronary ultrasound. In *Computers in Cardiology 1994*. Los Alamitos: IEEE Computer Society Press; 1994:277–280.

26 Mallery JA, Tobis JM, Griffith J, Gessert J, McRae M, Moussabeck O, *et al.*: Assessment of normal and atherosclerotic arterial wall thickness with an intravascular ultrasound imaging catheter. *Am Heart J* 1990, 119:1392–1400.

27 Bland JM, Altman DG: Statistical methods for assessing agreement between two methods of clinical measurement. *Lancet* 1986, ii:307–310.

28 Pitman EJG: A note on normal correlation. *Biometrika* 1939, 31:9–12.

29 de Feyter PJ, Serruys PW, Davies MJ, Richardson P, Lubsen J, Oliver MF: Quantitative coronary angiography to measure progression and regression of coronary atherosclerosis: value, limitations, and implications for clinical trials. *Circulation* 1991, 84:412–423.

30 Benkeser PJ, Churchwell AL, Lee C, Abouelnasr DM: Resolution limitations in intravascular ultrasound imaging. *J Am Soc Echocardiogr* 1993, 6:158–165.

31 Dhawale PJ, Griffin N, Wilson DL, Hodgson J McB: Calibrated 3D reconstruction of coronary arteries using intravascular ultrasound with cardiac gating and catheter motion compensation. In *Computers in Cardiology 1992*. Los Alamitos: Computer Society Press; 1992:30–33.

32 Dhawale PJ, Wilson DL, Hodgson JMcB: Optimal data acquisition for volumetric intracoronary ultrasound. *Cathet Cardiovasc Diagn* 1994, 32:288–299.

33 Slager CJ, Laban M, von Birgelen C, Krams R, Oomen JAF, den Boer A, *et al.*: 'ANGUS': a new approach to three-dimensional reconstruction of geometry and orientation of coronary lumen and plaque by combined use of coronary angiography and IVUS [abstract]. *J Am Coll Cardiol* 1995, 25 (suppl):144A.

PART II

APPLICATION, POTENTIAL, AND LIMITATIONS

Chapter 5

Quantification of the minimal luminal cross-sectional area after coronary stenting by two-dimensional and three-dimensional intravascular ultrasound versus edge detection and videodensitometry

C von Birgelen, MJB Kutryk, R Gil, Y Ozaki, C Di Mario,
JRTC Roelandt, PJ de Feyter,
PW Serruys

Reprinted with permission from *Am J Cardiol* 1996;78:520-525

Quantification of the Minimal Luminal Cross-Sectional Area After Coronary Stenting by Two- and Three-Dimensional Intravascular Ultrasound Versus Edge Detection and Videodensitometry

Clemens von Birgelen, MD, Michael J.B. Kutryk, MD, PhD, Robert Gil, MD, Yukio Ozaki, MD, PhD, Carlo Di Mario, MD, PhD, Jos R.T.C. Roelandt, MD, PhD, Pim J. de Feyter, MD, PhD, and Patrick W. Serruys, MD, PhD

The use of 2-dimensional intravascular ultrasound (2-D IVUS) to improve the outcome of coronary stenting has gained clinical acceptance, and recently 3-D IVUS has been introduced to clinical practice. However, there have been no comprehensive studies comparing the measurements of the coronary dimensions after stenting obtained by the different approaches of IVUS and quantitative coronary angiography. We examined the minimal luminal cross-sectional area of 38 stents using 2-D IVUS, 3-D IVUS, and 2 standard methods of quantitative coronary angiography, edge detection (ED) and videodensitometry (VD). Correlations between 2-D IVUS and ED ($r = 0.72$; $p < 0.0001$), VD ($r = 0.87$; $p < 0.0001$), and 3-D IVUS ($r = 0.81$; $p < 0.0001$) were higher than the correlations seen between 3-D IVUS and ED ($r = 0.58$; $p < 0.0005$) and VD ($r = 0.70$; $p < 0.0001$). The measurements by 2-D and 3-D IVUS (8.32 ± 2.50 mm^2 and 8.05 ± 2.66 mm^2) were larger than the values obtained by the quantitative angiographic techniques ED and VD (7.55 ± 2.22 mm^2 and 7.27 ± 2.21 mm^2). Thus, concordance was seen among all of the 4 techniques, confirming the validity of using IVUS for determination of the minimal luminal cross-sectional area after coronary stenting. A particularly good correlation was found between VD and IVUS, perhaps because measurement of the luminal area is the basic quantification approach of both techniques, whereas the lower correlations of ED with IVUS and VD may be explained by the dependence of ED on the angiographic projections used, which is especially important in eccentric stent configurations.

(Am J Cardiol 1996;78:520–525)

The use of computerized methods of quantitative angiographic evaluation after coronary interventions has gained wide acceptance.[1–4] Edge detection (ED) is considered the gold standard, whereas the videodensitometry (VD) method, which is independent of luminal shape of the target stenosis but is based on the optical density of the lumen, is restricted to research applications.[3,5–8] Intravascular ultrasound (IVUS) is used to guide coronary stenting,[9,10] permitting stenting without anticoagulation. Previous studies have demonstrated the potential of conventional 2-dimensional (2-D) IVUS, which permits reliable assessment of vessel and stent geometry, and 3-D IVUS, which allows a comprehensive assessment along the entire segment studied, including detection of the site of minimal luminal area and evaluation of stent symmetry.[9–17] However, there are no comprehensive studies comparing these techniques with ED and VD. As ED, VD, 2-D IVUS, and 3-D IVUS are available on-line, information concerning the agreement among the 4 diagnostic approaches in measuring the minimal luminal cross-sectional area after coronary stenting is of notable clinical interest.

From the Thoraxcenter, Division of Cardiology, University Hospital Rotterdam-Dijkzigt, Erasmus University Rotterdam, The Netherlands. Dr. von Birgelen is the recipient of a fellowship of the German Research Society (DFG, Bonn, Germany). Dr. Kutryk is the recipient of a Clinician Scientist Award of the Medical Research Council of Canada (Ottawa, Canada). Manuscript received December 11, 1995; revised manuscript received and accepted March 19, 1996.

Address for reprints: Patrick W. Serruys, MD, PhD, Division of Interventional Cardiology, Thoraxcenter, Erasmus University Rotterdam, Cardiac Catheterization and Intracoronary Imaging Laboratory, P.O. Box 1738, 3000 DR Rotterdam, The Netherlands.

METHODS

Study group and intervention procedure: The study group comprised 33 patients (23 men; mean age 61 ± 9 years). All patients received 250 mg aspirin and 10,000 U heparin intravenously. We examined 38 stents, implanted in the left anterior descending ($n = 11$), left circumflex ($n = 1$), or right ($n = 19$) coronary arteries, or saphenous bypass grafts ($n = 7$). A predilation of the lesions was performed by conventional balloon angioplasty before implantation of the stents (19 Wallstents [Schneider, Bülach, Switzerland] and 19 Palmaz-Schatz stents [Johnson & Johnson, Warren, New Jersey]). Delivery balloons with a diameter corresponding to the interpolated reference diameter were used to implant the Palmaz-Schatz stents. The interpolated angiographic reference lumen diameter by quantitative coronary angiography, the lesion length, and the presence of adjacent side branches were taken into account to select an appropriately sized self-expandable Wallstent. Additional balloon inflations were performed inside all stents, using a low-compliance balloon

catheter with a diameter ≥0.25 mm larger than the interpolated angiographic lumen reference and a pressure of ≥14 atm. Progression to larger balloons was permitted to achieve a satisfactory angiographic result (maximal nominal diameter 3.88 ± 0.55 mm with a pressure of 14.9 ± 3.2 atm). The procedural end point was the angiographic appearance of a smooth lumen of the stented segment and a minimal intrastent lumen diameter larger than a distal reference (≤1 cm distal to stent) at an angiographically undiseased site. Subsequently, the stented segment was examined angiographically and by IVUS after intracoronary administration of nitrates. During the entire procedure, the activated clotting time was measured hourly, and intravenous heparin was administered if required to maintain an activated clotting time of >300 seconds.

Quantitative coronary angiography: The minimal instent lumen area was determined on end-diastolic frames by ED and VD (Figure 1) using a computer-based Coronary Angiography Analysis System (CAAS II; Pie Medical, Maastricht, The Netherlands), previously described and validated in detail.[18] The measurements were performed on-line in 2 orthogonal angiographic views after intracoronary application of nitrates.

EDGE DETECTION: Based on the weighted sum of the first and second derivative functions applied to the digitized brightness silhouette, automated detection of the coronary artery contours was performed. The diameter function of the coronary artery lumen was determined by computing the shortest distances between the edge points of the right and left contours. The absolute angiographic diameter of the stenosis was determined using a contrast-free guiding catheter as a scaling device.[19] The minimal lumen diameter was measured by ED in the stented segment of the artery, and the minimal cross-sectional area was calculated assuming a circular model ($\pi \cdot r^2$).

VIDEODENSITOMETRY: The contours and diameter values of the analyzed coronary segment were obtained from the CAAS II system, described earlier. The profile of brightness of multiple scan lines, perpendicular to the local centerline direction of the coronary artery, was measured, and this brightness profile was transformed by a logarithmic transfer function into an absorption profile (gross absorption). By computing the linear regression line through the background points directly right and left of the contours of the coronary silhouette, we estimated the background contribution and subtracted it from the previous gross absorption profile to obtain the net cross-sectional absorption profile within the vessel contours. Thus, a luminal cross-sectional area function along the analyzed coronary artery segment was obtained.[3] Calibration of the VD area values was performed by comparing reference lumen areas, calculated from diameter measurements assuming a circular lumen configuration, with corresponding densitometric reference areas. The measurement by VD has been validated previously in vitro[5] and in vivo.[19]

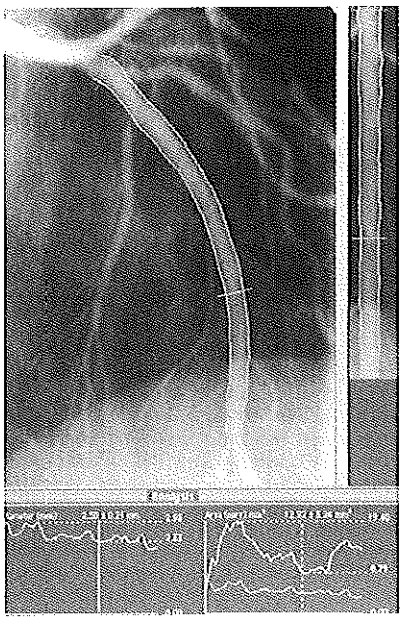

FIGURE 1. Quantitative coronary angiography by the CAAS II system after implantation of a Wallstent. The site of the instent minimal luminal diameter is indicated on the angiogram *(arrow, left upper panel)* of the left anterior descending coronary artery (cranial view) and on the edge-detection–based diameter function of the coronary artery lumen *(vertical line, left lower panel)*. The *right lower panel* shows the videodensitometric measurement of the instent minimum *(vertical dotted line)* of the luminal cross-sectional area function *(upper curve)*, which has been derived from subtraction of the background contribution *(lower curve)* from the gross brightness absorption profile.

Intravascular ultrasound: A 30 MHz single-element ultrasound catheter with a 2.9Fr echo-transparent distal sheath (MicroView, CVIS, Sunnyvale, California) was used to examine the stented segment at the end of the angiographically guided procedure. The common lumen of the sheath accommodates either the imaging core or the guidewire. The IVUS images were acquired during a motorized uniform-speed (1 mm/s) pullback of the transducer inside the stationary imaging sheath, which allowed the transducer and the handgrip to move at the same speed inside the pullback device, and were recorded on a high-resolution videotape for the 2-D analysis. The site of conventional manual tracing of the minimal intrastent lumen area was determined by scrolling the videotape back and forth.

With acquisition of the images on videotape, video signals were transferred simultaneously to a 3-D IVUS system (EchoQuant; Indec Systems Inc., Capitola, California) that automatically acquires 8.5 images/s, allowing for on-line reconstruction of contiguous tomographic IVUS image slices (118 μm apart) within 2 minutes (Figure 2). The 3-D system, operated by a second analyst, provided a longitudi-

nally reconstructed view that could be rotated around the long axis of the vessel segment. A cylindrical format, which was cut open lengthwise, was also displayed, permitting direct inspection of the inner vascular surface. Automated image segmentation, based on a pattern-recognition algorithm (Acoustic Quantification),[11] provided the measurement of lumen area on the cross-sectional IVUS images of the entire segment. The detected contour indicating the lumen-intima boundary was rapidly checked. If necessary, manual corrections outside of the detected luminal structure were made. A display of the lumen area measurements (Figure 2) facilitated the 3-D IVUS assessment.

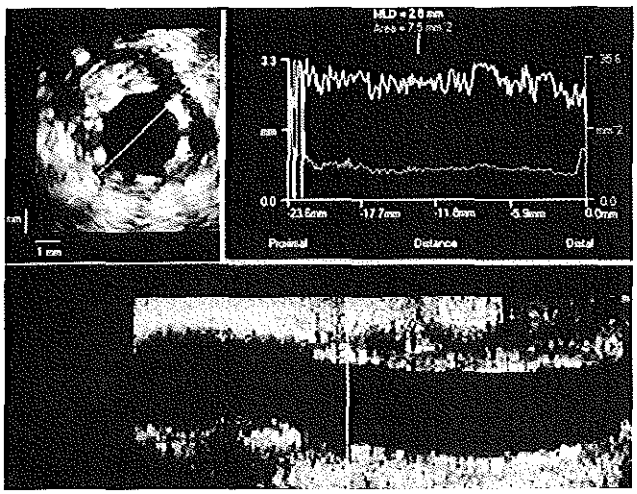

FIGURE 2. Three-dimensional intravascular ultrasound analysis of a well-expanded Palmaz-Schatz stent in a coronary segment with an eccentric atherosclerotic plaque. A 3-dimensional analysis system (EchoQuant) was used to acquire the intravascular ultrasound images automatically. A longitudinally reconstructed view *(lower panel)* was obtained that could be rotated around the long axis of the vessel segment. Automated image segmentation was performed by a pattern-recognition algorithm (Acoustic Quantification), which identified the blood pool inside the lumen. The luminal contours were rapidly checked and, if necessary, manual corrections were made on individual ultrasonic images. A display of the lumen area and corresponding diameter measurements facilitated on-line assessment and quantification of the luminal dimensions *(right upper panel)*. MLD=minimal luminal diameter.

Statistics: Results are given as mean ± 1 SD. Analysis of variance was performed, and when differences were found, the 2-tailed Student's *t* test for paired data analysis was used to compare the measurements provided by the different techniques. Linear regression analysis was performed to assess the strength of the relation between the different techniques for determining the minimal luminal cross-sectional area. According to the approach of Bland and Altman,[20] between-method agreement was assessed by determining mean ± SD of the between-method differences. A p value <0.05 was considered statistically significant.

RESULTS

Measurements by 2-D and 3-D IVUS were larger than those by the quantitative angiographic techniques ED and VD (8.32 ± 2.50 mm^2, 8.05 ± 2.66 mm^2, 7.55 ± 2.22 mm^2, and 7.27 ± 2.21 mm^2, respectively). The differences between the results of 2-D IVUS and both ED and VD ($p < 0.02$ and $p < 0.0001$), as well as between 3-D IVUS and VD ($p < 0.02$), were statistically significant.

Significant correlations between 2-D IVUS and ED, VD, and 3-D IVUS (Figure 3, left) were observed ($r = 0.72$, 0.87, and 0.81, respectively; $p < 0.0001$ for all). The agreement between 2 diagnostic methods also is shown (Figure 3, right); the figure shows the mean between-method difference and the range between +2 SD and −2 SD. The between-method differences were −0.77 ± 1.78 mm^2 (ED − 2-D IVUS), −1.05 ± 1.24 mm^2 (VD − 2-D IVUS), and −0.26 ± 1.58 mm^2 (3-D IVUS − 2-D IVUS).

Correlations were also found for 3-D IVUS and both ED ($r = 0.58$; $p < 0.0005$) and VD ($r = 0.70$; $p < 0.0001$) (Figure 4, left). Between-method differences (Figure 4, right) were −0.50 ± 2.28 mm^2 (ED − 3-D IVUS) and −0.79 ± 1.93 mm^2 (VD − 3-D IVUS). The correlation between ED and VD was high ($r = 0.84$; $p < 0.0001$), and the between-method difference was 0.28 ± 1.26 mm^2 (ED − VD) (Figure 4).

DISCUSSION

Intravascular ultrasound versus edge detection: For almost 2 decades, angiography has been the standard means of examining coronary interventions,[2] despite its capacity to display only the opacified luminal silhouette. This limitation can be overcome by IVUS, which visualizes the vessel lumen and wall,[21] depicts the stent architecture, and permits assessment of stent dimensions and apposition to the vessel wall.[9,10,15,22] Only the agreement and correlation between the techniques can be assessed in humans, as the true dimension remains unknown. As in several previous studies,[23–25] here the minimal luminal area determined by IVUS was consistently larger than that by ED, which may be explained in part by the dependence of the ultrasonic beam on the angle of incidence and a distortion of the IVUS image because of a noncentered position of the imaging catheter in the vessel lumen. In the present study, the correlation between 2-D IVUS and ED is comparable to previous findings in angiographically nondiseased coronary segments ($r = 0.73$ to 0.89),[21,23,26]

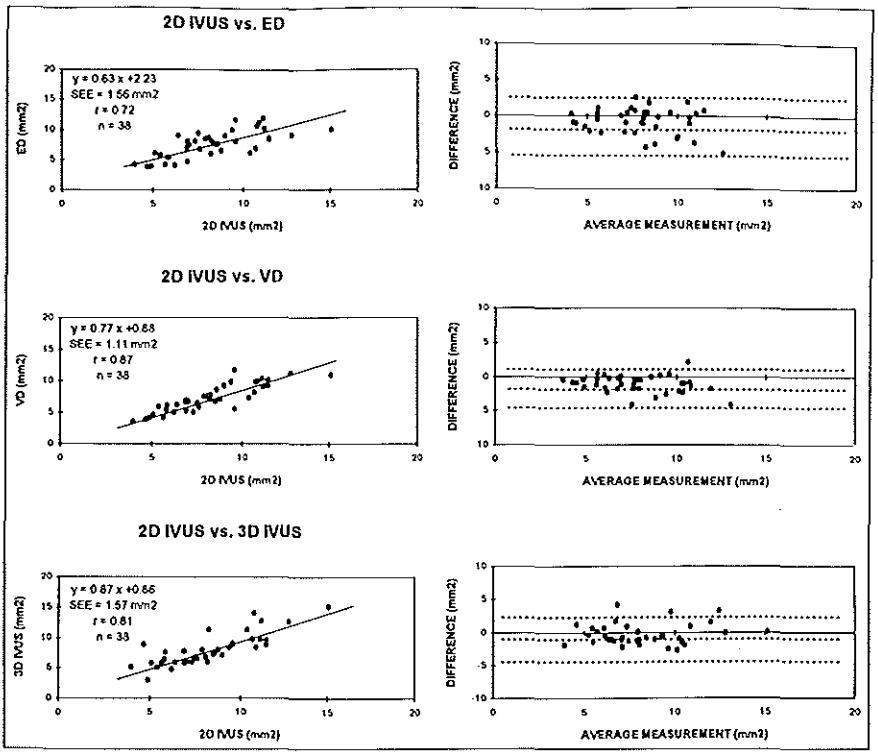

FIGURE 3. Comparison between the results of 2-dimensional intravascular ultrasound (2-D IVUS) and edge detection (ED), videodensitometry (VD), and 3-D IVUS. The results of the linear regression analyses are presented *(left)*. Significant correlations were found ($p < 0.0001$) and the regression lines are displayed. *Right*, the between-method difference is plotted against the average of the corresponding findings obtained from the methods being compared. *Dotted horizontal lines* indicate the mean between-method difference and +2 SD and −2 SD. The between-method difference ± 1 SD was −0.77 ± 1.78 mm², −1.05 ± 1.24 mm², and −0.26 ± 1.58 mm², respectively.

which were superior to correlations after balloon angioplasty (r = 0.28 to 0.69).[23,25,26] A previous report on coronary stenting[22] showed a lower correlation than our study, which may reflect differences in the IVUS and quantitative angiographic approaches used. In addition, because of high-pressure stenting, there is a low probability of insufficient stent expansion with contrast flow between the stent and vessel wall. Matar et al[12] evaluated the correlation of lumen volume measurements by ED and 3-D IVUS (r = 0.71), but our study is the first comparing the minimal luminal cross-sectional area.

Two- versus three-dimensional intravascular ultrasound: The relatively high variability of manual IVUS measurement can be minimized by automated boundary detection in 3-D IVUS.[11,15,27,28] In the present study, we obtained similar results by 2-D and 3-D IVUS, which may be partly explained by the use of a motorized pullback device, ensuring that images of the entire vascular segment were equally displayed. Automated lumen detection by 3-D IVUS was sometimes impaired by the acoustic shadowing behind larger deposits of calcium, because the algorithm may misinterpret the acoustic shadowing as lumen. Occasionally, manual correction was required because blood speckling near the stent was sometimes misinterpreted as tissue, explaining the slightly lower measurements by 3-D compared with 2-D IVUS.

These limitations and artifacts resulting from the systolic-diastolic movement of the imaging catheter[11,13,15] emphasize the need for careful interpretation of the 3-D IVUS measurements by an investigator experienced in this technique. Refinement of the segmentation algorithms will help to improve 3-D IVUS approaches in the future.

Videodensitometry: Unlike ED, VD is not dependent on the geometric stenosis profile; measurements rely on the optical density of the opacified lumen.[3,6–8] Measurement of luminal area is the basic quantification approach and, as observed in this study, a good correlation between IVUS and VD may thus be expected. Differences between the results obtained by ED and VD are less likely in a

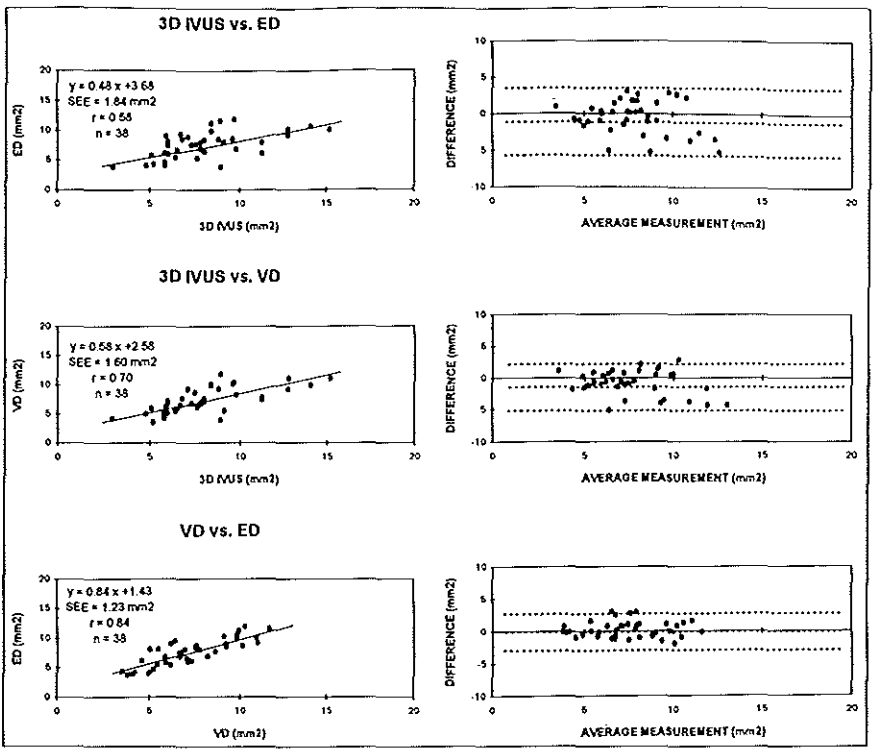

FIGURE 4. Comparison between the measurements obtained from 3-dimensional intravascular ultrasound (3-D IVUS) and edge detection (ED) and videodensitometry (VD), and between the findings of VD and ED. The results of the linear regression analyses are presented *(left)*. *Right,* the between-method difference is plotted against the average of the corresponding findings obtained from the methods being compared. *Dotted horizontal lines* indicate the mean between-method difference and +2 SD and −2 SD. The between-method difference ± 1 SD was −0.50 ± 2.28 mm², −0.79 ± 1.93 mm², and 0.28 ± 1.26 mm², respectively.

circular symmetric lumen, because luminal circularity is an elementary assumption in calculation of the minimal luminal area based on ED.[3] Accordingly, we found a good agreement between ED and VD, which confirmed previous observations after stenting and rotational atherectomy (r = 0.83 and 0.70, respectively).[4,7]

In the present study, the minimal luminal cross-sectional area, as measured by ED, was on average slightly larger than that by VD. This may reflect the dependence of ED on the angiographic projections used, particularly in relative luminal eccentricity. Moreover, side branches or other radiopaque structures projected on the reference segments may interfere with VD by increasing the brightness profile of the reference and may result in an underestimated minimal luminal cross-sectional area.[3] However, a previous in vitro study demonstrated a slight overestimation, potentially reflecting a contribution of the stent to the densitometrically determined values.[29] Based on current knowledge, the discordance between these observations and the results of the present study cannot be clarified. This unanswered question and the lack of comprehensive information about the correlation between IVUS and VD underline the necessity to define further the role of VD in the assessment of coronary interventions. The effort is certainly justified, as the effect of the new, highly radiopaque stents on VD measurements has yet to be determined. Our results clearly indicate a potential for VD in the assessment of luminal dimensions after coronary stenting.

1. Serruys PW, de Jaegere P, Kiemeneij F, Macaya C, Rutsch W, Heyndrickx G, Emanuelsson H, Marco J, Legrand V, Materne P, Belardi J, Sigwart U, Colombo A, Goy JJ, vd Heuvel P, Delcan J, Morel AA, for the Benestent Study Group. A comparison of balloon expandable stent implantation with balloon angioplasty in patients with coronary artery disease. *N Engl J Med* 1994;331:489–495.

2. Mancini GBJ. Quantitative coronary arteriographic methods in the interventional catheterization laboratory: an update and perspective. *J Am Coll Cardiol* 1991;17:23B–33B.

3. Escaned J, Haase J, Foley DP, Di Mario C, Den Boer A, Montauban van Swijndregt E, Serruys PW. Videodensitometry in percutaneous coronary interventions: a critical appraisal of its contributions and limitations. In: Serruys PW, Foley DP, de Feyter PJ, eds. Quantitative Coronary Angiography in Clinical Practice. Dordrecht: Kluwer Academic Publishers, 1994:69–87.

4. von Birgelen C, Umans V, Di Mario C, Keane D, Gil R, Prati F, de Feyter PJ, Serruys PW. Mechanism of high-speed rotational atherectomy and adjunc-

tive balloon angioplasty revisited by quantitative coronary angiography: edge detection versus videodensitometry. *Am Heart J* 1995;130:405–412.
5. Di Mario C, Haase J, den Boer A, Reiber JHC, Serruys PW. Edge detection versus densitometry in the quantitative assessment of stenosis phantoms: an in vivo comparison in porcine coronary arteries. *Am Heart J* 1992;124:1181–1189.
6. Serruys PW, Reiber JHC, Wijns W, v.d. Brand M, Kooijman CJ, ten Katen HJ, Hugenholtz PG. Assessment of percutaneous transluminal coronary angioplasty by quantitative coronary angiography: diameter versus densitometric area measurements. *Am J Cardiol* 1984;54:482–488.
7. Strauss BH, Juilliere Y, Rensing BJ, Reiber JHC, Serruys PW. Edge detection versus densitometry for assessing coronary stenting quantitatively. *Am J Cardiol* 1991;67:484–490.
8. Umans VA, Strauss BH, de Feyter PJ, Serruys PW. Edge detection versus videodensitometry for quantitative angiographic assessment of directional coronary atherectomy. *Am J Cardiol* 1991;68:534–539.
9. Colombo A, Hall P, Nakamura S, Almagor Y, Maiello L, Martini G, Gaglione A, Goldberg SL, Tobis JM. Intravascular stenting without anticoagulation accomplished with intravascular ultrasound guidance. *Circulation* 1995;91:1676–1688.
10. Goldberg SL, Colombo A, Nakamura S, Almagor Y, Maiello L, Tobis JM. Benefit of intravascular ultrasound in the deployment of Palmaz-Schatz stents. *J Am Coll Cardiol* 1994;24:996–1003.
11. Di Mario C, von Birgelen C, Prati F, Soni B, Li W, Bruining N, de Feyter PJ, Serruys PW, Roelandt JRTC. Three-dimensional reconstruction of two-dimensional intravascular ultrasound: clinical or research tool? *Br Heart J* 1995;73(suppl 2):26–32.
12. Matar FA, Mintz GS, Douek P, Farb A, Virmani R, Javier SP, Popma JJ, Pichard AD, Kent KM, Satler LF, Keller M, Leon MB. Coronary artery lumen volume measurement using three-dimensional intravascular ultrasound: validation of a new technique. *Cathet Cardiovasc Diagn* 1994;33:214–220.
13. Roelandt JRTC, Di Mario C, Pandian NG, Li W, Keane D, Slager CJ, de Feyter PJ, Serruys PW. Three-dimensional reconstruction of intravascular ultrasound images: rationale, approaches, problems, and directions. *Circulation* 1994;90:1044–1055.
14. Rosenfield K, Losordo DW, Ramaswamy K, Pastore JO, Langevin E, Razvi S, Kosowsky BD, Isner JM. Three-dimensional reconstruction of human coronary and peripheral arteries from images recorded during two-dimensional intravascular ultrasound examination. *Circulation* 1991;84:1938–1956.
15. von Birgelen C, Gil R, Ruygrok P, Prati F, Di Mario C, van der Giessen WJ, de Feyter PJ, Serruys PW. Optimized expansion of the Wallstent compared to the Palmaz-Schatz stent: online observations with two and three-dimensional intracoronary ultrasound after angiographic guidance. *Am Heart J* 1996;131:1067–1075.
16. Mintz GS, Pichard AD, Satler LF, Popma JJ, Kent KM, Leon MB. Three-dimensional intravascular ultrasonography: reconstruction of endovascular stents in vitro and in vivo. *Clin Ultrasound* 1993;21:609–615.
17. Mintz GS, Griffin J, Chuang YC, Pichard AD, Kent KM, Satler LF, Popma JJ, Leon MB. Reproducibility of the intravascular ultrasound assessment of stent implantation in saphenous vein grafts. *Am J Cardiol* 1995;75:1267–1270.
18. Haase J, Escaned J, van Swijndregt EM, Ozaki Y, Gronenschild E, Slager CJ, Serruys PW. Experimental validation of geometric and densitometric coronary measurements on the new generation cardiovascular angiography analysis system. *Cathet Cardiovasc Diagn* 1993;30:104–114.
19. Haase J, Keane D, Di Mario C, Escaned J, Slager CJ, Serruys PW. How reliable are geometric coronary measurements? In vitro and in vivo validation of digital and cinefilm-based quantitative coronary analysis systems. In: Serruys PW, Foley DP, de Feyter PJ, eds. Quantitative Coronary Angiography in Clinical Practice. Dordrecht: Kluwer Academic Publishers, 1994:27–49.
20. Bland JM, Altman DG. Statistical methods for assessing agreement between two methods of clinical measurement. *Lancet* 1986;1:307–310.
21. Ge J, Erbel R, Gerber T, Gorge G, Koch L, Haude M, Meyer J. Intravascular ultrasound imaging of angiographically normal coronary arteries: a prospective study in vivo. *Br Heart J* 1994;71:572–578.
22. Mudra H, Blasini R, Regar E, Klauss V, Rieber J, Theisen K. Intravascular ultrasound assessment of the balloon-expandable Palmaz-Schatz coronary stent. *Coron Artery Dis* 1993;4:791–799.
23. Haase J, Ozaki Y, Di Mario C, Escaned J, De Feyter PJ, Roelandt JRTC, Serruys PW. Can intravascular ultrasound correctly assess the luminal dimensions of coronary artery lesions? A comparison with quantitative angiography. *Eur Heart J* 1995;16:112–119.
24. Lowry RW, Kleiman NS, Raizner AE, Young JB. Is intravascular ultrasound better than quantitative coronary arteriography to assess cardiac allograft arteriopathy? *Cathet Cardiovasc Diagn* 1994;31:110–115.
25. Nakamura S, Mahon DJ, Maheswaran B, Gutfinger DE, Colombo A, Tobis J. An explanation for discrepancy between angiographic and intravascular ultrasound measurements after percutaneous transluminal coronary angioplasty. *J Am Coll Cardiol* 1995;25:633–639.
26. Hodgson J McB, Reddy KG, Suneja R, Nair RN, Lesnefsky EJ, Sheehan HM. Intracoronary ultrasound imaging: correlation of plaque morphology with angiography, clinical syndrome and procedural results in patients undergoing coronary angioplasty. *J Am Coll Cardiol* 1993;21:35–44.
27. Sonka M, Zhang X, Siebes M, DeJong S, McKay CR, Collins SM. Automated segmentation of coronary wall and plaque from intravascular ultrasound image sequences. In: Computers in Cardiology 1994. Los Alamitos, CA: IEEE Computer Society Press, 1994:281–284.
28. von Birgelen C, Slager CJ, Di Mario C, de Feyter PJ, Serruys PW. Volumetric intracoronary ultrasound: a new maximum confidence approach for the quantitative assessment of progression-regression of atherosclerosis? *Atherosclerosis* 1995;118(suppl):S103–113.
29. Strauss BH, Rensing BJ, Den Boer A, van der Giessen WJ, Reiber JHC, Serruys PW. Do stents interfere with the densitometric assessment of a coronary artery lesion? *Cathet Cardiovasc Diagn* 1991;24:259–264.

Chapter 6

Optimized expansion of the Wallstent compared with the Palmaz-Schatz stent: On-line observations with two- and three-dimensional intracoronary ultrasound after angiographic guidance

C von Birgelen, R Gil, P Ruygrok, F Prati, C Di Mario,
WJ van der Giessen, PJ de Feyter,
PW Serruys

Reprinted with permission from *Am Heart J* 1996;131:1067-1075

Optimized expansion of the Wallstent compared with the Palmaz-Schatz stent: On-line observations with two- and three-dimensional intracoronary ultrasound after angiographic guidance

Clemens von Birgelen, MD, Robert Gil, MD, Peter Ruygrok, MD, Francesco Prati, MD, Carlo Di Mario, MD, PhD, Wim J. van der Giessen, MD, PhD, Pim J. de Feyter, MD, PhD, and Patrick W. Serruys, MD, PhD *Rotterdam, The Netherlands*

Optimized stent expansion by high-pressure inflations of oversized balloons has initially been derived from experience obtained with the Palmaz-Schatz stent, whereas there is little experience with this strategy in the Wallstent. By using this approach with quantitative coronary angiographic guidance, 20 Wallstents and 20 Palmaz-Schatz stents were implanted in 34 patients and consecutively examined by conventional two-dimensional (2D) intracoronary ultrasound (ICUS) and three-dimensional (3D) ICUS on the basis of the application of a pattern recognition algorithm. Ultrasound criteria of adequate stent expansion were defined as a complete apposition of the stent to the vessel wall, a stent symmetry index (SSI = minimum/maximum lumen diameter) ≥0.7, and a stent-reference lumen area ratio (SRR = Minimum intrastent lumen area/Average of proximal and distal reference lumen area) ≥0.8. In all cases a smooth angiographic lumen and a negative diameter stenosis, on the basis of a distal reference, was achieved. For the Wallstents ICUS showed a higher SSI (2D, 0.95 ± 0.04 vs 0.85 ± 0.09; $p < 0.001$; 3D, 0.90 ± 0.09 vs 0.82 ± 0.11, $p < 0.05$) and a lower SRR (2D, 0.66 ± 0.12 vs 0.81 ± 0.13, $p < 0.005$; 3D, 0.63 ± 0.14 vs 0.74 ± 0.15, $p < 0.05$) than for the Palmaz-Schatz stents. Ninety percent of failure in meeting these criteria resulted from a low SRR. The incidence of incomplete stent apposition (one in both stents) or SSI <0.7 was low and generally associated with an SRR <0.8. The Wallstents met the ICUS criteria less often (2D, 2 (10%) vs 10 (50%), $p < 0.01$; 3D, 3 (15%) vs 9 (45%), $p < 0.05$), were significantly longer (35.1 ± 7.7 mm and 14.3 ± 3.3 mm, $p < 0.0001$), and generally demonstrated a larger vessel tapering, measured as proximal minus distal ICUS reference lumen area (1.33 ± 2.91 mm² vs 0.44 ± 1.97 mm², not significant). Wallstents meeting the ICUS criteria, however, showed less vessel tapering (0.18 ± 1.64 mm²). Thus optimized stent expansion was followed by excellent angiographic results for both Palmaz-Schatz and Wallstent. Although angiographic results and visual assessment of the ICUS examination suggested a good outcome, few Wallstents met the ICUS criteria in contrast to the Palmaz-Schatz stents. The low value of the SRR in the Wallstents is likely to be caused by vessel tapering, suggesting that this criterion may be unsuitable in assessing the adequacy of the expansion of relatively long stents such as the Wallstent. (Am Heart J 1996;131:1067-75.)

From the Thoraxcenter, Division of Cardiology, University Hospital, Erasmus University.

Dr. von Birgelen is a recipient of a fellowship of the German Research Society (DFG, Bonn, Germany).

Received for publication Sept. 12, 1995; accepted Oct. 23, 1995.

Reprint requests: Patrick W. Serruys, MD, PhD, Thoraxcenter, Erasmus University Rotterdam, Cardiac Catheterization and Intracoronary Imaging Laboratory, P.O. Box 1738, 3000 DR Rotterdam, The Netherlands.

0002-8703/96/$5.00 + 0 4/1/71360

Until recently coronary stenting has in many centers been performed only for acute or threatening vessel occlusion after balloon angioplasty.[1-8] The initial enthusiasm for coronary stenting[9] had been tempered by the high incidence of subacute thrombosis, which now appears to be significantly reduced by many factors, including coating the stent with heparin.[10] Optimization of the results of stenting, first promoted by the Milano group,[11-13] which performed high-pressure inflations of oversized balloons inside stents with intracoronary ultrasound (ICUS) guidance, is an alternative approach to meet the challenge of subacute stent thrombosis. Initial experience suggests[11] that this approach may even reduce the incidence of restenosis after coronary stenting.[14, 15] By changing the technique of coronary stenting from a more restrained to this vigorous approach, the problem of subacute occlusion[16] could be minimized, permitting stenting without anticoagulation and the inherent risk of bleeding.[11] The reduced incidence of subacute thrombosis by optimized stent deployment is achieved at the expense of a small but not insignificant risk of coronary dissection and rupture,[12, 17] emphasizing the necessity of defining certain criteria for safe and effective guidance of the intervention.

Table I. Characteristics of the population and stenting procedures

	Wallstent	*Palmaz-Schatz stent*
Stents	20	20
Patients	18	16
Patients with multiple stents	2 (15%)	4 (25%)
Age (yrs)	60.5 ± 8.8	60.9 ± 8.4
Male sex	13 (72%)	11 (69%)
Vessels		
LAD	3 (15%)	9 (45%)
LCX	0	1 (5%)
RCA	9 (45%)	10 (50%)
SVG	8 (40%)	0
Nominal stent length (mm)	35.1 ± 7.7	14.3 ± 3.3 $p < 0.00001$
Largest balloon (mm)	4.2 ± 0.6	3.6 ± 0.4 $p < 0.005$
Maximum pressure* (atm)	14.7 ± 3.7	15.1 ± 2.6 NS
Balloon:artery ratio	1.4 ± 0.3	1.3 ± 0.2 NS

LAD, Left anterior descending coronary artery; *LCX*, left circumflex coronary artery; *RCA*, right coronary artery; *SVG*, saphenous vein graft.
*Maximum pressure in the largest balloon.

Because the new concept has initially been applied with Palmaz-Schatz stents (Johnson & Johnson, Warren, N.J.), the ICUS criteria for optimized stent deployment[11-13] were primarily made on the basis of this stent with little experience in high-pressure expansion of the Wallstent (Schneider, Bulach, Switzerland), which has a characteristic structural design, length, and clinical application[18-22] that differs considerably from the Palmaz-Schatz stent.[23, 24] This observational study compares the practice and results of the optimized deployment of 20 Wallstents and 20 Palmaz-Schatz stents with quantitative angiography for guiding the procedure and ICUS for assessing the result. Because the potential of two- (2D) and three-dimensional (3D) ICUS in assessing the vessel wall[25-29] and stent[30, 31] geometry and the adequacy of stent deployment[11-13, 32-36] has recently been demonstrated, both conventional 2D and on-line reconstructed 3D ICUS were applied.

METHODS

Study population. The results of implantation of 20 Wallstents and 20 Palmatz-Schatz stents in American College of Cardiology/American Heart Association type B or C lesions[37, 38] without angiographic evidence of major calcification were examined on-line by quantitative coronary angiography and ICUS. The Wallstents were implanted in 18 patients and the Palmaz-Schatz stents in 16 patients aged 60.7 ± 8.5 years (range 46 to 73 years). The Wallstents were significantly longer than the Palmaz-Schatz stents ($p < 0.0001$). Table I gives further details.

Interventional procedure. All patients received 250 mg aspirin and 10,000 U heparin intravenously. During the entire procedure the activated clotting time was measured hourly and intravenous heparin was administered if required to maintain an activated clotting time of >300 seconds. After intracoronary injection of isosorbide dinitrate, the initial on-line quantitative coronary angiography (QCA) was performed. Predilation of the lesion by conventional balloon angioplasty was performed. The interpolated angiographic reference lumen diameter provided by QCA, the lesion length, and the presence of adjacent side branches were taken into account to select an appropriately sized self-expandable Wallstent. The nominal Wallstent diameter chosen was generally 1.5 mm larger than the interpolated reference diameter. A delivery balloon with a diameter corresponding to the interpolated reference lumen diameter was used to implant the Palmaz-Schatz stents.

Additional balloon inflations were performed inside all stents with a low-compliance balloon catheter with at least an 0.25 mm larger diameter than the interpolated angiographic lumen reference and a pressure of at least 14 atm. Progression to larger balloons was permitted to achieve a satisfactory angiographic result. Thus balloons with a maximum size of 4.2 ± 0.6 mm for the Wallstent and 3.6 ± 0.4 mm for the Palmaz-Schatz stent ($p < 0.005$) were inflated with maximum pressures of 14.7 ± 3.7 atm and 15.1 ± 2.6 atm (not significant, NS), respectively (Table I). The balloon/artery ratio was 1.4 ± 0.3 and 1.3 ± 0.2, respectively (NS). In the relatively long Wallstents the largest balloon size and the maximum pressure were frequently applied to only the proximal part of the stented segment. An angiographic appearance of a smooth lumen of the stented segment and a negative distal reference-based diameter stenosis were considered to be the procedural end points on the basis of QCA. After administration of intracoronary nitrates, the stented segment was examined by ICUS.

Quantitative coronary angiography. The computer-based Coronary Angiography Analysis System (CAAS II, Pie Medical Data, Maastricht, The Netherlands), previously described and validated in detail,[39, 40] was used to perform a geometric quantitative analysis. The boundaries of a selected coronary segment were detected by using a weighted sum of the first and second derivative functions of the brightness profile of each vessel scan. The absolute angiographic diameter of the stenosis was determined by using a contrast-free guiding catheter as a scaling device.[39] The measurements were performed on-line after intracoronary nitrates in two orthogonal views. Before stenting, the diameter function was used to determine the minimal lumen diameter, a computer-derived estimation of an interpolated reference diameter at the site of the lesion, and the obstruction length (Fig. 1). The *interpolated diameter stenosis before stenting* was calculated as (Intrastent minimal lumen diameter/Interpolated reference diameter) × 100%.

Because the segments directly adjacent to the stent are involved in the process of luminal enlargement after opti-

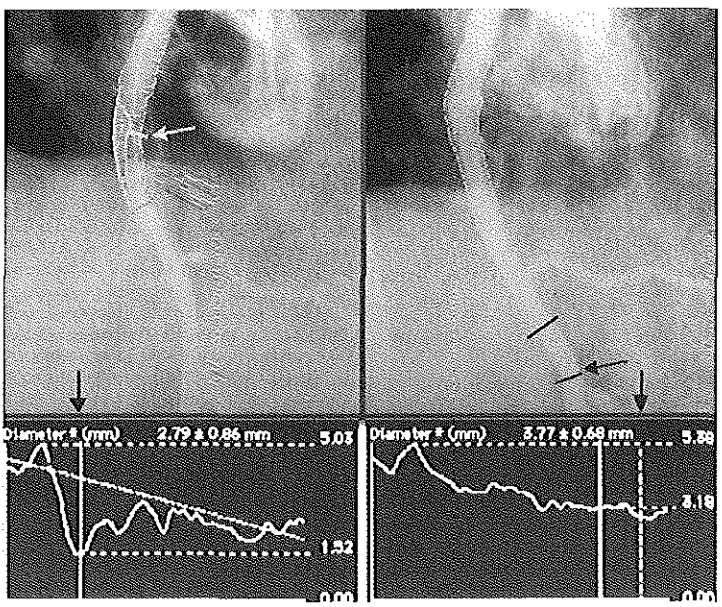

Fig. 1. Quantitative coronary angiography before *(left)* and after implantation of Wallstent *(right)* by CAAS II analysis system. On angiograms site of minimum lumen diameter is indicated by *line*. *Arrowhead* indicates site of reference measurement. Before stenting *(left)* interpolated reference at site of minimal lumen diameter was used to measure interpolated diameter stenosis. To calculate diameter stenosis after stenting *(right)* angiographically undiseased site up to 1 cm distal to stent was used as reference, showing diameter similar to interpolated reference before stenting.

mized stenting, the interpolated reference diameter was not used to calculate the percent diameter stenosis after stenting but the lumen diameter of an angiographically undiseased reference up to 1 cm distal to the stent without major side branches between the stent and the reference site (Fig. 1). The minimal lumen diameter was measured in the stented segment of the artery and the *distal reference-based diameter stenosis after stenting* was calculated as (Intrastent minimum lumen diameter/Distal reference lumen diameter) × 100%.

Image acquisition of ICUS. A 30-MHz single-element long-monorail ultrasound catheter with a 2.9F echotransparent distal sheath was used (MicroView, CVIS, Sunnyvale, Calif.). The common lumen of the sheath accomodates the imaging core and the guide wire but never both simultaneously. ICUS imaging was performed during a motorized uniform speed (1 mm/sec) pullback of the transducer inside the stationary imaging sheath, which allowed the transducer to move at the same speed as the ICUS handgrip inside the pullback device. The video signal was recorded on a high-resolution super VHS tape for conventional ICUS analysis.

Assessment by ICUS. After the pullback of the ultrasound catheter was completed, the videotape was used to obtain lumen area measurements of the ICUS references that were by definition 3 to 5 mm proximal and distal to the stented segment. Stent apposition to the vessel wall was reviewed over the entire stented segment. The ICUS image with the minimal intrastent lumen area was found by scrolling the videotape back and forth. On this cross-section, the lumen area was manually traced and the stent symmetry was assessed by measuring the minimum and maximum lumen diameter.

3D reconstruction of ICUS. Simultaneously with the video recording on s-VHS tape, video signals were also transferred to a 3D ICUS system (EchoQuant, Indec Systems Inc., Capitola, Calif.) that automatically acquires 8.5 images per second so that contiguous tomographic ICUS image slices, 118 μm apart, could be reconstructed on-line. The memory capacity of the 3D system operated by a second analyst allowed the acquisition and processing of a maximum of 255 images within 2 minutes; thus segments up to 30 mm long could be reconstructed. If Wallstents were longer than 30 mm, ICUS images recorded on videotape were used to reconstruct the proximal part of these stents.

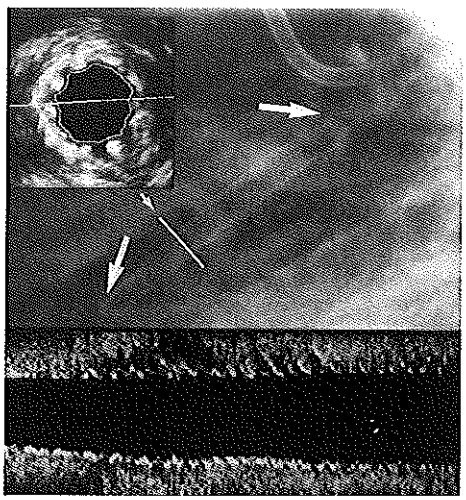

Fig. 2. Wallstent after implantation in left anterior descending coronary artery. *Arrowheads* indicate proximal and distal ends of stent on radiographic image *(upper panel)*. Location of 2D ICUS image *(insert)* is indicated by *small arrowhead*. Cross-sectional image is derived from 3D analysis system, performing semiautomated detection of blood pool on basis of application of pattern recognition algorithm. Longitudinal view *(lower panel)* is reconstructed, showing smooth tapering of luminal dimensions from proximal *(right)* to distal *(left)*. Besides 3D, conventional 2D analysis was performed in this study on basis of review of videotape and manual contour tracing.

Assessment by 3D ICUS. The 3D system provided a longitudinally reconstructed view (Fig. 2) that could be rotated around the longitudinal axis of the vessel segment. Furthermore, a cylindrical format was displayed cut open lengthwise and tilted back. The cylindrical view and more frequently the longitudinal display were used to evaluate the adequacy of stent strut apposition to the vessel wall. Automated image segmentation, on the basis of a pattern recognition algorithm (Acoustic Quantification)[25] that has previously been validated,[41] provided on the cross-sectional ICUS images of the entire reconstructed segment the measurement of the lumen area and the minimum and maximum diameters. The detected contour, indicating the lumen-intima boundary, was rapidly checked and manual correction could be performed on individual ICUS cross-sections. A display of the lumen area and corresponding diameter measurements facilitated the assessment. The minimum lumen area and the minimum and maximum lumen diameters were measured.

Adequate stent expansion by ICUS. During the ultrasound examination of the entire segment, criteria on the basis of our previous experience and slightly modified criteria of the Italian group[11] were applied to define adequate stent deployment. First, good *apposition to the vessel wall* had to be found at all sites of the stented segment. Moreover, the *stent symmetry index* (SSI), defined as ratio of minimal divided by maximal intrastent diameter, had to be ≥0.7 at the site of the minimal intrastent lumen area. The adequacy of the intrastent lumen area finally achieved was assessed by the *stent-reference lumen area ratio* (SRR), a ratio of the minimum intrastent divided by reference lumen area, which had to be ≥0.8. The reference lumen area was defined as the mean of the proximal and distal reference measurements; however, if only a single reference could be measured (e.g., ostial lesion), this measurement was used alone to calculate the SRR. During both 2D and 3D ICUS examinations, these criteria were applied to define an adequate result after the stenting procedure. After this examination was completed, each operator was free to perform additional balloon inflations inside the stent on the basis of the clinical situation and the angiographic or ICUS findings.

Statistics. Measurements of continuous parameters are given as mean ± 1 SD. The two-tailed student's *t* test for unpaired data analysis was used to compare the Wallstent group with the Palmaz-Schatz stent group, and a p value of <0.05 was considered statistically significant. Categorical variables were assessed using chi-square statistics.

RESULTS

Initial QCA. In the Wallstent and Palmaz-Schatz stent groups the minimal lumen diameter was 1.26 ± 0.48 mm and 1.04 ± 0.23 mm (NS) before stenting, and the obstruction length was 12.24 ± 4.25 mm and 8.18 ± 3.21 mm ($p < 0.005$), respectively. The interpolated reference diameter was 3.04 ± 0.76 mm and 2.86 ± 0.55 mm (NS), and the interpolated diameter stenosis was 58.1% ± 12.6% and 60.9% ± 9.2% (NS), respectively.

Angiographic results and clinical outcome. After stenting, a smooth lumen of the stented segment was obtained in all angiographic views and the QCA analysis revealed a negative distal reference-based diameter stenosis in all Wallstents and Palmaz-Schatz stents. The QCA results after the Wallstent and Palmaz-Schatz stent implantation did not differ significantly. In both the Wallstent and Palmaz-Schatz stent groups, a significant increase in the minimal lumen diameter and reduction of the percent diameter stenosis (Fig. 3) was observed ($p <$ 0.0001 for both). The minimal lumen diameter after stenting was 2.95 ± 0.39 mm for the Wallstent and 3.19 ± 0.51 mm for the Palmaz-Schatz stent (NS), and the distal reference-based diameter stenosis was −18.0% ± 11.2% and −17.3% ± 10.0% (NS), respectively. The interpolated reference diameter obtained before stenting and the distal reference diameter after stenting (2.84 ± 0.39 mm and 2.95 ± 0.45 mm

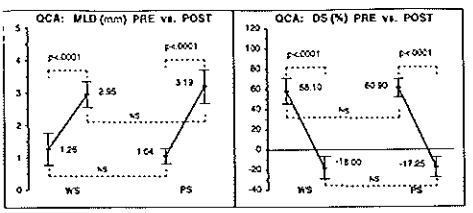

Fig. 3. QCA measurements before (PRE) and after (POST) implantation of Wallstent (WS) or Palmaz-Schatz stent (PS). In both stent groups minimal lumen diameter (MLD) increased significantly after stenting *(left panel)*. Diameter stenosis (DS), derived from interpolated reference before and distal reference measurement after stenting, was significantly reduced by intervention. Between Wallstents and Palmatz-Schatz stents no significant difference was observed.

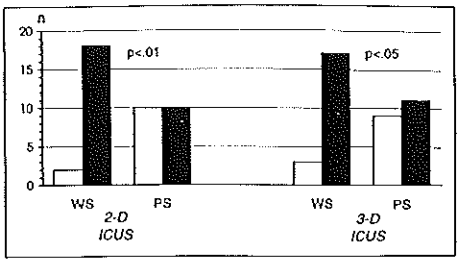

Fig. 4. ICUS criteria of adequate stent expansion met *(white bars)* or not met *(black bars)*. Both conventional 2D and 3D analysis of ICUS images demonstrated that Wallstents *(WS)* met ICUS criteria less frequently than the Palmaz-Schatz stents *(PS)*.

(NS) for the Wallstent group and Palmaz-Schatz stent group, respectively) did not differ significantly.

On the basis of QCA criteria of a smooth stented segment lumen and the realization of a negative percent diameter stenosis, all Wallstents and Palmaz-Schatz stents were successfully implanted. Anticoagulation was performed with aspirin and coumadine or ticlopidine at the operator's discretion. No procedural or post-procedural complications were encountered in either group before discharge.

ICUS assessment after stenting. The stent symmetry index (SSI) was significantly higher in the Wallstent than Palmaz-Schatz stent group (Table II). This difference was even more pronounced in the 2D ($p < 0.001$) than the 3D ICUS results ($p < 0.05$), demonstrating an SSI of 0.95 ± 0.04 and 0.90 ± 0.09 for the Wallstent group and 0.85 ± 0.09 and 0.82 ± 0.11 for the Palmaz-Schatz stent group, respectively. A significantly lower value of the stent-reference lumen area ratio (SRR) was measured in the Wallstent group compared with the Palmaz-Schatz stent group with both 2D (0.66 ± 0.12 vs 0.81 ± 0.13, $p < 0.005$) and 3D ICUS (0.63 ± 0.14 vs 0.74 ± 0.15, $p < 0.05$). The minimal lumen area of the Wallstents was slightly lower (NS) than the minimal lumen area of the Palmaz-Schatz stents (7.65 ± 2.05 mm^2 vs 8.98 ± 2.78 mm^2 by 2D ICUS and 7.62 ± 2.01 mm^2 vs 8.49 ± 3.18 mm^2 by 3D ICUS). No significant difference between the results of 2D and 3D ICUS measurements for the different parameters was found (Table II).

Two (10%) Wallstents and 10 (50%) Palmaz-Schatz stents ($p < 0.01$) met the ICUS criteria of adequate stenting by 2D ICUS (Fig. 4). By using 3D ICUS, 3 (15%) Wallstents and 9 (45%) Palmaz-Schatz stents were found to meet the ICUS criteria of adequate stent expansion ($p < 0.05$). A low SRR was the main reason for >90% of the failures in meeting the criteria. The incidence of an incomplete stent apposition to the vessel wall or an SSI <0.7 was low and mostly associated with a low SRR (Table III). The average ICUS reference lumen area was 12.50 ± 3.41 mm^2 proximally and 11.17 ± 3.07 mm^2 distally for the Wallstent group and 11.34 ± 2.68 mm^2 proximally and 10.89 ± 3.13 mm^2 distally for the Palmaz-Schatz stent group. Consequently, the tapering of the lumen area along the entire stented segment was higher (NS) in the Wallstent group (1.33 ± 2.91 mm^2) compared with the Palmaz-Schatz stent group (0.44 ± 1.97 mm^2). The Wallstents, which met the ultrasound criteria by 2D or 3D ICUS, had an average tapering of the lumen area of 0.18 ± 1.64 mm^2, and all but one were implanted in bypass grafts.

DISCUSSION

Procedure and anglographic assessment. On the initial angiogram the minimal stenosis lumen diameter, the reference lumen diameter, and the balloon-artery ratio were slightly higher for the Wallstent group, whereas the diameter of the maximum size balloon was significantly higher for these cases when compared with the Palmaz-Schatz stent group. This finding may reflect the fact that 40% of Wallstents were implanted in saphenous vein grafts, which usually show larger luminal dimensions than native coronary arteries. Indeed, the relatively long Wallstent is frequently implanted in vein grafts[18, 19] or mid–right coronary arteries without concern for side branches.

Recently, the effect of "conventional" nonopti-

Table II. 2D and 3D ICUS parameters after stenting

	Wallstent	*Palmaz-Schatz stent*	*p*
2D SSI	0.95 ± 0.04	0.85 ± 0.09	<0.001
3D SSI	0.90 ± 0.09	0.82 ± 0.11*	<0.05
2D MLA (mm^2)	7.65 ± 2.05	8.98 ± 2.78	NS
3D MLA (mm^2)	7.62 ± 2.01	8.49 ± 3.18*	NS
2D SRR	0.66 ± 0.12	0.81 ± 0.13	<0.005
3D SRR	0.63 ± 0.14	0.74 ± 0.15*	<0.05

MLA, Minimum lumen area.
*No significant difference between measurements by 2D and 3D intracoronary ultrasound.

Table III. Adequacy of stent expansion by ICUS

	Wallstent	*Palmaz-Schatz stent*
2D ICUS		
ICUS criteria fulfilled	2 (10%)	10 (50%)
ICUS criteria not fulfilled	18 (90%)	10 (50%)
SRR <80%	18	9
SSI <0.7 or incomplete apposition	0	1
SRR <80% and SSI <0.7	0	0
3D ICUS		
ICUS criteria fulfilled	3 (15%)	9 (45%)
ICUS criteria not fulfilled	17 (85%)	11 (55%)
SRR <80%	16	9
SSI <0.7 or incomplete apposition	0	0
SRR <80% and SSI <0.7	1	2

mized deployment of self-expandable and balloon-expandable stents on the stenosis geometry have been examined by our group on the basis of QCA, which demonstrated a similar improvement in stenosis geometry despite major differences in design and mechanical characteristics of the two stent types.[42] Also after angiographic optimization of the Palmaz-Schatz and Wallstent expansion in this study, the residual minimal lumen diameter did not show a statistically significant difference, although the minimal lumen diameter was slightly higher in the Palmaz-Schatz stent group. Nevertheless a smooth lumen contour with a negative distal reference-based diameter stenosis was observed in all stents. Thus no difference between the Palmaz-Schatz and Wallstents was observed in accomplishing an angiographic success.

ICUS assessment. For almost 2 decades angiography has been the standard method of examining the adequacy of coronary interventions.[39] However, it displays only the opacified luminal silhouette of the vessel. ICUS imaging visualizes the lumen and vessel wall[43-45] and depicts the stent architecture, permitting careful examination of its dimensions and apposition to the vessel wall.[11-13, 32-35, 46-48] The comprehensive insight into vessel and stent geometry provided by ICUS has played an important educational role in triggering and developing the concept of optimized stent deployment.[11-13] In this study the minimal lumen area of the Wallstent group and Palmaz-Schatz stent group did not differ significantly after stent implantation; however, a tendency towards a smaller minimal luminal dimension was found for the Wallstent group in accord with the angiographic findings.

Adequacy of stent expansion by ICUS. The ICUS criteria for safe and effective guidance to optimize stent expansion were developed on the basis of experience with Palmaz-Schatz stents,[11-13] although there has been little experience with the Wallstent with its characteristic design, length, and application.[18-22] In this study ICUS criteria employed in our center, derived from the experience with Palmaz-Schatz stents, were applied to both Palmaz-Schatz stents and Wallstents to help assess the criteria's value in evaluating optimized Wallstent expansion and to compare the application in the two different types of stents.

No difference in stent apposition to the vessel wall was observed between Palmaz-Schatz stents and Wallstents, but the SSI of both groups differed significantly and demonstrated a more symmetrical lumen shape in the Wallstent. Differences in stent design and mechanical properties between the tubular-slotted Palmaz-Schatz stent and the self-expandable wire-mesh Wallstent, which continues to exert active radial force on the vessel wall after deployment, may explain this finding.

A result that fulfilled the criteria for optimized stenting was achieved in 10% to 15% of the Wallstents compared with 45% to 50% of the Palmaz-Schatz stents. Incomplete stent apposition or an SSI <0.7 were infrequently observed and not significantly different between the Palmaz-Schatz and Wallstent groups. However, an SRR <0.8 despite an optimal angiographic result was responsible for the frequent ICUS-based judgment of inadequate stent deployment and accounted for the differences in fulfillment of the criteria of adequate stent expansion between Palmaz-Schatz stents and Wallstents.

The extent of vessel tapering[49] along the stented segment appears to be crucial for the SRR and may explain the significant difference between the SRR of Palmaz-Schatz and Wallstents despite good results by angiography and visual assessment of the ICUS images for both stent types (Fig. 5). In this study, segments treated by Wallstents, which were significantly longer than Palmaz-Schatz stents, showed relatively more pronounced vessel tapering, demon-

strated by the difference between the ICUS-measured proximal and distal reference lumen area that for the Wallstent was almost threefold greater than for the Palmaz-Schatz stent. Indeed, it is evident that a minimal lumen area at the distal end of a tapering stent may not meet the criterion of an SRR ≥0.8 if the difference between the distal and proximal reference lumen area is great, resulting in a relatively large mean reference lumen area. This is supported by the finding that the difference between proximal and distal reference lumen area of the Wallstents that met the SRR criterion was particularly low. The ICUS adequacy of the Palmaz-Schatz stent group supports previous observations reporting a 40% incidence of inadequate results after angiographically optimized stent expansion,[11] but data for the Wallstent have yet to be reported.

2D and 3D ICUS. Similar results for the various parameters were obtained by 2D and 3D ICUS. Measurements of the minimal lumen area by 3D ICUS were almost identical to those of 2D ICUS for the Wallstents. For the Palmaz-Schatz stents, a nonsignificant overestimation by the 2D ICUS was observed, but it remains unclear why this slight difference between 2D and 3D measurements was only observed in the relatively shorter Palmaz-Schatz stents and not in Wallstents. An overestimation of the minimal lumen area measurements by 2D ICUS may be expected because some sites of the vessel segment may be missed by visual examination and conventional 2D assessment. The differences between 2D and 3D measurements in this study may be small for two reasons. First, a motorized pullback of the ICUS transducer was performed, ensuring that 2D ICUS images of all sites of the entire vascular segment were equally displayed. This view may not always be guaranteed if the ICUS catheter is manipulated by hand. Second, the experience of the analysts who had previously performed more than 100 3D ICUS examinations enabled them to mentally obtain an approximate spatial picture of the vessel segment by 2D ICUS information.

Limitations. This study provides an insight into the clinical practice of the optimized expansion of the Palmaz-Schatz stent and Wallstent. The patient population was unselected and included a number of Wallstents in vein grafts. Because vein grafts show less vessel tapering than native coronary arteries and most Wallstents with adequate stent expansion by ICUS were placed in bypass grafts, differences between the ICUS findings of Palmaz-Schatz and Wallstents observed in this study are likely to be even more pronounced in a series of native coronary arteries. Further trials should try to address the issues raised by this study in homogeneous populations of either native coronary arteries or venous bypass grafts. Coronary angiography displays only the silhouette of the opacified lumen and provides no direct information on the apposition of the stent to the vessel wall. In clinical practice quantitative angiography[39] is further limited by foreshortening and overlapping vessels. The use of a distal reference diameter to calculate the percent diameter stenosis after stenting introduces certain subjectivity; however, this on-line QCA approach is feasible for the analysis after optimized stent deployment and takes the frequently fusiform angiographic shape of the stented vessel into account.

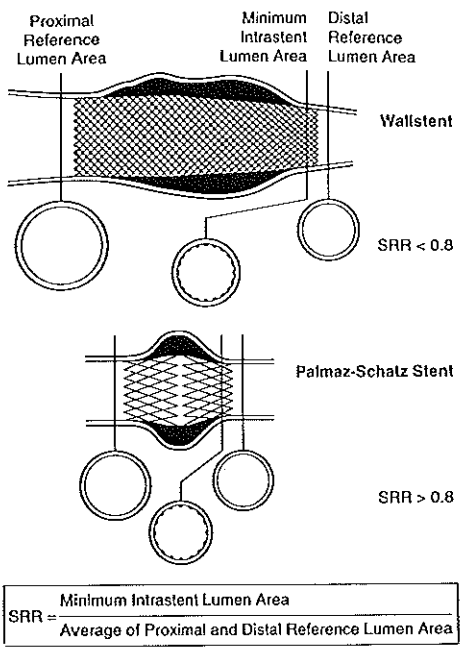

Fig. 5. Possible explanation for difficulty in achieving SRR ≥0.8 after Wallstent implantation. In this scheme Wallstent clearly tapers and does not fulfill SRR criterion because minimal lumen area is located near distal reference site, with lumen dimensions significantly smaller than proximal reference. Example of Palmaz-Schatz stent, however, shows little vessel tapering and is much more likely to fulfill SRR criterion.

ICUS consistently yields larger values of the luminal dimensions compared with quantitative angiography[50] and has some inherent limitations, such as the dependence on the angle of incidence of the

ultrasound beam and the relatively high variability of measurements on the basis of manual tracing.[51] The variability of measurements can be minimized by semiautomated boundary detection in 3D reconstructed ICUS.[25, 29, 41, 52-54] In this 3D ICUS study, the automated lumen detection was sometimes impaired by the echo shade behind larger deposits of calcium, and the quality of the 3D reconstruction was occasionally limited by artifacts resulting from the cyclic movement of the ICUS catheter and systolic-diastolic changes of the lumen dimensions.[25, 27, 29] The latter problem will be solved in the future by ECG-gated 3D reconstruction.[29] Because the 3D reconstructed view does not depict the true spatial orientation of the vessel segment,[29] careful interpretation by an experienced investigator was required.

Conclusions. Optimized stent expansion by high-pressure inflations of oversized balloons provided excellent angiographic results for both Palmaz-Schatz stents and Wallstents. 2D and 3D ICUS provided on-line valuable additional information without significant differences between the two approaches. The ultrasound criteria for adequate stent expansion, which evolved from the use of ICUS in Palmaz-Schatz stents, indicated a good result in half of the Palmaz-Schatz stents but few Wallstents, although the angiographic findings and visual assessment of the ICUS images suggested a good outcome. Stent symmetry index and apposition to the vessel wall could be well examined in the Wallstents, whereas the stent-reference lumen area ratio (SRR) infrequently fulfilled the ICUS criteria for adequate stent expansion. We suggest that this is likely caused by vessel tapering and differences between the proximal and distal reference lumen dimensions. Thus the standard SRR criterion appears to be unsuitable in assessing relatively long stents such as the Wallstent.

REFERENCES

1. Colombo A, Goldberg SL, Almagor Y, Maiello L, Finci L. A novel strategy for stent deployment in the treatment of acute or threatened closure complicating balloon coronary angioplasty: use of a short or standard (or both) single or multiple Palmaz-Schatz stents. J Am Coll Cardiol 1993;22:1687-91.
2. De Feyter PJ, De Scheerder I, Van den Brand M, Laarman GJ, Suryapranata H, Serruys PW. Emergency stenting for refractory acute coronary artery occlusion during coronary angioplasty. Am J Cardiol 1993;66:1147-50.
3. Fishman DL, Savage MP, Leon MB, Schatz RA, Ellis SG, Cleman MW, et al. Effect of intracoronary stenting on intimal dissection after balloon angioplasty: results of quantitative coronary analysis. J Am Coll Cardiol 1991;18:1445-51.
4. George BS, Voorhees WD, Roubin GS, Fearnot NE, Pinkerton CA, Raizner AE, et al. Multicenter investigation of coronary stenting to treat accute or threatened closure after percutaneous transluminal coronary angioplasty: clinical and angiographic outcomes. J Am Coll Cardiol 1993;22:135-43.
5. Haude M, Erbel R, Straub U, Dietz U, Schatz R, Meyer J. Results of intracoronary stents for management of coronary dissection after balloon angioplasty. Am J Cardiol 1991;67:691-6.
6. Herrman HC, Buchbinder M, Clemen MW, Fishman D, Goldberg S, Leon MB, et al. Emergent use of balloon-expandable coronary artery stenting for failed percutaneous transluminal coronary angioplasty. Circulation 1992;86:812-9.
7. Maiello L, Colombo A, Gianrossi R, McCanny R, Finci L. Coronary stenting for treatment of acute or threatened closure following dissection after coronary balloon angioplasty. Am Heart J 1993;125: 1670-5.
8. Roubin GS, Cannon AD, Agrawal SK, Macander PJ, Dean LS, Baxley WA, et al. Intracoronary stenting for acute and threatened closure complicating percutaneous transluminal coronary angioplasty. Circulation 1992;85:916-27.
9. Sigwart U, Puel J, Mirkovitch V, Joffre F, Kappenberger L. Intravascular stents to prevent occlusion and restenosis after transluminal angioplasty. N Engl J Med 1987;316:701-6.
10. van Beusekom HMM, Serruys PW, van der Giessen WJ. Coronary stent coatings. Coron Art Dis 1994;5:590-6.
11. Colombo A, Hall P, Nakamura S, Almagor Y, Maiello L, Martini G, et al. Intracoronary stenting without anticoagulation accomplished with intravascular ultrasound guidance. Circulation 1995;91:1676-88.
12. Goldberg SL, Colombo A, Nakamura S, Almagor Y, Maiello L, Tobis JM. Benefit of intracoronary ultrasound in the deployment of Palmaz-Schatz stents. J Am Coll Cardiol 1994;24:996-1003.
13. Nakamura S, Colombo A, Gaglione A, Almagor Y, Goldberg SL, Maiello L, et al. Intracoronary ultrasound observations during stent implantation. Circulation 1994;89:2026-34.
14. Fishman DL, Leon MB, Baim DS, Schatz RA, Savage MP, Penn I, et al. for the Stent REStenosisi Study (STRESS) Investigators. A randomized comparison of coronary stent placement and balloon angioplasty in the treatment of coronary artery disease. N Engl J Med 1994;331:496-501.
15. Serruys PW, de Jaegere P, Kiemeneij F, Macaya C, Rutsch W, Hendrickx G, et al. for the Benestent Study Group. A comparison of balloon expandable stent implantation with balloon angioplasty in patients with coronary artery disease. N Engl J Med 1994;331:489-95.
16. Haude M, Erbel R, Issa H, Straub U, Rupprecht HJ, Treese N, et al. Subacute thrombotic complications after intracoronary implantation of Palmaz-Schatz stents. Am Heart J 1993;126:15-22.
17. Reimers B, von Birgelen C, van der Giessen WJ, Serruys PW. A word of caution on optimizing stent deployment in calcified lesions: a case of acute coronary rupture with cardiac tamponade. Am Heart J 1996;131:192-4.
18. Strauss BH, Serruys PW, Bertrand ME, Puel J, Meier B, Goy JJ, et al. Quantitative angiographic follow-up of the coronary Wallstent in native vessels and bypass grafts (European experience—March 1986 to March 1990). Am J Cardiol 1992;69:476-81.
19. Keane D, Buis B, Reifart N, Plokker TH, Ernst J, Mast E, et al. Clinical and angiographic outcome following implantation of the less shortening Wallstent in aorto-coronary vein grafts: introduction of a second generation stent in the clinical arena. J Interven Cardiol 1994;7:557-64.
20. Keane D, de Jaegere P, Serruys PW. Structural design, clinical experience, and current indications of the coronary Wallstent. Cardiology Clinics 1994;12:689-97.
21. Serruys PW, Strauss BH, Beatt KJ, Bertrand M, Puel J, Rickards AF, et al. Angiographic follow-up after placement of a self-expanding coronary stent. N Engl J Med 1991;324:13-7.
22. Strauss BH, Serruys PW. The coronary Wallstent. In: Topol EJ, editor. Textbook of Interventional Cardiology, 2nd ed. Philadelphia: WB Saunders, 1994:687-701.
23. Schatz RA, Baim DS, Leon M, Ellis SG, Goldberg S, Hirshfeld JW, et al. Clinical experience with the Palmaz-Schatz coronary stent (initial results of a multicenter study). Circulation 1991;83:148-61.
24. Haude M, Erbel R, Straub U, Dietz U, Meyer J. Short and long term results after intracoronary stenting in human coronary arteries: monocenter experience with the balloon-expandable Palmaz-Schatz stent. Br Heart J 1991;66:337-45.
25. Di Mario C, von Birgelen C, Prati F, Soni B, Li W, Bruining N, et al. Three-dimensional reconstruction of two-dimensional intracoronary

ultrasound: clinical or research tool? Br Heart J 1995;73(2 Suppl):26-32.
26. Matar FA, Mintz GS, Douek P, Farb A, Virmani R, Javier SP, et al. Coronary artery lumen volume measurement using three-dimensional intravascular ultrasound: validation of a new technique. Cathet Cardiovasc Diagn 1994;33:214-20.
27. Roelandt JRTC, Di Mario C, Pandian NG, Li W, Keane D, Slager CJ, et al. Three-dimensional reconstruction of intracoronary ultrasound images: rationale, approaches, problems, and directions. Circulation 1994;90:1044-55.
28. Rosenfield K, Losordo DW, Ramaswamy K, Pastore JO, Langevin E, Razvi S, et al. Three-dimensional reconstruction of human coronary and peripheral arteries from images recorded during two-dimensional intravascular ultrasound examination. Circulation 1991;84:1938-56.
29. von Birgelen C, Di Mario C, Prati F, Bruining N, Li W, de Feyter PJ, et al. Intracoronary ultrasound: three-dimensional reconstruction techniques. In: de Feyter PJ, Di Mario C, Serruys PW, editors. Quantitative coronary imaging. Rotterdam: Barjesteh Meeuwes, 1995:181-97.
30. Mintz GS, Pichard AD, Satler LF, Popma JJ, Kent KM, Leon MB. Three-dimensional intravascular ultrasonography: reconstruction of endovascular stents in vitro and in vivo. Clin Ultrasound 1993;21:609-16.
31. Schryver TE, Popma JJ, Kent KM, Leon MB, Eldredge S, Mintz GS. Use of intracoronary ultrasound to identify the "true" coronary lumen in chronic coronary dissection treated with intracoronary stenting. Am J Cardiol 1992;69:1107-8.
32. Mudra H, Klauss V, Blasini R, Kroetz M, Rieber J, Regar E, et al. Ultrasound guidance of Palmaz-Schatz intracoronary stenting with a combined intravascular ultrasound balloon catheter. Circulation 1994;90:1252-61.
33. Painter JA, Mintz GS, Wong SC, Popma JJ, Pichard AD, Kent KM, et al. Serial intravascular ultrasound studies fail to show evidence of chronic Palmaz-Schatz stent recoil. Am J Cardiol 1995;75:398-400.
34. Kiemeneij F, Laarman GJ, Slagboom T. Mode of deployment of coronary Palmaz-Schatz stents after implantation with the stent delivery system: an intravascular ultrasound study. Am Heart J 1995;123:638-44.
35. Laskey WL, Brady ST, Kussmaul WG, Waxler AR, Krol J, Herrmann HC, et al. Intravascular ultrasonographic assessment of the results of coronary artery stenting. Am Heart J 1993;125:1576-83.
36. Prati F, Di Mario C, von Birgelen C, Gil R, de Feyter PJ, de Jaegere P, et al. Usefulness of on-line 3D reconstruction for stent implantation [abstract]. J Am Coll Cardiol 1995;25:9-10A.
37. Ellis SG, Vandormael MG, Cowley MJ, Di Sciascio G, Deligonul U, Topol EJ, et al. and the multivessel angioplasty prognosis group. Coronary morphologic and clinical determinants of procedural outcome with angioplasty for multivessel coronary disease. Circulation 1990;82:1193-202.
38. Ryan TJ, Faxon DP, Kennedy JW, King SB III, Loop FD, Peterson KL, et al. Guidelines for percutaneous transluminal coronary angioplasty: a report of the American College of Cardiology/American Heart Association task force on assessment of diagnostic and therapeutic cardiovascular procedures (subcommittee on percutaneous transluminal coronary angioplasty). J Am Coll Cardiol 1988;12:529-45 and Circulation 1988;78:486-502.
39. Keane D, Serruys PW. Quantitative coronary angiography: an integral component of interventional cardiology. In: Topol EJ, Serruys PW, editors. Current review of interventional cardiology, 2nd ed. Philadelphia: Current Medicine, 1995:205-33.
40. Haase J, Escaned J, van Swijndregt EM, Ozaki Y, Gronenschild E, Slager CJ, et al. Experimental validation of geometric and densitometric coronary measurements on the new generation cardiovascular angiography analysis system. Cathet Cardiovasc Diagn 1993;30:104-14.
41. Hausmann D, Friedrich G, Sudhir K, Mullen WL, Soni B, Fitzgerald PJ, et al. 3D intravascular ultrasound imaging with automated border detection using 2.9 F Catheters [abstract]. J Am Coll Cardiol 1994;23:174A.
42. De Jaegere PP, Strauss BH, van der Giessen WJ, de Feyter PJ, Serruys PW. Immediate changes in stenosis geometry following stent implantation: comparison between a self-expandable and a balloon expandable stent. J Interven Cardiol 1992;5:71-8.
43. Ge J, Erbel R, Gerber T, Gorge G, Koch L, Haude M, et al. Intravascular ultrasound imaging of angiographically normal coronary arteries: a prospective study in vivo. Br Heart J 1994;71:572-8.
44. Nissen SE, Gurley JC, Grines CL, Booth DC, McClure R, Berk M, et al. Intravascular ultrasound assessment of lumen size and wall morphology in normal subjects and patients with coronary artery disease. Circulation 1991;84:1087-99.
45. Tobis JM, Mallery J, Mahon D, Lehmann K, Zalesky P, Griffith J, et al. Intravascular ultrasound imaging of human coronary arteries in vivo. Circulation 1991;83:913-26.
46. Mudra H, Blasini R, Regar E, Klauss V, Rieber J, Theisen K. Intravascular ultrasound assessment of the balloon-expandable Palmaz-Schatz coronary stent. Coron Art Dis 1993;4:791-99.
47. Slepian MJ. Application of intraluminal ultrasound imaging to vascular stenting. Int J Card Imaging 1991;6:285-311.
48. Tenaglia AN, Kisslo K, Kelly S, Hamm MA, Crowely R, Davidson CJ. Ultrasound guide wire-directed stent deployment. Am Heart J 1993;125:1213-6.
49. Javier SP, Mintz GS, Popma JJ, Pichard AD, Kent KM, Satler LF, et al. Intravascular ultrasound assessment of the magnitude and mechanism of coronary artery and lumen tapering. Am J Cardiol 1995;75:177-80.
50. Haase J, Ozaki Y, Di Mario C, Escaned J, De Feyter PJ, Roelandt JRTC, et al. Can intracoronary ultrasound correctly assess the luminal dimensions of coronary artery lesions? A comparison with quantitative angiography. Eur Heart J 1995;16:112-9.
51. Hausmann D, Lundkvist AJS, Friedrich GJ, Mullen WL, Fitzgerald PJ, Yock PG. Intracoronary ultrasound imaging: intraobserver and interobserver variability of morphometric measurements. Am Heart J 1994;128:674-80.
52. von Birgelen C, Di Mario C, Li W, Camenzind E, Ozaki Y, de Feyter PJ, et al. Volumetric quantification in intracoronary ultrasound: validation of a new automatic contour detection method with integrated user interaction [abstract]. Circulation 1994;90:I-550.
53. von Birgelen C, Di Mario C, Li W, Schuurbiers JCH, Slager CJ, Ruygrok P, et al. Clinical application of a new computerized method measuring coronary artery dimensions by three-dimensional intracoronary ultrasound: reproducibility in vivo during coronary interventions [abstract]. Eur Heart J 1995;16:428.
54. Sonka M, Zhang X, Siebes M, DeJong S, McKay CR, Collins SM. Automated segmentation of coronary wall and plaque from intravascular ultrasound image sequences. In: Computers in cardiology 1994. Los Alamitos, Calif.: IEEE Computer Society Press, 1994:281-4.

Chapter 7

Electrocardiogram-gated intravascular ultrasound image acquisition after coronary stent deployment facilitates on-line three-dimensional reconstruction and automated lumen quantification

C von Birgelen, GS Mintz, A Nicosia, DP Foley,
WJ van der Giessen, N Bruining, SG Airiian,
JRTC Roelandt, PJ de Feyter,
PW Serruys

Reprinted with permission from *J Am Coll Cardiol* 1997;30:436-443

Electrocardiogram-Gated Intravascular Ultrasound Image Acquisition After Coronary Stent Deployment Facilitates On-Line Three-Dimensional Reconstruction and Automated Lumen Quantification

CLEMENS VON BIRGELEN, MD,* GARY S. MINTZ, MD, FACC,† ANTONINO NICOSIA, MD, DAVID P. FOLEY, MB, MRCPI, PHD, WIM J. VAN DER GIESSEN, MD, PHD, NICO BRUINING, BSC, SERGEI G. AIRIAN, MD, JOS R. T. C. ROELANDT, MD, PHD, FACC, PIM J. DE FEYTER, MD, PHD, FACC, PATRICK W. SERRUYS, MD, PHD, FACC

Rotterdam, The Netherlands and Washington, D.C.

Objectives. This study evaluates the feasibility, reliability and reproducibility of electrocardiogram (ECG)-gated intravascular ultrasound (IVUS) image acquisition during automated transducer withdrawal and automated three-dimensional (3D) boundary detection for assessing on-line the result of coronary stenting.

Background. Systolic-diastolic image artifacts frequently limit the clinical applicability of such automated analysis systems.

Methods. In 30 patients, after successful angiography-guided implantation of 34 stents in 30 target lesions, we carried out IVUS examinations on-line with the use of ECG-gated automated 3D analyses and conventional manual analyses of two-dimensional images from continuous pullbacks. These on-line measurements were compared with off-line 3D reanalyses. The adequacy of stent deployment was determined by using ultrasound criteria for stent apposition, symmetry and expansion.

Results. Gated image acquisition was successfully performed in all patients to allow on-line 3D analysis within 8.7 ± 0.6 min (mean ± SD). Measurements by on-line and off-line 3D analyses correlated closely ($r \geq 0.95$), and the minimal stent lumen differed only minimally (8.6 ± 2.8 mm^2 vs. 8.5 ± 2.8 mm^2, p = NS). The conventional analysis significantly overestimated the minimal stent lumen (9.0 ± 2.7 mm^2, $p < 0.005$) in comparison with results of both 3D analyses. Fourteen stents (41%) failed to meet the criteria by both 3D analyses, all of these not reaching optimal expansion, but only 7 (21%) were detected by conventional analysis ($p < 0.02$). Intraobserver and interobserver comparison of stent lumen measurements by the automated approach revealed minimal differences (0.0 ± 0.2 mm^2 and 0.0 ± 0.3 mm^2) and excellent correlations ($r = 0.99$ and 0.98, respectively).

Conclusions. ECG-gated image acquisition after coronary stent deployment is feasible, permits on-line automated 3D reconstruction and analysis and provides reliable and reproducible measurements; these factors facilitate detection of the minimal lumen site.

(J Am Coll Cardiol 1997;30:436–43)

Intravascular ultrasound (IVUS) permits detailed, high quality cross-sectional imaging of the coronary arteries in vivo. The normal coronary artery architecture, the major components of the atherosclerotic plaque and, in particular, changes that occur in coronary artery dimensions and anatomy during and after transcatheter therapy can be studied in vivo in a manner otherwise not possible (1–4). This includes direct visualization of intensely echoreflective (but radiolucent) stainless steel stent struts (5–11). In an attempt to reduce both the analysis time and the variability involved in planar IVUS measurements, automated three-dimensional (3D) image reconstruction and analysis systems have been developed (10–20). However, cyclic changes in coronary dimensions and the movement of the IVUS catheter relative to the coronary vessel wall frequently cause image artifacts (Fig. 1) that generally represent an important limitation to the applicability of 3D systems for quantitative analysis (17,21,22).

One method of limiting cyclic artifacts combines electrocardiogram (ECG)-gated image acquisition (22) and a previously validated program for automated 3D IVUS boundary detection (18,19). We applied this technique to the analysis of 34 coronary stents after successful angiography-guided implantation to determine the feasibility, reliability and reproducibility of this approach to assessing on-line procedural results.

From the Thoraxcenter, Division of Cardiology, University Hospital Rotterdam-Dijkzigt and Erasmus University, Rotterdam, The Netherlands; and †Washington Hospital Center, Washington, D.C. Dr. von Birgelen is the recipient of a fellowship of the German Research Society (DFG, Bonn, Germany).

Manuscript received December 10, 1996; revised manuscript received March 25, 1997, accepted April 16, 1997.

*Present address: Department of Cardiology, University Hospital Essen, Hufelandstrasse 55, 45122 Essen, Germany.

Address for correspondence: Patrick W. Serruys, Thoraxcenter, University Hospital Dijkzigt, P.O. Box 1738, 3000 DR Rotterdam, The Netherlands.

Abbreviations and Acronyms
CSA = cross-sectional area
ECG = electrocardiogram, electrocardiographic
IVUS = intravascular ultrasound
3D = three-dimensional
2D = two-dimensional

Methods

Study patients. The study was approved by the Medical Ethical Committee of the Erasmus University Hospital, Rotterdam. All patients provided written informed consent. The study group consisted of 30 patients (24 men, 6 women, mean age ± SD 59.1 ± 8.4 years) who had 34 stents implanted in 30 target lesions. To simplify the ECG-gated acquisition procedure, we chose for the study only patients who had 1) sinus rhythm, 2) ≤10 extrasystoles/min, and 3) no permanent or temporary pacemaker implantation.

Intervention procedures and coronary angiography. All patients received intravenous aspirin (250 mg) and heparin (10,000 U), and subsequent heparin was administered hourly to maintain an activated clotting time >300 s. The percutaneous transluminal angioplasty procedures were performed by using 8F femoral artery sheaths and 8F guiding catheters. All patients were undergoing elective stent implantation for stable (n = 14) or unstable (n = 16) angina; therefore, conservative balloon predilation was performed to enable stent placement but avoid unnecessary dissection. The stents were placed in the right (n = 20), left anterior descending (n = 9) and left circumflex (n = 5) coronary arteries. The following stents were used: Palmaz-Schatz stent (Johnson & Johnson Interventional Systems, n = 15); Wallstent (Schneider, Bulach, Switzerland, n = 11); Cordis balloon expandable coiled stent (Cordis Corporation, n = 4), Multilink stent (Advanced Cardiovascular Systems, n = 2); AVE Microstent (Applied Vascular Engineering, Edmonton, Alberta, Canada, n = 1); and NIR stent (Medinol, Ltd., Tel Aviv, Israel, n = 1). After the procedure, all patients were treated with an antiplatelet regimen of aspirin and ticlopidine.

On-line quantitative coronary angiography was performed with the CAAS II system (Pie Medical, Maastricht, The Netherlands) according to previously described methodology (10,11). The maximal diameter of the target segment and the interpolated reference diameter were used to select the diameter of the balloon-expandable stents. The interpolated reference diameter of the stented coronary segments ranged from 2.5 to 4.7 mm. The proximal and distal vessel diameter, interpolated reference diameter and lesion length were taken into account to select an appropriately sized self-expanding Wallstent (11). Adjunct balloon angioplasty was performed by using low compliance balloon catheters with a maximal nominal size of 3.74 ± 0.44 mm (balloon/preintervention reference = 1.24 ± 0.21; balloon/postintervention reference = 1.04 ± 0.14) at a maximal pressure of 16.4 ± 1.7 atm.

After IVUS imaging was performed, any further treatment was left to the discretion of the operator. Although additional IVUS examinations were not part of the protocol, and were, in fact, not performed, the operator was free to perform them, if he or she considered them necessary.

Angiographic end points. All procedures had achieved angiographic success before IVUS examinations were performed. A procedure was considered angiographically successful if all of the following three criteria were met: 1) smooth contour of the lumen silhouette in the stented segment, 2) diameter stenosis inside the stent in the "worst" (of at least two orthogonal) views <15% by quantitative on-line analysis, and 3) no inflow or outflow obstruction. IVUS examination was then performed.

IVUS imaging. IVUS imaging was performed after bolus injection of intracoronary nitroglycerin with use of a commercially available mechanical sector scanner (CardioVascular Imaging Systems) and 2.9F sheath-based IVUS catheters (MicroView, CardioVascular Imaging Systems). This catheter incorporates a 15-cm long sonolucent distal imaging sheath that alternatively houses the guide wire (during catheter introduction) or, after the guide wire has been pulled back, the 30-MHz beveled single-element transducer (during imaging).

First, a continuous motorized pullback of the IVUS transducer at a pullback speed of 0.5 mm/s (within the imaging sheath) was performed for conventional on-line two-dimensional (2D) cross-sectional IVUS analysis. Next, the transducer was readvanced for ECG-gated image acquisition. The basic settings of the IVUS machine remained unchanged to ensure an equal image quality during both pullbacks. Between both pullbacks there were no significant changes in the patients' heart rate and no differences in the occurrence of arrhythmias. The ECG-triggered pullback device uses a step-

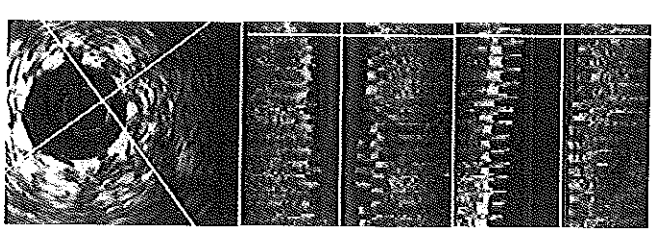

Figure 1. Cyclic artifact in 3D IVUS image set of stented coronary segment. Center and right panels, Saw-shaped artifacts in two perpendicular longitudinal sections after *non-gated* image acquisition, resulting from the cyclic movement of the echo-transducer relative to the coronary wall, may limit the on-line applicability of systems for automated contour detection. Left panel, Cross-sectional image corresponding to the horizontal cursor in the longitudinal sections.

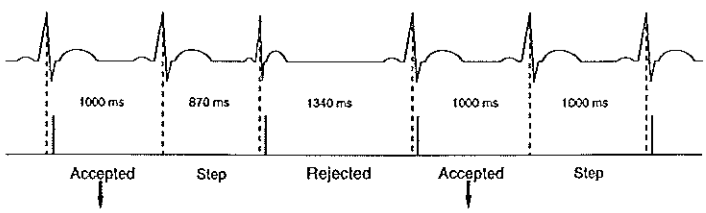

Figure 2. Principle of ECG-gated image acquisition and stepwise pullback. Images were acquired 40 ms after the peak of the R wave and only *accepted* for computer storage (arrows) if the time interval between two successive R waves met a predefined range. This range was based on data (mean RR interval ± 50 ms), taken before imaging was performed. If an RR interval was too long or short, images were *rejected*, and the transducer remained at this site until the image could be acquired during a heart cycle with an appropriate RR interval length. During the following heart cycle, the transducer was withdrawn 200 μm (Step) to the adjacent image acquisition site.

ping motor to withdraw the transducer in 0.2-mm axial increments through the stationary imaging sheath. The ECG-triggered pullback device is controlled by a 3D ultrasound work station (23) (EchoScan, TomTec, Munich, Germany). The work station receives a video input from the IVUS machine and an ECG signal from the patient. It measures the RR intervals over a 2-min period preceding the imaging sequence to define the upper and lower limits of acceptable RR intervals (mean value ± 50 ms). During the imaging sequence it considers heart rate variability and checks for the presence of extrasystoles. If the RR interval meets the preset range, images are 1) acquired 40 ms after the peak of the R wave, 2) digitized (by the work station), and 3) stored in the computer memory. After an image is acquired, the IVUS transducer is withdrawn 0.2 mm to acquire the next image at that site (Fig. 2).

IVUS analysis protocol. All 34 stented lesions were analyzed on-line by two experienced IVUS analysts who had no knowledge of each other's results. One analyst (called the "2D analyst") performed conventional manual tracing of the cross-sectional IVUS images. The second analyst (called the "3D analyst") analyzed the ECG-gated 3D IVUS images (18,19). The senior interventional cardiologists of the department decided that, to be clinically useful, all on-line analyses should be completed within ≤10 min.

After an interval of ≥4 weeks, the 3D analyst performed a blinded off-line reanalysis of the stored ECG-gated image set from all 34 stents. This off-line reanalysis had no time limit. Each image was carefully checked, the videotape was used to confirm the automated measurements, even small deviations were corrected, and the results were approved by two independent cardiologists, experienced in the use and analysis of IVUS imaging. The off-line reanalysis was performed within 28.7 ± 5.9 min and represented the maximal confidence measurements.

Intraobserver and interobserver variability of on-line 3D measurements of the stent cross-sectional area were determined from 10 randomly selected digitized stent image data sets (for a total of 1,112 cross-sectional IVUS images). Because actual on-line conditions cannot be reproduced, this comparison was obtained from simulated on-line conditions, especially a maximal analysis time of 10 min. Intraobserver variability was determined from repeated measurements performed by the 3D analyst; interobserver variability was determined by comparing the measurements of the 3D analyst and those of a third analyst who had no knowledge of previous data.

2D quantitative IVUS analysis. By using previously validated manual contour tracing techniques (24), the minimal lumen cross-sectional area (CSA) within the stented segment was measured and compared with the proximal and distal reference lumen CSA. These reference measurements were obtained from the most normal-looking cross-sections within 5 mm proximal and distal to the stent edges. In addition, the stent symmetry index (minimal/maximal stent diameter) was measured at the minimal lumen CSA site.

3D quantitative IVUS analysis. Quantitative 3D IVUS analysis was performed by using a contour detection program (Fig. 3) developed at the Thoraxcenter, Rotterdam. This system allows the automated analysis of up to 200 IVUS images. Two longitudinal sections are constructed in which contour detection is performed to identify regions of interest (center and range for boundary searching) on planar images. This procedure facilitates automated detection of the lumen boundary on the planar images with use of the minimum cost algorithm (18,19). The axial location of an individual planar image is indicated by a cursor that is used to scroll through the entire set of planar IVUS images to review the detected contours (Fig. 3). Corrections may be performed by "forcing" the contour through a visually identified point (minimum cost), which causes the entire data set to be updated (dynamic programming). This algorithm has been validated with use of a tubular phantom (18) and in histologic studies (19). Furthermore, the intraobserver and interobserver reproducibility of in vivo CSA measurements after nongated acquisition of IVUS images from nonstented atherosclerotic coronary arteries have been reported (18).

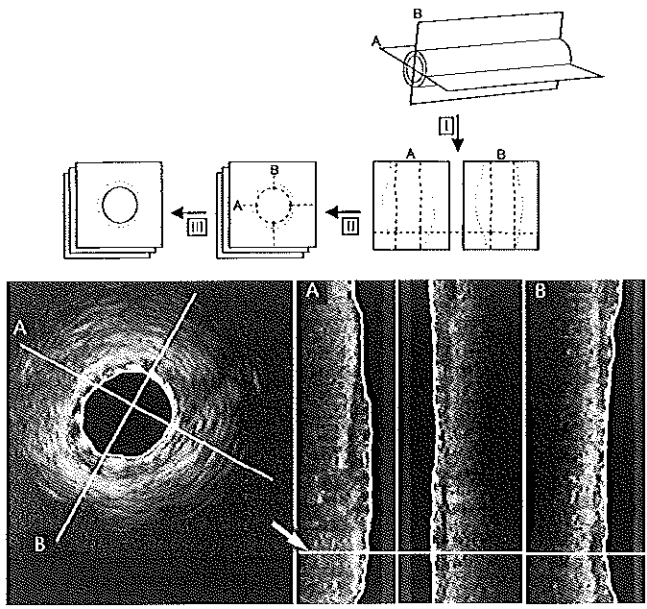

Figure 3. 3D quantitative IVUS analysis. **Upper panel,** Principle of automated lumen contour detection. Two perpendicular longitudinal sections (A, B) were reconstructed from image data of the entire 3D "stack" of images. The lumen contours were detected (I) by use of a minimum cost algorithm. Edge information of these longitudinal contours was represented as points on the planar images (II) and defined regions of interest (center and range of the boundary searching) that guided the final automated contour detection of the lumen boundary on the planar images. **Lower panel,** Clinical example of contour analysis in a stented coronary segment. A horizontal cursor (arrow) could be used to scroll through the entire set of planar images (**left**). This cursor indicated on the two perpendicular longitudinal sections (A, B) the site corresponding to the planar image displayed. On the longitudinal sections, note the relative smoothness of both lumen and external vascular boundaries.

Although the algorithm can also be used to detect the external vessel boundary (18,19), only the measurement of the lumen CSA (inside the echo-reflective struts of the metallic stents) and the stent symmetry ratio (i.e., minimal divided by maximal stent diameter) were used in the current study. Reference lumen CSA measurements were obtained at minimally diseased sites 5 mm proximal and distal to the stented segment.

IVUS criteria for optimal stent deployment. Three IVUS criteria, based on the experience of the Milan group (5,6) and our own data (11), were used to define optimal stent deployment: 1) apposition = complete stent apposition to vessel wall along the entire stented segment; 2) symmetry = ratio of minimal/maximal stent diameter (stent symmetry index) ≥0.7; 3) expansion = ratio of minimal stent CSA/mean reference lumen CSA ≥0.8; or, ratio of minimal stent CSA/distal reference lumen CSA ≥0.8 (if the site of the minimal stent CSA was in the distal third of the stent).

Statistical analysis. Quantitative data were given as mean value ± 1 SD; qualitative data were presented as frequencies. Continuous variables were compared by using a two-tailed Student *t* test and linear regression analysis; categoric variables were compared by the chi-square test or Fisher exact test. As proposed by Bland and Altman (25), the agreement of the different approaches was assessed by determining the mean value ± SD of the between-method differences. A p value < 0.05 was considered statistically significant.

Table 1. Comparison of On-Line and Off-Line Intravascular Ultrasound Analyses

	On-Line 2D	On-Line 3D	Off-Line 3D	Δ On-Line 2D vs. On-Line 3D	Δ On-Line 2D vs. Off-Line 3D	Δ On-Line 3D vs. Off-Line 3D
Stent						
Minimal lumen CSA (mm^2)	9.0 ± 2.7	8.6 ± 2.8	8.5 ± 2.8	0.4 ± 0.6*	0.4 ± 0.7†	0.1 ± 0.2
Symmetry index	0.83 ± 0.09	0.81 ± 0.07	0.81 ± 0.08	0.02 ± 0.07	0.02 ± 0.08	0 ± 0.02
Reference						
Proximal lumen CSA (mm^2)	12.7 ± 3.8	12.1 ± 3.8	12.4 ± 4.2	0.6 ± 2.3	0.3 ± 2.2	−0.3 ± 1.3
Distal lumen CSA (mm^2)	10.1 ± 2.8	10.1 ± 3.8	10.1 ± 3.7	0 ± 1.8	0 ± 2.1	0 ± 0.9
Suboptimal stent deployment	7 (21%)	14 (41%)	14 (41%)	−7 (−21%)‡	−7 (−21%)‡	0

*$p < 0.005$; †$p < 0.001$; ‡$p < 0.02$; all other differences were not significant. Values are expressed as mean value ± 1 SD or number (%) of stents. CSA = cross-sectional area; Δ = between-method difference; 3D, 2D = three- and two-dimensional intravascular ultrasound (IVUS) measurements, respectively.

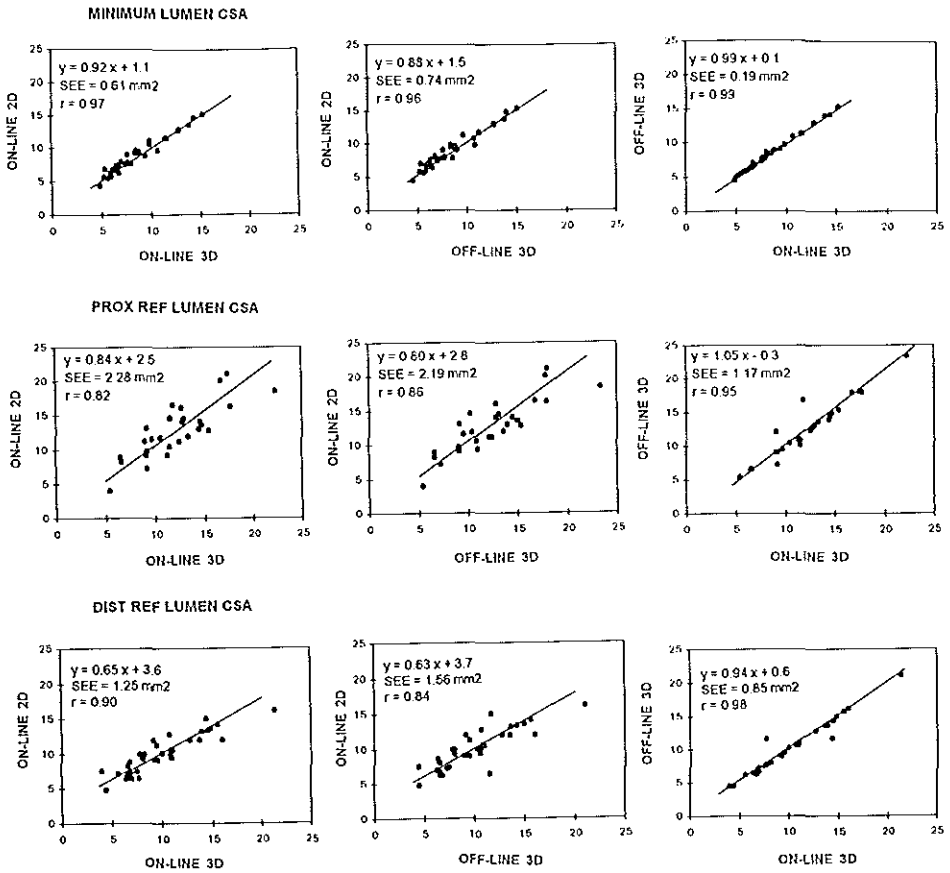

Figure 4. Results of linear regression analyses, comparing the lumen CSA measurements of the minimal stent (upper panels), proximal reference (PROX REF, center panels) and distal reference (DIST REF, lower panels), as obtained from on-line 2D and both on-line and off-line 3D IVUS analyses. Correlations were excellent, especially between on-line and off-line 3D IVUS measurements (the off-line 3D reanalysis represents the maximal confidence approach).

Results

Quantitative angiographic data. Before intervention, the minimal lumen diameter was 0.87 ± 0.42 mm, and the diameter stenosis 70.6 ± 13.7%. After stenting, a smooth angiographic lumen was achieved in all cases, with absence of inflow or outflow obstruction. The final minimal lumen diameter was 3.29 ± 0.41 mm with a corresponding diameter stenosis of 8.4 ± 3.4% (range 1% to 14%). According to the quantitative angiographic criteria, all stents were implanted successfully.

Feasibility of ECG-gated 3D IVUS image acquisition and analysis. After angiographically successful stent deployment, ECG-gated image acquisition was successfully performed in all patients with excellent tolerance. No subjective complaints of the patients were reported, and continuous ECG monitoring showed no evidence of ST segment alteration or increased frequency of arrhythmias during both gated and nongated IVUS imaging runs. The ECG-gated image acquisition required on average 4.6 ± 1.4 min (range 3.6 to 7.8), whereas the image acquisition during conventional continuous pullbacks required 1.7 ± 0.3 min (range 1.5 to 2.4, $p < 0.0001$). The on-line 3D analysis required 8.7 ± 0.6 min (range 7.3 to 10.0),

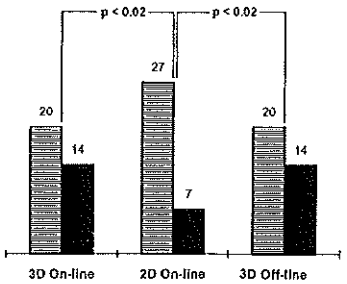

Figure 5. Detection of suboptimal stent deployment based on defined IVUS criteria. After angiography-guided stent implantation, off-line 3D analysis (providing the maximal confidence results) as well as on-line 3D analysis demonstrated that 14 stents (41%) failed to meet the IVUS criteria of optimal stent deployment, but only 7 (21%) of these stents were so classified by the on-line 2D analysis. **Striped bars** = IVUS criteria fulfilled; **solid bars** = IVUS criteria not fulfilled.

whereas reviewing the videotape and manually tracing the 2D IVUS images took 5.8 ± 0.7 min (range 4.8 to 7.4, $p < 0.001$).

IVUS measurements after stent deployment. The results of the different IVUS analyses are given in Table 1. There was a slight but significant overestimation of the minimal stent lumen CSA by the on-line 2D IVUS analysis when results were compared with those of both on-line and off-line 3D analyses ($p < 0.005$ and $p < 0.001$, respectively). The other variables measured (stent symmetry, proximal and distal reference lumen CSA) did not differ among analyses.

The between-method measurement variability, expressed as the standard deviation of the between-methods differences, was consistently higher for the on-line 2D measurement versus both the on-line and the off-line 3D measurements than for the two 3D measurements (Table 1). Nevertheless, the correlations among the CSA measurements obtained from the on-line 2D, on-line 3D and off-line 3D analyses were excellent (Fig. 4). Correlations of the stent symmetry measurements ranged from 0.62 (on-line 2D vs. 3D) to 0.98 (on-line 3D vs. off-line 3D).

IVUS criteria of optimal stent deployment. With the off-line 3D analysis (which provided the maximal confidence results), 14 (41%) of the 34 stents failed to meet the IVUS criteria of optimal stent deployment (Table 1). Only 7 of these stents were so classified by the on-line 2D analysis ($p < 0.02$), whereas all 14 stents were also identified by the on-line 3D analysis ($p < 0.02$ vs. on-line 2D analysis) (Fig. 5). Inadequate stent expansion was the constant reason for the failure to meet the deployment criteria ($n = 14$). There were no instances of incomplete stent apposition; the one case of stent asymmetry (which also had inadequate stent expansion) was revealed by both on-line 3D and off-line 3D analyses, but not by on-line 2D analysis.

Procedural outcome. After completion of the study protocol, any further treatment was left to the discretion of the operator. Additional angiography-guided balloon dilations were performed in six stents that had not met the criteria by both 2D and 3D IVUS ($n = 2$) or by 3D IVUS alone ($n = 4$). Lack of further stent expansion despite high pressure dilation with oversized balloons was the principal reason for omitting further balloon dilations. There were no procedural or post-procedural in-hospital complications.

Reproducibility of on-line 3D IVUS analysis. The intraobserver and interobserver differences of stent CSA measurements were 0.0 ± 0.2 mm^2 and 0.0 ± 0.3 mm^2 (relative SD 2.0% and 3.1%). The correlations were high (Fig. 6).

Discussion

IVUS insights into vessel and stent geometry (5–11) have played a central role in developing the concept of optimized stent deployment using adjunct high pressure balloon inflations (5,6,8,11,26). IVUS-guided stent implantation has reduced the incidence of stent thrombosis and permitted stenting without anticoagulation (5). These studies used planar IVUS analysis; however, changes of the stent dimensions observed during a transducer pullback are frequently smooth and gradual, and thus the minimal lumen area may be difficult to reliably identify visually. Automated 3D reconstruction and

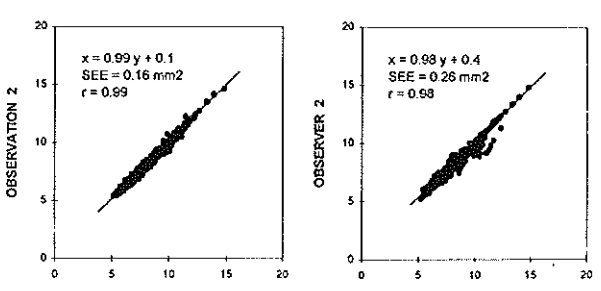

Figure 6. Intraobserver and interobserver measurement variability of on-line 3D IVUS. Correlation between the stent lumen CSA measurements (mm^2), provided by repeated analyses of the same observer (**left panel**, observations 1 and 2) and two independent observers (**right panel**, observers 1 and 2) using the 3D automated analysis method in ECG-gated IVUS image sets. Because actual on-line conditions cannot be reproduced, these data were obtained by using simulated on-line conditions, especially a maximal analysis time of 10 min.

analysis may therefore help to resolve this problem, but it must be both reliable and feasible during on-line application.

Previously, 3D reconstruction performed after stent implantation has been marred by cyclic image artifacts (18) (Fig. 1) that limited on-line application of automated 3D contour detection and analysis systems.

In the present study, to overcome this important limitation, we used ECG-gated IVUS image acquisition (23) and a validated automated 3D analysis system (18,19,27) on-line after angiography-guided stent deployment. The importance of ECG-gated image acquisition for off-line automated 3D IVUS measurements has been demonstrated by other groups (16,21) using alternative 3D contour detection systems. Sonka and colleagues (16) have stated that the correlation between observer-defined and automated lumen contours by their system improved as a result of ECG gating ($r = 0.91$ and 0.98 for nongated and ECG-gated, respectively) (16). We found that ECG-gated image acquisition resulted in much smoother vessel boundaries, readily facilitating the on-line contour detection process.

The main results of this study were that ECG-gated IVUS image acquisition and automated on-line 3D analysis 1) were feasible to evaluate the procedural results after stent deployment, 2) provided reliable and reproducible measurements of the lumen dimensions within the stented segment, and 3) facilitated the detection of the minimal lumen site. Despite the high correlation of the minimal lumen area measurements provided by the on-line 2D and 3D analyses, there was a significant overestimation of minimal lumen area with use of the 2D approach; this was confirmed by the off-line measurement. As a result, there were significant differences between the on-line 2D and 3D analyses in judging the adequacy of stent deployment by using the defined IVUS criteria. The high reliability of the on-line 3D approach in scrutinizing such criteria was confirmed by the off-line measurement. The on-line 3D analysis time (8.7 ± 0.6 min) of the present study is acceptably within the 10-min range set by the board of the Thoraxcenter senior interventional cardiologists. Nevertheless, in parallel with the advances in computer technology and further refinements in the software, further reduction of the analysis time can be expected.

Clinical implications. Although good clinical and angiographic results have been reported for coronary stenting without the use of IVUS (28,29), previous studies using conventional IVUS techniques (5,6,11) have suggested a considerable frequency of suboptimal results, a finding that is again confirmed by our methodology. We also found that conventional 2D IVUS itself underestimated the frequency of suboptimal stenting.

Numerous interventional cardiologists have praised IVUS as helpful in guiding (difficult) stent procedures and in investigating ambiguous angiographic results, but there is no blanket recommendation concerning the use of IVUS in routine stenting (26). However, the indication for stenting is currently broadening to smaller vessels, longer lesions, unfavorable morphology, multivessel disease and unstable syndromes, and the number of different types of stents available is increasing rapidly (30). Considering this increasing complexity of stenting procedures, a feasible and reliable IVUS analysis approach will remain at least extremely valuable, often necessary, and perhaps cost-effective, depending on long-term clinical results; this aspect will undoubtedly be an objective of future trials evaluating the usefulness of IVUS guidance in complex coronary stenting.

Study limitations. Nonuniform transducer rotation of mechanical IVUS catheters, noncoaxial catheter position or vascular curvatures may create image distortion and artifacts in both planar images and 3D reconstructions (17); however, segments are generally relatively straight after stenting. Although coronary angiography itself has several limitations, combined approaches using both angiographic and IVUS data for 3D reconstruction of the vessel may resolve many of the problems mentioned, but these techniques are laborious and still restricted to research (22). As 3D reconstructions of IVUS images generally do not depict the true spatial coronary geometry, careful interpretation by an experienced investigator is required.

Our experience suggests that ECG-gated image acquisition is feasible in 90% to 95% of patients referred for coronary intervention, but it may be difficult in patients with arrhythmias and even impossible in the presence of atrial fibrillation, unless cardiac pacing is performed. ECG-gated image acquisition (23) requires more time than conventional motorized pullbacks at a uniform speed; this longer duration may limit its use before interventions in patients with critical coronary stenoses. Further miniaturization of the IVUS catheters and the use of imaging wires (31,32) may soon help to overcome this limitation.

Conclusions. ECG-gated acquisition of IVUS images during automated transducer pullbacks is feasible after coronary stent deployment. The approach is clinically relevant, as it permits on-line automated 3D reconstruction and analysis, provides reliable and reproducible measurements of lumen dimensions and facilitates the detection of the minimal lumen area, thus guiding optimized stent deployment.

References

1. Fitzgerald PJ, St. Goar FG, Connolly AJ, et al. Intravascular ultrasound imaging of coronary arteries: is three layers the norm? Circulation 1992;86: 154–8.
2. Mintz GS, Painter JA, Pichard AD, et al. Atherosclerosis in angiographically "normal" coronary artery reference segments: an intravascular ultrasound study with clinical correlations. J Am Coll Cardiol 1995;25:1479–85.
3. Erbel R, Ge J, Bockisch A, et al. Value of intracoronary ultrasound and Doppler in the differentiation of angiographically normal coronary arteries: a prospective study in patients with angina pectoris. Eur Heart J 1996;17: 850–9.
4. Pinto FJ, St. Goar FG, Gao SZ, al. Immediate and one-year safety of intracoronary ultrasound imaging: evaluation with serial quantitative angiography. Circulation 1993;88:1709–14.
5. Colombo A, Hall P, Nakamura S, et al. Intravascular stenting without anticoagulation accomplished with intravascular ultrasound guidance. Circulation 1995;91:1676–88.
6. Goldberg SL, Colombo A, Nakamura S, Almagor Y, Maiello L, Tobis JM.

Benefit of intracoronary ultrasound in the deployment of Palmaz-Schatz stents. J Am Coll Cardiol 1994;24:936–1003.
7. Mudra H, Klauss V, Blasini R, et al. Ultrasound guidance of Palmaz-Schatz intracoronary stenting with a combined intravascular ultrasound balloon catheter. Circulation 1994;90:1252–61.
8. Görge G, Haude M, Ge J, et al. Intravascular ultrasound after low and high inflation pressure coronary artery stent implantation. J Am Coll Cardiol 1995;26:725–30.
9. Dussaillant GR, Mintz GS, Pichard AD, et al. Small stent size and intimal hyperplasia contribute to restenosis: a volumetric intravascular ultrasound analysis. J Am Coll Cardiol 1995;26:720–4.
10. von Birgelen C, Kutryk MJB, Gil R, et al. Quantification of the minimal luminal cross-sectional area after coronary stenting by two- and three-dimensional intravascular ultrasound versus edge detection and videodensitometry. Am J Cardiol 1996;78:520–5.
11. von Birgelen C, Gil R, Ruygrok P, et al. Optimized expansion of the Wallstent compared with the Palmaz-Schatz stent: online observations with two- and three-dimensional intracoronary ultrasound after angiographic guidance. Am Heart J 1996;131:1067–75.
12. Rosenfield K, Losordo DW, Ramaswamy K, et al. Three-dimensional reconstruction of human coronary and peripheral arteries from images recorded during two-dimensional intravascular ultrasound examination. Circulation 1991;84:1938–56.
13. Coy KM, Park JC, Fishbein MC, et al. In vitro validation of three-dimensional intravascular ultrasound for the evaluation of arterial injury after balloon angioplasty. J Am Coll Cardiol 1992;20:692–700.
14. Mintz GS, Pichard AD, Satler LF, Popma JJ, Kent KM, Leon MB. Three-dimensional intravascular ultrasonography: reconstruction of endovascular stents in vitro and in vivo. Clin Ultrasound 1993;21:609–15.
15. Matar FA, Mintz GS, Douek P, et al. Coronary artery lumen volume measurement using three-dimensional intravascular ultrasound: validation of a new technique. Cathet Cardiovasc Diagn 1994;33:214–20.
16. Sonka M, Liang W, Zhang X, De Jong S, Collins SM, McKay CR. Three-dimensional automated segmentation of coronary wall and plaque from intravascular ultrasound pullback sequences. In: Computers in Cardiology 1995. Los Alamitos (CA): IEEE Computer Society, 1995:637–40.
17. Roelandt JRTC, Di Mario C, Pandian NG, et al. Three-dimensional reconstruction of intracoronary ultrasound images: rationale, approaches, problems, and directions. Circulation 1994;90:1044–55.
18. von Birgelen C, Di Mario C, Li W, et al. Morphometric analysis in three-dimensional intracoronary ultrasound: an in-vitro and in-vivo study using a novel system for the contour detection of lumen and plaque. Am Heart J 1996;132:516–27.
19. von Birgelen C, van der Lugt A, Nicosia A, et al. Computerized assessment of coronary lumen and atherosclerotic plaque dimensions in three-dimensional intravascular ultrasound correlated with histomorphometry. Am J Cardiol 1996;78:1202–9.
20. Gil R, von Birgelen C, Prati F, Di Mario C, Ligthart J, Serruys PW. Usefulness of three-dimensional reconstruction for interpretation and quantitative analysis of intracoronary ultrasound during stent deployment. Am J Cardiol 1996;77:761–4.
21. Dhawale PJ, Wilson DL, Hodgson J McB. Optimal data acquisition for volumetric intracoronary ultrasound. Cathet Cardiovasc Diagn 1994;32:288–99.
22. von Birgelen C, Slager CJ, Di Mario C, de Feyter PJ, Serruys PW. Volumetric intracoronary ultrasound: a new maximum-confidence approach for the quantitative assessment of progression-regression of atherosclerosis? Atherosclerosis 1996;118 Suppl:S103–13.
23. Bruining N, von Birgelen C, Di Mario C, et al. Dynamic three-dimensional reconstruction of ICUS images based on an ECG-gated pull-back device. In: Computers in Cardiology 1995. Los Alamitos (CA): IEEE Computer Society, 1995:633–6.
24. Hodgson J McB, Graham SP, Savakus AD, et al. Clinical percutaneous imaging of coronary anatomy using an over-the-wire ultrasound catheter system. Int J Cardiac Imaging 1989;4:186–93.
25. Bland JM, Altman DG. Statistical methods for assessing agreement between two methods of clinical measurement. Lancet 1986;2:307–10.
26. Tobis JM, Colombo A. Do you need IVUS guidance for coronary stent deployment? Cathet Cardiovasc Diagn 1996;37:360–1.
27. Li W, von Birgelen C, Di Mario C, et al. Semi-automatic contour detection for volumetric quantification of intracoronary ultrasound. In: Computers in Cardiology 1994. Los Alamitos (CA): IEEE Computer Society, 1994:277–80.
28. Serruys PW, de Jaegere P, Kiemeneij F, et al., for the Benestent Study Group. A comparison of balloon expandable stent implantation with balloon angioplasty in patients with coronary artery disease. N Engl J Med 1994;331:489–95.
29. Fishman DL, Leon MB, Baim DS, et al., for the Stent REStenosis Study (STRESS) Investigators. A randomized comparison of coronary stent placement and balloon angioplasty in the treatment of coronary artery disease. N Engl J Med 1994;331:496–501.
30. Serruys PW, Kutryk MJB. The state of the stent: current practices, controversies, and future trends. Am J Cardiol 1996;78(Suppl 3A):4–7.
31. Di Mario C, Fitzgerald PJ, Colombo A. New developments in intracoronary ultrasound. In: Reiber JHC, van der Wall EE, editors. Cardiovascular Imaging. Dordrecht, The Netherlands: Kluwer Academic, 1996;257–75.
32. von Birgelen C, Mintz GS, de Feyter PJ, et al. Reconstruction and quantification with three-dimensional intracoronary ultrasound: an update on techniques, challenges, and future directions. Eur Heart J 1997;18:1056–67.

Chapter 8

Coronary Wallstents show significant late, post-procedural expansion despite implantation with adjunct high-pressure balloon inflations

C von Birgelen, SG Airiian, PJ de Feyter,
DP Foley, WJ van der Giessen,
PW Serruys

Reprinted with permission from *Am J Cardiol* 1998;82:129-134

Coronary Wallstents Show Significant Late, Postprocedural Expansion Despite Implantation With Adjunct High-Pressure Balloon Inflations

Clemens von Birgelen, MD,* Segei G. Airiian, MD, Pim J. de Feyter, MD, PhD, David P. Foley, MB, MRCPI, PhD, Wim J. van der Giessen, MD, PhD, and Patrick W. Serruys, MD, PhD

Adjunct high-pressure balloon inflations following the delivery of oversized self-expandable Wallstents may affect their implied late, postprocedural self-expansion. Consequently, we examined 15 "Magic" Wallstents, which were implanted following a strategy of stent oversizing and subsequent adjunct high-pressure balloon inflations (16 ± 2 atm; all ≥12 atm). The excellent radiographic visibility of this stent permitted reliable quantitative coronary angiographic measurement of both lumen and stent dimensions (before and after stenting, and at follow-up). At follow-up, extent and distribution of in-stent neointimal proliferation were evaluated with volumetric intravascular ultrasound. Between postintervention and follow-up examination, mean stent diameter increased from 3.7 ± 0.4 to 4.2 ± 0.4 mm ($p < 0.0001$); there was no significant difference in late stent expansion between proximal, mid-, and distal stent subsegments. Late stent expansion showed a significant (reverse) relation to maximum balloon size ($r = -0.56$, $p < 0.04$), but not with follow-up lumen size or late lumen loss. On average, 52 ± 18% of the stent was filled with neointimal ingrowth; neointimal volume/cm stent length was 64 ± 22 mm^3. Both late stent expansion ($r = 0.36$, $p < 0.02$) and maximum balloon pressure ($r = 0.41$, $p < 0.001$) were related to neointimal volume/cm stent but not to follow-up lumen size. Thus, despite high-pressure implantation, Wallstents showed significant late self-expansion, which resulted in larger stent dimensions at follow-up that assisted in accommodating in-stent neointimal proliferation. Conversely, late stent expansion had a significant relation to the extent of in-stent neointimal ingrowth. Beneficial and disadvantageous effects of the late stent expansion appear to be balanced, because a relation to late lumen loss or follow-up lumen dimensions was not found to be present.

(Am J Cardiol 1998;82:129–134)

During the last decade, implantation of coronary stents has become a rapidly expanding approach for percutaneous transluminal catheter-based therapy of significant atherosclerotic lesions.[1–10] In the short, balloon-expandable slotted tube stents, the extent and mechanisms of late lumen renarrowing and in-stent neointimal proliferation have been carefully evaluated with quantitative coronary angiography and intravascular ultrasound (IVUS).[11–14] However, insights gained in this particular stent design cannot simply be transferred to self-expandable stents such as the Wallstent,[1,2,15–17] because the deployment characteristics differ considerably.[18,19] After high-pressure implantation of balloon-expandable slotted tube stents, no change in stent size was observed between the final postintervention examination and follow-up.[16,17,20] However, high-pressure balloon inflation after delivery of self-expandable Wallstents may have a significant effect on the implied late, postprocedural changes in stent dimensions. Consequently, we examined 15 oversized, self-expandable "Magic" Wallstents (Schneider, Bülach, Switzerland), which have an excellent radiographic visibility that permits reliable quantitative coronary angiographic (QCA) measurement of stent dimensions after stent implantation, and at 6-month follow-up (Figure 1). In addition, extent and distribution of neointimal ingrowth were evaluated with a volumetric IVUS analysis system.[14,21–24]

From the Thoraxcenter, University Hospital Rotterdam-Dijkzigt and Erasmus University Rotterdam, Rotterdam, The Netherlands. Dr. von Birgelen is the recipient of a fellowship of the German Research Society (DFG, Bonn, Germany). Manuscript received November 6, 1997; revised manuscript received and accepted February 20, 1998.

Address for reprints: Patrick W. Serruys, MD, PhD, Thoraxcenter, University Hospital Dijkzigt, Bd 418, P.O. Box 1738, 3000 DR Rotterdam, The Netherlands.

*Current address: Department of Cardiology, University Hospital Essen, Hufelandstrasse 55, D45122 Essen, Germany.

METHODS

Patient group: The study group consisted of 15 patients (12 men and 3 women, aged 61 ± 9 years) with symptomatic 1-vessel (n = 9) or 2-vessel disease (n = 6), who had Magic Wallstents (n = 15) implanted. All lesions were nonostial and located in right coronary arteries. The study was approved by the medical ethical committee of the Erasmus University Hospital, Rotterdam; all patients provided written informed consent.

Intervention procedures: All patients received 250 mg of aspirin and 10,000 U of heparin intravenously, and subsequent heparin was administered hourly to maintain an activated clotting time of >300 seconds. Balloon angioplasty and stent deployment were per-

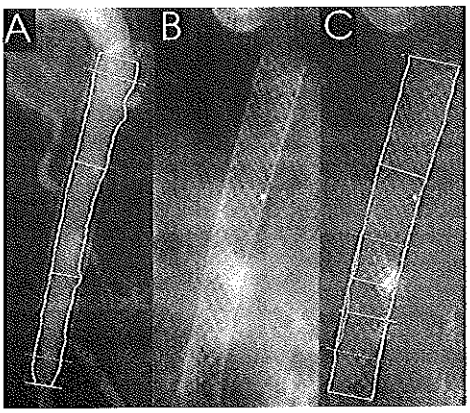

FIGURE 1. "Magic" Wallstent at 6-month follow-up. Note the excellent definition of the stent boundaries outside the opacified lumen *(A)*. The high radiographic visibility on contrast-free angioframes *(B)* permits reliable QCA analysis of the stent dimensions *(C)*.

formed according to standard clinical practice at the Thoraxcenter Rotterdam[17] using the femoral approach and 8Fr femoral arterial sheaths. The percutaneous transluminal angioplasty procedures were performed with 8Fr guiding catheters. All patients were undergoing elective stent implantation, so conservative balloon predilatation was performed to enable stent placement but avoid unnecessary dissection.

The proximal, distal, and maximum lumen diameter, the interpolated reference diameter, and the lesion length as provided by on-line quantitative coronary angiography were taken into account to select the stent size. Stents had a nominal diameter of 5.1 ± 0.7 mm and a length of 33 ± 7 mm. Following a strategy of stent oversizing, the Wallstents had a nominal diameter that was on average 1.5 mm larger than the maximum lumen diameter of the segment to be stented, as measured by on-line QCA. Adjunct balloon dilatation was performed inside all stents, using low-compliance balloon catheters at maximum pressures of at least 12 atm. Balloon sizing was left to the discretion of the operator. The largest balloon was frequently sized according to the (rounded-up) proximal reference diameter. In long Wallstents the largest balloon was often used in the proximal and midportion of the stent only, whereas the distal portion was dilated by a balloon sized according to the distal or the mean (proximal and distal) reference. In addition, angiographic signs of reference segment disease were considered when sizing balloons. After the procedure, all patients were treated with an antiplatelet regimen of aspirin and ticlopidine. Follow-up cardiac catheterization, angiography, and IVUS examination were performed according to a standard protocol.

Quantitative coronary angiography: The QCA analysis was performed with the CAAS II system (Pie Medical, Maastricht, The Netherlands) according to previously described methodology.[17,25] Measurements were performed in multiple (≥2) matched angiographic views after intracoronary nitrates were administered, they included analysis of proximal, mid-, and distal subsegments (equal length) of the stented segment (Figure 2). The boundaries of a selected coronary segment were detected using a weighted sum of the first and second derivative functions of the brightness profile of each vessel scan. The absolute angiographic diameter of the stenosis was determined using a contrast-free guiding catheter as a scaling device. As in many previous QCA studies using the CAAS system,[6,9,16–18] the diameter function was used to determine the minimal lumen diameter and a computer-derived estimation of an interpolated reference diameter at the minimal lumen site. The interpolated diameter stenosis was calculated as [(reference diameter − minimal lumen diameter)/reference diameter] × 100.

The excellent radiographic visibility of the Magic Wallstent (Figure 1) permitted measurement of the stent dimensions on contrast-free image frames both after the procedure and at follow-up.

Intravascular ultrasound imaging: The IVUS imaging at follow-up was performed after intracoronary nitroglycerin bolus injection using a commercially available mechanical sector scanner (CardioVascular Imaging Systems, Sunnyvale, California) and 2.9Fr sheath-based IVUS catheters (MicroView, CardioVascular Imaging Systems). This catheter incorporated a 15-cm-long sonolucent distal imaging sheath that alternatively housed the guidewire (during catheter introduction) or, after the guidewire had been pulled back, the 30-MHz beveled single-element transducer (during imaging). A continuous motorized pullback of the IVUS transducer at a pullback speed of 0.5 mm/s (within the imaging sheath) was performed. The entire IVUS imaging run was recorded on videotape for off-line analysis.

Volumetric measurement of neointimal ingrowth: The measurement of in-stent neointimal ingrowth was performed with a validated computerized volumetric IVUS analysis system (Figure 3), which performs a boundary detection based on the application of a minimum-cost algorithm and has previously been described in detail.[14,21–24] In brief, this system allowed reconstruction of 2 perpendicular longitudinal sections in which contour detection of the echo-reflective stent and the lumen-neointimal boundary was performed to identify regions of interest for the boundary search on the planar IVUS images. On the planar images, the regions of interest guided the automated detection of the lumen and stent contours, which were used for the volumetric measurement of neointimal ingrowth based on Simpson's rule (neointimal volume = stent volume − lumen volume). To compensate for differences in stent length, the neointimal volume/cm stent length was calculated from the absolute values of neointimal volume and stent length.

In vitro, the algorithm has been validated in a tubular phantom consisting of several segments.[21] The automated measurements revealed a high correlation with the true phantom volumes ($r = 0.99$); mean

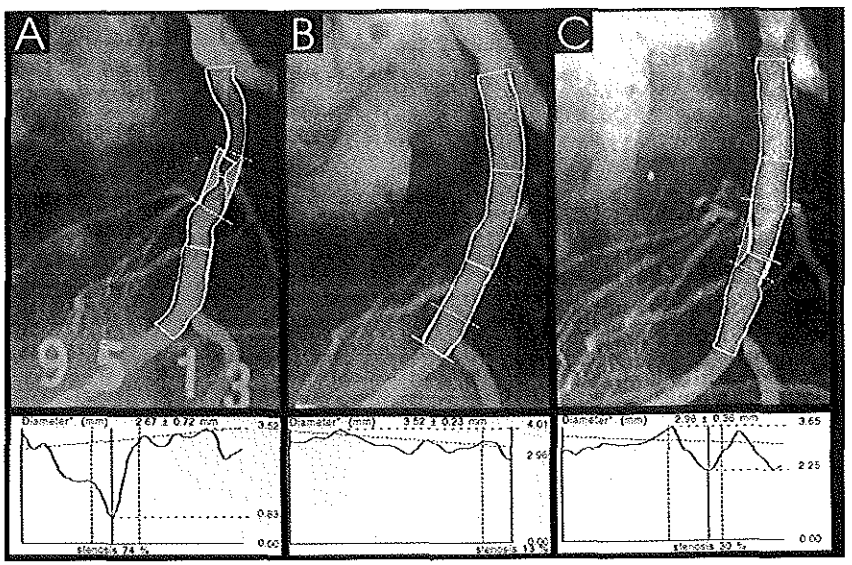

FIGURE 2. Example of QCA lumen analysis. Lumen dimensions were measured before intervention *(A)*, after intervention *(B)*, and at follow-up *(C)*. Note at follow-up the relatively focal lumen obstruction at the transition between the distal and midsegment of the stent (see Figure 3 for corresponding IVUS images).

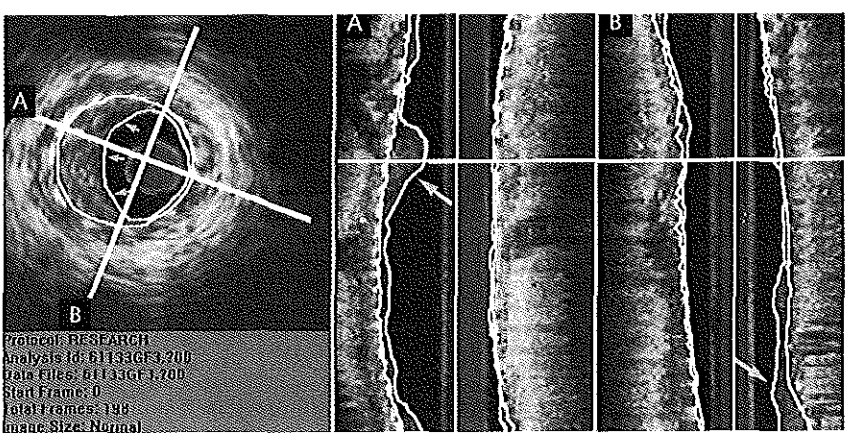

FIGURE 3. Volumetric IVUS analysis of in-stent neointimal proliferation. On 2 perpendicular longitudinal images *(A and B)*, reconstructed from the 3-dimensional data set, coronary lumen, stent struts, and neointimal ingrowth *(arrowheads)* can be well distinguished. The origin of the planar IVUS image *(left-hand side)* is indicated by a horizontal cursor on the longitudinal images; it shows focal neointimal proliferation *(smaller arrowheads)*.

differences were <1.8% (SD <3.8%) for volumes of the various segments.[21] A comparison between automated 3-dimensional IVUS measurements in coronary specimens in vitro and morphometric measurements on the corresponding histologic sections revealed good correlations for volumetric measurements (r = 0.83 to 0.98).[22] In vitro, volume measurements by the automated system agreed well with results obtained by manual tracing of IVUS images, showing low between-method differences with the SD not exceeding 4.3%, and high correlation coefficients (r = 0.99).[22] In vivo, intra- and interobserver comparisons of volumetric measurements revealed high correlations (r = 0.99) and small mean differences (<1.2%), with SD ≤3.2%.[21,24]

Statistical analysis: Quantitative data were given as mean ± 1 SD; qualitative data were presented as frequencies. Continuous variables were compared by

TABLE I Minimal Lumen Diameter (mm) in Proximal, Mid-, and Distal Stent Segments

	PRE	POST	FUP
Proximal segment	1.9 ± 0.8	3.4 ± 0.4†	2.3 ± 0.7
Midsegment	1.5 ± 0.4*	3.2 ± 0.4	2.4 ± 0.6
Distal segment	2.0 ± 0.5	3.1 ± 0.4	2.2 ± 0.7

*p = 0.01 versus distal subsegments.
†p <0.01 versus mid- and distal subsegments.
FUP = follow-up; POST = final result after the intervention; PRE = before intervention.

analysis of variance, 2-tailed Student's *t* test, and linear regression analysis. A p value <0.05 was considered statistically significant.

RESULTS

Procedural details: All 15 Wallstents were successfully deployed. The stents were oversized by 1.6 ± 0.5 mm relative to the maximum lumen diameter. Adjunct balloon dilatation was performed using low-compliance balloon catheters with a maximum diameter of 4.0 ± 0.6 mm at an inflation pressure of 16 ± 2 atm. The balloon-to-artery ratio was 1.1 ± 0.1 using the postinterventional reference diameter as a reference.

Quantitative coronary angiography before and after stenting: During the intervention, overall the minimal lumen diameter increased from 1.0 ± 0.5 to 3.1 ± 0.4 mm (p <0.0001), the reference diameter increased from 3.1 ± 0.6 to 3.4 ± 0.4 mm (p = 0.01), and the diameter stenosis decreased from 66 ± 16% to 10 ± 4% (p <0.0001). Analysis of the proximal, mid-, and distal subsegments (Table I) demonstrated that before intervention the minimal lumen diameter was smallest in the midsegments.

Quantitative coronary angiography at follow-up: At follow-up, 5 patients had symptoms of angina and a diameter stenosis ≥50%. Overall, the minimal lumen and reference diameters decreased to 1.9 ± 0.6 mm (p <0.0001) and 3.0 ± 0.8 mm (p = 0.01), respectively, corresponding to a diameter stenosis of 35 ± 14% (p <0.0001). There was no significant difference in follow-up minimal lumen diameter between the subsegments (Table I).

Between postintervention examination and follow-up, a late self-expansion of the Wallstents was noted (Figure 4); the mean stent diameter increased from 3.7 ± 0.4 to 4.2 ± 0.4 mm (p <0.0001). There was no significant difference in late stent expansion between subsegments (Table II). Late stent expansion showed a reverse relation to the maximum balloon size used for postdilatation (r = −0.56; y = −1.2x + 4.3; p <0.04), but not to the follow-up lumen dimensions or late lumen loss.

Volumetric intravascular ultrasound at follow-up: On average, 52 ± 18% of the stent was filled with neointimal ingrowth (52 ± 20%, 54 ± 19%, and 50 ± 23% in the proximal, mid-, and distal subsegment), as demonstrated by IVUS; the neointimal volume/cm stent length was 64 ± 22 mm^3 (68 ± 28 mm^3, 68 ± 25 mm^3, and 59 ± 26 mm^3 in the subsegments; p = NS). Both late stent expansion (r = 0.36, y = 30x + 49; p <0.02) and maximum balloon pressure (r = 0.41; y = 5x − 11; p <0.001) showed a significant correlation to neointimal volume/cm stent length (Figure 5).

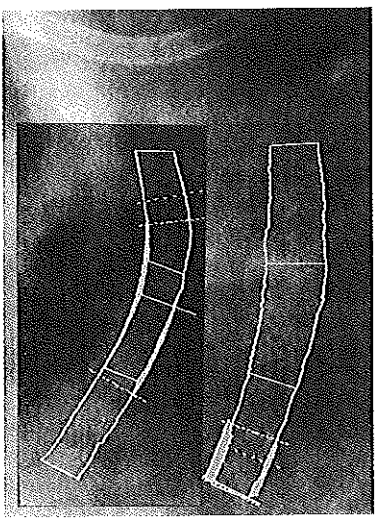

FIGURE 4. Example of late, postprocedural self-expansion of Wallstent. Between postintervention *(insert)* and follow-up, an evident increase in stent diameter was observed (contrast-free images correspond with Figure 2, *B and C*).

TABLE II Mean Stent Diameter (mm) After Intervention and at Follow-Up

	POST	FUP	p Value
Proximal segment	3.86 ± 0.41	4.36 ± 0.45	<0.0001
Midsegment	3.69 ± 0.36	4.30 ± 0.36	<0.0001
Distal segment	3.61 ± 0.37	4.06 ± 0.36	<0.0005
All segments	3.72 ± 0.39	4.24 ± 0.41	<0.0001

Abbreviations as in Table I.

DISCUSSION

The characteristic design of the Wallstent accounts for the self-expandable feature of this stent.[1,2,15–18] Initially, the self-expanding force of the Wallstent was thought to be sufficient for further gradual expansion after stent delivery. However, adjunct balloon dilatations were required to achieve stent dimensions that were sufficiently large to minimize the rate of subacute stent thrombosis. Recently, high-pressure balloon inflations after Wallstent delivery have been suggested,[17] but the presence and extent of late postprocedural stent expansion after such high-pressure inflations inside the Wallstent have not been reported. Because most other stent designs are radiolucent after deployment and difficult to perceive on the angiogram, IVUS has frequently been used for the direct

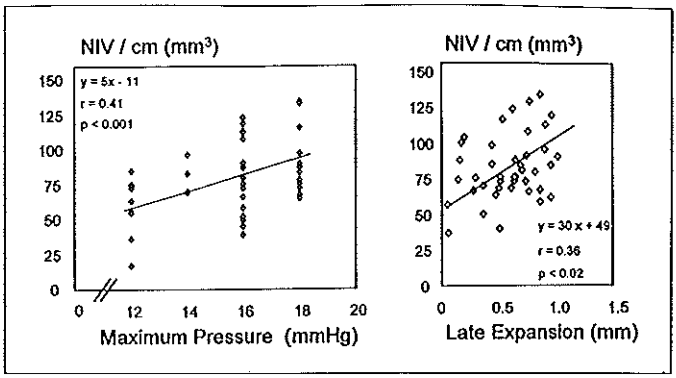

FIGURE 5. Neointimal proliferation versus late stent expansion and maximum balloon pressure. The late, postprocedural expansion of the Wallstents *(right panel)* and the maximum balloon pressure during adjunct balloon inflation inside the stents *(left panel)* showed a significant relation to the extent of neointimal volume/cm stent length (NIV/cm), as measured by volumetric IVUS.

cross-sectional assessment of stent struts[10,20,23] and in-stent neointimal proliferation at follow-up.[11–14] However, the excellent radiographic visibility of the new Magic Wallstent, consisting of round wire struts of a cobalt-based alloy with an inner platinum core, was ideal for reliable QCA analysis of late expansion of the Wallstent.

Late self-expansion of the Wallstent: We compared the stent dimensions after intervention and at follow-up and demonstrated that the self-expandable Wallstent showed a significant late expansion despite high-pressure (12 to 18 atm) in-stent balloon inflation after stent delivery. Late stent expansion was not only found to be present in the proximal and distal stented segments but also in the midportion, which frequently covered the highest burden of atherosclerotic plaque. The extent of late self-expansion was higher if balloon inflation after Wallstent delivery was performed with smaller balloons; conversely, larger balloons partly anticipated the late self-expansion of stents. Recent preliminary QCA data of a nitinol coronary stent also describe a late expansion of that self-expandable stent after implantation with balloon pressures of 10 to 14 atm.[26]

In our study we followed a strategy of substantial stent oversizing. The Wallstents had a nominal diameter that was on average 1.5 mm larger than the maximum lumen diameter of the segment to be stented, whereas currently oversizing Wallstents by 1 mm is suggested.[17] The concept of substantially oversizing stents, applied in this particular series of patients, may partly account for the relatively high extent of late stent expansion observed and may contribute to the procedure-related increase in reference diameter. On average, late stent expansion was comparable to the extent of oversizing the Wallstents above the current suggestion of 1 mm. We believe that the stents, as examined after 6 months, may have reached a state of final expansion; nevertheless, our data do not exclude the possibility that this process may continue even beyond 6 months.

Late stent expansion and neointimal proliferation: Late self-expansion of the oversized Wallstents resulted in larger stent dimensions at follow-up, which helped to accommodate the in-stent neointimal proliferation. In contrast, late stent expansion may be a parameter of potential vascular injury,[27,28] showing a significant relation to the extent of in-stent neointimal ingrowth. The beneficial and disadvantageous effects of late stent self-expansion appear to be balanced, because a significant relation between late stent expansion and both late lumen loss and follow-up lumen dimensions was not found to be present.

The neointimal ingrowth in Wallstents, as measured by IVUS, was significantly larger than that previously reported for short slotted tube stents[11–13]; however, the dimensions of the Wallstent in itself (diameter after intervention: 3.7 ± 0.4 mm) were significantly larger than those reported for slotted tube stents.[11–13] At follow-up, this contrast was even higher, as the Wallstent diameter increased to 4.2 ± 0.4 mm.

Study limitations and potential sources of error: (1) The degree of late stent expansion with a more conservative stent selection strategy is not known from the current data. (2) The number of stents examined does not permit calculation of an actual restenosis rate; however, this was not the intention of this study. (3) Coronary angiography and QCA delineate the vessel lumen as a silhouette and foreshorten vessel segments depending on the projection used.[25] (4) Linear 3-dimensional IVUS approaches, as used in this study, do not account for vessel curvatures and provide approximate values of volumetric parameters[24]; nevertheless, coronary segments are relatively straight after stent implantation.[23]

Clinical implications: High-pressure implantation of substantially oversized coronary Wallstents resulted in late self-expansion of the stents, which helped to accommodate neointimal ingrowth. But a relation between late stent expansion and follow-up lumen dimensions was not found to be present, because the

increase in stent dimensions is currently balanced by an increased neointimal proliferation. Our data suggest that at this time excessive oversizing of the Wallstent or application of extremely high balloon pressures during adjunct balloon inflations may not help to further improve the follow-up lumen dimensions. However, with the advent of clinically effective antiproliferative strategies (e.g., radiation or pharmacologic approaches), the mechanical properties of the Wallstent may offer a chance to achieve particularly large long-term lumen dimensions after coronary stent implantation.

1. Sigwart U, Puel J, Mirkovitch V, Joffre F, Kappenberger L. Intravascular stents to prevent occlusion and restenosis after transluminal angioplasty. *N Engl J Med* 1987;316:701–706.
2. Serruys PW, Strauss BH, Beatt KJ, Bertrand M, Puel J, Rickards AF, Kappenberger L, Meier B, Goy JJ, Vogt P, Sigwart U. Angiographic follow-up after placement of a self-expanding coronary stent. *N Engl J Med* 1991;324:13–17.
3. Schatz RA, Baim DS, Leon M, Ellis SG, Goldberg S, Hirshfeld JW, Cleman MW, Cabin HS, Walker C, Stagg J, Buchbinder M, Teirstein PS, Topol EJ, Savage M, Perez JA, Curry RC, Levine SL, Palmaz JC. Clinical experience with the Palmaz-Schatz coronary stent. Initial results of a multicenter study. *Circulation* 1991;83:148–161.
4. Haude M, Erbel R, Straub U, Dietz U, Meyer J. Short and long term results after intracoronary stenting in human coronary arteries: monocenter experience with the balloon-expandable Palmaz-Schatz stent. *Br Heart J* 1991;66:337–345.
5. Roubin GS, Cannon AD, Agrawal SK, Macander PJ, Dean LS, Baxley WA, Breland J. Intracoronary stenting for acute and threatened closure complicating percutaneous transluminal coronary angioplasty. *Circulation* 1992;85:916–927.
6. Serruys PW, de Jaegere P, Kiemeneij F, Macaya C, Rutsch W, Heyndrickx G, Emanuelsson H, Marco J, Legrand V, Materne P, Belardi J, Sigwart U, Colombo A, Goy JJ, vd Heuvel P, Delcan J, Morel AA, for the Benestent Study Group. A comparison of balloon expandable stent implantation with balloon angioplasty in patients with coronary artery disease. *N Engl J Med* 1994;331:489–495.
7. Fishman DL, Leon MB, Baim DS, Schatz RA, Savage MP, Penn I, Detre K, Veltri L, Ricci D, Nobuyoshi M, Cleman M, Heuser R, Almond D, Teirstein PS, Fish RD, Colombo A, Brinker J, Goldberg S, for the Stent REStenosis Study (STRESS) Investigators. A randomized comparison of coronary stent placement and balloon angioplasty in the treatment of coronary artery disease. *N Engl J Med* 1994;331:496–501.
8. Schömig A, Neumann FJ, Kastrati A, Schühlen H, Blasini R, Hadamitzky, Walter H, Zitzmann-Roth EM, Richardt G, Eckhard AH, Schmitt C, Ulm K. A randomized comparison of antiplatelet and anticoagulant therapy after the placement of coronary stents. *N Engl J Med* 1996;334:1084–1089.
9. Serruys PW, Emanuelsson H, van der Giessen WJ, Lunn AC, Kiemeney F, Macaya C, Rutsch W, Heyndrickx G, Suryapranata H, Legrand V, Goy JJ, Materne P, Bonnier H, Morice MC, Fajadet J, Belardi J, Colombo A, Garcia E, Ruygrok P, de Jaegere P, Morel MA, on behalf of the Benestent-II Study Group: Heparin coated Palmaz-Schatz stents in human coronary arteries: early outcome of the BENESTENT II pilot study. *Circulation* 1996;93:412–422.
10. Colombo A, Hall P, Nakamura S, Almagor Y, Maiello L, Martini G, Gaglione A, Goldberg SL, Tobis JM. Intracoronary stenting without anticoagulation accomplished with intravascular ultrasound guidance. *Circulation* 1995;91:1676–1688.
11. Dussaillant GR, Mintz GS, Pichard AD, Kent KM, Satler LF, Popma JJ, Wong SC, Leon MB. Small stent size and intimal hyperplasia contribute to restenosis: a volumetric intravascular ultrasound analysis. *J Am Coll Cardiol* 1995;26:720–724.
12. Hoffmann R, Mintz GS, Dussaillant GR, Popma JJ, Pichard AD, Satler LF, Kent KM, Griffin J, Leon MB. Patterns and mechanisms of in-stent restenosis: a serial intravascular ultrasound study. *Circulation* 1996;94:1247–1254.
13. Mudra H, Regar E, Klauss V, Werner F, Henneke K-H, Sbarouni E, Theisen K. Serial follow-up after optimized ultrasound-guided deployment of Palmaz-Schatz stents: in-stent neointimal proliferation without significant reference segment response. *Circulation* 1997;95:363–370.
14. von Birgelen C, Kutryk MJB, Serruys PW. Three-dimensional intravascular ultrasound analysis of coronary stent deployment and in-stent neointimal volume: current clinical practice and the concepts of TRAPIST, ERASER, and ITALICS. *J Invas Cardiol* 1998;10:17–26.
15. Strauss BH, Serruys PW, Bertrand ME, Puel J, Meier B, Goy JJ, Kappenberger L, Rickards AF, Sigwart U. Quantitative angiographic follow-up of the coronary Wallstent in native vessels and bypass grafts (European experience—March 1986 to March 1990). *Am J Cardiol* 1992;69:475–481.
16. Keane D, Buis B, Reifart N, Plokker TH, Ernst J, Mast E, Renkin J, Heyndrickx G, Morel MA, de Jaegere P, Serruys PW. Clinical and angiographic outcome following implantation of the less shortening Wallstent in aorto-coronary vein grafts: introduction of a second generation stent in the clinical arena. *J Interven Cardiol* 1994;7:557–564.
17. Ozaki Y, Keane D, Ruygrok P, van der Giessen WJ, de Feyter PJ, Serruys PW. Six-month clinical and angiographic outcome of the new, less shortening Wallstent in native coronary arteries. *Circulation* 1996;93:2114–2120.
18. von Birgelen C, Gil R, Ruygrok P, Prati F, Di Mario C, van der Giessen WJ, de Feyter PJ, Serruys PW. Optimized expansion of the Wallstent compared with the Palmaz-Schatz stent: online observations with two- and three-dimensional intracoronary ultrasound after angiographic guidance. *Am Heart J* 1996;131:1067–1075.
19. de Jaegere P, Strauss BH, van der Giessen WJ, de Feyter PJ, Serruys PW. Immediate changes in stenosis geometry following stent implantation: comparison between a self-expandable and a balloon expandable stent. *J Interven Cardiol* 1992;5:71–78.
20. Görge G, Haude M, Ge J, Voegele E, Gerber T, Rupprecht HJ, Meyer J, Erbel R. Intravascular ultrasound after low and high inflation pressure coronary artery stent implantation. *J Am Coll Cardiol* 1995;26:725–730.
21. von Birgelen C, Di Mario C, Li W, Schuurbiers JCH, Slager CJ, de Feyter PJ, Roelandt JRTC, Serruys PW. Morphometric analysis in three-dimensional intracoronary ultrasound: an in-vitro and in-vivo study using a novel system for the contour detection of lumen and plaque. *Am Heart J* 1996;132:516–527.
22. von Birgelen C, van der Lugt A, Nicosia A, Mintz GS, Gussenhoven EJ, de Vrey E, Maltus MT, Roelandt JRTC, Serruys PW, de Feyter PJ. Computerized assessment of coronary lumen and atherosclerotic plaque dimensions in three-dimensional intravascular ultrasound correlated with histomorphometry. *Am J Cardiol* 1996;78:1202–1209.
23. von Birgelen C, Mintz GS, Nicosia A, Foley DP, van der Giessen WJ, Bruining N, Airiian SG, Roelandt JRTC, de Feyter PJ, Serruys PW. Electrocardiogram-gated intravascular ultrasound image acquisition after coronary stent deployment facilitates on-line three-dimensional reconstruction and automated lumen quantification. *J Am Coll Cardiol* 1997;30:436–443.
24. von Birgelen C, de Vrey EA, Mintz GS, Nicosia A, Bruining N, Li W, Slager CJ, Roelandt JRTC, Serruys PW, de Feyter PJ. ECG-gated three-dimensional intravascular ultrasound: feasibility and reproducibility of an automated analysis of coronary lumen and atherosclerotic plaque dimensions. *Circulation* 1997;96:2944–2952.
25. Escaned J, Baptista J, Di Mario C, Haase J, Ozaki Y, Linker DT, Feyter PJ, Roelandt JRTC, Serruys PW. Significance of automated stenosis detection during quantitative angiography: insights gained from intracoronary ultrasound. *Circulation* 1996;94:966–972.
26. Roguin A, Beyar R, Grenadier E, Markiewicz W. Continued expansion of the nitinol self-expanding coronary stent during angiographic follow-up (abstr). *Eur Heart J* 1997;18:156.
27. Schwartz RS, Huber KC, Murphy JG, Edwards WD, Camrud AR, Vlietstra RE, Holmes DR. Restenosis and the proportional neointimal response to coronary injury: results in a porcine model. *J Am Coll Cardiol* 1992;19:267–274.
28. Rogers C, Edelman ER. Endovascular stent design dictates experimental restenosis and thrombosis. *Circulation* 1995;91:2995–3001.

Chapter 9

Structural and functional characterization of an intermediate stenosis with intracoronary ultrasound and Doppler: A case of "reverse Glagovian modeling"

C von Birgelen, C Di Mario,
PW Serruys

Reprinted with permission from *Am Heart J* 1996;132:694-696

Structural and functional characterization of an intermediate stenosis with intracoronary ultrasound and Doppler: A case of "reverse Glagovian modeling"

Clemens von Birgelen, MD, Carlo Di Mario, MD, PhD, and Patrick W. Serruys, MD, PhD
Rotterdam, The Netherlands

A compensatory enlargement of the coronary arterial wall as plaque increases has been described by Glagov et al.,[1] whereas a paradoxical shrinkage of the arterial wall at the site of vascular stenoses was observed by Pasterkamp et al.[2] in femoral arteries. We report a case of a "reverse Glagovian modeling" in a coronary artery detected during the comprehensive assessment of an intermediate lesion with intracoronary ultrasound and Doppler.

A 60-year-old woman complaining of chest pain at rest and during exercise for 1 year, despite treatment with a beta blocker, displayed a slowly ascending depression of the ST segment of 1.5 mm in leads V_5 and V_6 at maximum effort during a bicycle stress test. Coronary angiography revealed no luminal obstruction of the right and left circumflex coronary arteries. The left anterior descending coronary artery (LAD) had a stenosis in the proximal segment and minor luminal irregularities in the midsegment. After intracoronary injection of nitrates, quantitative coronary angiography of the proximal lesion was performed online (CAAS, PieMedical, Maastricht, The Netherlands) and revealed a minimal luminal diameter of 1.92 mm with a 42% diameter stenosis (Fig. 1). The value of this quantitative angiographic analysis, however, was in all projections limited by the superimposition of an intermediate and a septal branch. Subsequently, a 0.014-inch 15-MHz Doppler guide wire (FloWire, Cardiometrics, Mountain View, Calif.) was advanced into the LAD distal to the lesion. Coronary flow velocity was measured at baseline and after intracoronary injection of a bolus of 18 μg of adenosine. Coronary flow reserve, calculated as the ratio between hyperemic and baseline average peak velocity, was 3.3 (Fig. 1). After a new intracoronary injection of 3 mg isosorbide dinitrate, a 2.9F 30-MHz mechanical intracoronary ultrasound (ICUS) catheter (Microview, CVIS, Sunnyvale, Calif.) was advanced distal to the lesion, and a slow, continuous withdrawal of the ICUS catheter was performed with a motorized pullback device at a speed of 0.5 mm/sec. The reference site distal to the plaque showed a mild concentric intimal thickening with a 21% cross-sectional area stenosis. At the site of the angiographic luminal narrowing, a focal noncalcified highly eccentric plaque was found showing a 58% cross-sectional area stenosis and a minimal luminal diameter of 2.0 mm (Fig. 2). A custom-designed analysis system, developed at the Thoraxcenter, was used to obtain a computerized assessment of luminal and plaque dimensions of the entire vascular segment visualized with ICUS.[3,4] Reduction of the total vessel area from the distal reference segment to the proximal LAD stenosis was observed (Fig. 2). On the basis of the information provided by ICUS imaging and Doppler, no coronary intervention was performed. The absence of inducible ischemia in the myocardial territory subtended by the LAD was confirmed by a dobutamine stress-echocardiography test, which demonstrated a normal thickening and motion of the anterior wall and the interventricular septum at a maximum level of dobutamine (40 μg/kg/min plus 2 mg intravenous atropine).

New intracoronary ultrasound techniques permit a morphologic and functional assessment of coronary stenoses, which may be particularly helpful in patients with angiographically intermediate stenoses[5,6] when the presence of myocardial ischemia has not been unequivocally demonstrated with noninvasive tests before the cardiac catheterization. Measurement of coronary flow reserve with the

From the Thoraxcenter, Cardiac Catheterization Laboratory, Erasmus University Rotterdam and University Hospital Rotterdam-Dijkzigt.

Dr. von Birgelen is the recipient of a fellowship of the German Research Society.

Reprint requests: Patrick W. Serruys, MD, PhD, Cardiac Catheterization and Intracoronary Imaging Laboratories, Thoraxcenter, Bd 432, P.O. Box 1738, 3000 DR Rotterdam, The Netherlands.

Am Heart J 1996;132:694-6.

0002-8703/96/$5.00 + 0 4/4/71989

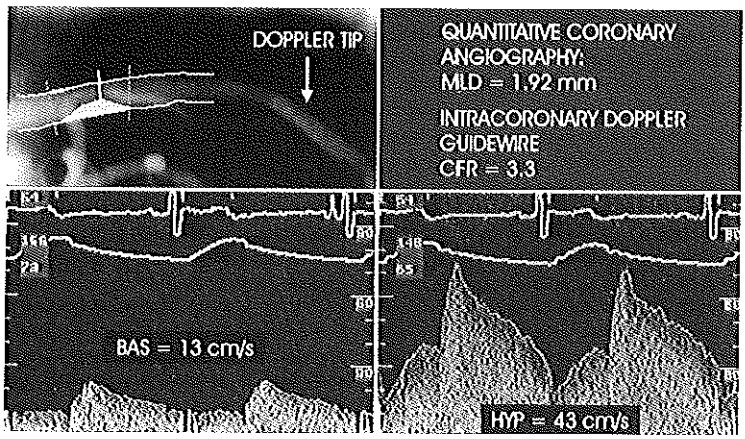

Fig. 1. Quantitative coronary angiography *(left upper panel)* of intermediate lesion in proximal segment of left anterior descending coronary artery. A 42% diameter stenosis was found but angiographic analysis was limited by sidebranches and overlapping vessels in all projections. Assessment of coronary flow velocity with Doppler guide wire distal to stenosis revealed normal coronary flow reserve of 3.3, calculated as ratio between average peak flow velocity at baseline *(left lower panel)* and hyperemia *(right lower panel). Arrowhead* indicates position of Doppler tip during flow velocity measurement. *BAS*, Baseline; *CFR*, coronary flow reserve; *HYP*, hyperemia; *MLD*, minimal luminal diameter.

Doppler guide wire is well correlated with the results of radioisotope perfusion tests and permits a reliable assessment of the hemodynamic significance of coronary stenoses. The safety of deferring coronary interventions in nonsignificant lesions on the basis of results of flow velocity measurements has recently been demonstrated.[6] In this case a normal coronary flow reserve was found in the LAD distal to the lesion, excluding a significant hemodynamic impairment. ICUS permits direct inspection and measurement of the plaque burden and is not affected by vessel overlapping or other causes of insufficient angiographic visualization. The feasibility and clinical value of ICUS for decision making in intermediate coronary lesions have recently been reported.[5] In this case the lesion fulfilled the ICUS criteria for deferral of coronary interventions (minimal luminal diameter <2 mm) proposed by Mintz et al.[5] on the basis of their clinical experience.

Enlargement of the total vessel dimension is a well known mechanism of the vascular wall to preserve the dimension of the lumen during the early stage of atherosclerosis.[1,7] This mechanism can compensate for an increase of plaque burden until it occupies 40% of the internal elastic membrane area.[1] However, the vessel wall does not uniformly respond to progressive plaque accumulation because the mechanism depends on the integrity of the endothelium-mediated response to the increase in shear stress as luminal narrowing starts to develop. When this compensatory mechanism fails, a "reverse modeling" may occur as described in atherosclerotic human femoral arteries showing a paradoxical shrinkage of the total vessel area at the site of the target stenosis.[2] The ICUS findings of this case suggest that a reverse modeling can also occur in coronary lesions. The complementary information obtained with ICUS imaging and Doppler can be valuable in the process of clinical decision making in patients with intermediate lesions. The question whether coronary lesions with "reverse Glagovian modeling" have a specific prognosis or a different response to treatment is of interest but requires further clinical investigation.

REFERENCES

1. Glagov S, Weisenberg E, Zaris CK, Stancunavicus R, Kolettis GJ. Compensatory enlargement of human atherosclerotic coronary arteries. N Engl J Med 1989;316:1371-5.
2. Pasterkamp G, Wensing PJW, Post MJ, Hillen B, Mali WPTM, Borst C. Paradoxical arterial wall shrinkage may contribute to luminal narrowing of human atherosclerotic femoral arteries. Circulation 1995; 91:1444-9.
3. von Birgelen C, Di Mario C, Li W, Schuurbiers JCH, Slager CJ, de Feyter PJ, et al. Morphometric analysis in three-dimensional intracoronary ultrasound: An in vitro and in vivo study performed with a novel system for the contour detection of lumen and plaque. Am Heart J 1996;132:516-27.
4. Di Mario C, von Birgelen C, Prati F, Soni B, Li W, Bruining N, et al. Three-dimensional reconstruction of two-dimensional intracoronary ultrasound: clinical or research tool? Br Heart J 1995;73(Suppl 2):26-32.
5. Mintz GS, Bucher TA, Kent KM, Pichard AD, Satler LF, Popma JJ, Morgan K, Leon MB. Clinical outcomes of patients not undergoing coronary artery revascularization as a result of intravascular ultrasound (abstract). J Am Coll Cardiol 1995;25:61A.
6. Kern MJ, Donohue TJ, Aguirre FV, Bach RG, Caracciolo EA, Wolford T, et al. Clinical outcome of deferring angioplasty in patients with nor-

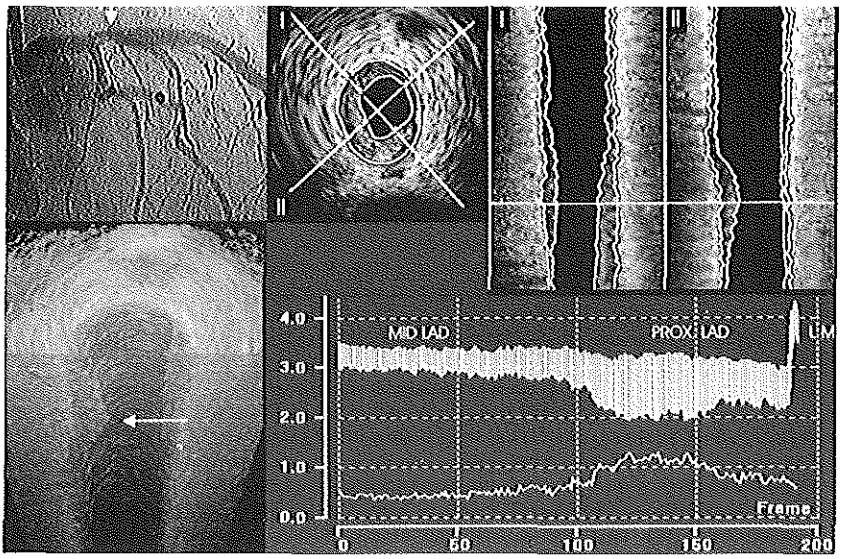

Fig. 2. Proximal stenosis of left anterior descending coronary artery (LAD) *(left upper panel)* assessed by new system for quantitative analysis of three-dimensional intracoronary ultrasound images.[3,4] Cross-sectional ultrasound images were reconstructed in two perpendicular longitudinal sections (I and II, *right upper panels*) and computerized contour detection was performed providing a three-dimensional view *(left lower panel)* and dimensions of lumen, plaque, and total vessel, calculated from area measurements. Mean diameter measurements (mm) of 200 consecutive ultrasound frames *(right lower panel)* are displayed, with plaque shown as white area between total vessel and lumen diameter. Note reduction of total vessel diameter from distal reference (mid-LAD) to target stenosis. *Arrowheads* in three-dimensional view and angiogram indicate site of stenosis, which is also displayed in cross-sectional ultrasound view *(mid-left upper panel)*. *LM*, Left main coronary artery; *PROX*, proximal.

mal translesional pressure-flow velocity measurements. J Am Coll Cardiol 1995;25:178-87.

7. Ge J, Erbel R, Zamorano J, Koch L, Kearney P, Gorge G, et al. Coronary artery remodeling in artherosclerotic disease: an intravascular ultrasonic study in vivo. Coronary Artery Disease 1993;4:981-6.

Chapter 10

Atherosclerotic coronary lesions with inadequate compensatory enlargement have smaller plaque and vessel volumes: Observations with three-dimensional intravascular ultrasound in vivo

C von Birgelen, GS Mintz, EA de Vrey, T Kimura, JJ Popma,
SG Airiian, MB Leon, M Nobuyoshi, PW Serruys,
PJ de Feyter

Reprinted with permission from *Heart* 1998;79:137-143

Atherosclerotic coronary lesions with inadequate compensatory enlargement have smaller plaque and vessel volumes: observations with three dimensional intravascular ultrasound in vivo

C von Birgelen, G S Mintz, E A de Vrey, T Kimura, J J Popma, S G Airiian, M B Leon, M Nobuyoshi, P W Serruys, P J de Feyter

Abstract

***Objective*—To compare vessel, lumen, and plaque volumes in atherosclerotic coronary lesions with inadequate compensatory enlargement versus lesions with adequate compensatory enlargement.**

***Design*—35 angiographically significant coronary lesions were examined by intravascular ultrasound (IVUS) during motorised transducer pullback. Segments 20 mm in length were analysed using a validated automated three dimensional analysis system. IVUS was used to classify lesions as having inadequate (group I) or adequate (group II) compensatory enlargement.**

***Results*—There was no significant difference in quantitative angiographic measurements and the IVUS minimum lumen cross sectional area between groups I (n = 15) and II (n = 20). In group I, the vessel cross sectional area was 13.3 (3.0) mm^2 at the lesion site and 14.4 (3.6) mm^2 at the distal reference ($p < 0.01$), whereas in group II it was 17.5 (5.6) mm^2 at the lesion site and 14.0 (6.0) mm^2 at the distal reference ($p < 0.001$). Vessel and plaque cross sectional areas were significantly smaller in group I than in group II (13.3 (3.0) *v* 17.5 (5.6) mm^2, $p < 0.01$; and 10.9 (2.8) *v* 15.2 (4.9) mm^2, $p < 0.005$). Similarly, vessel and plaque volume were smaller in group I (291.0 (61.0) *v* 353.7 (110.0) mm^3, and 177.5 (48.4) *v* 228.0 (92.8) mm^3, $p < 0.05$ for both). Lumen areas and volumes were similar.**

***Conclusions*—In lesions with inadequate compensatory enlargement, both vessel and plaque volume appear to be smaller than in lesions with adequate compensatory enlargement.**

(*Heart* 1998;79:137–142)

Keywords: intravascular ultrasound; ultrasonics; remodelling; coronary artery disease

Thoraxcenter, University Hospital Rotterdam-Dijkzigt, Rotterdam, Netherlands
C von Birgelen
S G Airiian
P W Serruys
P J de Feyter

Kokura Memorial Hospital, Kitakyushu, Japan
T Kimura
M Nobuyoshi

Washington Hospital Center, Washington DC, USA
G S Mintz
E A de Vrey
J J Popma
M B Leon

Correspondence to:
Dr de Feyter, Thoraxcenter, Bd 381, PO Box 1738, University Hospital Rotterdam-Dijkzigt 3000 DR Rotterdam, Netherlands.

Accepted for publication
2 October 1997

Intravascular ultrasound provides transmural images of coronary arteries in vivo. The coronary vascular wall, the cross sectional area of the atherosclerotic plaque, the consequences of plaque accumulation, and the mechanisms of lesion formation can be studied in humans in a manner previously not possible.[1-9]

Atherosclerotic arteries tend to undergo compensatory vascular enlargement to accommodate increasing plaque burden during the early stages of plaque accumulation.[10-12] Because of this adaptation, lumen dimensions are preserved and an angiographic underestimation of coronary atherosclerosis often occurs.[13] This concept was initially derived from anatomical and histopathological studies in vitro.[10-12] It has been confirmed using intravascular and epicardial ultrasound studies in vivo.[14-18] Recently, Clarkson *et al*[19] suggested that failure of adaptive remodelling may be an important factor for the development of significant atherosclerotic lesions. The histopathological and intravascular ultrasound data of Pasterkamp *et al*[20,21] in peripheral arteries, and intravascular ultrasound observations of Wong *et al*,[22] Nishioka *et al*,[23] and Mintz *et al*[24] have also shown evidence of inadequate compensatory enlargement.

In the present study, we examined 35 atherosclerotic coronary lesions which were classified as having inadequate (group I) or adequate compensatory enlargement (group II). Automated three dimensional intravascular ultrasound analysis of the lumen, vessel, and plaque dimensions was performed[25-29] to gain insight into the volumetric characteristics[6] of these lesions.

Methods

PATIENT POPULATION

The study population consisted of 35 patients with primary (not restenotic) atherosclerotic lesions examined using preintervention intravascular ultrasound. Inclusion criteria were: angiography documented non-curved lesion segments; limited plaque calcification throughout a lesion length of 20 mm; absence of a complete occlusion of the stenotic lumen during the ultrasound imaging run; and absence of major side branches. Thirty two men and three women (mean (SD) age 61 (9) years) were examined. Lesions were located in the left anterior descending coronary artery (n = 20), right coronary artery (n = 10), and left circumflex coronary artery (n = 5); 32 were proximal and three were in the mid-portion. The study was approved by the Local Council on Human Research. All patients signed a written informed consent form, approved by the local medical ethics committees.

INTERVENTIONAL PROCEDURE AND INTRAVASCULAR ULTRASOUND IMAGING

The patients received 250 mg aspirin and 10 000 U heparin intravenously. If the duration of the entire catheterisation procedure exceeded one hour, the activated clotting time was measured, and intravenous heparin was given in order to maintain a clotting time of more than 300 s. Intravascular ultrasound imaging was performed after intracoronary injection of 0.2 mg glyceryl trinitrate, starting at least 10 mm distal to the lesion segment. A mechanical intravascular ultrasound system (ClearView, CardioVascular Imaging Systems, Sunnyvale, California, USA) and a sheath based imaging catheter were used. The catheter incorporated a 30 MHz bevelled, single element transducer rotating at 1800 rpm (MicroView, CardioVascular Imaging Systems). This catheter is equipped with a 2.9 F 15 cm long sonolucent distal sheath that has a common lumen that either houses the guide wire (during catheter introduction) or the transducer (during imaging after the guide wire has been pulled back), but not both. This design avoids direct contact of the imaging core with the vessel wall.[25] The ultrasonic transducer was withdrawn through the stationary imaging sheath using a motorised pullback device at a constant speed of 0.5 mm/s. All intravascular ultrasound examinations were recorded on high resolution s-VHS videotape for later offline quantitative analysis. After the intravascular ultrasound examination, all patients were successfully treated by balloon angioplasty, coronary stent implantation, or directional coronary atherectomy; there were no procedural or postprocedural in hospital complications.

INTRAVASCULAR ULTRASOUND IMAGE ANALYSIS

Twenty millimeter long lesion segments (10 images/mm axial arterial length), centered on the target lesion site, were analysed off-line using a computerised intravascular ultrasound analysis system (fig 1).[25-28] Reference images with the smallest plaque burden were acquired no more than 3 mm distal to the lesion segment. Cross sectional area measurements at the reference site were obtained with the computerised analysis system (single frame mode); care was taken to avoid any major side branch between the lesion segment and the reference site.

Cross sectional area measurements (mm^2) included the lumen and vessel cross sectional area. The vessel cross sectional area was measured by tracing the border between the hypoechoic media and the echoreflective adventitia. As in many previous studies using intravascular ultrasound, the cross sectional area (and thickness) of plaque plus media was used as a measure of atherosclerotic plaque area (and thickness) because ultrasound cannot measure media thickness accurately.[29] Plaque cross sectional area was calculated as vessel cross sectional area minus lumen cross sectional area. The cross sectional area plaque burden was calculated as plaque cross sectional area divided by vessel cross sectional area.

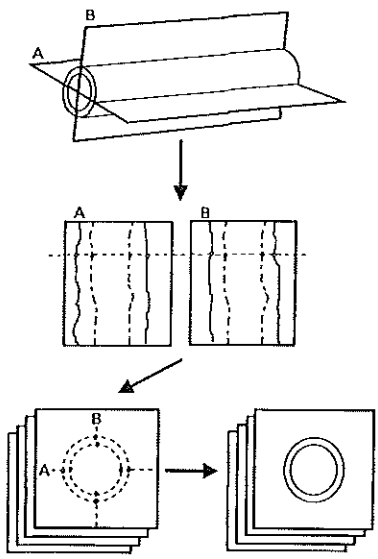

Figure 1 Principle of automated three dimensional intravascular ultrasound image analysis. Detection of the contours corresponding to the lumen–tissue and media–adventitia interfaces is first performed on two perpendicular longitudinal sections (A, B), reconstructed from the image data of the entire three dimensional "stack" of images. Edge information of the longitudinal contours are represented as points on the planar images, defining there the centre and range of the final contour detection process.

Compensatory enlargement was considered inadequate (group I) if the *vessel* cross sectional area at the site of the minimum *lumen* cross sectional area was smaller than that at the distal reference site (fig 2).[25] If the vessel cross sectional area at the site of the minimum *lumen* cross sectional area was larger than or equal to the distal reference site (fig 3), compensatory enlargement was considered adequate (group II).

Volume measurements (mm^3) of the lumen, vessel, and plaque (based on 10 intravascular ultrasound images/mm axial arterial length) were calculated according to Simpson's rule as

$$\text{Volume} = \sum_{i=1}^{n} \text{cross sectional area}_i \times H$$

where H = thickness of a coronary artery slice represented by a single tomographic intravascular ultrasound image, and n = number of images in the three dimensional image set. The volume plaque burden (%) was calculated as plaque volume divided by vessel volume.

The overall plaque eccentricity index was calculated as mean value of the eccentricity indices of all individual image slices; these were derived as previously described (minimum plaque thickness divided by maximum plaque thickness).[31] A higher value of that index indicated a more concentric plaque distribution (the maximum value 1.0 would indicate perfectly concentric plaque distribution along the entire lesion segment), whereas a lower

value indicated a more eccentric plaque distribution.

The overall lumen symmetry index was calculated as mean value of the lumen symmetry indices (minimum lumen diameter divided by maximum lumen diameter) of all individual image slices. A higher value of that index indicated a more symmetrical lumen shape (the maximum value 1.0 would indicate a perfectly circular lumen along the entire lesion segment).

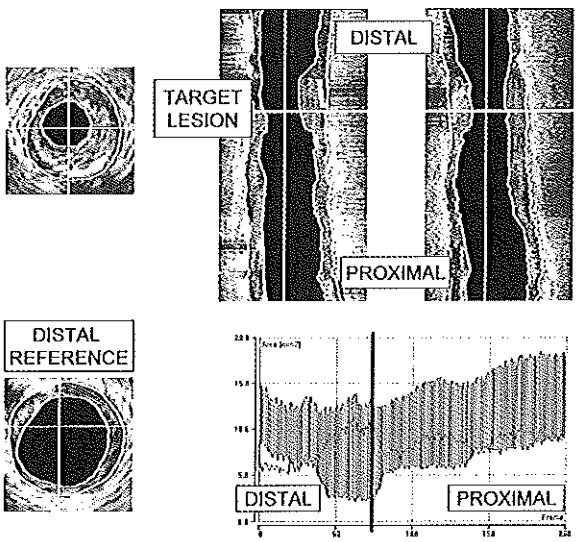

Figure 2 Analysis of a 20 mm long mid-right coronary segment with inadequate compensatory vascular enlargement (group I). The vessel cross sectional area is smallest at the target lesion site. Markers indicate that site on the longitudinal sections (right upper panels) and the display of the cross sectional area measurements (right lower panel). Linear functions of the vessel and lumen cross sectional area form the upper and lower boundaries of the greyish area, which represents the plaque cross sectional area. Alternatively, the values of plaque cross sectional area can be derived directly from a linear function (single black line), which here partly overlaps the greyish area.

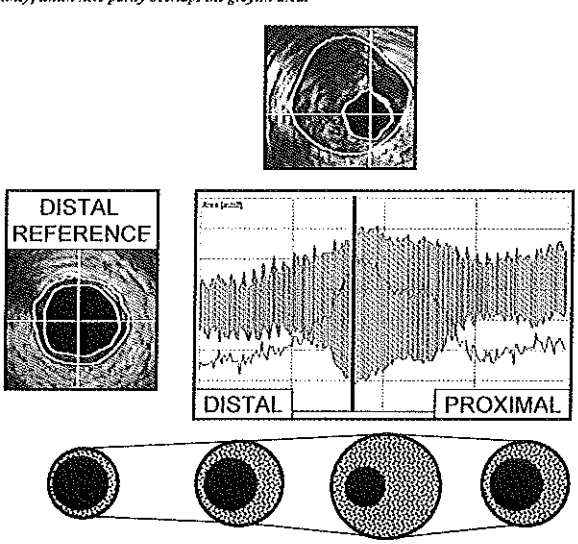

Figure 3 Adequate compensatory vascular enlargement, as observed in one of the lesion of group II. The vessel cross sectional area is larger at the target lesion site (upper panel) than at the reference site (left mid panel). The lower panel illustrates and underlines the principle of compensatory vascular enlargement.

COMPUTERISED INTRAVASCULAR ULTRASOUND ANALYSIS METHOD

The analysis was performed offline using a computerised intravascular ultrasound analysis system.[25 28] The analysis system used the Windows™ (Microsoft, Redmond, Washington, USA) operating system on a personal computer. The computerised analysis required the digitisation of a stack of intravascular ultrasound images from videotape. Two longitudinal sections were automatically reconstructed (fig 1), and the contours corresponding to the lumen–tissue and media–adventitia interfaces were automatically identified. The longitudinal contours were visually checked and, if necessary, edited with computer assistance (see below). The longitudinal contours generated individual edge points on the planar images defining the centre and range of the automated boundary search on the planar images. Subsequently, contour detection of the planar images was performed. The axial location of an individual planar image (on the longitudinal contours) was indicated by a cursor; the cursor was used to scroll through the entire set of planar images while the planar contours were visually checked. Finally, the contour data of the planar images were used for the computation of the results.

Automated contour detection and computer assisted contour editing were based on the application of a minimum cost algorithm to detect the luminal and external vessel boundaries.[26–28] Each digitised intravascular ultrasound image was resampled in a radial format (64 radii per image), and a cost matrix representing the edge strength was calculated from the image data. For the boundary between lumen and plaque, the cost value was defined by the spatial first derivative. For the external vessel boundary a cross correlation pattern matching process was used for the cost calculations. The path with the smallest accumulated value was determined by dynamic programming techniques.

The computer assisted editing differed considerably from conventional manual contour tracing. The computer mouse was used to indicate the correct boundary. This forced the contour through the manually entered point by assigning this point a very low value in the cost matrix. Editing the contour of a single slice caused the entire dataset to be updated (dynamic programming). Side branches with relatively small ostium and small calcified portions of the plaque were generally ignored by the algorithm as a result of its robustness, which means that the automated contour detection did not follow every abrupt change in the cost path.

This algorithm has been validated in tubular phantoms.[27] A comparison between automated three dimensional intravascular ultrasound

Table 1 Quantitative coronary angiographic measurements

Variables	Group I (n = 15)	Group II (n = 20)
Minimum lumen diameter (mm)	1.03 (0.33)	1.16 (0.33)
Interpolated reference diameter (mm)	3.05 (0.39)	3.31 (0.65)
Diameter stenosis (%)	66 (10)	63 (15)

Values are mean (SD); all non-significant.
Groups I and II, lesions with and without inadequate compensatory vascular enlargement, respectively.

measurements in atherosclerotic coronary specimen in vitro, and morphometric measurements on the corresponding histological sections revealed good correlations ($r = 0.80$ to 0.94 for cross sectional area, and $r = 0.83$ to 0.98 for volume measurements).[25] Both area and volume measurements by the automated system agreed well with results obtained by manual tracing of intravascular ultrasound images (mean differences $\leq 3.7\%$; areas: $r \geq 0.97$, and volumes: $r = 0.99$).[26] In vivo, intraobserver and interobserver comparisons of the analysis method revealed high correlations ($r = 0.95$ to 0.98 for area and $r = 0.99$ for volume) and small mean differences ($\leq 1.1\%$), with SD of lumen, vessel, and plaque not exceeding 7.3%, 4.5%, and 10.9% for areas, and 2.7%, 0.7%, and 2.8% for volumes, respectively.[27]

QUANTITATIVE CORONARY ANGIOGRAPHY

Quantitative angiographic analysis was performed off-line as previously described[32 33] on end diastolic frames with homogeneous opacification of the coronary lumen, acquired after intracoronary application of nitrates. We used a computer based coronary angiography analysis system (CAAS, Pie Medical, Maastricht, Netherlands). The measurements were performed by an experienced analyst in at least two projections, obtained from opposite (ideally orthogonal) angiographic views without overlapping side branches or foreshortening. Briefly, automated detection of the coronary artery contours was performed on the basis of the weighted sum of the first and second derivative functions applied to the digitised brightness silhouette. The diameter function of the coronary artery lumen was determined by computing the shortest distances between the edge points of the right and left contours. The absolute angiographic diameter of the stenosis was determined using the non-tapering part of the contrast-free guiding catheter as a scaling device. The minimum lumen diameter was measured by edge detection; the interpolated reference diameter was based on a computerised estimation of the original arterial dimension at the site of the obstruction. The diameter stenosis was derived from the measured minimum luminal diameter and the interpolated reference diameter.

STATISTICAL ANALYSIS

Quantitative data are given as mean values (SD). Dichotomous variables are expressed as frequencies. Continuous variables are compared using the two tailed Student t test and linear regression analysis. Probability (p) values < 0.05 are considered statistically significant.

Results

ADAPTIVE REMODELLING STATE

Inadequate compensatory enlargement was found in 15 lesions (group I); in these cases the vessel cross sectional area at the site of the minimum lumen area was smaller than at the distal reference (13.3 (3.0) *v* 14.4 (3.6) mm^2, $p < 0.01$). In the other 20 lesions (group II), the vessel cross sectional area at the minimum lumen area was larger than that at the distal reference (17.5 (5.6) *v* 14.0 (6.0) mm^2, $p < 0.001$).

The patients in the two groups did not differ in age (61 (6) years *v* 62 (10) years) or sex (male: 14/15 *v* 18/20). Lesion location was also similar for both groups: left anterior descending (9/15 *v* 11/20), right (5/15 *v* 5/20), and left circumflex coronary arteries (1/15 *v* 4/20).

PLANAR INTRAVASCULAR ULTRASOUND

Quantitative coronary angiographic measurements were similar in both groups (table 1)

QUANTITATIVE ANGIOGRAPHIC ANALYSES

Reference segment measurements were similar in both groups (table 2). There was no difference in minimum lumen cross sectional area or cross sectional area plaque burden (table 2); however, both vessel and plaque cross sectional area were significantly smaller in group I (lesions with inadequate remodelling).

Table 2 Cross sectional area (CSA) measurements with intravascular ultrasound

Variables	Group I (n = 15)	Group II (n = 20)	p value
Minimum lumen site			
Lumen CSA (mm^2)	2.4 (1.0)	2.3 (1.5)	NS
Vessel CSA (mm^2)	13.3 (3.0)	17.5 (5.6)	< 0.01
Plaque CSA (mm^2)	10.9 (2.8)	15.2 (4.9)	< 0.005
CSA plaque burden (%)	82 (7)	87 (7)	< 0.05
Reference site			
Lumen CSA (mm^2)	7.2 (3.6)	7.4 (4.1)	NS
Vessel CSA (mm^2)	14.4 (3.6)	14.0 (6.0)	NS
Plaque CSA (mm^2)	7.3 (2.5)	6.5 (3.0)	NS
CSA plaque burden (%)	52 (15)	49 (16)	NS

Values are mean (SD).
Groups I and II, lesions with and without inadequate compensatory vascular enlargement, respectively.
Reference images were acquired no more than 3 mm distal to the 20 mm long lesion segments.

Table 3 Volumetric measurements by intravascular ultrasound

Variables	Group I (n = 15)	Group II (n = 20)	p value
Lumen volume (mm^3)	113.6 (44.0)	125.7 (49.9)	NS
Vessel volume (mm^3)	291.0 (61.0)	353.7 (110.0)	< 0.05
Plaque volume (mm^3)	177.5 (48.4)	228.0 (92.8)	< 0.05
Volumetric plaque burden (%)	61 (11)	64 (10)	NS

Values are mean (SD).
Groups I and II, lesions with and without inadequate compensatory vascular enlargement, respectively; segment length was 20 mm.

INTRAVASCULAR ULTRASOUND VOLUMETRIC ANALYSIS

Overall, an average of 62.8(10.8)% of the vessel volume (326.9 (7.0) mm^3) was filled with plaque (206.4 (80.1) mm^3); this defined the volumetric plaque burden. The residual lumen volume measured 120.5 (47.2) mm^3. Plaque and vessel volumes were smaller in group I than

in group II ($p < 0.05$ for both) (table 3); there was no significant difference in lumen volume or in volumetric plaque burden.

The eccentricity index (minimum plaque thickness divided by maximum plaque thickness) was significantly higher in group I than in group II (0.28 (0.07) *v* 0.21 (0.11), $p < 0.05$), indicating a more concentric plaque distribution in group I. The lumen shape was significantly more symmetrical in group I; this was shown by the higher lumen symmetry index (minimum lumen diameter divided by maximum lumen diameter) in group I (0.86 (0.02) *v* 0.84 (0.03), $p < 0.05$).

Discussion

Three dimensional intravascular ultrasound was initially used for visual assessment of the spatial configuration of plaques and dissection membranes,[36 37] whereas contemporary three dimensional intravascular ultrasound systems are equipped with algorithms for computer assisted analysis of the plaque or lumen volumes and dimensions.[6 25-29 35 38 39] The three dimensional intravascular ultrasound analysis system used in the current study has been extensively validated; it permits the rapid automated analysis of lumen and plaque volumes and dimensions on a large number of planar image slices.[6 26-28]

We used this three dimensional intravascular ultrasound analysis system to compare 15 lesions with inadequate compensatory enlargement to 20 lesions with adequate compensatory enlargement. Compared to lesions with adequate compensatory enlargement, lesions with inadequate compensatory enlargement had smaller plaque and vessel volumes, more concentric plaque distribution, more symmetrical lumen shapes, and similar lumen volumes and dimensions.

Importantly, lumen volumes and dimensions were similar in both groups, whether assessed by intravascular ultrasound or by quantitative coronary angiography. This emphasises the significance of intravascular ultrasound in the assessment of human atherosclerosis in vivo.

Our observations corroborate recent studies, which showed that inadequate compensatory enlargement may contribute to the development of significant luminal narrowing.[19-25] In these previous studies, despite intracoronary injection of nitrates before the ultrasound examination, local vasospastic activity could not be excluded[23]; and a collapse of the coronary artery could have resulted from a decrease in coronary arterial pressure, attributable to subtotal occlusion of the residual lumen during the ultrasound imaging run. However, neither local vasospasm nor collapse of the coronary artery can explain the significantly smaller vessel and plaque volumes of lesions with inadequate compensatory enlargement, as observed in the current study.

LIMITATIONS AND POTENTIAL SOURCES OF ERROR

As all previous studies of the natural history of coronary atherosclerosis in human were performed at a single point in time, the time course and magnitude of vascular response to plaque growth remains unknown.

Imaging with intravascular ultrasound can be hampered by eccentric catheter position, non-uniform transducer rotation, and non-coaxial catheter position.

As the external vascular boundary cannot be seen in the acoustic shadow behind calcium, we did not include lesions with severe plaque calcification. As in all studies with intravascular ultrasound, intracoronary injections of nitrates were performed before the ultrasound examination to prevent vasospasm; no angiographic changes before and after the intravascular ultrasound imaging procedure were observed, but this does not exclude local vasospastic activity.

Linear three dimensional systems, as used in the current study, provide approximate volumetric indices because they do not account for the presence of vascular curvatures.[28 29 42] In the current study, only relatively straight coronary segments on the angiogram were included to minimise the curve induced error in the volume calculation. Approaches that combine data obtained from angiography and intravascular ultrasound can provide information on the real spatial geometry of the vessel, but these sophisticated techniques are still subject to refinement and ongoing research.[29]

CONCLUSIONS

Planar intravascular ultrasound analysis identified a population of coronary artery lesions with inadequate compensatory vascular enlargement. Volumetric intravascular ultrasound analysis showed that these lesions have less atherosclerotic plaque. Serial intravascular ultrasound studies will be required to determine whether the adaptive remodelling state of atherosclerotic lesions has any implication for the success of catheter based or pharmacological treatment strategies.

CvB is the recipient of a fellowship of the German Research Society (DFG, Bonn, Germany).

1 Anderson MH, Simpson IA, Katritsis D, *et al.* Intravascular ultrasound imaging of the coronary arteries: an in vitro evaluation of measurement of area of the lumen and atheroma characterization. *Br Heart J* 1992;68:276–81.
2 Ge J, Erbel R, Gerber T, *et al.* Intravascular ultrasound imaging in angiographically normal coronary arteries: a prospective study in vivo. *Br Heart J* 1994;71:572–8.
3 Pinto FJ, St Chenzbraun A, Botas J, *et al.* Feasibility of serial intracoronary ultrasound imaging for assessment of progression of intimal proliferation in cardiac transplant recipients. *Circulation* 1994; 90:2348–55.
4 Alfonso F, Macaya C, Goicolea J, *et al.* Intravascular ultrasound imaging of angiographically normal coronary segments in patients with coronary artery disease. *Am Heart J* 1994;127:536–44.
5 Kearney PP, Starkey IR, Sutherland GR. Intracoronary ultrasound: current state of the art. *Br Heart J* 1995; 73(suppl 2):16–25.
6 von Birgelen C, Slager CJ, Di Mario C, *et al.* Volumetric intracoronary ultrasound: a new maximum confidence approach for the assessment of progression–regression of atherosclerosis? *Atherosclerosis* 1995;118(suppl):S103–13.
7 Hausmann D, Johnson JA, Sudhir K, *et al.* Angiographically silent atherosclerosis detected by intravascular ultrasound in patients with familial hypercholesterolemia and familial combined hyperlipidemia: correlation with high density lipoproteins. *J Am Coll Cardiol* 1996;27:1562–70.
8 Erbel R, Ge J, Bockisch A, *et al.* Value of intracoronary ultrasound and Doppler in the differentiation of angiographically normal coronary arteries: a prospective study in patients with angina pectoris. *Eur Heart J* 1996;17:880–9.
9 Peters RJC, Kok WEM, Di Mario C, *et al.* Prediction of restenosis after coronary balloon angioplasty: results of PICTURE (Post-IntraCoronary Treatment Ultrasound

Result Evaluation), a prospective multicenter intracoronary ultrasound imaging study. *Circulation* 1997;95:2254–61.
10 Bond MG, Adams MR, Bullock. Complicating factors in evaluating coronary arterial atherosclerosis. *Artery* 1981; 51:434–9.
11 Armstrong ML, Heistad DD, Marcus ML, *et al.* Structural and hemodynamic response of peripheral arteries of macaque monkeys to atherogenic diet. *Arteriosclerosis* 1985; 5:336–46.
12 Glagov S, Weisenberg E, Zaris CK, *et al.* Compensatory enlargement of human atherosclerotic coronary arteries. *N Engl J Med* 1987;316:13371–5.
13 Stiel GM, Stiel LSG, Schofer J, *et al.* Impact of compensatory enlargement of atherosclerotic coronary arteries on angiographic assessment of coronary artery disease. *Circulation* 1989;80:1603–9.
14 McPherson DD, Sims SJ, Hiratzka LF, *et al.* Coronary artery remodeling studied by high-frequency epicardial echocardiography: an early compensatory mechanism in patients with obstructive coronary atherosclerosis. *J Am Coll Cardiol* 1991;17:79–86.
15 Ge J, Erbel R, Zamorano J, *et al.* Coronary artery remodeling in atherosclerotic disease: an intravascular ultrasonic study in vivo. *Coronary Art Dis* 1993;4:981–6.
16 Hermiller JB, Tenaglia AN, Kisslo KB, *et al.* In vivo validation of compensatory enlargement of atherosclerotic coronary arteries. *Am J Cardiol* 1993;71:665–8.
17 Gerber TC, Erbel R, Gorge G, *et al.* Extent of atherosclerosis and remodeling of the left main coronary artery determined by intravascular ultrasound. *Am J Cardiol* 1994;73:666–71.
18 Losordo DW, Rosenfield K, Kaufman J, *et al.* Focal compensatory enlargement of human arteries in response to progressive atherosclerosis: in vivo documentation using intravascular ultrasound. *Circulation* 1994;89:2570–7.
19 Clarkson TB, Prichard RW, Morgan TM, *et al.* Remodeling of coronary arteries in human and nonhuman primates. *JAMA* 1994;271:289–94.
20 Pasterkamp G, Wensing PJW, Post MJ, *et al.* Paradoxical arterial wall shrinkage may contribute to luminal narrowing of human atherosclerotic femoral arteries. *Circulation* 1995;91:1444–9.
21 Pasterkamp G, Borst C, Post MJ, *et al.* Atherosclerotic arterial remodeling in the superficial femoral artery: individual variation in local compensatory enlargement response. *Circulation* 1996;93:1818–25.
22 Wong CB, Porter TR, Xie F, *et al.* Segmental analysis of coronary arteries with equivalent plaque burden by intravascular ultrasound in patients with and without angiographically significant coronary artery disease. *Am J Cardiol* 1995;76:598–601.
23 Nishioka T, Luo H, Eigler NL, *et al.* Contribution of inadequate compensatory enlargement to development of human coronary artery stenosis: an in vivo intravascular ultrasound study. *J Am Coll Cardiol* 1996;27:1571–6.
24 Mintz GS, Kent KM, Pichard AD, *et al.* Contribution of inadequate arterial remodeling to the development of focal coronary artery stenoses: an intravascular ultrasound study. *Circulation* 1997;95:1791–8.
25 von Birgelen C, Di Mario C, Serruys PW. Structural and functional characterization of an intermediate stenosis with intracoronary ultrasound: a case of "reverse Glagovian modeling". *Am Heart J* 1996;132:694–6.
26 von Birgelen C, van der Lugt A, Nicosia A, *et al.* Computerized assessment of coronary lumen and atherosclerotic plaque dimensions in three-dimensional intravascular ultrasound correlated with histomorphometry. *Am J Cardiol* 1996;78:1202–9.
27 von Birgelen C, Di Mario C, Li W, *et al.* Morphometric analysis in three-dimensional intracoronary ultrasound: an in-vitro and in-vivo study using a novel system for the contour detection of lumen and plaque. *Am Heart J* 1996;132: 516–27.
28 von Birgelen C, de Vrey EA, Mintz GS, *et al.* ECG-gated three-dimensional intravascular ultrasound: feasibility and reproducibility of the automated analysis of coronary lumen and atherosclerotic plaque dimensions in humans. *Circulation* 1997;96:2944–52.
29 von Birgelen C, Mintz GS, de Feyter PJ, *et al.* Reconstruction and quantification with three-dimensional intracoronary ultrasound: an update on techniques, challenges, and future directions. *Eur Heart J* 1997;18:1056–67.
30 Mallery JA, Tobis JM, Griffith J, *et al.* Assessment of normal and atherosclerotic arterial wall thickness with an intravascular ultrasound imaging catheter. *Am Heart J* 1990;119: 1392–400.
31 Honye J, Mahon DJ, Jain A, *et al.* Morphological effects of coronary balloon angioplasty in vivo assessed by intravascular ultrasound imaging. *Circulation* 1992;85:1012–25.
32 Escaned J, Baptista J, Di Mario C, *et al.* Significance of automated stenosis detection during quantitative angiography: insights gained from intracoronary ultrasound. *Circulation* 1996;94:966–72.
33 von Birgelen C, Kutryk MJB, Gil R, *et al.* Quantification of the minimal luminal cross-sectional area after coronary stenting by two- and three-dimensional intravascular ultrasound versus edge detection and videodensitometry. *Am J Cardiol* 1996;78:520–5.
34 Kitney RI, Moura L, Straughan K. 3-D visualization of arterial structures using ultrasound and voxel modeling. *Int J Cardiac Imag* 1989;4:135–43.
35 Rosenfield K, Losordo DW, Ramaswamy K, *et al.* Three-dimensional reconstruction of human coronary and peripheral arteries from images recorded during two-dimensional intravascular ultrasound examination. *Circulation* 1991;84:1938–56.
36 Coy KM, Park JC, Fishbein MC, *et al.* In vitro validation of three-dimensional intravascular ultrasound for the evaluation of arterial injury after balloon angioplasty. *J Am Coll Cardiol* 1992;20:692–700.
37 Roelandt JRTC, Di Mario C, Pandian NG, *et al.* Three-dimensional reconstruction of intracoronary ultrasound images: Rationale, approaches, problems, and directions. *Circulation* 1994;90:1044–55.
38 Di Mario C, von Birgelen C, Prati F, *et al.* Three-dimensional reconstruction of two-dimensional intracoronary ultrasound: clinical or research tool? *Br Heart J* 1995; 73(suppl 2):26–32.
39 von Birgelen C, Mintz GS, Nicosia A, *et al.* Electrocardiogram-gated intravascular ultrasound image acquisition after coronary stent deployment facilitates on-line three-dimensional reconstruction and automated lumen quantification. *J Am Coll Cardiol* 1997;30:436–43.
40 Evans JL, Ng KH, Wiet SG, *et al.* Accurate three-dimensional reconstruction of intravascular ultrasound data: spatially correct three-dimensional reconstructions. *Circulation* 1996;93:567–76.

Chapter 11

Successful directional atherectomy of de novo coronary lesions assessed with three-dimensional intravascular ultrasound and angiographic follow-up

C von Birgelen, GS Mintz, EA de Vrey, PJ de Feyter, T Kimura, JJ Popma, M Nobuyoshi, PW Serruys, MB Leon

Reprinted with permission from *Am J Cardiol* 1997;80:1540-1545

Successful Directional Atherectomy of De Novo Coronary Lesions Assessed With Three-Dimensional Intravascular Ultrasound and Angiographic Follow-Up

Clemens von Birgelen, MD, Gary S. Mintz, MD, Evelyn A. de Vrey, MD, Pim J. de Feyter, MD, PhD, Takeshi Kimura, MD, Jeffrey J. Popma, MD, Masakiyo Nobuyoshi, MD, Patrick W. Serruys, MD, and Martin B. Leon, MD

Recent histopathologic and intravascular ultrasound (IVUS) data indicate that inadequate compensatory enlargement of atherosclerotic lesions contributes to the development of significant arterial stenoses. Such lesions may contain less plaque, which may have implications for atheroablative interventions. In this study, we compared lesions with (group A, n = 16) and without inadequate compensatory enlargement (group B, n = 30) as determined by IVUS. The acute results and the follow-up lumen dimensions of angiographically successful directional coronary atherectomy procedures were compared. Inadequate compensatory enlargement was considered present when the preintervention arterial cross-sectional area at the target lesion site was smaller than that at the (distal) reference site. Three-dimensional IVUS analysis and quantitative angiography were performed in 46 patients before and after intervention. IVUS measurements included the arterial, lumen, and plaque (arterial minus lumen) cross-sectional areas at the target lesion site (i.e., smallest lumen site) and the (distal) reference site. Angiographic follow-up was performed in 42 patients. Preintervention and postintervention angiographic measurements and IVUS lumen cross-sectional area measurements were similar in both groups. However, at follow-up, the angiographic minimum lumen and reference diameters were significantly smaller in group A compared with group B (1.71 ± 0.47 mm vs 2.14 ± 0.73 mm, p <0.03, and 2.97 ± 0.29 mm vs 3.39 ± 0.76 mm, p <0.02; group A vs B). The data of this observational study suggest that lesions with inadequate compensatory enlargement, as determined by IVUS before intervention, may have less favorable long-term lumen dimensions after directional coronary atherectomy procedures. ©1997 by Excerpta Medica, Inc.

(Am J Cardiol 1997;80:1540–1545)

Histopathologic studies in primates and humans have demonstrated that atherosclerotic arteries tend to undergo compensatory enlargement to accommodate an increasing plaque burden to preserve luminal dimensions until the progressive accumulation of plaque exceeds the ability of the vessel to compensate.[1,2] Subsequently, Clarkson et al[3] extended this concept by suggesting that failure of compensatory enlargement may be important in the development of significant arterial stenoses. Intravascular ultrasound (IVUS) provides transmural images of coronary vessels in vivo. The coronary vascular wall, the cross-sectional area of the atherosclerotic plaque, accurate lumen dimensions, and the serial changes that occur with the atherosclerotic disease process can be studied in humans in a manner previously not possible.[4–7] The initial studies with IVUS and epicardial ultrasound confirmed the concept of compensatory vascular enlargement.[4–8] However, recent histopathologic and IVUS data in atherosclerotic peripheral[9] and coronary arteries[10,11] supported the hypothesis of Clarkson et al[3] and showed evidence of inadequate compensatory vascular enlargement. Lesions with inadequate compensatory enlargement have been shown to contain less plaque burden; this may have implications for atheroablative interventions such as directional coronary atherectomy.[11–20] Therefore, we compared lesions with and without inadequate compensatory enlargement, as determined by preintervention IVUS, with regard to the acute results and follow-up lumen dimensions following successful directional coronary atherectomy procedures.

From the Washington Hospital Center, Washington, DC; Thoraxcenter, Erasmus University Rotterdam, Rotterdam, The Netherlands; and Kokura Memorial Hospital, Kitakyushu, Japan. Manuscript received and accepted September 11, 1997.

Address for reprints: Gary S. Mintz, MD, The Washington Hospital Center, Room 4 B1, 110 Irving Street N.W., Washington, DC 20010

METHODS

Study population: The study groups consisted of 46 symptomatic patients who were treated by directional coronary atherectomy procedures at the Washington Hospital Center, the Kokura Memorial Hospital, or the Thoraxcenter Rotterdam. Patients were included if they met the following criteria: (1) successful directional atherectomy (with or without adjunctive balloon angioplasty) of a single, primary nonostial lesion with limited calcification throughout its length, (2) high-quality IVUS recordings using motorized transducer pull-back through a stationary imaging sheath both before and after the intervention, and (3) lack of complete occlusion of the stenotic lumen during the initial IVUS imaging run. There were 38 men and 8 women who ranged in age from 37 to 76 years (mean 59 ± 9). Lesion location was the left anterior descend-

ing coronary artery (n = 29), right coronary artery (n = 12), and left circumflex coronary artery (n = 5); 37 lesions were proximal and 9 were midvessel.

Lesions were divided into 2 groups based on preintervention IVUS measurements: (1) lesions with inadequate compensatory enlargement (group A) and (2) lesions with adequate compensatory enlargement (group B). There was no significant difference between group A and B with regard to the characteristics of the patients and lesion location. The study was approved by the Local Councils on Human Research. All patients signed a written informed consent form approved by the Local Medical Ethics Committees.

Interventional procedure: All patients received 250-mg aspirin and 10,000-U heparin intravenously. If the duration of the entire catheterization procedure was >1 hour, the activated clotting time was measured, and intravenous heparin was administered in order to maintain an activated clotting time of >300 seconds. After intracoronary injection of 0.2-mg nitroglycerin, the coronary artery was examined with IVUS. Directional coronary atherectomy (Devices for Vascular Intervention, Redwood City, California) was performed according to standard protocols. If required, predilation before the atherectomy (but after the initial IVUS run) was performed (n = 3). A final IVUS imaging run was then performed at the end of the procedure. In the patients with adjunctive balloon angioplasty, the final IVUS imaging run was performed after the balloon dilation. Follow-up angiography was performed after 6 months in 42 patients (91.4%), using a standard cardiac catheterization and angiography protocol.

Atherectomy was performed using an average of 23 ± 10 cuts and a mean pounds per square inch (lbs/in^2) of 26 ± 11. The maximum cutter size of the atherectomy device was 7Fr in 43 patients and 6Fr in 3 patients. In 31 patients (67.4%), adjunctive balloon angioplasty was performed, using a nominal balloon size of 3.9 ± 0.6 mm at a maximum pressure of 10.0 ± 4.9 atm. There was no significant difference between group A and B with regard to the characteristics of the interventional procedures; adjunctive balloon angioplasty was performed in 68.7% (11 of 16 patients) and 66.7% (20 of 30 patients), respectively.

Intravascular ultrasound imaging: A mechanical IVUS system (CardioVascular Imaging Systems Inc., San Jose, California) and a sheath-based imaging catheter were used. The catheter incorporated a 30-MHz beveled, single-element transducer rotating at 1,800 rpm within a stationary echolucent imaging sheath. Two catheter designs were used: (1) a 3.2Fr short monorail version or (2) a 2.9Fr long monorail version. The common distal lumen of the latter version alternatively houses the guidewire (during catheter introduction) or the transducer (during imaging after the guidewire is pulled back), but not both. These sheath-based catheter designs avoid direct contact of the imaging core with the vessel wall. The ultrasonic transducer was withdrawn through the stationary imaging sheath using a motorized pull-back device at a constant speed of 0.5 mm/s. The IVUS catheter was advanced ≥10 mm distal to the lesion segment, the motorized transducer pull-back device was then activated, and imaging continued (uninterrupted) until the transducer reached the aorto-ostial junction. All IVUS studies were recorded on high-resolution s-VHS videotape for off-line quantitative analysis.

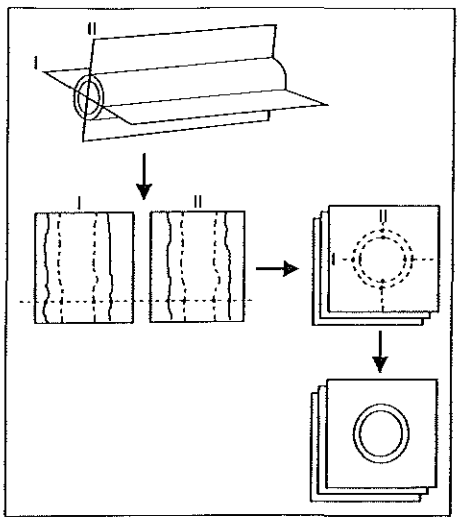

FIGURE 1. Automated contour detection of the luminal and arterial boundaries was first performed on 2 perpendicular longitudinal sections *(I, II)* that were reconstructed from the image data of a 3-dimensional stack of IVUS images. The 3-dimensional approach permitted interpretation in the longitudinal dimension and facilitated the detection of the contours on the planar images. Edge information from the longitudinal contours was represented as points on the planar images, defining the center and range for the final automated contour detection process. The contours on the planar images were checked and edited if required. Measurements were derived from these contours.

Intravascular ultrasound contour detection algorithm: All preintervention and postintervention IVUS studies were analyzed with a computerized analysis system operating in either a single-frame mode (to analyze a preselected single reference image) or in 3-dimensional mode (to perform a segmental analysis of the entire lesion segment).[21-23] In 3-dimensional mode, a "stack" of IVUS images (10 images/mm of arterial length) was digitized from videotape. Two longitudinal sections were automatically reconstructed (Figure 1), and the contours corresponding to the lumen-tissue and media-adventitia interfaces were automatically identified. The automatic contour detection was then visually checked; if necessary, the longitudinal contours were edited.

The longitudinal contours generated 8 individual points on the corresponding planar images (4 for the lumen-tissue interface and 4 for the media-adventitia interface) which defined the range of interest for contour detection on the planar images.[21-23] Automated detection and computer-assisted editing of the contours assigned to the tissue-lumen and media-adven-

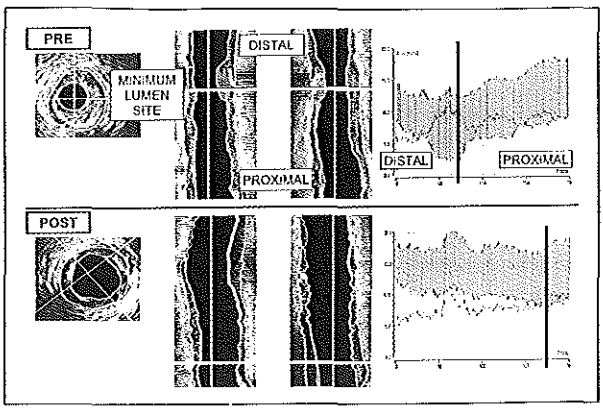

FIGURE 2. Three-dimensional IVUS analysis of an entire lesion segment (i.e., the treated vascular segment) before *(PRE, upper panels)* and after directional coronary atherectomy with adjunctive balloon angioplasty *(POST, lower panels)*; lesion location was the mid-segment of a right coronary artery. The cut-planes of the longitudinally reconstructed IVUS sections *(middle panels)* are indicated on the planar IVUS images *(left panels)*, which represent the target lesion sites (i.e., minimum lumen site). Markers on both, the longitudinal sections *(white horizontal markers)* and the result displays *(black vertical markers, right panels)* indicate the site of the image with the smallest lumen cross-sectional area. The results of cross-sectional area measurements (in square millimeters) on 200 planar IVUS frames are displayed in the right panels. Linear functions of the arterial and lumen cross-sectional area form the upper and lower boundaries of the grayish area, which represents the plaque plus media cross-sectional area. Note that before the intervention *(right upper panel)*, the arterial area was smallest at the target lesion site (12.9 mm^2), indicating inadequate compensatory enlargement.

titia interfaces on the planar image slices were based on the application of a minimum-cost algorithm. Each digitized IVUS image was resampled in a radial format (64 radii per image); a cost matrix representing the edge strength was calculated from the image data. For the boundary between lumen and plaque, the cost value was defined by the spatial first derivative. For the media-adventitia boundary a cross-correlation pattern matching process was used for the cost calculations. The path with the smallest accumulated value was determined by dynamic programming techniques. Small side branches or small calcified deposits were generally ignored by the algorithm as a result of its robustness.

The axial location of an individual planar image on the longitudinal presentation was indicated by a cursor; this cursor was used to scroll through the entire set of planar images to visually check the contours. Careful checking and editing of the contours of the planar images was performed. The computer-assisted editing differed considerably from conventional manual contour tracing. The computer mouse was pointed on the correct boundary to give that site a very low value in the cost matrix, which "forced" the contour through that point. Editing the contour of a single slice caused the entire data set to be updated. Finally, the contour data of the planar images were used for the computation of the results (Figure 2).

Previous validation of this algorithm has been performed in tubular phantoms.[22] A comparison between automated 3-dimensional IVUS measurements in atherosclerotic coronary specimen in vitro and morphometric measurements on the corresponding histologic sections revealed good correlations ($r = 0.80$ to 0.94 for cross-sectional area measurements).[21] The cross-sectional area measurements agreed well with results obtained by manual tracing of IVUS images (mean differences $\pm$ 3.7%; $r = 0.97$).[21] In vivo, the intraobserver and interobserver comparison of the analysis method revealed a high correlation ($r = 0.95$ to 0.98 for cross-sectional area measurements) and small mean differences ($\pm$1.1%), with SD, for lumen, arterial, and plaque plus media cross-sectional areas not exceeding 7.3%, 4.5%, and 10.9%.[22]

Intravascular image analysis: The arterial cross-sectional area was measured as the area within the border between the hypoechoic media and the echoreflective adventitia. As in many previous studies using IVUS,[17,18,23,24] the plaque plus media cross-sectional area was used as a measure of atherosclerotic plaque, because ultrasound cannot measure media thickness accurately.[25]

As in previous 3-dimensional IVUS studies,[24] the entire lesion segment (i.e., entire region of treatment) was identified by (1) comparing the ultrasound images before and after the intervention, noting lumen increase, topographical landmarks (such as side branches and calcification), and typical postintervention findings of plaque defects and flaps; and (2) the tape-recorded comments of the operator. The lesion segments (19.3 $\pm$ 4.3 mm) were digitized (193 $\pm$ 43 images/segment) and analyzed with the contour detection system. The target lesion site (i.e., the site of the smallest lumen cross-sectional area) was automatically identified from the computerized analysis of the entire lesion segment. The reference site was visually determined from the preintervention IVUS study as the image slice with the smallest plaque burden within 3 mm distal to the lesion segment, but before any major side branch (on average 10.2 $\pm$ 2.9 mm distal to center of the lesion site). Measurements at the target lesion and reference sites included the arterial, lumen, and plaque plus media (arterial minus lumen) cross-sectional area and the cross-sectional area plaque burden (plaque plus media divided by arterial cross-sectional area).

Inadequate compensatory enlargement was determined from preintervention IVUS imaging, comparing the target lesion with the distally located reference site. Using a definition, initially suggested by Nishioka et al[10]: "inadequate compensatory enlargement was considered present when the arterial cross-sec-

TABLE 1 Intravascular Ultrasound Data of Target Lesion Sites

	Group A	Group B	p Value
Preintervention			
Arterial CSA (mm^2)	13.2 ± 3.0	17.6 ± 5.1	<0.001
Lumen CSA (mm^2)	2.5 ± 1.0	2.7 ± 1.5	NS
Plaque + media CSA (mm^2)	10.8 ± 2.8	14.9 ± 4.4	<0.0005
CSA plaque burden (%)	84.6 ± 6.5	80.9 ± 7.5	NS
Postintervention			
Arterial CSA (mm^2)	15.4 ± 2.3†	18.4 ± 6.3	<0.03
Lumen CSA (mm^2)	6.4 ± 1.5‡	6.9 ± 2.2‡	NS
Plaque + media CSA (mm^2)	9.1 ± 1.5*	11.5 ± 5.1†	<0.03
CSA plaque burden (%)	58.7 ± 6.5‡	61.2 ± 8.8‡	NS

Data are mean values ± 1 SD.
Pre- versus postintervention data: *p <0.01; †p <0.001; ‡p <0.0001.
CSA = cross-sectional area.
Target lesion sites were determined by the smallest lumen cross-sectional area.

tional area at the target lesion site was smaller than that at the reference site."

Quantitative coronary angiography: Quantitative angiographic analysis was performed offline on end-diastolic frames with homogeneous opacification of the coronary lumen acquired after intracoronary application of nitrates, as previously described.[14] We used a computer-based Coronary Angiography Analysis System (CAAS, PieMedical, Maastricht, The Netherlands). The measurements were performed by an experienced analyst in 22 angiograms and obtained from opposite (ideally orthogonal) angiographic views without overlapping side branches or foreshortening. The absolute angiographic diameter of the stenosis was determined using the nontapering part of the contrast-free guiding catheter as a scaling device. The minimal lumen diameter was measured by edge detection; the interpolated reference diameter was based on a computerized estimation of the original lumen dimension at the site of the obstruction. The diameter stenosis was derived from the measured minimal lumen diameter and the reference diameter.

Statistical analysis: Quantitative data were given as mean value ± SD. Dichotomous variables were expressed as frequencies and compared using chi-square statistics. Continuous variables were compared using the 2-tailed Student's *t* test and linear regression analysis. A p value <0.05 was considered statistically significant.

RESULTS

Intravascular ultrasound data (Table I): Inherent with the IVUS-based classification, in group A the preintervention arterial cross-sectional area was smaller at the target lesion than at the reference site (13.2 ± 3.0 mm^2 vs 14.4 ± 3.5 mm^2, p <0.003; difference: −0.1 to −3.2 mm^2). In group B the arterial cross-sectional area was larger at the target lesion site than at the reference site (17.6 ± 5.1 mm^2 vs 14.0 ± 5.3 mm^2, p <0.0001; difference: 0.1 to 9.6 mm^2). Both the arterial cross-sectional area and the plaque plus media cross-sectional area of the target lesion site were smaller in group A than in group B (p <0.001).

During intervention, lumen dimensions increased significantly (p <0.0001) with a residual cross-sectional area plaque burden of 58.7 ± 6.5% versus 61.2 ± 8.8% for groups A and B, respectively. Residual arterial and plaque plus media cross-sectional areas were smaller in group A (p <0.03 for both).

Quantitative angiographic measurements (Table II): During the intervention, overall the minimal lumen diameter increased significantly from 1.13 ± 0.35 mm to 2.7 ± 0.49 mm (p <0.0001); the reference diameter increased from 3.26 ± 0.57 mm to 3.44 ± 0.51 mm (p <0.002); and the diameter stenosis decreased from 64 ± 13% to 21 ± 12% (p <0.0001). When group A was compared with group B, there was no significant difference in pre- and postintervention reference diameter, minimal lumen diameter, or diameter stenosis.

Angiographic follow-up was available in 42 patients (91.4%) (group A, 15 of 16 or 93.7%, and group B, 27 of 30 or 90%). Overall, the minimal lumen diameter measured 1.99 ± 0.68 mm, the reference diameter 3.24 ± 0.66 mm, and the diameter stenosis 39 ± 14%. Both the reference and minimal lumen diameters measured at follow-up were significantly smaller in group A than in group B (Figure 3). Because the reference diameters at follow-up were significantly smaller in group A, there was no difference in diameter stenosis (42 ± 15% vs 38 ± 14%, p = 0.37); a diameter stenosis of 50% was found in 5 patients of each group (group A, 5 of 15 or 33.3%, and group B, 5 of 27 or 18.5%, p = 0.28).

DISCUSSION

In the current study inadequate compensatory enlargement was present before intervention in 35% of the de novo coronary lesions treated with directional coronary atherectomy. The main finding of the present study is that despite similar postintervention lumen dimensions of both lesions with and without inadequate compensatory enlargement, the angiographic minimal lumen and reference diameters at follow-up were significantly smaller in lesions with inadequate compensatory enlargement, as determined by IVUS before intervention.

Quantitative coronary angiography[26] and planar IVUS studies[27] have previously shown that the postintervention lumen dimensions and the residual cross-sectional area plaque burden at the lesion site are predictors of the follow-up lumen dimensions. The findings of this study suggest that the arterial remodeling state before directional atherectomy procedures could be another factor that may influence the follow-up lumen dimensions.

As in previous IVUS studies, both plaque ablation and vessel wall stretch accounted for the procedural lumen gain in the present study. The residual postintervention cross-sectional area plaque burden at the

TABLE II Quantitative Angiographic Data

	Group A	Group B	p Value
Preintervention			
Reference diameter (mm)	3.14 ± 0.50	3.32 ± 0.60	NS
MLD (mm)	1.08 ± 0.38	1.16 ± 0.33	NS
Diameter stenosis (%)	66 ± 10	64 ± 14	NS
Postintervention			
Reference diameter (mm)	3.26 ± 0.45	3.54 ± 0.52	NS
MLD (mm)	2.65 ± 0.45	2.74 ± 0.51	NS
Diameter stenosis (%)	18 ± 12	22 ± 12	NS
Follow-up			
Reference diameter (mm)	2.97 ± 0.29	3.39 ± 0.76	<0.02
MLD (mm)	1.71 ± 0.47	2.14 ± 0.73	<0.03
Diameter stenosis (%)	42 ± 15	38 ± 14	NS

Data are mean values ± 1 SD.
MLD = minimal lumen diameter.

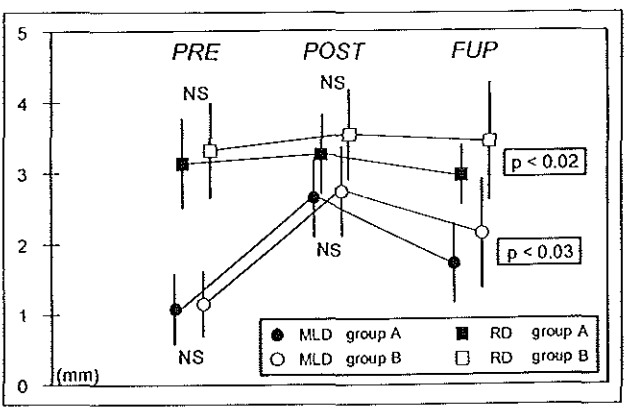

FIGURE 3. Between groups A and B, there was no significant difference in pre-(PRE) and postintervention (POST) reference diameter (RD) and minimal lumen diameter (MLD) as measured by quantitative coronary angiography. However, at 6-month angiographic follow-up (FUP) both minimal lumen and reference diameters were significantly smaller in group A.

smallest lumen site (60%) was comparable to that of most previous studies using planar IVUS analyses.[15–18,24,28]

Three-dimensional IVUS image analysis: Three-dimensional reconstruction of the ultrasonic images was initially used to visually assess the spatial configuration of the lumen and plaque and to perform elementary measurements.[29,30] Recently, algorithms for automated quantification of the lumen dimensions have been introduced.[21–23,31] The automated 3-dimensional IVUS analysis system applied in the present study (Figure 2) can be used to detect the tissue-lumen boundary as well as the media-adventitia (external elastic membrane) boundary on a relatively larger number of IVUS images per millimeter arterial length.[21–23] In addition, it facilitates the detection of the target lesion site with the smallest lumen size.[31]

Study limitations and potential sources of error: (1) Because our data were derived from a nonconsecutive series of patients (only successful directional atherectomy procedures), no conclusion regarding the primary success rate of directional coronary atherectomy in lesions with or without inadequate compensatory enlargement can be made. (2) Because the external vascular boundary cannot be seen in the acoustic shadowing behind calcium, we excluded cases with severe calcification. (3) Intracoronary injections of nitrates were used to prevent vasospasm, and no angiographic changes were observed before and after the IVUS imaging procedure; nevertheless, local vasospastic activity cannot completely be excluded. (4) The follow-up examination was performed with angiography only (no IVUS follow-up); however, coronary angiography is not able to distinguish between late unfavorable remodeling and intimal hyperplasia, the principal mechanisms of lesion recurrence at follow-up. (5) Coronary angiography delineates only the vessel lumen as a silhouette and foreshortens vessel segments, depending on the projection used. (6) Electrocardiographic gated image acquisition can facilitate the automated quantitative analysis of 3-dimensional IVUS image sets,[23,31] but at the time of the present study, the electrocardiographic gated approach was not yet available.

Clinical implications: Coronary lesions with inadequate compensatory enlargement, as defined by IVUS, may have less favorable long-term lumen dimensions, despite initially successful directional atherectomy procedures. Selection of lesions with more favorable remodeling before intervention may help to improve the long-term outcome after directional coronary atherectomy.

1. Armstrong ML, Heistad DD, Marcus ML, Megan MB, Piegors DJ. Structural and hemodynamic response of peripheral arteries of macaque monkeys to atherogenic diet. *Arteriosclerosis* 1985;5:336–346.
2. Glagov S, Weisenberg E, Zaris CK, Stankunavicius R, Kolettis GJ. Compensatory enlargement of human atherosclerotic coronary arteries. *N Engl J Med* 1987;316:1371–1375.
3. Clarkson TB, Prichard RW, Morgan TM, Petrick GS, Klein KP. Remodeling of coronary arteries in human and nonhuman primates. *JAMA* 1994;271:289–294.
4. Ge J, Erbel R, Zamorano J, Koch L, Kearney P, Görge G, Gerber T, Meyer J. Coronary artery remodeling in atherosclerotic disease: an intravascular ultrasonic study in vivo. *Coron Artery Dis* 1993;4:981–986.
5. Hermiller JB, Tenaglia AN, Kisslo KB, Phillips HR, Bashore TM, Stack RS, Davidson CJ. In vivo validation of compensatory enlargement of atherosclerotic coronary arteries. *Am J Cardiol* 1993;71:665–668.
6. Gerber TC, Erbel R, Görge G, Ge J, Rupprecht HJ, Meyer J. Extent of atherosclerosis and remodeling of the left main coronary artery determined by intravascular ultrasound. *Am J Cardiol* 1994;73:666–671.
7. Losordo DW, Rosenfield K, Kaufman J, Pieczek A, Isner JM. Focal compensatory enlargement of human arteries in response to progressive atherosclerosis:

in vivo documentation using intravascular ultrasound. *Circulation* 1994;89: 2570–2577.
8. McPherson DD, Sirna SJ, Hiratzka LF, Thorpe L, Armstrong ML, Marcus ML, Kerber RE. Coronary artery remodeling studied by high-frequency epicardial echocardiography: an early compensatory mechanism in patients with obstructive coronary atherosclerosis. *J Am Coll Cardiol* 1991;17:79–86.
9. Pasterkamp G, Wensing PJW, Post MJ, Hillen B, Mali WPTM, Borst C. Paradoxical arterial wall shrinkage may contribute to luminal narrowing of human atherosclerotic femoral arteries. *Circulation* 1995;91:1444–1449.
10. Nishioka T, Luo H, Eigler NL, Berglund H, Kim CJ, Siegel RJ. Contribution of inadequate compensatory enlargement to development of human coronary artery stenosis: an in vivo intravascular ultrasound study. *J Am Coll Cardiol* 1996;27:1571–1576.
11. Mintz GS, Kent KM, Pichard AD, Satler LF, Popma JJ, Leon MB. Contribution of inadequate arterial remodeling to the development of focal coronary artery stenoses: an intravascular ultrasound study. *Circulation* 1997;95:1791–1798.
12. Topol EJ, Leya F, Pinkerton CA, Whitlow PL, Hofling B, Simonton CA, Masden RR, Serruys PW, Leon MB, Williams DO et al, for the CAVEAT Study Group. A comparison of directional atherectomy with coronary angioplasty in patients with coronary artery disease. *N Engl J Med* 1993;329:221–227.
13. Safian RD, Gelbfish JS, Erny RE, Schnitt SJ, Schmidt DA, Baim DS. Coronary atherectomy: clinical, angiographic, and histological findings and observations regarding potential mechanisms. *Circulation* 1990;82:69–79.
14. Umans VA, Keane D, Foley D, Boersma E, Melkert R, Serruys PW. Optimal use of directional coronary atherectomy is required to ensure long-term angiographic benefit: a study with matched procedural outcome after atherectomy and angioplasty. *J Am Coll Cardiol* 1996;28:637–644.
15. Tenaglia AN, Buller CE, Kisslo KB, Stack RS, Davidson CJ. Mechanisms of balloon angioplasty and directional coronary atherectomy as assessed by intracoronary ultrasound. *J Am Coll Cardiol* 1992;20:685–691.
16. Suneja R, Nair RN, Reddy KG, Rasheed Q, Sheehan HM, Hodgson JMcB. Mechanisms of angiographically successful directional coronary atherectomy: evaluation by intracoronary ultrasound and comparison with transluminal coronary angioplasty. *Am Heart J* 1993;126:507–514.
17. Braden GA, Herrington DM, Downes TR, Kutcher MA, Little WC. Quantitative and qualitative contrasts in the mechanisms of lumen enlargement by coronary balloon angioplasty and directional coronary atherectomy. *J Am Coll Cardiol* 1994;23:40–48.
18. Di Mario C, Gil R, Camenzind E, Ozaki Y, von Birgelen C, Umans V, de Jaegere P, de Feyter PJ, Roelandt JRTC, Serruys PW. Quantitative assessment with intracoronary ultrasound of the mechanisms of restenosis after percutaneous transluminal coronary angioplasty and directional coronary atherectomy. *Am J Cardiol* 1995;75:772–777.
19. Matar FA, Mintz GS, Farb A, Douek P, Pichard AD, Kent KM, Satler LF, Popma JJ, Keller MB, Pinnow E, Merritt AJ, Lindsay J Jr, Leon MB. The contribution of tissue removal to lumen improvement after directional coronary atherectomy. *Am J Cardiol* 1994;74:647–650.
20. Weissman NJ, Palacios IF, Nidorf SM, Dinsmore RE, Weyman AE. Three-dimensional intravascular ultrasound assessment of plaque volume after successful atherectomy. *Am Heart J* 1995;130:413–419.
21. von Birgelen C, van der Lugt A, Nicosia A, Mintz GS, Gussenhoven EJ, de Vrey E, Mallus MT, Roelandt JRTC, Serruys PW, de Feyter PJ. Computerized assessment of coronary lumen and atherosclerotic plaque dimensions in three-dimensional intravascular ultrasound correlated with histomorphometry. *Am J Cardiol* 1996;78:1202–1209.
22. von Birgelen C, Di Mario C, Li W, Schuurbiers JCH, Slager CJ, de Feyter PJ, Roelandt JRTC, Serruys PW. Morphometric analysis in three-dimensional intracoronary ultrasound: an in-vitro and in-vivo study using a novel system for the contour detection of lumen and plaque. *Am Heart J* 1996;132:516–527.
23. von Birgelen C, de Vrey EA, Mintz GS, Nicosia A, Bruining N, Li W, Slager CJ, Roelandt JRTC, Serruys PW, de Feyter PJ. ECG-gated three-dimensional intravascular ultrasound: feasibility and reproducibility of an automated analysis of coronary lumen and atherosclerotic plaque dimensions in humans. *Circulation*; in press.
24. Matar FA, Mintz GS, Pinnow E, Saturnino PJ, Popma JJ, Kent KM, Satler LF, Pichard AD, Leon MB. Multivariate predictors of intracoronary ultrasound end points after directional coronary atherectomy. *J Am Coll Cardiol* 1995;25: 318–324.
25. Mallery JA, Tobis JM, Griffith J, Gessert J, McRae M, Moussabeck O, Bessen M, Moriuchi M, Henry WL. Assessment of normal and atherosclerotic arterial wall thickness with an intravascular ultrasound imaging catheter. *Am Heart J* 1990;119:1392–1400.
26. Kuntz RE, Gibson CM, Nobuyoshi M, Baim DS. Generalized model of restenosis after conventional balloon angioplasty, stenting and directional atherectomy. *J Am Coll Cardiol* 1993;21:15–25.
27. Mintz GS, Popma JJ, Pichard AD, Kent KM, Satler LF, Chuang YC, Griffin J, Leon MB. Intravascular ultrasound predictors of restenosis after percutaneous transcatheter coronary revascularization. *J Am Coll Cardiol* 1996;27:1678–1687.
28. Dussaillant GR, Mintz GS, Popma JJ, Kent KM, Pichard AD, Satler LF, Leon MB. Intravascular ultrasound, directional coronary atherectomy, and the Optimal Atherectomy Restenosis Study (OARS). *Coron Art Dis* 1996;7:294–298.
29. Rosenfield K, Losordo DW, Ramaswamy K, Pastore JO, Langevin RE, Razvi S, Kosowsky BD, Isner JM. Three-dimensional reconstruction of human coronary and peripheral arteries from images recorded during two-dimensional intravascular ultrasound examination. *Circulation* 1991;84:1938–1956.
30. Coy KM, Park JC, Fishbein MC, Laas T, Diamond GA, Adler L, Maurer G, Siegel RJ. In vitro validation of three-dimensional intravascular ultrasound for the evaluation of arterial injury after balloon angioplasty. *J Am Coll Cardiol* 1992; 20:692–700.
31. von Birgelen C, Mintz GS, Nicosia A, Foley DP, van der Giessen WJ, Bruining N, Airiian SG, Roelandt JRTC, de Feyter PJ, Serruys PW. Electrocardiogram-gated intravascular ultrasound image acquisition after coronary stent deployment facilitates on-line three-dimensional reconstruction and automated lumen quantification. *J Am Coll Cardiol* 1997;30:436–443.

Chapter 12

Volumetric intracoronary ultrasound: A new maximum confidence approach for the quantitative assessment of progression-regression of atherosclerosis ?

C von Birgelen, CJ Slager, C Di Mario, PJ de Feyter,
PW Serruys

Reprinted with permission from *Atherosclerosis* 1995;118(Suppl.):S103-S113

Volumetric intracoronary ultrasound: A new maximum confidence approach for the quantitative assessment of progression-regression of atherosclerosis?

Clemens von Birgelen, Cornelis J. Slager, Carlo Di Mario, Pim J. de Feyter, Patrick W. Serruys*

Thoraxcenter, Division of Cardiology, University Hospital Rotterdam-Dijkzigt and Erasmus University, Rotterdam, The Netherlands

Abstract

Quantitative assessment of atherosclerosis during its natural history and following therapeutic interventions is important, as cardiovascular disease remains the most significant cause of morbidity and mortality in industrial societies. While coronary angiography delineates the vessel lumen, permitting only the indirect determination of atherosclerotic wall changes encroaching upon the lumen, intracoronary ultrasound permits direct plaque assessment and quantification. The angiographic percent diameter stenosis, previously suggested as measure of a maximum confidence approach, is still commonly used to quantify stenosis severity, but the reference segments which are required for angiographic interpolation of the normal vessel dimensions are frequently involved in the general process of atherosclerosis, including progression or regression. Considering also the variability of vascular remodeling during the evolution of atherosclerosis, including compensatory enlargement and paradoxical arterial shrinkage, intracoronary ultrasound appears currently to be the only reliable technique to measure plaque burden and progression or regression of atherosclerosis. However, correct matching of the site of measurement at follow-up with the site of the initial ultrasound study is often difficult to achieve, but is significantly facilitated by the use of volumetric intracoronary ultrasound. This approach permits not only area measurement, but also measurement of plaque volume, which appears to be the ideal measure for quantifying the atherosclerotic plaque, as it is highly reproducible and directly reflects the changes of an entire arterial segment.

Keywords: Coronary artery disease; Progression-regression; Vascular remodeling; Intravascular ultrasound; Volumetric quantification; Plaque volume; Atherosclerosis; Three-dimensional reconstruction

* Corresponding author, Thoraxcenter, Bd 432, Cardiac Catheterization and Intracoronary Imaging Laboratories, P.O. Box 1738, 3000 DR Rotterdam, The Netherlands. Tel.: + 31 10 436 0511; Fax: + 31 10 436 9154.

1. Introduction

Coronary artery disease (CAD) remains the cause of death and disability in the industrialized countries, despite our increased knowledge about

the pathogenetic mechanisms of atherosclerosis [1–5] and our subsequently increased awareness and management of unfavourable risk factors including hypercholesterolemia hypertension, obesitas, smoking and psychological stress. The search for effective interventions remains and the reliable quantitative assessment of atherosclerosis during its natural history and various therapeutical interventions is thus of paramount importance and required in order to define the efficacy of these therapeutical measures [6].

During the last two decades, coronary angiography has been considered the standard method to evaluate the coronary anatomy. The development of semi-automated quantitative angiography in the late 1970s [7] and its clinical application to interventional cardiology in the early 1980s [8] allowed the replacement of visual assessment by a semi-automated approach [9–11], providing objective and reproducible measurements of luminal dimensions. However, coronary angiography delineates only the vessel lumen as a silhouette, a perspective that is incapable of reflecting the irregular nature of the atherosclerotic vessel wall changes. Thus, plaques may be present in angiographically normal segments.

A prognostic value of angiographic endpoints has been demonstrated for both visual assessment and semi-automated coronary angiography [12,13], but the limitations of angiography may explain the minimal changes in luminal dimensions observed in large angiographic studies, aimed at the assessment of progression or regression of coronary atherosclerosis during pharmacologic or dietary interventions [14]. Particularly the use of the relative percent diameter stenosis, recently suggested as the angiographic measure of a maximum confidence approach to quantify stenosis severity [15], nowadays appears to be doubtful, as the angiographic reference segments themselves are frequently involved in the general process of atherosclerosis, including progression or regression. Accordingly, new quantitative coronary imaging techniques such as intracoronary ultrasound, which permits the direct qualitative and quantitative assessment of the coronary plaque, may provide an important addition to the understanding of the natural history and prognosis of coronary atherosclerosis as well as the potential of pharmacological interventions [11,16,17]

2. Current angiographic measures and their limitations

The distribution of atherosclerosis can be either focal or diffuse [18]. If the process of atherosclerosis is predominantly diffuse, relative measurements are unable to quantify plaque severity, explaining the findings of several pathologic studies which indicate that angiography may underestimate the extent and severity of the atherosclerotic changes [19–22]. The angiographic percent diameter stenosis [15] is commonly used to quantify stenosis severity, but the 'normal' reference segments which are required for the calculation of the relative lumen diameter stenosis are frequently involved in a general process of atherosclerosis including progression or regression, thus suggesting pseudo-progression or pseudo-regression [11,23–25]. Furthermore, a relative parameter does not accurately reflect the functional significance of the lesion [26], since lesion length and absolute luminal dimensions are not taken into account. Indeed, such an approach to quantify progression or regression of atherosclerosis appears to be far away from 'a maximal confidence'.

Absolute measurements such as minimal or mean luminal diameter generally appear to be superior indicators of stenosis severity [27–29] or progression of atherosclerosis [30]. However, the minimal luminal diameter which is the most important determinant of the functional significance of coronary stenoses [26,27] is also crucial, since an increase of the lumen diameter at the site of the minimal luminal cross-section can be associated with an overall reduction of the mean lumen diameter. Nevertheless, the mean lumen diameter is the best angiographic measure to determine progression or regression of diffuse atherosclerosis of entire coronary segments [23].

3. Potential and limitations of two-dimensional intracoronary ultrasound

Intracoronary ultrasound is a relatively new method which provides cross-sectional images of both the vessel lumen and wall. The size of the ultrasound transducers had gradually been re-

duced so that recently introduced ultrasound catheters have a distal tip diameter of even less than 1 mm.

The sensitivity of intracoronary ultrasound in detecting minimal atherosclerosis is superior to angiography [31–35] and additional qualitative information on the plaque composition [31,36–40] is provided. Plaque thickness can be directly quantified by ultrasound [41], a feature which was first utilized during epicardial high-frequency ultrasound imaging [42], a forerunner of intracoronary ultrasound. Direct measurement of the vascular dimensions by intracoronary ultrasound can nowadays be performed with high accuracy [31]. Finally, the safety of the invasive intracoronary ultrasound examination, particularly if performed during diagnostic catheterization [43], should be emphasized.

Many problems of the first generation intracoronary ultrasound catheters have been solved or minimized and the image quality has been significantly improved, but the angle of incidence of the ultrasonic beam is still important, since a non-coaxial position of the transducer may result in a distortion of the ultrasound image [44]. Plaque compression by the ultrasound catheter at vessel curvatures and the lateral or out-of-plane resolution of current ultrasound transducers remain fields of future improvement [45].

4. Insights gained from studies of vascular remodeling

Coronary angiography detects atherosclerotic changes in the vessel wall only if the plaque encroaches the lumen. This does not occur during the early stage of plaque expansion as demonstrated by Armstrong et al., who detected in monkeys during an atherogenic diet an enlargement of the coronary artery in response to luminal encroachment by the coronary plaque [46–48]. These experimental findings were confirmed by Glagov et al. [46] in human coronary arteries, demonstrating in histological sections of the arteries an enlargement of the total vessel area as plaque area increases. This mechanism appears to be capable of compensating for an increase of plaque burden until the plaque occupies 40 percent of the internal elastic membrane area.

As a consequence of the compensatory enlargement of the vessel, luminal area may be preserved, as seen angiographically despite extensive CAD. Stiel et al. confirmed in a study comparing post-mortem quantitative angiography with morphometric analysis on histologic sections of the coronary arteries that compensatory enlargement of diseased coronary segments results in a significant angiographic underestimation of coronary atherosclerosis during the early stage of the disease [49].

The compensatory enlargement of the coronary arteries during the early progression of atherosclerosis does not represent any problem for the quantitative assessment by intracoronary ultrasound. The method itself can even be used to study the mechanism of the arterial remodeling [50]. Ultrasonic confirmation of the compensatory enlargement during evolving atherosclerosis was first performed non-invasively, using epicardial high-frequency echocardiography [51] and carotid duplex scanners [52], and was subsequently demonstrated by intravascular ultrasound in coronary [53–55] and femoral arteries [56].

Thus, coronary angiography is unable to detect and quantify the early stage of evolving atherosclerosis, while intracoronary ultrasound permits direct inspection and measurement of the plaque burden without need for interpolation or reference segments, clearly demonstrating its superiority in assessing the early phase of atherosclerosis.

In order to correct the angiographic measurement of the percent diameter stenosis during later stages of atherosclerosis, a correction for the compensatory enlargement of the artery could theoretically be performed, if coronary remodeling occurs in all arteries in the same way. However there is evidence that some arteries show remodeling while others do not enlarge and even seem to show a reverse modeling. Such a 'paradoxical arterial wall shrinkage' has been described by Pasterkamp et al. in human atherosclerotic femoral arteries [57]. It remains unclear in how many cases this 'reverse Glagovian modeling' accounts for or contributes to the luminal narrowing. Current concepts of vascular remodeling are based on a complex interaction between growth

factors, vasoactive substances, pressure, flow, and shear stress, while the endothelium plays an important role as the sensor and transducer of signals [50,58–60]. Disturbance of this balance or the enlargement of the distal post-stenotic reference segment may result in 'arterial shrinkage'.

Our experience with three-dimensional intracoronary ultrasound (Fig. 1) demonstrates that a reverse vascular modeling also occurs in coronary arteries. In this light, a correction of the percent diameter stenosis, measured by quantitative coronary angiography, appears to be highly questionable. If there is such a variability of vascular remodeling and if the plaque may grow inside or outside of the coronary lumen, intracoronary ultrasound appears to be currently the only reliable technique which permits a direct measurement of plaque burden and progression or regression of atherosclerosis.

5. The benefit of the third dimension in intracoronary ultrasound

After the introduction of intracoronary ultrasound in research and clinical use, a substantial role of this technique in the assessment of progression or regression of coronary atherosclerosis will be expected. Indeed, the accuracy [61] and in vivo feasibility [62,63] of intracoronary ultrasound has been well demonstrated in experimental stud-

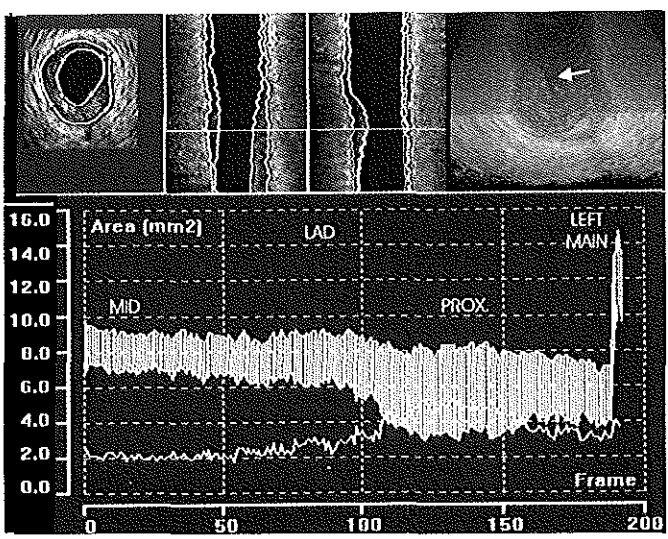

Fig. 1. Primary lesion in the proximal segment of the left anterior descending coronary artery (LAD), assessed by a new system for quantitative analysis of three-dimensional intracoronary ultrasound images. The cross-sectional ultrasound images, representing a segment of round 10 mm length, were reconstructed in two perpendicular longitudinal sections (mid panels). A computerized contour detection was performed providing a three-dimensional view (right upper panel; arrowhead indicates target stenosis) and area measurements (mm^2) of the lumen, plaque, and total vessel on 200 consecutive ultrasound frames (lower panel). The values of the plaque area are shown as a white field between two lines, representing the absolute values of the total vessel and lumen areas. The absolute value of the plaque area can be derived from this white field, but is also displayed as a single white line. The area stenosis at the site of the mid segment of the LAD was round 20%. According to the mechanism described by Glagov, an enlargement of the total vessel area, partly compensating the plaque burden, may be expected at the site of a relatively focal plaque. In the measurement display of this case, however, a paradoxical reduction of the total vessel area from the distal reference in the early mid LAD (MID) to the target stenosis in the proximal segment (PROX) was observed. Plaque volume of the entire arterial segment was 32 mm^3.

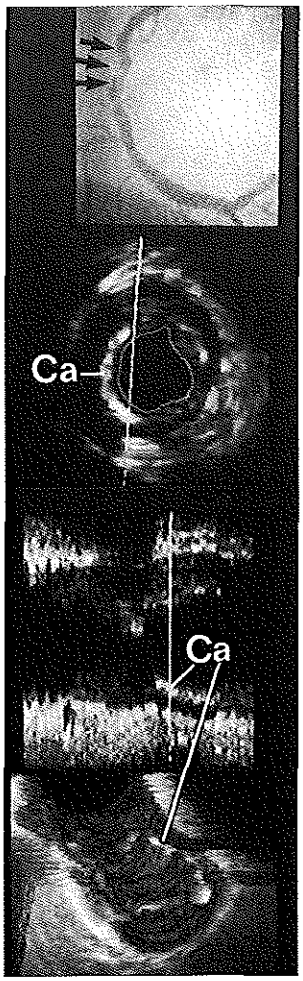

Fig. 2. Calcified lesion in a mid right coronary artery. Arrowheads in the angiogram indicate the segment which was reconstructed. The superficial calcification is visible in the cross-sectional, longitudinal, and three-dimensional cylindrical view (upper mid, lower mid, and low panel respectively). The longitudinal and cylindrical displays permit a much more comprehensive insight into the complex spatial distribution of the plaque.

ies of progression or regression of atherosclerosis. The principal reason why this technique has not yet been introduced to major human progression-regression trials are the difficulties with correctly matching the sites of measurement in serial ultrasonic studies [62–70], but a reliable serial evaluation of progression or regression of atherosclerosis depends critically on the correct matching of the images. This limitation results from the lack of the third dimension in conventional two-dimensional ultrasound [67]. This procedure can be significantly facilitated by the use of three-dimensional reconstruction of intracoronary ultrasound images, permitting in serial ultrasound studies the assessment of the same site of the artery.

6. Volumetric intracoronary ultrasound

Three-dimensional reconstruction of intracoronary ultrasound images was first used [71] to visually assess the spatial configuration of atherosclerotic plaques (Fig. 2). Examination of dissections and stents by this technique has provided valuable clinical information [72–76].

The basic cross-sectional intracoronary ultrasound images are acquired while the ultrasound catheter is pulled back through the coronary artery segment of interest. A continuous pull-back at a uniform speed resulting in an equidistant spacing of adjacent images [77] is still the most common approach. A stepping motor, developed at the Thoraxcenter, performs an electrocardiogram (ECG)-gated withdrawal of the ultrasound catheter and can also be used to perform an ECG-gated image acquisition [78]. This approach allows to minimize artifacts induced by the cyclic movement of the ultrasound catheter in the lumen and the systolic-diastolic pulsation of the vessel wall.

Subsequently, the stack of cross-sectional images is reconstructed. The reconstruction systems differ mainly in the image segmentation, a processing step which performs a distinction between vessel wall structures and the blood-pool. The semi-automated detection facilities of commercial analysis systems are limited to the distinction between the blood-pool in the lumen and the vessel wall [71,79–83]. They are based on the definition of grey-level thresholds or acoustic quantification (Fig. 3).

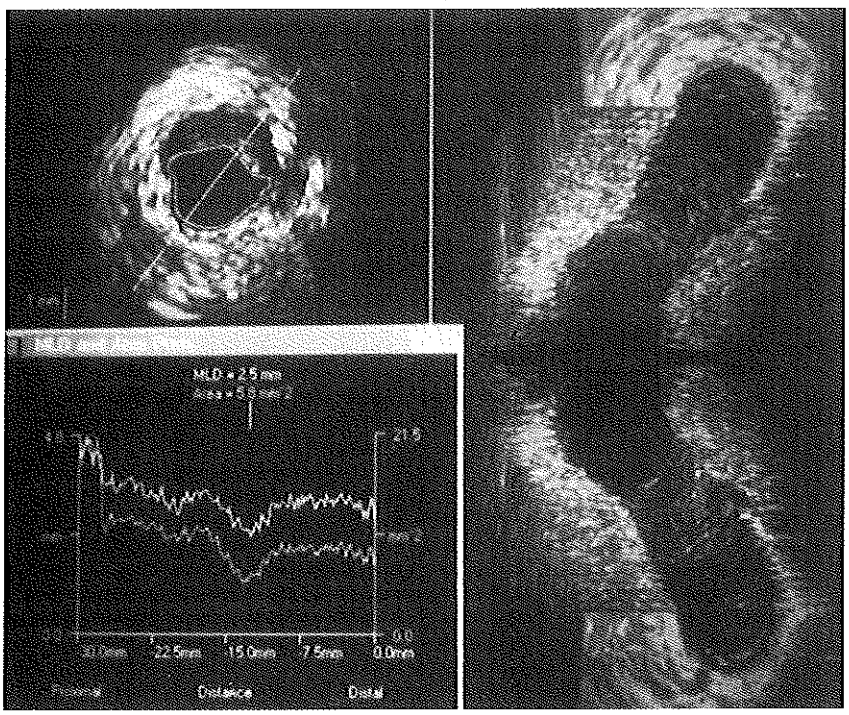

Fig. 3. Three-dimensional reconstruction of a short eccentric atherosclerotic plaque of relatively low echogenicy in the proximal segment of a coronary artery. A semi-automated distinction between the blood-pool and the vessel wall was performed by an acoustic quantification method, based on the recognition of the blood speckle, which shows a quite uniform pattern in the vessel wall and a varying pattern in flowing blood. Measurement of the lumen area and the mean luminal diameter are displayed in the left lower panel. Currently, no automated measurements of plaque area or volume can be performed by this approach.

At the Thoraxcenter, a computerized analysis system has been developed which performs a contour detection, based on the application of a minimum cost algorithm, and permits the identification of both the boundaries between the lumen and plaque as well as the plaque-media complex and adventitia (Fig. 1) using the complete volumetric information of the stack of intracoronary ultrasound images [68,84]. During the interactive contour detection on the longitudinal images, dynamic programming techniques are used to permit frequent up-dates of the displays including a cross-sectional plus two longitudinal views (Fig. 4). The visual information from both the cross-sectional and the longitudinal views facilitates the detection of the external boundary of the vessel wall. The advantage of this approach is particularly evident if calcium or stent struts obscure parts of the underlying vessel wall, rendering the morphometric measurement on sole cross-sectional images impossible. Even with short circumferential calcifications of the plaque, a reliable interpolation of the external vessel contour can be performed. The longitudinal contours guide the otherwise automated contour detection on the cross-sectional images, which is finally checked and may be manually corrected. Using the whole set of volumetric information, the analysis system performs a semi-

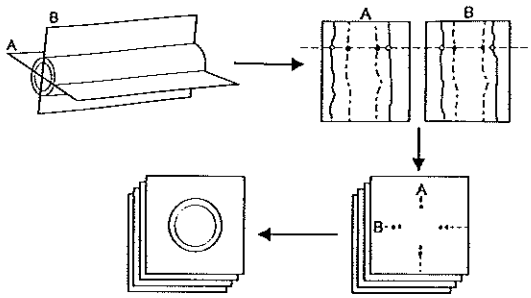

Fig. 4. Principle of the contour detection method, developed at the Thoraxcenter [68,84,85]. The intracoronary ultrasound images, obtained during a motorized pull-back of the ultrasound catheter, are used to reconstruct two longitudinal sections from the voxel space (voxel = volume unit). An automated contour detection of the intimal leading edge and the external boundary of the vessel is performed, based on the application of a minimum-cost algorithm, dynamic programming techniques, and user interaction. The longitudinal contours are represented as individual edge points in the whole stack of cross-sectional images. These points define center and range of the final contour detection process on the cross-sectional ultrasound images. Finally, the contours are checked and may be corrected. The analysis system provides information about areas, mean diameters and volumes of the lumen, total vessel and plaque (Fig. 1).

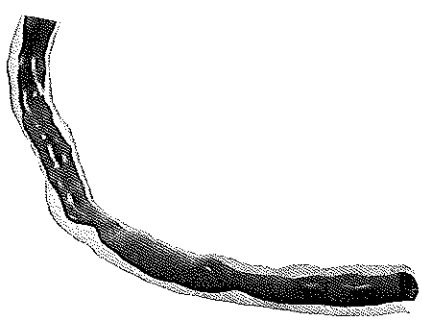

Fig. 5. Combined use of biplane angiography and three-dimensional intracoronary ultrasound by ANGUS, a new method which allows the analysis of the true geometry of the vessel lumen and plaque, taking vessel curvatures and catheter bends into account [88]. A reconstruction of a diseased right coronary artery is displayed in a frontal projection. Ultrasound data provided by the contour detection method were spatially arranged and interpolated, using biplane data on both the pull-back trajectory and the angiogram.

automated measurement of plaque volume. It reflects a function of the plaque area over the length of the reconstructed segment and can be calculated as the mean plaque area times the length of the reconstructed segment. Minimal differences in the start and end in repeated studies are unlikely to impair the accuracy of the changes in plaque volume measurements, assessed for an entire coronary arterial segment.

Volumetric measurements by the Thoraxcenter analysis system have been studied in a phantom in vitro showing a high accuracy [68]. The volumetric measurement has a lower intraobserver and interobserver variability than the measurement of areas on individual cross-sectional images [85], reflecting an averaging of the differences of the area measurement. Measurement of plaque volume [68–70,86] is particularly promising to quantify atherosclerotic plaques in progression-regression trials since it directly reflects changes of the plaque burden of an entire arterial segment with a high reproducibility.

7. Perspective of volumetric intracoronary ultrasound

Some limitations of three-dimensional reconstruction remain [67], but artifacts resulting from the movement of the ultrasound catheter during the cardiac cycle and systolic-diastolic changes in vessel dimensions can be minimized by the use of an ECG-gated pull-back system [67,87].

Combined use of biplane angiography and three-dimensional intracoronary ultrasound by a new method (ANGUS) may in the future help to analyze the true geometry of the vessel lumen and plaque, taking vessel curvatures and catheter bends into account [88]. In Fig. 5, a clinical example of a spatial reconstruction by ANGUS is given, showing a diseased right coronary artery in frontal projection. Ultrasound data on the intimal leading edge and the external boundary of the total vessel, provided by the contour detection method, were spatially arranged and interpolated, using biplane data on the pull-back trajectory and on the contrast angiogram. The example demonstrates that the external contour of the vessel provides additional information which cannot be obtained from a silhouette of the lumen which is normally provided by the angiogram [89]. This approach may permit a more distinct assessment of the progression or regression of atherosclerosis, an issue which is interesting as plaque progression or regression of the outer and inner curve of a bended coronary segment may differ significantly.

8. Conclusions

Coronary angiography depicts the silhouette of the vessel lumen permitting only an indirect analysis of the 'footprints' induced by the atherosclerosis of the coronary wall, not reflecting the early stage and the complex nature of the disease. Intracoronary ultrasound directly assesses and quantifies atherosclerotic plaques and is currenly the only reliable technique to measure progression or regression of atherosclerosis in the cardiac catheterization laboratory. The reliability of serial ultrasound studies can be further improved by using volumetric intracoronary ultrasound, which allows reliable and highly reproducible quantification of the plaque volume of entire arterial segments.

Acknowledgements

We gratefully acknowledge the contribution of Dr W. Li in developing the three-dimensional reconstruction system of the Thoraxcenter, the assistance of Dr A.G. Violaris in reviewing the manuscript, and the expert technical assistance of J. Ligthart, N. Bruining and E. van der Leur. Dr. C. von Birgelen is recipient of a Fellowship of the German Research Society.

References

[1] Ross R. The pathogenesis of atherosclerosis — an update. N Engl J Med 1986;314:488.
[2] Fuster V, Badimon L, Badimon JJ, Chesebro JH. The pathogenesis of coronary artery disease and the acute coronary syndromes (I). N Engl J Med 1992;326:242.
[3] Fuster V, Badimon L, Badimon JJ, Chesebro JH. The pathogenesis of coronary artery disease and the acute coronary syndromes (II). N Engl J Med 1992;326:310.
[4] Stary HC. Evolution and progression of atherosclerotic lesions in coronary arteries of children and young adults. Arteriosclerosis 1989;9(Suppl.)1:19.
[5] Ross R. The pathogenesis of atherogenesis of atherosclerosis: A perspective for the 1990s. Nature 1993;362:801.
[6] Kuller LH. Why measure atherosclerosis? Circulation 1993;87(Suppl.):II–34.
[7] Reiber JHC, Booman F, Troost GJ et al. A cardiac image analysis system: Objective quantitative processing of angiocardiograms. In: Computers in Cardiology. Los Alamitos IIEEE Computer Society Press, 1978:239.
[8] Serruys PW, Booman F, Troost GJ et al. Computerized quantitative coronary angiography applied to percutaneous transluminal coronary angioplasty: Advantages and limitations. In: Kaltenbach M, Gruntzig A, Rentrop K and Bussmann WD (eds). Transluminal Coronary Angiography and Intracoronary Thrombolysis, Coronary Heart Disease IV. Berlin: Springer-Verlag, 1982:110.
[9] Zir LM, Miller SW, Dismore RE et al. Interobserver variability in coronary arteriography. Circulation 1976;53:627.
[10] Goldberg RK, Kleiman NS, Minor ST et al. Comparison of quantitative coronary angiography to visual estimates of lesion severity pre and post PTCA. Am Heart J 1990;178.
[11] Waters D, Lesperance J, Craven TE, Hudson G, Gillam LD. Advantages and limitations of serial coronary arteriography for the assessment of progression and regression of coronary atherosclerosis. Implications for clinical trials. Circulation 1993;87(Suppl.):II–38.
[12] Buchwald H, Matts JP, Fitch LL et al. for the Surgical Control of the Hyperlipidaemias (POSCH) Group. Changes in sequential coronary angiograms and subsequent coronary events. J Am Med Assoc 1992;268:1429.
[13] Applegate RJ, Herrington DM, Little WC. Coronary angiography: more than meets the eye. Circulation 1993;87:1399.

[14] Vos J, de Feyter PJ, Simoons ML, Tijssen JGP, Deckers JW. Retardation and arrest of progression or regression of coronary artery disease: A review. Prog Cardiovasc Dis 1993;35:435.
[15] Brown BG, Hillger LA, Lewis C et al. A maximum confidence approach for measuring progression and regression of coronary artery disease in clinical trials. Circulation 1993;87(Suppl.):II–66.
[16] Badimon L, Badimon JJ, Gold HK, Fuster V. Coronary atherosclerosis: Morphology and characteristics to identify by evolving imaging technology. Am J Card Imag 1992;6:278.
[17] Waller BF, Pinkerton CA, Slack JD. Intravascular ultrasound: A historical study of vessels during life: the new 'gold standard' for vascular imaging. Circulation 1992;85:2305.
[18] de Feyter PJ, Serruys PW, Davies MJ, Richardson P Lubsen J, Oliver MF. Quantitative coronary angiography to measure progression and regression of coronary atherosclerosis: Value, limitations, and implications for clinical trials. Circulation 1991;84:412.
[19] Stone PH, Gibson CM, Pasternak RC et al. for the Harvard Atherosclerosis Reversibility Project Study Group. Natural history of coronary atherosclerosis using quantitative angiography in men, and implications for clinical trials of coronary regression. Am J Cardiol 1993;71:766.
[20] Waller BF. Anatomy, histology, and pathology of the major epicardial coronary arteries relevant to echocardiographic imaging techniques. J Am Soc Echo 1989;2:232.
[21] Grodin CM, Dyrda I, Pasternac A, Campeau, Bourassa MG Lesperance J. Discrepancies between cineangiographic and postmortem findings in patients with coronary artery disease and recent myocardial revascularization. Circulation 1974;49:703.
[22] Schwartz JN, Kong Y, Hackel DB, Bartel AG. Comparison of angiographic and postmortem findings in patients with coronary artery disease. Am J Cardiol 1975;36:174.
[23] Hutchins GM, Buckley BH, Ridolfi RL et al. Correlation of coronary arteriograms and left ventriculaograms with postmortem studies. Circulation 1977;56:32.
[24] Arnett RN, Isner JM, Redwood D. Coronary artery narrowing in coronary heart disease. Comparison of cineangiographic and necropsy findings. Ann Intern Med 1979;36:174.
[25] Leung WH, Alderman EL, Lee TC, Stadius ML. Quantitative arteriography of apparently normal coronary segments with nearby or distant disease suggests presence of occult, nonvisualized atherosclerosis. J Am Coll Cardiol 1995;25:311.
[26] Zijlstra F, van Ommeren J, Reiber JHC, Serruys PW. Does quantitative assessment of coronary artery dimensions predict the physiological significance of coronary stenosis? Circulation 1987;75:1154.
[27] Harrison DG, White CW, Hiratzka LF et al. The value of lesion cross-sectional area determined by quantitative coronary angiography in assessing the physiologic significance of proximal left anterior descending arterial stenoses. Circulation 1984;69:1111.
[28] Marcus ML, Armstrong ML, Heistad DD, Eastham CL, Mark AL. Comparison of three methods of evaluating coronary obstructive lesions: Postmortem arteriography, pathologic examination and measurement of the regional myocardial perfusion during maximal vasodilation. Am J Cardiol 1982;49:1699.
[29] White CW, Wright CB, Doty DB et al. Does visual interpretation of the coronary angiogram predict the physiologic importance of a coronary stenosis? N Engl J Med 1984;310:819.
[30] Ellis S, Sanders W, Goulet C et al. Optimal detection of the progression of coronary artery disease: Comparison of methods suitable for risk factor intervention trials. Circulation 1986;76:1235.
[31] St Goar FG, Pinto FJ, Alderman EL, Fitzgerald PJ Stadius ML, Popp RL. Intravascular ultrasound imaging of angiographically normal coronary arteries: An in vivo comparison with quantitative angiography. J Am Coll Cardiol 1991;18:952.
[32] St Goar FG, Pinto FJ, Alderman EL et al. Detection of coronary atherosclerosis in young adult hearts using intravascular ultrasound. Circulation 1992;86:756.
[33] St Goar FG, Pinto FJ, Alderman EL et al. Intracoronary ultrasound in cardiac transplant recipients: In vivo evidence of 'angiographically silent' intimal thickening. Circulation 1992;85:979.
[34] Yamagishi M, Miyatake K, Tamai J, Nakatani S, Kojama J, Nissen SE. Intravascular ultrasound detection of atherosclerosis at the site of focal vasospasm in angiographically normal or minimally narrowed coronary segments. J Am Coll Cardiol 1994;23:352.
[35] Hermiller JB, Buller CE, Tenaglia et al. Unrecognized left main coronary artery disease in patients undergoing interventional procedures. Am J Cardiol 1993;71:173.
[36] Nissen SE, Gurley JC, Grines CL et al. Intravascular ultrasound assessment of lumen size and wall morphology in normal subjects and patients with coronary artery disease. Circulation 1991;84:1087.
[37] Yock PG, Linker DT. Intravascular ultrasound: Looking below the surface of vascular disease. Circulation 1990;81:1715.
[38] Di Mario C, The SHK, Madretsma S et al. Detection and characterization of vascular lesions by intravascular ultrasound: An in vitro study correlated with histology. J Am Soc Echo 1992;5:135.
[39] Mintz GS, Popma JJ, Pichard AD et al. Patterns of calcification in coronary artery disease: A statistical analysis of intravascular ultrasound and coronary angiography in 1155 lesions. Circulation 1995;91:1959.
[40] Friedrich GJ, Moes NY, Muehlberger VA et al. Detection of intralesional calcium by intracoronary ultrasound depends on the histologic pattern. Am Heart J 1994;128:435.
[41] Pignoli P, Tremoli E, Poli A, Oreste P, Paoletti R. Intimal plus medial thickness of the arterial wall: A direct measurement with ultrasound imaging. Circulation 1986;74:1399.

[42] McPherson DD, Sirna SJ, Hiratzka LF et al. Coronary arterial remodeling studied by high-frequency epicardial echocardiography: An early compensatory mechanism in patients with obstructive coronary atherosclerosis. J Am Coll Cardiol 1991;17:79.
[43] Hausmann D, Erbel R, Alibelli-Chemarin MJ et al. The safety of intracoronary ultrasound: A multicenter survey of 2207 examinations. 1995;91:623.
[44] Di Mario C, Madrestma S, Linker D et al. The angle of incidence of the ultrasonic beam: A critical factor for the image quality in intravascular ultrasound. Am Heart J 1993;125:442.
[45] Benkeser PJ, Churchwell AL, Lee C, Abouelnasr DM. Resolution limitations in intravascular ultrasound imaging. J Am Soc Echocardiogr 1993;6:158.
[46] Glagov S, Weisenberg E, Zaris CK, Stancunavicus R Kolettis GJ. Compensatory enlargement of human atherosclerotic coronary arteries. N Engl J Med 1989;316:1371.
[47] Armstrong ML, Warner ED, Connor WE. Regression of coronary atheromatosis in rhesus monkeys. Circ Res 1970;27:59.
[48] Armstrong ML, Heistad DD, Marcus ML, Megan MB, Piegors DJ. Structural and hemodynamic response of peripheral arteries of macaque monkeys to atherogenic diet. Arteriosclerosis 1985;5:336.
[49] Stiel GM, Stiel LSG, Schofer J, Donath K, Mathey DG. Impact of compensatory enlargement of atherosclerotic coronary arteries on angiographic assessment of coronary artery disease. Circulation 1989;80:1603.
[50] Gibbons GH, Dzau VJ. The emerging concept of vascular remodeling. N Engl J Med 1994;330:1431.
[51] Mc Pherson DD, Sirna SJ, Hiratzka LF et al. Coronary arterial remodeling studied by high-frequency epicardial echocardiography: An early compensatory mechanism in patients with obstructive coronary atherosclerosis. J Am Coll Cardiol 1991;17:79.
[52] Steinke W, Els T, Hennerici M. Compensatory carotid artery dilatation in early atherosclerosis. Circulation 1994;89:2578.
[53] Gerber TC, Erbel R, Görge G, Ge J, Rupprecht H-J Meyer J. Extent of atherosclerosis and remodeling of the left main coronary artery determined by intravascular ultrasound. Am J Cardiol 1994;73:666.
[54] Ge J, Erbel R, Zamorano J et al. Coronary artery remodeling in atherosclerotic disease: An intravascular ultrasonic study in vivo. Cor Art Dis 1993;4:981.
[55] Hermiller JB, Tenaglia AN, Kisslo KB et al. In vivo validation of compensatory enlargement of atherosclerotic coronary arteries. Am J Cardiol 1993;71:665.
[56] Losordo DW, Rosenfield K, Kaufman J, Pieczek A, Isner JM. Focal compensatory enlargement of human arteries in response to progressive atherosclerosis. In vivo documentation using intravascular ultrasound. Circulation 1994;89:257.
[57] Pasterkamp G, Wensing PJW, Post MJ, Hillen B, Mali WPTM, Borst C. Paradoxical arterial wall shrinkage may contribute to luminal narrowing of human atherosclerotic femoral arteries. Circulation 1995;91:1444.
[58] Glagov S, Zaris C, Giddens DP, Ku DN. Hemodynamics and atherosclerosis. Arch Pathol Lab Med 1988;112:1018.
[59] Langille BL, O'Donnell F. Reductions in arterial diameter produced by chronic decreases in blood flow are endothelium-dependent. Science 1986;231:405.
[60] Vita JA, Treasure CB, Ganz P, Cox DA, Fish RD, Selwyn AP. Control of shear stress in the epicardial coronary arteries of humans: Impairment by atherosclerosis. J Am Coll Cardiol 1989;14:1193.
[61] Hausmann D, Goupta M, Connolly AJ, Paemley WW Fitzgerald PJ, Yock PG. Accuracy of intravascular ultrasound to assess progression and regression of experimental aortic atherosclerosis (abstr). Circulation 1993;88:I–501.
[62] Gupta M, Connolly AJ, Zhu BQ et al. Quantitative analysis of progression and regression of atherosclerosis by intravascular ultrasound: Validation in a rabbit model (abstr). Circulation 1992;86:I–518.
[63] Lassetter JE, Krall RC, Moddrelle DS, Jenkins RD. Morphologic changes of the arterial wall during regression of experimental atherosclerosis (abstr). Circulation 1992;86:I–518.
[64] Kovach JA, Mintz GS, Kent KM et al. Serial intravascular studies indicate that chronic recoil is an important mechanism of restenosis following transcatheter therapy (abstr). J Am Coll Cardiol 1993;21:484A.
[65] Mintz GS, Kovach JA, Pichard AD et al. Geometric remodeling is the predominant mechanism of clinical restenosis after coronary angioplasty (abstr). J Am Coll Cardiol 1994;23:138A.
[66] Di Mario C, Gil R, Camenzind E et al. Quantitative assessment with intracoronary ultrasound of the mechanisms of restenosis after percutaneous transluminal coronary angioplasty and directional coronary atherectomy. Am J Cardiol 1995;75:772.
[67] Roelandt JRTC, Di Mario C, Pandian et al. Three-dimensional reconstruction of intracoronary ultrasound images: Rationale, approaches, problems and directions. Circulation 1994;90:1044.
[68] von Birgelen C, Di Mario C, Li W et al. Volumetric quantification in intracoronary ultrasound: Validation of a new automatic contour detection method with integrated user interaction (abstr). Circulation 1994;90:I–550.
[69] Dhawale PJ, Rasheed Q, Berry J, Hodgson J McB. Quantification of lumen and plaque volume with ultrasound: Accuracy and short term variability in patients (abstr). Circulation 1994;90:I–164.
[70] Dhawale PJ, Rasheed Q, Mecca W, Nair R, Hodgson J McB. Analysis of plaque volume during DCA using a volumetrically accurate three-dimensional ultrasound technique (abstr). Circulation 1993;88:I–550.
[71] Rosenfield K, Losordo DW, Ramaswamy K, Isner JM. Three-dimensional reconstruction of human coronary and

peripheral arteries from images recorded during two-dimensional intravascular ultrasound examination. Circulation 1991;84:1938.

[72] Cavaye DM, White RA, Lerman RD et al. Usefulness of intravascular ultrasound imaging for detecting experimentally induced aortic dissection in dogs and for determining the effectiveness of endoluminal stenting. Am J Cardiol 1992;69:705.

[73] Schryver TE, Popma JJ, Kent KM, Leon MB, Mintz GS. Use of intracoronary ultrasound to identify the true coronary lumen in chronic coronary dissection treated with intracoronary stenting. Am J Cardiol 1992;69:107.

[74] Coy KM, Park JC, Fishbein MC, Laas T et al. In vitro validation of three-dimensional intravascular ultrasound for the evaluation of arterial injury after balloon angioplasty. J Am Coll Cardiol 1992;20:692.

[75] Mintz GS, Leon MB, Popma JJ, Kent KM. Three-dimensional reconstruction of endovascular stents (abstr). J Am Coll Cardiol 1992;19:224A.

[76] Prati F, Di Mario C, von Birgelen C et al. Usefulness of on-line 3D reconstruction for stent implantation (abstr). J Am Coll Cardiol 1995;25:9A.

[77] Mintz GS, Keller MB, Fay FG. Motorized IVUS transducer pull-back permits accurate quantitative axial measurements (abstr). Circulation 1992;86:I–323.

[78] Di Mario C, von Birgelen C, Prati F et al. Three-dimensional reconstruction of two-dimensional intracoronary ultrasound: Clinical or research tool? Br Heart J 1995;73(Suppl.2):26.

[79] Rosenfield K, Kaufman J, Pieczek A, Langevin RE, Razvi S, Ilsner JM. Real-time three-dimensional reconstruction of intravascular ultrasound images of iliac arteries. Am J Cardiol 1992;70:412.

[80] Chandrasekaran K, D'Adamo AJ, Sehgal CM. Three-dimensional reconstruction of intravascular ultrasound images. In: Yock PG, Tobis JM, (eds), Intravascular Ultrasound Imaging, New York: Churchill-Livingston, 1992;141.

[81] Kitney R, Moura L, Straughan K. 3-D visualization of arterial structures using ultrasound and voxel modelling. Int J Cardiac Imag 1989;4:135.

[82] Hausmann D, Friedrich G, Sudhir K et al. 3D intravascular ultrasound imaging with automated border detection using 2.9 F catheters (abstr). J Am Coll Cardiol 1994;23:174A.

[83] Prati F, Di Mario C, von Birgelen C et al. On-line automated lumen volumen measurement with 3-D intracoronary ultrasound during coronary interventions (abstr). J Am Coll Cardiol 1995;25:345A.

[84] Li W, von Birgelen C, Di Mario C et al. Semi-automated contour detection for volumetric quantification of intracoronary ultrasound. Proc Comput Cardiol, IEEE Computer Society Press, Los Alamitos, 1994;267.

[85] von Birgelen C, Di Mario C, Li W et al. Clinical Application of a new computerized method measuring coronary artery dimensions by three-dimensional intracoronary ultrasound: Reproducibility in-vivo during coronary interventions (abstr). Eur Heart J 1995;16: 428.

[86] Galli FC, Sudhir K, Kao AK, Fitgerald PJ, Yock PG. Direct measurement of plaque volume by three-dimensional ultrasound: Potential and pitfalls (abstr). J Am Coll Cardiol 1992;19:115A.

[87] Dhawale PJ, Wilson DL, McB Hodgson J. Optimal data acquisition for volumetric intracoronary ultrasound. Cathet Cardiovasc Diagn 1994;32:288.

[88] Slager CJ, Laban M, von Birgelen C et al. ANGUS: A new approach to three-dimensional reconstruction of geometry and orientation of coronary lumen and plaque by combined use of coronary angiography and IVUS (abstr). J Am Coll Cardiol 1995;25:144A.

[89] von Birgelen C, Umans V, Di Mario C et al. Mechanism of high-speed rotational atherectomy and adjunctive balloon angioplasty revisited by quantitative coronary angiography: edge detection versus videodensitometry. Am Heart J 1995;130:405.

Chapter 13

Reconstruction and quantification with three-dimensional intracoronary ultrasound: An update on techniques, challenges, and future directions

C von Birgelen, GS Mintz, PJ de Feyter, N Bruining,
A Nicosia, C Di Mario, PW Serruys,
JRTC Roelandt

Reprinted with permission from *Eur Heart J* 1997;18:1056-1067

Reconstruction and quantification with three-dimensional intracoronary ultrasound

An update on techniques, challenges, and future directions

C. von Birgelen, G. S. Mintz*, P. J. de Feyter, N. Bruining, A. Nicosia, C. Di Mario, P. W. Serruys and J. R. T. C. Roelandt

*Thoraxcenter, University Hospital Rotterdam-Dijkzigt, Erasmus University Rotterdam, The Netherlands, and the *Washington Hospital Center, Washington DC, U.S.A.*

Introduction

Conventional two-dimensional intracoronary ultrasound enables the extent, distribution, and therapy of atherosclerotic plaques to be studied as it provides a unique tomographic visualization of both the vascular lumen and wall[1–7]. The most important limitation of two-dimensional intracoronary ultrasound in pre/post-studies is the matching of the target sites for serial measurement. This problem is caused by the lack of a third dimension in conventional intracoronary ultrasound examinations. Three-dimensional reconstruction of intracoronary ultrasound images[8–10] permits a more advanced assessment of vessel, lumen and plaque morphology.

Measurement of the plaque area in an entire coronary segment may provide more detail of the complex plaque architecture and avoids the difficult mental conceptualization process[11–15]. Moreover, during online three-dimensional reconstruction (Fig. 1) measurements of the target lesion and the reference segments may be accessed immediately in a reconstructed longitudinal view. This may facilitate selecting the best type and sized interventional device or the evaluation of complications, as the relevant coronary segments can be carefully examined before and/or after interventional procedures[9,16–21].

Key Words: Intravascular ultrasound, three-dimensional reconstruction, image processing, coronary artery disease.

Dr von Birgelen is the recipient of a Fellowship of the German Research Society (Deutsche Forschungsgemeinschaft, Bonn, Germany.

Correspondence: Professor Jos R. T. C. Roelandt, MD, PhD, Director of the Division Cardiology, University Hospital Rotterdam-Dijkzigt, Thoraxcenter, P.O. Box 1738, 3000 DR Rotterdam, The Netherlands.

Basic processing steps

The basic processing steps to obtain a three-dimensional reconstruction from the two-dimensional intracoronary ultrasound images are similar for all systems currently available.

Image acquisition

The better the two-dimensional intracoronary ultrasound images the better the three-dimensional reconstructions. Thus machine settings must be optimized before image acquisition is performed. Starting distal to the stenosis, the imaging catheter is withdrawn through the arterial segment to be reconstructed. The imaging core of sheath-based intracoronary ultrasound catheters, which are designed for repeated pull-backs and most frequently used with three-dimensional intracoronary ultrasound, does not have direct contact with the vessel wall. Such catheters are equipped with a 15 cm long transparent distal sheath which houses the transducer. There are two catheter designs: a 3·2F short monorail and a 2·9F common distal lumen catheter. The 2·9F design has a common distal lumen that houses the guide wire (during catheter introduction) or the transducer (during imaging when the guide wire has been pulled back) alternately. These intracoronary ultrasound catheter designs stabilize the transducer pull-back trajectory and reduce the risk of a non-uniform speed in continuous pull-backs, but

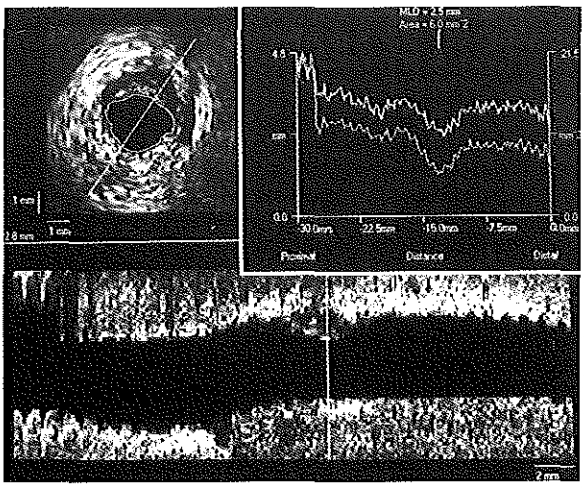

Figure 1 **Short eccentric plaque in a proximal coronary segment. The longitudinal reconstruction (lower panel) and the on-line measurement of the luminal cross-sectional area and minimal diameter (right upper panel) were obtained from the acoustic quantification system (Echo-Quant).**

during the first 5 to 10 s of a continuous pull-back there may be straightening of the imaging core inside the catheter before a constant withdrawal speed is attained.

There are different pull-back approaches which can be applied. A continuous-speed pull-back resulting in an equidistant spacing of adjacent images[22], is still the most common approach. Side-branches or spots of calcium are used as topographic landmarks to ensure a reliable comparison of the same arterial segment in serial studies. A modified concept of the continuous-speed pull-back is ECG-triggered video labelling during uniform pull-back of the intracoronary ultrasound transducer. Video frames coinciding with the R-wave of the ECG are automatically labelled and images acquired at the same phase of the cardiac cycle are used for off-line three-dimensional reconstruction. This approach displays the arterial segment and enables the vascular dimensions to be measured at any time during the cardiac cycle. It also minimizes the systolic–diastolic artifacts which are frequently observed in non-triggered uniform-speed pull-backs (Fig. 2).

By using an ECG-triggered pull-back device in combination with an ECG-gated image acquisition[23], the problem of cyclic motion artifacts can be overcome[24,25]. A dynamic three-dimensional reconstruction system, initially designed for three-dimensional reconstruction of echocardiographic images (Echoscan, TomTec, Munich, Germany)[23], can dynamically display the arterial segment, showing the motion of an entire cardiac cycle. Before image acquisition starts, the upper and lower limits of the RR interval are defined. A maximum number of 25 intracoronary ultrasound images per cardiac cycle can be sampled if the length of the RR interval meets the pre-set range (Fig. 3).

Image digitization and segmentation

Digitization of the intracoronary ultrasound images can be performed on- or off-line by sampling the video frames with a framegrabber at a defined digitization frame rate. The segmentation step identifying structures of interest in the intracoronary ultrasound images can be achieved by applying dedicated algorithms, which discriminate between the blood-pool inside the lumen and structures of the vessel wall[26]. The quality of the final three-dimensional reconstruction and the accuracy of the quantitative analysis are highly influenced by the quality of the segmentation algorithm. In addition to the threshold approaches (Fig. 4)[10], segmentation can be achieved by using either an acoustic quantification algorithm[21,27] or a contour detection algorithm[13,14,28,29].

The acoustic quantification method (Fig. 5) distinguishes between the blood pool and vessel wall using an algorithm for statistical pattern recognition (Echo-Quant, INDEC, CA, U.S.A.). Comparing the ultrasound speckle pattern of flowing blood to the pattern of the vessel wall, there is much more variation in time in blood[30]. The algorithm is able to distinguish between these two patterns and to detect the interface between blood and vessel wall. Finally, pixels (picture elements) identified as part of the blood pool are removed.

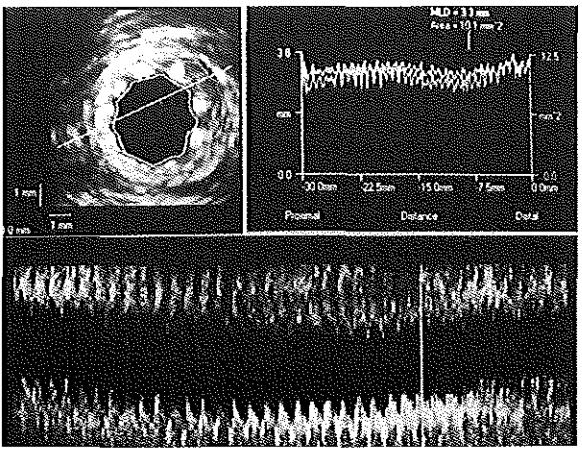

Figure 2 **Cyclic artifacts in a venous bypass graft. The longitudinally reconstructed image of a stented bypass graft shows enormous saw-shaped artifacts, resulting from cyclic vessel pulsation and the movement of the intracoronary ultrasound catheter inside ('catheter fluttering'). The artifacts are visible in both the longitudinal display and the graph, showing the measurements of the luminal cross-sectional area and the minimum diameter (right upper panel). (Reproduced with permission[54].)**

Another approach is a contour detection system (Fig. 6), which has been developed at the Thoraxcenter Rotterdam. A minimum cost algorithm detects the intimal leading edge and the external vascular boundary (external elastic lamina)[13,14,28,29]. Another semi-automated contour detection system, described by Sonka *et al.* detects the luminal contour and the contours of the internal and external elastic laminae. Initial in vitro studies show a good correlation with lumen and plaque area measurements obtained by manual tracing[31,32].

Image reconstruction and display

Different display formats can be used to present the three-dimensional image data sets. The most commonly generated is the longitudinal format (Fig. 1). A cylindrical format (Fig. 7). and a lumen cast format are also sometimes used. General programs for three-dimensional presentation can display oblique and tangential cuts through the reconstructed structures, comparable to the display options available in magnetic resonance imaging systems. A dynamic visualization of the artery after ECG-gated image acquisition is also possible[24].

Current three-dimensional reconstruction systems

Different systems are available. Each has a distinct technical approach with specific advantages and disadvantages in applicability, imaging, and quantification. The following systems are used at the Washington Hospital Center and/or the Thoraxcenter Rotterdam.

Acoustic quantification system

This system (EchoQuant), recently validated in rabbit aortas[27], can be used either on- or off-line, and it samples intracoronary ultrasound images with a digitization frame rate of 8·5 frames . s^{-1}. The length of the reconstructed coronary segment is determined by the pull-back speed since the image acquisition and digitization rates are fixed. Using a pull-back speed of 1·0 mm . s^{-1} images of 8 cm long segments can be acquired. Segmentation and reconstruction of a vascular segment 3 cm long can be performed within 3 min. The quality of the automated detection can be checked and manually corrected in individual cross-sectional images. No geometric assumptions of the lumen shape are required; and the program may therefore provide accurate segmentation of an irregularly shaped lumen. However, application of the algorithm may be hampered by the quality of the basic intracoronary ultrasound images[27,33]. Some parameters determining the automated identification process can be adjusted by the user; this is particularly important when the intracoronary ultrasound image quality is not optimal. Since the reconstruction is performed within a few minutes, it can be used in the catheterization laboratory[21].

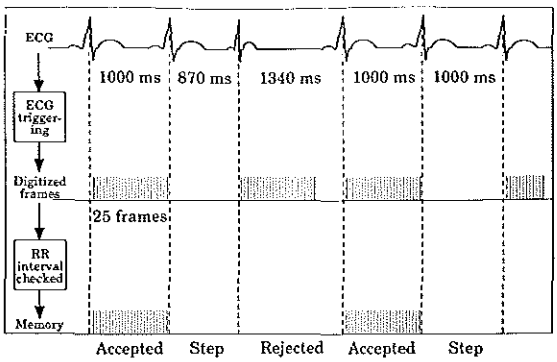

Figure 3 **The combined use of an ECG-gated pull-back device and image acquisition by the dynamic three-dimensional reconstruction system (Echoscan, TomTec, Munich, Germany) allows the problem of cyclic artifacts to be overcome and a dynamic visualization obtained. The range of the RR interval is defined (here: 1000 ± 100 ms) before the image acquisition starts. During the pull-back procedure, the maximum number of 25 intracoronary ultrasound images per cardiac cycle for each scanning site is digitized and sampled in the computer memory, unless the length of the RR interval fails to meet the pre-set range (here: third cardiac cycle). Each time a cycle is stored, the following heart beat is required to perform a pull-back step in order to reach the adjacent scanning site. (Reproduced with permission[24].)**

A selected cross-sectional image, a longitudinally reconstructed image (Fig. 1), and a cylindrical three-dimensional view (presenting the segment opened longitudinally) (Fig. 5) are displayed on the monitor. The measurements of the automated cross-sectional luminal area are displayed in a diagram. Although the algorithm is unable to detect the external contour of the total vessel, the current version of this program provides an option which allows manual tracing of the external contour of the vessel in selected two-dimensional images.

Thoraxcenter contour detection system

This analysis system digitizes a user-defined region of interest with a maximum of 200 tomographic images. Segments of approximately 2·5 cm (uniform pull-back) or 4 cm long (ECG-gated pull-back) can reliably be analysed. The method depends less on the image quality since it operates interactively. Reliable segmentation and three-dimensional reconstruction remain possible even when the image quality is not optimal. However, user interaction is required in the presence of irregular lumen shapes. On-line application of this system has recently been started using ECG-gated image acquisition.

The contour detection procedure (Fig. 6) consists of three steps[13,14,28]. First, the intracoronary ultrasound images are modelled in a voxel space[34]; and two perpendicular cut planes running parallel to the longitudinal axis of the vessel are selected. Data located at the interception of these cut planes and the voxel volume are derived to reconstruct two longitudinal images of the vascular segment. The angle and location of the cut planes is defined by the user in order to optimize the representation of the arterial segment on the longitudinal sections.

In a second step, the contours of the luminal and external vascular boundaries (external elastic lamina) are detected in the longitudinal images. This step is based on the application of a minimum cost algorithm[35], which has previously been validated[36] and applied in two-dimensional intracoronary ultrasound images[37]. The user is free to add markers, forcing the contours to pass through these sites. The optimal path of the longitudinal contours is updated serially, using dynamic programming techniques. The contours of the longitudinal images are then depicted as points in each cross-sectional image.

Finally, automated contour detection is performed in all the cross-sectional images, using the four edge points, derived from the longitudinal contours, as landmarks to guide the detection. The accuracy of the final contours can be checked and corrections may be performed. The system permits the quantitative analysis

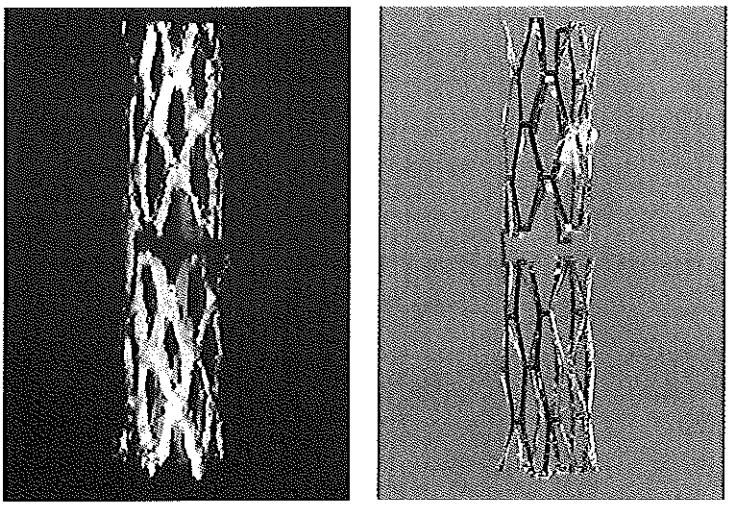

Figure 4 In vitro three-dimensional intracoronary ultrasound reconstruction (left panel) of a Palmaz-Schatz stent (Johnson & Johnson, Warren, U.S.A.) (right panel) based on segmentation by thresholding. The articulation of the Palmaz-Schatz stent and the typical strut pattern can be easily distinguished. (Reproduced with permission[120].)

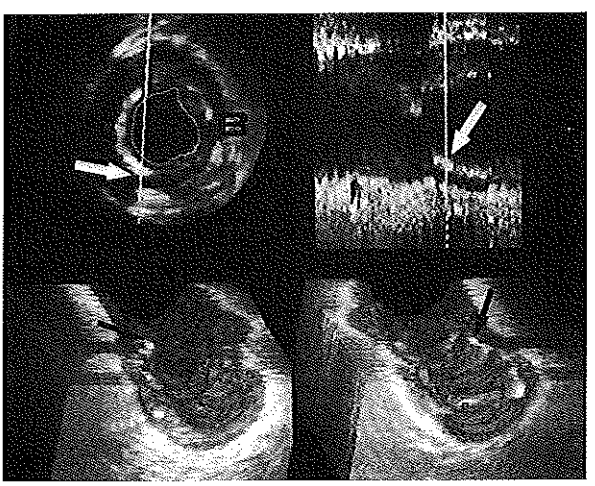

Figure 5 Complex coronary lesion in a mid right coronary artery before intervention. A large superficial calcification (arrowheads) is visible in the transverse (left upper panel), the longitudinally reconstructed (right upper panel), and the cylindrical view (lower panel). Segmentation is performed by acoustic quantification (EchoQuant, Indec, Capitola, CA, U.S.A.) which detects and consecutively removes the blood-pool (B) from the intracoronary ultrasound images. The length of the plaque calcification can easily be evaluated in the longitudinal reconstruction. The cursors (lines) in the transverse and longitudinal view permit the rotation of the longitudinal reconstruction and the selection of specific cross-sectional intracoronary ultrasound images.

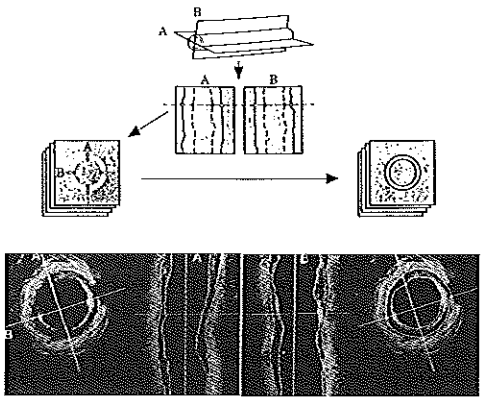

Figure 6 **The principle of the three-dimensional contour detection system. The intracoronary ultrasound images, obtained during a motorized pull-back, are stored in the computer memory as a 'volumetric space'. The method is based on the concept that edge points, derived from longitudinal contours which were previously detected on two longitudinally reconstructed images, guide and facilitate the final contour detection on the transverse intracoronary ultrasound images. The position of an individual transverse plane in the longitudinal sections is indicated by a horizontal cursor line which can be used to scroll through the whole series of transverse intracoronary ultrasound images. (Reproduced with permission[14].)**

of lumen and plaque, and even volumetric data (Fig. 8) can be obtained, as each cross-sectional image represents a slice of the reconstructed arterial segment[13–15]. Area and mean diameter measurements of the total vessel, lumen, and plaque are displayed in diagrams (Fig. 9). These diagrams also show diameter-stenosis, area-obstruction, and lumen symmetry functions[13,14,28].

Dynamic reconstruction system

The three-dimensional reconstruction tool installed in each Echoscan system (TomTec) uses a segmentation which is based on the definition of thresholds in the scale of gray levels. The applicability of this algorithm depends upon image quality. However, in instances with optimal two-dimensional image quality, remarkable dynamic reconstructions can be obtained (Fig. 10). As the ECG-gated three-dimensional reconstruction of a coronary segment requires sampling and processing of a large amount of data, the time of analysis is still slightly longer than for a conventional analysis.

Using volume rendering techniques, the dynamic reconstruction system allows dynamic visualization of the reconstructed segment[24] with a maximum of 25 frames per cardiac cycle. The reconstruction of various transverse and longitudinal sections is possible. The longitudinal reconstruction of a coronary artery segment is readily available in the cardiac catheterization laboratory and similar to computer tomography or magnetic resonance imaging, these longitudinal sections can pass through the centre of the vessel or cut the vessel wall tangentially.

Meanwhile, a version of the contour-detection-based analysis software of the Thoraxcenter, Rotterdam, has been customized for use with the Echoscan system[25,29]. The software package is available for users of Echoscan systems.

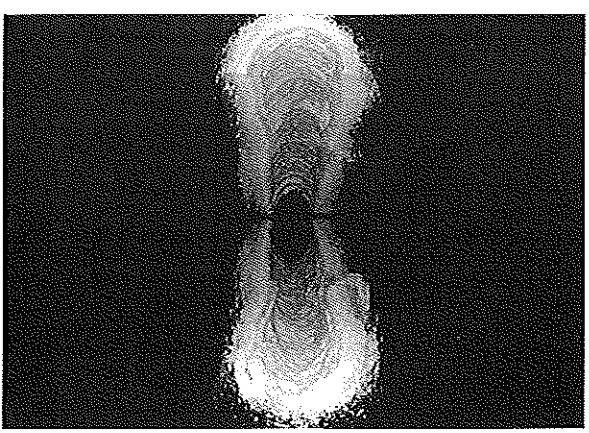

Figure 7 **Spatial view of a coronary segment (follow-up after previous directional coronary atherectomy), obtained from image data provided by the contour detection approach. This cylindrical display format is not required for the purpose of quantification, nevertheless additional insight into plaque disruption may sometimes be obtained. (Reproduced with permission[14].)**

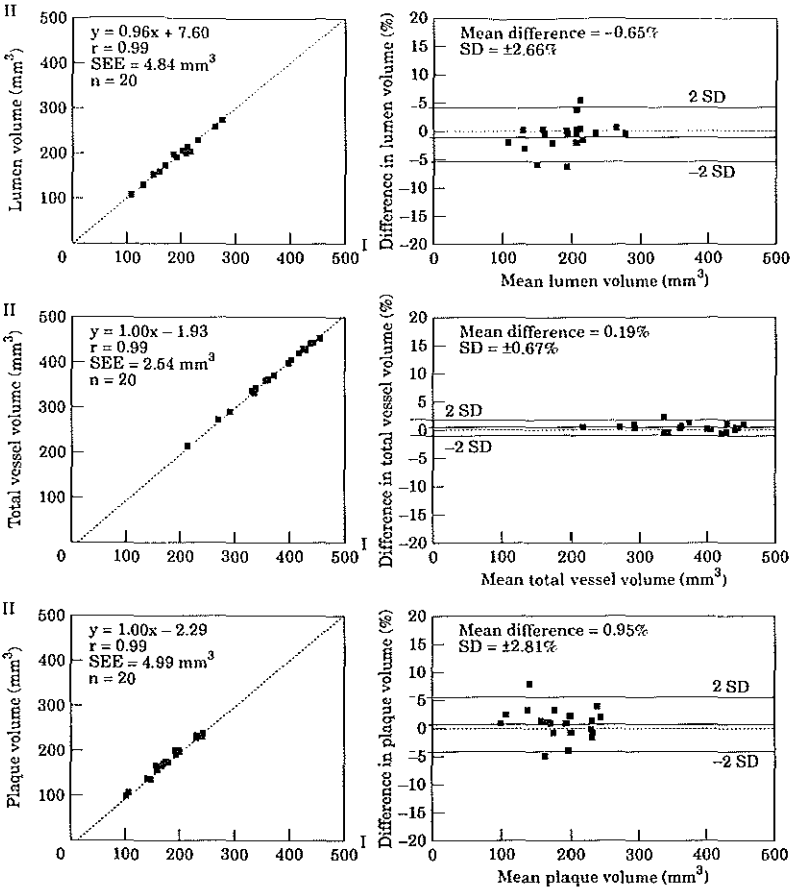

Figure 8 **Inter-observer variability of volume measurements in-vivo by the contour detection system. The lumen, total vessel, and plaque volume measurements in 20 coronary segments by two independent observers (I and II) showed a high reproducibility. In the right-hand panels relative inter-observer differences are plotted against the average of the two measurements. Solid lines indicate the mean difference and the range of 2 standard deviations (SD), and dotted lines mark the line of identity in all panels. (Reproduced with permission[14].)**

Challenges and future directions

Several factors, including problems related specifically to intracoronary ultrasound[39,40] as well as general limitations of the three-dimensional reconstruction[41], influence the quality of the reconstruction. Both lumen and plaque volume measurements showed minimal short-term biological variability upon repeated pull-back of the same coronary artery segment[42]. The quality of the basic intracoronary ultrasound image is crucial, as poor or incomplete visualization of the lumen–plaque and plaque–adventitia boundaries in the presence of calcification is a problem which hampers both reconstruction and quantification. Currently available intracoronary ultrasound transducers have a limited lateral resolution[43] and image distortion by non-uniform rotation or non-coaxial positioning of the intracoronary ultrasound catheter in the lumen may create complex artifacts in three-dimensional reconstructions[41]. Moreover, motorized pull-back devices or displacement sensors cannot always assure an equal distance between adjacent images, as bends of the ultrasound catheter may induce a difference between the movement of the distal transducer and the proximal part of the intracoronary ultrasound catheter.

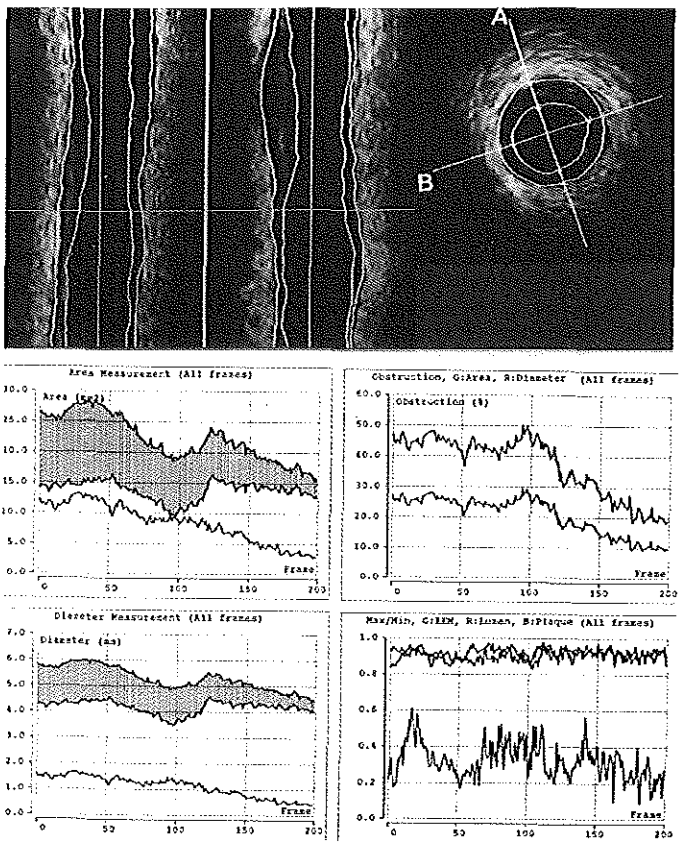

Figure 9 **Standard display of the results, by the contour detection method, of the Thoraxcenter, Rotterdam. The clinical example shows the results of an intracoronary ultrasound analysis performed 6 months after directional coronary atherectomy in a proximal left anterior descending coronary artery. The left mid and lower panels show area and mean diameter measurements of lumen, total vessel, and plaque. The gray areas represent the coronary plaque and the upper and lower boundaries of the gray zones correspond with the dimensions of the coronary lumen and the total vessel. The absolute plaque measurements are shown as a single line function for both area and diameter measurements (left mid and lower panels). Functions of the diameter-stenosis (%) and area-obstruction (%) are displayed in the mid right panel. The right lower panel shows the symmetry of the lumen and total vessel and the eccentricity of the plaque. (Reproduced with permission[14].)**

The cyclic movement of the intracoronary ultrasound catheter and systolic–diastolic changes in vessel dimensions can originate typical saw tooth-shaped image artifacts (Fig. 2)[41,44]. ECG-gated image acquisition and pull-back have the potential to minimize these cyclic artifacts and to optimize image acquisition, allowing reliable volumetric measurement[25,29,45]. However, compared to continuous pull-back, image acquisition by the ECG-gated approach requires a longer acquisition time which may cause problems in patients with very severe coronary stenoses.

Vessel curvatures with a radius of less than 5 cm may cause a significant distortion of the three-dimensional reconstructed image[46]. Over-estimation and under-estimation of certain portions of the plaque may be caused by vessel curvatures[47] as a result of the curved pull-back trajectory of the intracoronary ultrasound transducer. The contour detection system

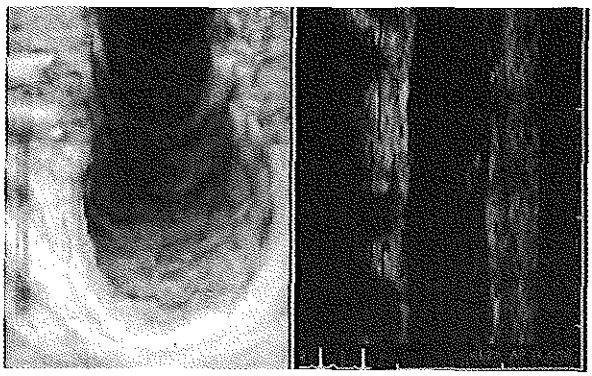

Figure 10 ECG-gated three-dimensional reconstruction of a proximal coronary artery with an eccentric plaque formation (on the right-hand side). A custom-designed pull-back device with a stepper motor, developed at the Thoraxcenter, Rotterdam, and the Echoscan (TomTec GmbH, Munich, Germany) were used to obtain this reconstruction. The plaque is visible on both a longitudinal section through the artery (right panel) and in a three-dimensionally reconstructed view (left panel).

demonstrates artificial curvatures caused by a localized eccentric plaque burden. Other three-dimensional reconstruction systems, as for instance the acoustic quantification system, straighten the display of the coronary segment artificially. The combined use of data obtained from biplane angiography and intracoronary ultrasound (Fig. 11) may help overcome many of these limitations to the provision of information on the real vessel curvatures and the orientation of the intracoronary ultrasound catheter[48,49]. Using ANGUS[49] — a technical approach which has been developed at the Thoraxcenter Rotterdam — in a geometric vessel phantom of known dimensions, a high accuracy was observed; and first applications in humans yielded good results. In the meantime, our findings have been confirmed by another group using a similar approach[50]. The use of new forward looking transducers[51] may also help to overcome some of the current limitations but the value of this device is still limited by the low image resolution and the large dimensions of the ultrasound transducers.

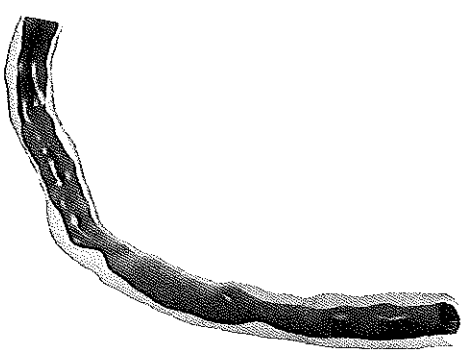

Figure 11 Combined use of biplane angiography and three-dimensional intracoronary ultrasound by ANGUS. This novel method allows the true geometry of the coronary lumen and plaque to be investigated, taking arterial curvatures and catheter bends into account. A reconstruction of an atherosclerotic right coronary artery is displayed in a frontal projection. Intracoronary ultrasound data provided by the contour detection method were spatially arranged and interpolated, using biplane data on both the pull-back trajectory and the angiogram. (Reproduced with permission[19].)

Miniaturization of the imaging catheters and improvements in the computer technology will also help to increase future applications of three-dimensional intracoronary ultrasound, which has the potential to largely replace quantitative coronary angiography in the future (Fig. 12) and permits volumetric quantification[13–15,29] without need for laborious manual tracing[52,53].

Conclusion

Until recently, three-dimensional intracoronary ultrasound appeared to be restricted to pure research applications, but we feel that the method will gain further importance and become a routine technique, if the interest, effort and technical developments in the field are sustained.

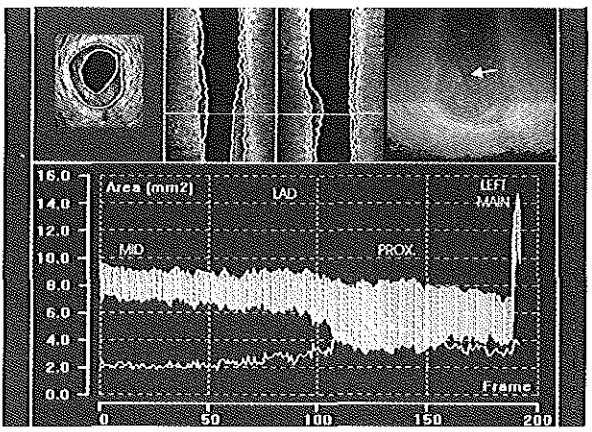

Figure 12 **Primary lesion in a proximal left anterior descending coronary artery (LAD), assessed by the three-dimensional intracoronary ultrasound contour detection system of the Thoraxcenter, Rotterdam. An arrowhead indicates the target stenosis in the cylindrical reconstruction. The measurements are shown in the lower panel: The white zone represents the coronary plaque and the upper and lower boundaries of this zone correspond with the values of the coronary lumen and the total vessel areas (mm^2). The absolute values of the plaque area (mm^2) are also shown as a single line. The area stenosis at the site of the mid segment of the LAD was approximately 20%. According to the mechanism described by Glagov, an enlargement of the total vessel area, partly compensating the plaque burden, may be expected at the site of relatively focal plaque formation. In this case, however, a paradoxical reduction of the total vessel area, from the distal reference in the mid LAD (MID) to the target stenosis in the proximal segment (PROX) was observed. (Reproduced with permission[169].)**

References

[1] Hodgson J McB, Graham SP, Sarakus AD *et al.* Clinical percutaneous imaging of coronary anatomy using an over-the-wire ultrasound catheter system. Int J Cardiac Imaging 1989; 4: 186–93.

[2] Yock PG, Linker DT. Intravascular ultrasound. Looking below the surface of vascular disease. Circulation 1990; 81: 1715–8.

[3] Nissen SE, Gurley JC, Grines CL *et al.* Intravascular ultrasound assessment of lumen size and wall morphology in normal subjects and patients with coronary artery disease. Circulation 1991; 84: 1087–99.

[4] Fitzgerald PJ, St. Goar FG, Connolly AJ, *et al.* Intravascular ultrasound imaging of coronary arteries: is three layers the norm? Circulation 1992; 86: 154–8.

[5] Ge J, Erbel R, Rupprecht HJ *et al.* Comparison of intravascular ultrasound and angiography in the assessment of myocardial bridging. Circulation 1994; 89: 1725–32.

[6] Mintz GS, Popma JJ, Pichard AD *et al.* Arterial remodeling after coronary angioplasty: a serial intravascular ultrasound study. Circulation 1996: 94; 35–43.

[7] Erbel R, Ge J, Bockisch A *et al.* Value of intracoronary ultrasound and Doppler in the differentiation of angiographically normal coronary arteries: a prospective study in patients with angina pectoris. Eur Heart J 1996; 17: 880–9.

[8] Matar FA, Mintz GS, Douek P *et al.* Coronary artery lumen volume measurement using three-dimensional intravascular ultrasound: validation of a new technique. Cathet Cardiovasc Diagn 1994; 33: 214–20.

[9] Rosenfield K, Kaufman J, Pieczek A, Langevin RE, Razvi S, Ilsner JM. Real-time three-dimensional reconstruction of intravascular ultrasound images of iliac arteries. Am J Cardiol 1992; 70: 412–5.

[10] Rosenfield K, Losordo DW, Ramaswamy K, Isner JM. Three-dimensional reconstruction of human coronary and peripheral arteries from images recorded during two-dimensional intravascular ultrasound examination. Circulation 1991; 84: 1938–56.

[11] Losordo DW, Rosenfield K, Peiczek A, Baker K, Harding M, Isner JM. How does angioplasty work? Serial analysis of human iliac arteries using intravascular ultrasound. Circulation 1992; 86: 1845–58.

[12] von Birgelen C, Di Mario C, Serruys PW. Structural and functional characterization of an intermediate stenosis with intracoronary ultrasound: a case of "reverse Glagovian modeling". Am Heart J 1996; 132: 694–6.

[13] von Birgelen C, van der Lugt A, Nicosia A *et al.* Computerized assessment of coronary lumen and atherosclerotic plaque dimensions in three-dimensional intravascular ultrasound correlated with histomorphometry. Am J Cardiol 1996; 78: 1202–9.

[14] von Birgelen C, Di Mario C, Li W *et al.* Morphometric analysis in three-dimensional intracoronary ultrasound: an in-vitro and in-vivo study using a novel system for the contour detection of lumen and plaque. Am Heart J 1996; 132: 516–27.

[15] von Birgelen C, Slager CJ, Di Mario C, de Feyter PJ, Serruys PW. Volumetric intracoronary ultrasound: a new maximum confidence approach for the quantitative assessment of progression/regression of atherosclerosis? Atherosclerosis 1995; 118 (Suppl): S103–13.

[16] Coy KM, Park JC, Fishbein MC *et al.* In vitro validation of three-dimensional intravascular ultrasound for the evaluation of arterial injury after balloon angioplasty. J Am Coll Cardiol 1992; 20: 692–700.

[17] Rosenfield K, Kaufman J, Pieczek AM *et al.* Human coronary and peripheral arteries: on-line three-dimensional reconstruction from two-dimensional intravascular US scans. Radiology 1992; 184: 823–32.

[18] Mintz GS, Leon MB, Satler LF *et al.* Clinical experience using a new three-dimensional intravascular ultrasound system before and after transcatheter coronary therapies. J Am Coll Cardiol 1992; 19: 292A.

[19] Schryver TE, Popma JJ, Kent KM, Leon MB, Eldredge S, Mintz GS. Use of intracoronary ultrasound to identify the true coronary lumen in chronic coronary dissection treated with intracoronary stenting. Am J Cardiol 1992; 69: 1107–8.

[20] Mintz GS, Pichard AD, Satler LF, Popma JJ, Kent KM, Leon MB. Three-dimensional intravascular ultrasonography: reconstruction of endovascular stents in vitro and in vivo. J Clin Ultrasound 1993; 21: 609–15.

[21] von Birgelen C, Gil R, Ruygrok P *et al.* Optimized expression of the Wallstent compared to the Palmaz-Schatz stent: online observations with two and three-dimensional intracoronary ultrasound after angiographic guidance. Am Heart J 1996; 131: 1067–75.

[22] Fuessel RT, Mintz GS, Pichard AD *et al.* In vivo validation of intravascular ultrasound length measurements using a motorized transducer pullback system. Am J Cardiol 1996; 77: 1115–8.

[23] Roelandt JRTC, ten Cate FJ, Vletter WB, Taams MA. Ultrasonic dynamic three-dimensional visualization of the heart with a multiplane transesophageal imaging transducer. J Am Soc Echocardiogr 1994; 7: 217–29.

[24] Bruining N, von Birgelen C, Di Mario C *et al.* Dynamic three-dimensional reconstruction of ICUS images based on an ECG gated pull-back device. In: Computers in Cardiology 1995, Los Alamitos: IEEE Computer Society Press, 1995: 633–6.

[25] von Birgelen C, Mintz GS, Nicosia A *et al.* ECG-gated intravascular ultrasound image acquisition after coronary stent deployment facilitates on-line three-dimensional reconstruction and automated lumen quantification. J Am Coll Cardiol 1997 (in press).

[26] Chandrasekaran K, D'Adamo AJ, Sehgal CM. Three-dimensional reconstruction of intravascular ultrasound images. In: Yock PG, Tobis JM, eds. Intravascular Ultrasound Imaging. New York: Churchill-Livingstone, 1992: 141–7.

[27] Hausmann D, Friedrich G, Sudhir K *et al.* 3D intravascular ultrasound imaging with automated border detection using 2.9F Catheters. J Am Coll Cardiol 1994; 23: 174A.

[28] Li W, von Birgelen C, Di Mario C *et al.* Semi- automatic contour detection for volumetric quantification of intracoronary ultrasound. In: Computers in Cardiology 1994, Los Alamitos: IEEE Computer Society Press, 1994: 277–80.

[29] von Birgelen C, de Vrey E, Mintz GS *et al.* ECG-gated three-dimensional intravascular ultrasound: feasibility and reproducibility of the automated analysis of coronary lumen and atherosclerotic plaque dimensions in humans. Circulation (in press).

[30] Li W, Gussenhoven EJ, Zhong Y *et al.* Temporal averaging for quantification of lumen dimensions in intravascular ultrasound images. Ultrasound Med Biol 1994; 20: 117–22.

[31] Sonka M, Zhang X, Siebes M, DeJong S, McKay CR, Collins SM. Automated segmentation of coronary wall and plaque from intravascular ultrasound image sequences. In: Computers in Cardiology 1994, Los Alamitos: IEEE Computer Society Press, 1994: 281–4.

[32] Sonka M, Zhang X, Siebes M *et al.* Semi-automated detection of coronary arterial wall and plaque borders in intravascular ultrasound images. Circulation 1994; 90: I-550.

[33] von Birgelen C, Kutryk MJB, Gil R *et al.* Quantification of the minimal luminal cross-sectional area after coronary stenting: two-dimensional and three-dimensional intravascular ultrasound versus edge detection and videodensitometry. Am J Cardiol 1996; 78: 520–5.

[34] Kitney R, Moura L, Straughan K. 3-D visualization of arterial structures using ultrasound and voxel modelling. Int J Cardiac Imag 1989; 4: 134–43.

[35] Li W, Bosch JG, Zhong Y *et al.* Image segmentation and 3D reconstruction of intravascular ultrasound images. In: Wei Y, Gu B, eds. Acoustical Imaging, Vol. 20. New York: Plenum Press, 1993: 489–96.

[36] Li W, Gussenhoven EJ, Zhong Y *et al.* Validation of quantitative analysis of intravascular ultrasound images. Int J Cardiac Imag 1991; 6: 247–54.

[37] Di Mario C, The SHK, Madretsma S *et al.* Detection and characterization of vascular lesions by intravascular ultrasound: an in-vitro study correlated with histology. J Am Soc Echocardiogr 1992; 5: 135–46.

[38] Masotti L, Pini R. Three-dimensional imaging. In: Wells, PNT, ed. Advances in Ultrasound Techniques and Instrumentation. New York: Churchill Livingstone, 1993: 69–77.

[39] Ge J, Erbel R, Seidel I *et al.* Experimentelle Überprüfung der Genauigkeit und Sicherheit des intraluminalen Ultraschalls. Z Kardiol 1991; 80: 595–601.

[40] Di Mario C, Madretsma S, Linker D *et al.* The angle of incidence of the ultrasonic beam: a critical factor for the image quality in intravascular ultrasonography. Am Heart J 1993; 125: 442–8.

[41] Roelandt JRTC, Di Mario C, Pandian NG *et al.* Three-dimensional reconstruction of intracoronary ultrasound images: Rationale, approaches, problems and directions. Circulation 1994; 90: 1044–55.

[42] Dhawale P, Rasheed Q, Berry J, Hodgson J McB. Quantification of lumen and plaque volume with ultrasound: accuracy and short term variability in patients. Circulation 1994; 90: I-164.

[43] Benkeser PJ, Churchwell AL, Lee C, Abouelnasr DM. Resolution limitations in intravascular ultrasound imaging. J Am Soc Echocardiogr 1993; 6: 158–65.

[44] Di Mario C, von Birgelen C, Prati F *et al.* Three-dimensional reconstruction of two-dimensional intracoronary ultrasound: clinical or research tool? Br Heart J 1995; 73 (Suppl 2): 26–32.

[45] Dhawale PJ, Wilson DL, Hodgson J McB. Optimal data acquisition for volumetric intracoronary ultrasound. Cathet Cardiovasc Diagn 1994; 32: 288–99.

[46] Waligora MJ, Vonesh MJ, Wiet SP, McPherson DD. Effect of vascular curvature on three-dimensional reconstruction of intravascular ultrasound images. Circulation 1994; 90: I-227.

[47] Klein HM, Günther RW, Verlande M *et al.* 3D-surface reconstruction of intravascular ultrasound images using personal computer hardware and a motorized catheter control. Cardiovasc Intervent Radiol 1992; 15: 97–101.

[48] Koch L, Kearney P, Erbel R *et al.* Three-dimensional reconstruction of intracoronary ultrasound images: roadmapping with simultaneously digitised coronary angiograms. In: Computers in Cardiology 1993, Los Alamitos: IEEE Computer Society Press, 1993: 89–91.

[49] Slager CJ, Laban M, von Birgelen C *et al.* ANGUS: A new approach to three-dimensional reconstruction of geometry and orientation of coronary lumen and plaque by combined use of coronary angiography and ICUS. J Am Coll Cardiol 1995; 25: 144A.

[50] Evans JL, Ng KH, Wiet SG *et al.* Accurate three-dimensional reconstruction of intravascular ultrasound data: spatially correct three-dimensional reconstructions. Circulation 1996; 93: 567–76.

[51] Ng K-H, Evans JL, Vonesh MJ *et al.* Arterial imaging with a new forward-viewing intravascular ultrasound catheter, II: three-dimensional reconstruction and display of data. Circulation 1994; 89: 718–23.
[52] Matar FA, Mintz GS, Farb A *et al.* The contribution of tissue removal to lumen improvement after directional coronary atherectomy. Am J Cardiol 1994; 74: 647–50.
[53] Dussaillant GR, Mintz GS, Pichard AD *et al.* Small stent size and intimal hyperplasia contribute to restenosis: a volumetric intravascular ultrasound analysis. J Am Coll Cardiol 1995; 26: 720–4.
[54] von Birgelen C, Di Mario C, Reimers B *et al.* Three-dimensional intracoronary ultrasound imaging: methodology and clinical relevance for the assessment of coronary arteries and bypass grafts. J Cardiovasc Surg 1996; 37: 129–39.

Chapter 14

Variations of remodeling in response to left main atherosclerosis assessed with intravascular ultrasound in vivo

C von Birgelen, SG Airiian, GS Mintz, WJ van der Giessen,
DP Foley, JRTC Roelandt, PW Serruys,
PJ de Feyter

Reprinted with permission from *Am J Cardiol* 1997;80:1408-1413

Variations of Remodeling in Response to Left Main Atherosclerosis Assessed With Intravascular Ultrasound In Vivo

Clemens von Birgelen, MD,* Sergei G. Airiian, MD, Gary S. Mintz, MD, Wim J. van der Giessen, MD, PhD, David P. Foley, MB, MRCPI, PhD, Jos R.T.C. Roelandt, MD, PhD, Patrick W. Serruys, MD, PhD, and Pim J. de Feyter, MD, PhD

Histopathologic studies have demonstrated that vessels enlarge to compensate for an increase in plaque burden; this has been confirmed in vivo using intravascular ultrasound (IVUS). The initial studies suggested a biphasic course of lesion formation with (1) preservation of lumen dimensions up to a plaque burden of approximately 40%, and (2) luminal narrowing as plaque burden further increases. In this study, we used IVUS and angiography to assess the extent of left main (LM) atherosclerosis in 107 patients undergoing catheter-based procedures of the left anterior descending or left circumflex coronary arteries. Using IVUS, atherosclerotic plaques were found in all LM arteries, but only 26 (24%) had varying degrees of luminal narrowing on the angiogram. Nevertheless, there was an inverse relation ($r = -0.62$, $p < 0.0001$) between the minimal lumen area and the plaque burden (i.e., plaque + media divided by total vessel area) that was *not* restricted to plaque burden values >40% (or >30%), but persisted at plaque burden values of 20% to 40%. In addition, LM arteries with a plaque burden <40% had a similar total vessel area as did LM arteries with a plaque burden ≥40% (22.9 ± 6.1 vs 21.8 ± 4.8 mm^2, $p = 0.30$). These data suggest that lumen dimensions may not be preserved even if plaque occupies no more than 20% to 40% of the total vessel area. Thus, there is more variation in remodeling response during earlier stages of plaque accumulation within the LM artery than is commonly suggested.
(Am J Cardiol 1997;80:1408–1413)

Coronary angiography is used to assess lesion formation[1]; however, early atherosclerosis is angiographically silent.[2–5] Histopathologic studies of diseased arterial segments have demonstrated that compensatory enlargement of the vascular wall occurs to compensate for the accumulation of atherosclerotic plaque.[2,6] Intravascular ultrasound (IVUS) provides transmural images of coronary vessels in vivo including the coronary vascular wall, the area of atherosclerotic plaque, accurate lumen dimensions, and the serial changes that occur with the atherosclerotic disease process.[7–10] Intravascular and epicardial ultrasound studies of atherosclerotic coronary[3,5,11–13] and peripheral arteries[14–17] have provided insights into the consequences of plaque accumulation and mechanisms of lesion formation. Earlier studies have confirmed the initial histopathologic findings of a biphasic course of lesion formation: (1) early preservation of lumen dimensions until a plaque burden of approximately 40% is reached, and (2) luminal narrowing as plaque burden further increases.[3,4,6] More recent studies have shown evidence that inadequate or absent compensatory vascular enlargement may also be important in the development of arterial stenoses.[12,13,15–18] The left main (LM) coronary artery is one of the most important targets of atherosclerotic plaque accumulation.[5,6,19–25] In this study we used IVUS and quantitative coronary angiography to systematically assess the extent and characteristics of LM atherosclerosis in 107 patients undergoing catheter-based interventions of significant lesions of the left anterior descending or left circumflex coronary arteries.

From the Thoraxcenter, University Hospital Rotterdam-Dijkzigt, Erasmus University Rotterdam, Rotterdam, The Netherlands; and the Washington Hospital Center, Washington D.C. Manuscript received August 24, 1997, and accepted August 29, 1997.

*Current address: Department of Cardiology, University Hospital Essen, Hufelandstrasse 55, D-45147 Essen, Germany. Dr. von Birgelen is the recipient of a fellowship of the German Research Society (DFG, Bonn, Germany).

Address for reprints: Pim J. de Feyter, MD, PhD, Thoraxcenter, Bd 38, P.O. Box 1738, University Hospital Rotterdam-Dijkzigt, 3000 DR Rotterdam, The Netherlands.

METHODS

Patient population: Between August 1, 1995, and July 31, 1996, a prospective IVUS examination of the LM artery was performed in 107 patients. There were 84 men (78%) and 23 women (22%) who ranged in age from 32 to 80 years (mean 58 ± 11); all of them were symptomatic (87 had chronic stable angina and 20 unstable angina). This patient population represented a consecutive series of patients with IVUS-guided coronary interventions of significant narrowings in the left anterior descending or circumflex coronary arteries. None were considered to have significant disease of the LM artery. This study was approved by the local council on human research. All patients signed a written informed consent form approved by the medical ethical committee of the University Hospital Rotterdam-Dijkzigt.

Intervention procedures and coronary angiography: All patients received 250 mg of aspirin and 10,000 U of heparin intravenously. If the duration of the entire catheterization procedure exceeded 1 hour, the acti-

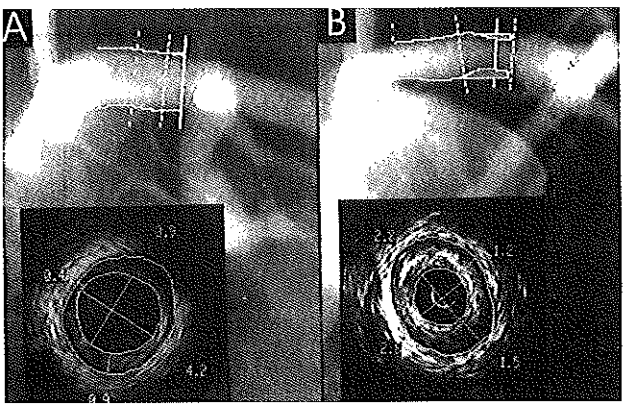

FIGURE 1. Examples of plaque formation in left main coronary arteries without *(A)* and with *(B)* luminal narrowing on the angiogram. The angiograms display the plaque interpolation and minimal lumen detection, as obtained from quantitative coronary angiography. The intravascular ultrasound images *(inserts)* depict the site of minimum lumen cross-sectional area; on these images the contours of the lumen and total vessel boundaries as well as the minimum and maximum diameters of lumen and plaque + media were traced.

vated clotting time was measured; intravenous heparin was administered in order to maintain an activated clotting time of >300 seconds. In all patients, successful catheter-based interventions of lesions in the left anterior descending (n = 91) or left circumflex coronary arteries (n = 16) were performed (63 with stent placement, 25 with directional atherectomy, and 19 with balloon angioplasty). At the end of the interventional procedure, intracoronary injection of 2 mg of isosorbide dinitrate was administered, ≥2 angiograms of the LM were recorded from opposite (ideally orthogonal) views without overlapping side branches or foreshortening, and the LM artery was interrogated using IVUS. There were no procedural or postprocedural in-hospital complications in these patients.

Angiographic analysis: The angiograms were first interpreted by 3 experienced coronary angiographers who were blinded to IVUS data. All angiographic projections were reviewed for the presence of atherosclerosis of the LM artery. If during the visual assessment of the LM artery, an indentation of the opacified luminal silhouette or a lumen narrowing of any degree was noticed, that LM artery was classified as "angiographically *ab*normal." Accordingly, only LM arteries without such findings were classified as "angiographically normal." Decisions for classification required at least 2 votes.

Quantitative coronary angiography of 2 angiographic views (ideally orthogonal views without overlapping side branches or foreshortening) was then performed off-line. End-diastolic frames acquired after intracoronary application of nitrates and having homogeneous opacification of the coronary lumen were selected for analysis. The computer-based Coronary Angiography Analysis System (CAAS II, Pie Medical, Maastricht, The Netherlands) was used for the analysis. This has previously been described in detail.[1]

Intravascular ultrasound imaging: After intracoronary injection of 2 mg of isosorbide dinitrate, the LM artery was examined using a mechanical IVUS system (CardioVascular Imaging Systems Inc, Sunnyvale, California) and a sheath-based IVUS catheter. The IVUS catheter incorporates a 30-MHz beveled, single-element transducer rotating at 1,800 rpm within a 2.9Fr long monorail imaging sheath. The distal 15-cm-long sonolucent segment of the imaging sheath has a common lumen that alternatively houses the guidewire (during catheter introduction) or the transducer (during imaging after the guidewire has been pulled back), but not both. This design avoids direct contact of the IVUS imaging core with the vessel wall. Before the IVUS imaging run, the guiding catheter was withdrawn from the ostium of the LM artery to assure complete scanning of the entire LM artery. All studies were performed using a motorized transducer pullback at 0.5 mm/s. All IVUS studies were recorded on 0.5-inch high-resolution sVHS tape for off-line analysis.

Intravascular ultrasound analysis: Each videotape was analyzed off-line by an experienced IVUS analyst and overread by 2 independent cardiologists experienced in the use and analysis of IVUS images.

QUANTITATIVE ANALYSIS: Validation of manual measurements by IVUS has been reported previously.[26] The site of the minimum lumen cross-sectional area was identified by carefully scrolling the tape back and forth; if there were multiple image slices with the same minimum lumen cross-sectional area, then the image slice with the largest plaque burden was selected. This was the image slice on which the IVUS measurements were performed (Figure 1). The cross-sectional area measurements included the lumen and total vessel cross-sectional area (interobserver differences: 0.1 ± 0.8 mm^2 [lumen], 0.0 ± 1.1 mm^2 [total vessel]). Plaque + media cross-sectional area was calculated as total vessel minus lumen cross-sectional area, and the plaque burden was calculated as plaque + media divided by total vessel cross-sectional area. The total vessel diameter was calculated as: square root of [(4 · total vessel cross-sectional area)/π]. The minimum and maximum lumen diameters (interobserver differences: 0.0 ± 0.3 mm [minimum lumen], 0.0 ± 0.3 mm [maximum lumen]), and the minimum and maximum plaque + media thickness (interobserver differences: 0.01 ± 0.02 mm [minimum plaque + media], 0.01 ± 0.09 mm [maximum plaque + media]) were measured. The total vessel cross-sectional area represents the area within the border between the hypoechoic media and the echoreflective adventitia. As in many previous studies using

TABLE I Quantitative Coronary Angiography and Intravascular Ultrasound Data

	All Patients (n = 107)	Plaque Burden <40% (n = 71)	Plaque Burden ≥40% (n = 36)	p Value*
IVUS				
Lumen CSA (mm^2)	15.1 ± 4.8	16.8 ± 4.7	11.6 ± 2.8	<0.0001
P + M CSA (mm^2)	7.5 ± 3.6	6.1 ± 2.9	10.3 ± 3.2	<0.0001
Total vessel CSA (mm^2)	22.6 ± 5.7	22.9 ± 6.1	21.8 ± 4.8	0.30
Plaque burden (%)	33.3 ± 12.9	26.6 ± 9.4	46.6 ± 7.3	<0.0001
Minimum lumen diameter (mm)	3.91 ± 0.75	4.18 ± 0.71	3.38 ± 0.54	<0.0001
Maximum lumen diameter (mm)	4.65 ± 0.75	4.92 ± 0.70	4.12 ± 0.54	<0.0001
Minimum P + M diameter (mm)	0.16 ± 0.22	0.08 ± 0.15	0.31 ± 0.25	<0.0001
Maximum P + M diameter (mm)	0.99 ± 0.42	0.85 ± 0.37	1.26 ± 0.40	<0.0001
Total vessel diameter (mm)	5.32 ± 0.65	5.36 ± 0.68	5.24 ± 0.57	0.34
Arc of plaque (°)	296 ± 83	270 ± 90	348 ± 22	<0.0001
Quantitative coronary angiography				
Minimum lumen diameter (mm)	3.84 ± 0.78	3.98 ± 0.70	3.59 ± 0.86	<0.05
Reference diameter (mm)	4.17 ± 0.75	4.30 ± 0.68	3.93 ± 0.84	<0.05
Diameter stenosis (%)	8.0 ± 7.0	7.6 ± 6.2	8.8 ± 8.3	0.43

*Plaque burden <40% versus plaque burden ≥40%.
Data are expressed as mean ± 1 SD.
CSA = cross-sectional area; IVUS = intravascular ultrasound; P + M = plaque + media.

IVUS, plaque + media cross-sectional area was used as a measure of atherosclerotic plaque, because ultrasound cannot measure media thickness accurately.[27] The circumferential arc of the LM artery containing plaque was measured (in degrees) using a protractor centered on the lumen. The plaque burden has been termed cross-sectional area obstruction, cross-sectional narrowing, or percent plaque area by other investigators.

QUALITATIVE ANALYSIS: Plaque composition was assessed visually. The presence of significant amounts of calcium, dense fibrous tissue, or soft plaque was tabulated. Calcium produced bright echoes (brighter than the reference adventitia) with acoustic shadowing (attenuation) of deeper arterial structures[8]; the largest arc of calcium within the LM artery was identified and measured (in degrees) using a protractor centered on the lumen. Although initially an arc of calcium >120° was predetermined to be an exclusion criterion (to assure reliable measurement of the total vessel and plaque + media cross-sectional area), *no* patient had this degree of LM calcification. Plaque tissue producing echoes that were as bright as or brighter than the reference adventitia, but without acoustic shadowing was classified as "fibrous." Tissue being less dense than the reference adventitia was classified as "soft." Plaques containing more than 1 type of tissue were classified as "mixed."

Statistical analysis: Categorical variables were presented as frequencies. Continuous variables were presented as mean ± 1 SD. Categorical variables were compared using chi-square analysis. Continuous variables were compared using the 2-tailed Student's *t* test and linear and nonlinear regression analyses. A p value <0.05 was considered statistically significant.

RESULTS

Overall angiographic and intravascular ultrasound data: With use of coronary angiography, only 26 LM arteries (24%) were classified as abnormal; however, IVUS revealed atherosclerotic plaques in all 107 LM arteries (p <0.0001 vs angiography). Twenty-five plaques were classified as soft, 22 were fibrous, and 50 were mixed. Plaque calcification was found in 30 LM lesions with an arc of calcium ranging from 20° to 120° in circumference. Data provided by both quantitative coronary angiography and IVUS are listed in Table I.

Data of angiographically normal versus abnormal main stems: The IVUS and quantitative coronary angiographic findings in patients with angiographically abnormal (n = 26) and normal LM arteries (n = 81) were then compared. The 2 groups were similar with regard to age (59 ± 10 vs 57 ± 11 years) and gender (77% vs 79% men). Patients with an angiographically abnormal LM artery had (1) a smaller quantitative angiographic minimal lumen diameter (3.30 ± 0.68 vs 4.02 ± 0.73 mm, p <0.0001), (2) a smaller quantitative angiographic reference diameter (4.01 ± 0.74 vs 4.23 ± 0.75 mm, p <0.0001), (3) a higher quantitative angiographic diameter stenosis (17.60 ± 6.85% vs 4.88 ± 3.15%, p <0.0001), and (4) a smaller IVUS minimal lumen cross-sectional area (13.0 ± 4.9 vs 15.7 ± 4.7 mm^2, p <0.05). In patients with an angiographically abnormal LM artery, the IVUS plaque burden tended to be higher (37.2 ± 14.2% vs 32.1 ± 14.2%, p = 0.10); however, the total vessel cross-sectional area tended to be even smaller (20.9 ± 6.4 vs 23.1 ± 5.4 mm^2, p = 0.10). There was no significant difference in plaque composition.

Assessment of vascular remodeling: The total vessel cross-sectional area by IVUS correlated directly with the plaque + media cross-sectional area (r = 0.54, p <0.0001, Figure 2).

In addition, the IVUS minimal lumen cross-sectional area correlated inversely with the plaque burden (r = −0.62, p <0.0001, Figure 3); this relation was very similar for the LM artery with a plaque burden ≥40% (r = −0.42, y = −0.17x + 19.0, p <0.01) and for the LM artery with a plaque burden <40% (r = −0.41, y = −0.21x + 22.3, p <0.001). Similar correlations were found for the LM artery with a plaque burden ≥30% and <30% (r = −0.48 and −0.42, respectively, both p <0.01). Various nonlinear regression approaches were tested and did not reveal relations with higher or equal significance.

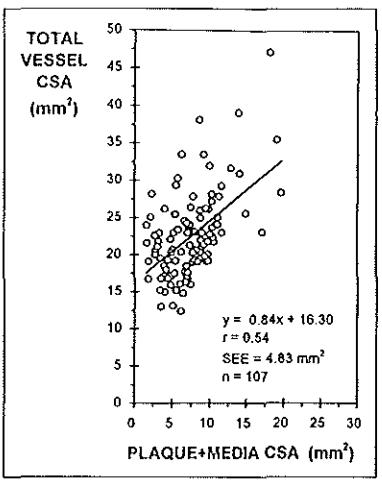

FIGURE 2. Correlation between total vessel cross-sectional area (CSA) and plaque + media cross-sectional area, measured with intravascular ultrasound in 107 left main coronary arteries.

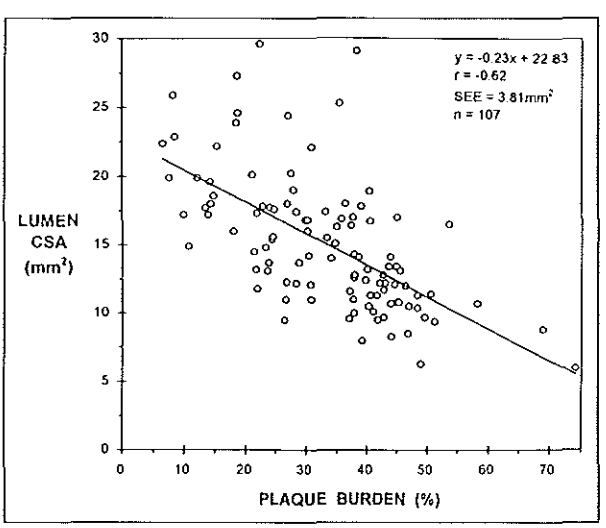

FIGURE 3. The minimal lumen cross-sectional area (CSA) by intravascular ultrasound correlated inversely with the plaque burden. This relation was observed not only in the 36 arteries with a plaque burden ≥40% ($r = -0.42$, $p < 0.01$), but also in the 71 arteries with a plaque burden <40% ($r = -0.41$, $p < 0.001$). Similar correlations were also found for both, arteries with a plaque burden ≥30% and <30% ($r = -0.48$ and -0.42, respectively, both $p < 0.01$).

Thirty-six of the 107 LM arteries had an IVUS plaque burden ≥40%; 71 had a plaque burden <40%. Both groups were similar with respect to age (58 ± 11 vs 57 ± 11 years) and gender (79% vs 78% men). Results of quantitative coronary angiography and IVUS analysis of these 2 subsets are listed in Table I. In the group with plaque burden ≥40%, IVUS plaque composition was less frequently soft (8% vs 31%, $p < 0.01$); the frequency of plaque calcification was higher (47% vs 18%, $p < 0.005$), and the arc of diseased vessel wall was significantly larger (348 ± 22° vs 270 ± 90°, $p < 0.0001$). In addition, in vessels with plaque burden ≥40%, the lumen cross-sectional area and diameters were significantly smaller; the plaque + media cross-sectional area and diameters were larger, but the total vessel cross-sectional area was similar (22.9 ± 6.1 vs 21.8 ± 4.8 mm², $p = 0.30$).

DISCUSSION

In the present study, careful IVUS examination during catheter-based interventions of major epicardial left coronary arteries in a consecutive series of 107 patients revealed the presence of LM plaques in all and demonstrated the superiority of IVUS in detecting early atherosclerotic changes in vivo.[1,2,8,19,20] These data are in agreement with previous IVUS findings in a smaller study group.[19]

Adaptive vascular remodeling: The absence of angiographic lumen narrowing despite the presence of ultrasound-confirmed plaque formation is generally thought to result from compensatory vascular enlargement. In addition, there were other signs of adaptive remodeling. First, the total vessel cross-sectional area measured 22.6 mm²; this is comparable to previous measurements in diseased LM arteries (22.0 to 23.3 mm²),[3,20] but larger than measurements in nondiseased LM arteries (19.0 mm²).[20] Second, despite an average plaque burden of 33%, the average lumen cross-sectional area was reduced by 20% compared with that in nondiseased LM arteries.[20]

As in previous histopathologic and IVUS studies,[2–6] we found a significant relation between plaque + media and total vessel cross-sectional area. This relation, which has previously been understood as an arithmetic expression of the adaptive remodeling process, appears to be less strong in the LM artery ($r = 0.46$ to 0.56)[3,5] than has been reported in other major epicardial coronary branches or in peripheral vessels ($r = 0.63$ to 0.85).[2,3,14–16] In addition, the value of the relation between plaque + media and total vessel area appears to be limited because (1) correlating plaque + media with total vessel cross-sectional area should have a significant positive relation because this is a correlation between α and $\alpha + \beta$, and (2) the regression equation will always show steeper slopes for mildly diseased vascular segments, falsely suggesting overcompensation of total vessel area in relation to plaque accumulation.[28]

Variations of remodeling response: However, the results of the current study also suggest that even during earlier stages of atherosclerotic plaque accu-

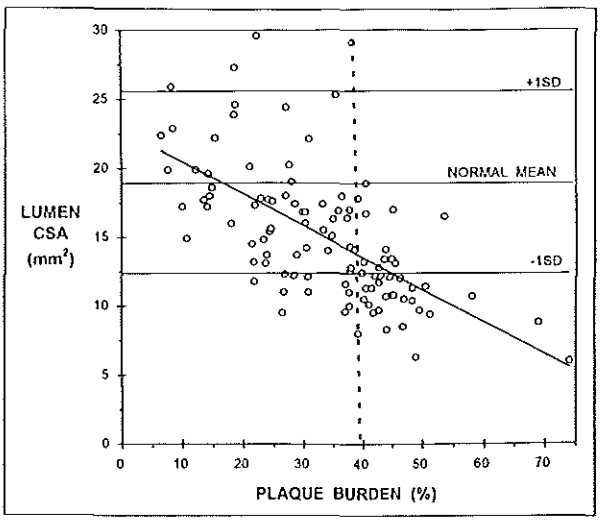

FIGURE 4. Intravascular ultrasound normal values from published reports, obtained in 61 main stems with ultrasound-documented absence of plaque formation (19.0 ± 6.5 mm²),[20] were used to evaluate the preservation of lumen cross-sectional area (CSA). The illustration displays (1) data of the current study compared with (2) mean ± 1 SD of the normal size *(3 horizontal lines)*, (3) a linear regression line, and (4) *a dotted line* indicating a plaque burden of 40%. In patients with a plaque burden <20% the lumen size was evenly distributed on both sides of the mean normal value, and in all patients the lumen was larger than the −1 SD margin. This may, to some extent, result from adaptive remodeling. Conversely, in several main stems with a plaque burden between 20% and 40%, the lumen was smaller than the −1 SD margin, which may reflect inadequacy or early cessation of the adaptive remodeling process.

mulation (i.e., plaque burden of 20% to 40%), compensatory vascular enlargement may be inadequate to preserve lumen dimensions in a considerable number of cases. For instance, there was a negative correlation between lumen cross-sectional area and plaque burden ($r = 0.62$), a relation that was not restricted to patients with a plaque burden > or <30% or 40%, as previously described.[3,6] In the present study, there was also no significant difference in total vessel cross-sectional area between (1) LM artery with a plaque burden <40% versus LM artery with a plaque burden ≥40%, or (2) angiographically normal versus angiographically abnormal LM arteries. The total vessel cross-sectional area was even slightly higher in the group with angiographically normal LM arteries. We used IVUS normal values from published data, obtained from 61 LM arteries with IVUS-documented absence of plaque formation (19.0 ± 6.5 mm²),[20] to evaluate the preservation of the lumen cross-sectional area. Figure 4 shows data of the current study compared with the mean ± 1 SD of the normal LM size. In patients with a LM plaque burden <20%, the lumen size was evenly distributed on both sides of the mean normal value; in all patients the lumen was larger than the −1 SD margin. This may, to some extent, result from adaptive remodeling. Conversely, in several patients with a LM plaque burden between 20% and 40%, the LM was smaller than the −1 SD margin; this may reflect an inadequacy or an early cessation of the adaptive remodeling process.

Variability of the adaptive remodeling process has previously been suggested by others.[6,12,15–17] Nevertheless, because these studies in humans were observations at one point in time, the time course and magnitude of vascular response to plaque growth remains unknown.

Limitations and potential sources of error: (1) All patients underwent catheter-based coronary interventions. Therefore, we were limited to assessment of LM arteries in patients *without* angiographically significant LM lesions, but *with* significant lesions of the left anterior descending or circumflex coronary arteries. (2) As in previous histopathologic or IVUS studies of vascular remodeling,[1–18] this study was observational and provided only a "snapshot-like view" on coronary artery disease. (3) Measurement accuracy may be affected by an eccentric position or a noncoaxial orientation of the IVUS catheter. (4) The accuracy of visual assessment of plaque composition on conventional IVUS images is known to be limited, and IVUS tissue classification does not necessarily correspond to histologic classification. (5) Intracoronary injections of nitrates were used to prevent vasospasm, and no angiographic changes were observed before and after the IVUS imaging procedure; nevertheless, this does not completely exclude local vasospastic activity.

Clinical implications: Although IVUS inspection reveals the presence of plaque formation within the LM artery in patients undergoing procedures of major left coronary branches, the extent of plaque accumulation is variable and should not be equated with hemodynamically significant disease. Nevertheless, our findings underline the standard recommendation to perform any cannulation of the LM artery with care. The current study demonstrates that compensatory vascular enlargement is a variable phenomenon, explaining a smaller lumen cross-sectional area in some cases even before the plaque occupies 40% of the total vessel cross-sectional area. Serial IVUS studies will be necessary to gain insight into (1) the time course of vascular remodeling, and (2) whether plaques with different patterns of remodeling require specific or different therapy with respect to the acute procedural success and long-term outcome.

1. Escaned J, Baptista J, Di Mario C, Haase J, Ozaki Y, Linker DT, de Feyter PJ, Roelandt JRTC, Serruys PW. Significance of automated stenosis detection during quantitative angiography: insights gained from intracoronary ultrasound. *Circulation* 1996;94:966–972.
2. Stiel GM, Stiel LSG, Schofer J, Donath K, Mathey DG. Impact of compen-

satory enlargement of atherosclerotic coronary arteries on angiographic assessment of coronary artery disease. *Circulation* 1989;80:1603–1609.
3. Hermiller JB, Tenaglia AN, Kisslo KB, Phillips HR, Bashore TM, Stack RS, Davidson CJ. In vivo validation of compensatory enlargement of atherosclerotic coronary arteries. *Am J Cardiol* 1993;71:665–668.
4. Ge J, Erbel R, Zamorano J, Koch L, Kearney P, Gorge G, Gerber T, Meyer J. Coronary artery remodeling in atherosclerotic disease: an intravascular ultrasonic study in vivo. *Coron Artery Dis* 1993;4:981–986.
5. Gerber TC, Erbel R, Gorge G, Ge J, Rupprecht HJ, Meyer J. Extent of atherosclerosis and remodeling of the left main coronary artery determined by intravascular ultrasound. *Am J Cardiol* 1994;73:666–671.
6. Glagov S, Weisenberg E, Zaris CK, Stankunavicius R, Koletis GJ. Compensatory enlargement of human atherosclerotic coronary arteries. *N Engl J Med* 1987;316:1371–1375.
7. Fitzgerald PJ, St. Goar FG, Connolly AJ, Pinto FJ, Billingham ME, Popp RL, Yock PG. Intravascular ultrasound imaging of coronary arteries: is three layers the norm? *Circulation* 1992;86:154–158.
8. Mintz GS, Painter JA, Pichard AD, Kent KM, Satler LF, Popma JJ, Chuang YC, Bucher TA, Sokolowicz LE, Leon MB. Atherosclerosis in angiographically "normal" coronary artery reference segments: an intravascular ultrasound study with clinical correlations. *J Am Coll Cardiol* 1995;25:1479–1485.
9. de Feyter PJ, Ozaki Y, Baptista J, Escaned J, Di Mario C, de Jaegere PPT, Serruys PW, Roelandt JRTC. Ischemia-related lesion characteristics in patients with stable or unstable angina: a study with intracoronary angioscopy and ultrasound. *Circulation* 1995;92:1408–1413.
10. von Birgelén C, van der Lugt A, Nicosia A, Mintz GS, Gussenhoven EJ, de Vrey E, Mallus MT, Roelandt JRTC, Serruys PW, de Feyter PJ. Computerized assessment of coronary lumen and atherosclerotic plaque dimensions in three-dimensional intravascular ultrasound correlated with histomorphometry. *Am J Cardiol* 1996;78:1202–1209.
11. McPherson DD, Sima SJ, Hiratzka LF, Thorpe L, Armstrong ML, Marcus ML, Kerber RE. Coronary artery remodeling studied by high-frequency epicardial echocardiography: an early compensatory mechanism in patients with obstructive coronary atherosclerosis. *J Am Coll Cardiol* 1991;17:79–86.
12. Nishioka T, Luo H, Eigler NL, Berglund H, Kim CJ, Siegel RJ. Contribution of inadequate compensatory enlargement to development of human coronary artery stenosis: an in vivo intravascular ultrasound study. *J Am Coll Cardiol* 1996;27:1571–1576.
13. Wong CB, Porter TR, Xie F, Deligonul U. Segmental analysis of coronary arteries with equivalent plaque burden by intravascular ultrasound in patients with and without angiographically significant coronary artery disease. *Am J Cardiol* 1995;76:598–601.
14. Losordo DW, Rosenfield K, Kaufman J, Pieczek A, Isner JM. Focal compensatory enlargement of human arteries in response to progressive atherosclerosis: in vivo documentation using intravascular ultrasound. *Circulation* 1994; 89:2570–2577.
15. Pasterkamp G, Wensing PJW, Post MJ, Hillen B, Mali WPTM, Borst C. Paradoxical arterial wall shrinkage may contribute to luminal narrowing of human atherosclerotic femoral arteries. *Circulation* 1995;91:1444–1449.
16. Pasterkamp G, Borst C, Post MJ, Mali WPTM, Wensing PJW, Gussenhoven EJ, Hillen B. Atherosclerotic arterial remodeling in the superficial femoral artery: individual variation in local compensatory enlargement response. *Circulation* 1996;93:1818–1825.
17. Mintz GS, Kent KM, Pichard AD, Satler LF, Popma JJ, Leon MB. Contribution of inadequate arterial remodeling to the development of focal coronary artery stenoses: an intravascular ultrasound study. *Circulation* 1997;95:1791–1798.
18. von Birgelen C, Di Mario C, Serruys PW. Structural and functional characterization of an intermediate stenosis with intracoronary ultrasound: a case of "reverse Glagovian modeling". *Am Heart J* 1996;132:694–696.
19. Hermiller JB, Buller CE, Tenaglia AN, Kisslo KB, Phillips HR, Bashore TM, Stack RS, Davidson CJ. Unrecognized left main coronary artery disease in patients undergoing interventional procedures. *Am J Cardiol* 1993;71:173–176.
20. Ge J, Liu F, Gorge G, Haude M, Baumgart D, Erbel R. Angiographically "silent" plaque in the left main coronary artery detected by intravascular ultrasound. *Coron Artery Dis* 1995;6:805–810.
21. Lim JS, Proudfit WL, Sones FM Jr. Left main coronary arterial obstruction: long-term follow-up of 141 non-surgical cases. *Am J Cardiol* 1975;36:131–135.
22. Bulkley BH, Roberts WC. Atherosclerotic narrowing of the left main coronary artery. Necropsy analysis of 152 patients with fatal coronary heart disease and varying degrees of left main narrowing. *Circulation* 1976;55:823–828.
23. Conti CR, Selby JH, Christie LG, Pepine CJ, Curry RC Jr, Nichols WW, Conetta DG, Feldman RL, Mehta J, Alexander JA. Left main coronary artery stenosis: clinical spectrum, pathophysiology, and management. *Prog Cardiovasc Dis* 1979;22:73–106.
24. Isner JM, Kishel J, Kent KM, Ronan JA, Ross AM, Roberts WC. Accuracy of angiographic determination of left main coronary arterial narrowing: angiographic-histologic correlative analysis in 28 patients. *Circulation* 1981;63:1056–1064.
25. Bergelson BA, Tommaso CL. Left main coronary artery disease: assessment, diagnosis, and therapy. *Am Heart J* 1995;129:350–359.
26. Hodgson J McB, Graham SP, Savakus AD, Dame SG, Stephens DN, Dhillon PS, Brands D, Sheehan H, Eberle MJ. Clinical percutaneous imaging of coronary anatomy using an over-the-wire ultrasound catheter system. *Int J Cardiac Imaging* 1989;4:186–193.
27. Mallery JA, Tobis JM, Griffith J, Gessert J, McRae M, Moussabeck O, Bessen M, Moriuchi M, Henry WL. Assessment of normal and atherosclerotic arterial wall thickness with an intravascular ultrasound imaging catheter. *Am Heart J* 1990;119:1392–1400.
28. Gussenhoven EJ, Gieselschap JH, van Lankeren W, Posthuma DJ, Aad van der Lugt. Remodeling of atherosclerotic coronary arteries assessed with intravascular ultrasound in vitro. *Am J Cardiol* 1997;79:699–702.

SUMMARY AND CONCLUSIONS

Summary

Three-dimensional (3D) intravascular ultrasound (IVUS) systems provide techniques for automated quantitative analysis of relatively large image sequences. This approach has the potential to reduce the subjectivity of manual boundary tracing and to facilitate volumetric IVUS measurements. In most studies (Chapters 1–4 and 7–11), a 3D *contour detection* system was used, which detects both the lumen and external vascular boundaries based on the application of a minimum cost algorithm. In Chapters 5 and 6, an *acoustic quantification* system was applied, which detects the lumen only, based on the application of an algorithm for statistical pattern recognition.

The thesis sheds a light on numerous studies with these quantitative 3D IVUS systems, performed at the Thoraxcenter and Erasmus University Rotterdam. Aim of this work was (1) to validate the method (Part I) and (2) to use the technique to gain further insights into the mechanisms of coronary atherosclerosis and percutaneous catheter-based coronary interventions, such as stent implantation and directional coronary atherectomy (Part II).

Chapter 1 reports on the in vitro validation of 3D IVUS *contour detection* in atherosclerotic human coronary arteries. Cross-sectional area and volume measurements by 3D IVUS agreed well with the results obtained by manual tracing, showing low between-method differences with low standard deviations (cross-sectional areas: ≤6.2%, volumes: ≤4.3%) and high correlation coefficients (r≥0.97). The 3D IVUS measurements also correlated well with the histomorphometric data (r≥0.80).

Chapter 2 presents a validation study in a tubular phantom with segments of various luminal dimensions. The 3D IVUS *contour detection* showed good agreement and high correlations with the true values. In addition, this chapter reports on the measurement variability of analyzing clinical 3D image sequences from continuous motorized transducer pullbacks, which was found to be low (cross-sectional areas: ≤10.8%, volumes: <2.8%). However, in this study, IVUS sequences of coronary segments with excessive cyclic movement were not considered for analysis, as the systolic-diastolic saw-shaped image artifacts on the longitudinally reconstructed sections hindered the automated contour detection.

Chapter 3 describes a novel ECG-gated approach. As systolic-diastolic changes in vascular dimensions and the cyclic movement of the IVUS catheter may cause imaging artifacts, a dedicated ECG-triggered pullback device was developed. In all 28 humans, ECG-gated image acquisition was successfully performed (within 3.9±1.5min) and well tolerated. There was an excellent agreement between automated *contour detection* with conventional manual measurements on 200 randomly chosen IVUS images (differences ≤1.6% with SD ≤9.1%). Although the coronary segments in this study were non-selected and included calcified portions and some sidebranches, 3D contour analyses of the ECG-gated image sets showed a low measurement variability (for cross-sectional area measurements ≤7.2%), which was considerably lower than that reported for a study with non-gated 3D IVUS (Chapter 2). Volumetric measurements showed a particularly low measurement variability (≤3.2%), which reflects an averaging of the differences of the cross-sectional area measurements.

Chapter 4 reports the impact of different sample spacings (distance along vessel's axis between two image slices) on volumetric measurements, based on the calculation by Simpson's rule. In coronary segments with mild-to-moderate atherosclerosis the width of the sample spacing had a relatively small but significant impact on the variability of volumetric IVUS measurements. Measurement variability of plaque volume for instance increased by 3%, when a sample spacing of 0.2mm was replaced by a sample spacing of 1mm. These findings should be considered, particularly when addressing with IVUS volumetric changes that are assumed small, such as those expected in studies of the progression and regression of atherosclerosis.

Chapter 5 compares in vivo measurements of the minimal luminal area of 38 stents, as provided by 3D IVUS (*acoustic quantification*), two-dimensional (2D) IVUS, and geometric and densitometric quantitative coronary angiography. Calcifications sometimes impaired automated lumen detection by 3D IVUS. The 2D IVUS measurements were slightly larger than those obtained by 3D IVUS, which may partly have resulted from a misinterpretation of slow blood flow near the vessel wall by the computer algorithm. Both IVUS measurements were significantly larger than the angiographic data. Nevertheless, significant correlations were found between all four techniques ($r = 0.58–0.87$). High correlation between videodensitometry and IVUS data suggests a particular potential for videodensitometry.

Chapter 6 reports on a series of on-line observations with 3D (*acoustic quantification*) and 2D IVUS after successful angiography-guided implantation of 20 Wallstents and 20 Palmaz-Schatz stents. Insights with IVUS into the acute result of coronary stenting showed evidence of significant differences between short (14.3± 3.3mm) balloon-expandable Palmaz-Schatz stent and long (35.1±7.7 mm) self-expandable Wallstent. Although angiographic results and visual assessment of the IVUS examination suggested a good outcome in both stent designs, only few Wallstents reached a stent-reference lumen area ratio (= minimal stent area divided by average reference area) ≥0.8. The lower values of this ratio in Wallstents are most likely to be caused by vessel tapering, suggesting that this criterion, which had been derived from experience with the Palmaz-Schatz stent, may not be suitable for assessing the adequacy of relatively long stents such as the Wallstents.

Chapter 7 presents a study with ECG-gated IVUS image acquisition and 3D *contour detection* on-line after coronary stenting (34 stents). The study was performed to evaluate the feasibility and reliability of this diagnostic approach in this particular clinical setting. ECG-gated image acquisition was successfully performed in all patients to allow on-line 3D analysis within 8.7± 0.6min. Analyzing the luminal dimensions along an entire stented segment using 3D IVUS was not only feasible, but also provided more accurate results than conventional manual analysis on 2D video-images, recorded during continuous pullbacks. The conventional approach significantly overestimated the minimal stent lumen area in comparison with both on-line 3D analysis and off-line 3D re-analysis ($p<0.005$). In addition, by both on-line and off-line 3D IVUS analyses, 14 stents (41%) failed to meet a predefined ratio of stent expansion, however, only half of them ($n=7$) were detected by the conventional 2D analysis ($p<0.02$). The overestimation of the minimal stent area by conventional 2D analysis may have most probably resulted from performing the measurements slightly proximal or distal to the site of the true minimal

lumen.

Chapter 8 reports on 15 "*Magic*" Wallstents (good radiographic visibility), which were implanted following a strategy of stent oversizing and subsequent adjunct high-pressure balloon inflations. Between post-intervention and follow-up examination, quantitative coronary angiography showed an increase in mean stent diameter from 3.7±0.4mm to 4.2±0.4mm ($p<0.0001$). Follow-up 3D IVUS (contour detection) examination demonstrated that 52±18% of the stent volume was filled by neointimal ingrowth; neointimal volume/cm stent length was 64±22mm^3. Late stent self-expansion assisted in accommodating the neointimal proliferation, however it also showed a significant relation with the extent of in-stent neointimal ingrowth. Beneficial and disadvantageous effects of the late stent expansion appear to be balanced, as a relation with late lumen loss or follow-up lumen dimensions was not found to be present.

Chapter 9 reports on an intermediate coronary lesion, in which the vessel area at the smallest lumen site (as measured by 3D IVUS *contour detection*) was smaller than that at the distal reference site. Angioplasty was deferred, because of a normal distal coronary flow reserve, as measured with a 0.014-inch Doppler guide wire. This case report is the first 3D IVUS characterization of a lesion with inadequate compensatory enlargement (i.e. "reverse Glagovian modeling") ever reported.

Chapter 10 addresses with 3D IVUS (*contour detection*) the question, whether lesions with and without inadequate compensatory enlargement show differences in volumetric lesion characteristics. The results of this study were particularly interesting in the light of recent criticism, arguing that observation of lesions with inadequate compensatory enlargement with conventional 2D IVUS might result from local vasospasm or vessel collapse, induced by the insertion of the IVUS imaging catheter itself. In a series of 35 patients, treated by catheter-based coronary interventions, 15 lesions showed inadequate compensatory enlargement (vessel area of the minimum lumen site < distal reference). Lesions with inadequate compensatory enlargement differed significantly from the rest of the lesions, as both plaque and vessel volumes of lesions with inadequate compensatory enlargement were significantly smaller ($p<0.05$).

Chapter 11 evaluates whether differences in the preintervention remodeling state, as examined with quantitative 3D IVUS (*contour detection*), may have implications for the long-term lumen dimensions following successful directional coronary atherectomy. For lesions with ($n=16$) and without ($n=30$) inadequate vascular enlargement, there was no difference in both preintervention and postintervention quantitative angiographic data and IVUS lumen dimensions. However, quantitative angiography at 6 months follow-up revealed smaller minimal lumen diameters ($p<0.03$) and reference lumen diameters ($p<0.02$) in lesions with inadequate compensatory enlargement prior to the intervention. Thus, lesions with inadequate compensatory enlargement appear to have less favorable lumen dimensions after directional coronary atherectomy procedures, despite primary angiographic success.

Chapter 12 shows the limitations of quantitative angiography with regards to the assessment of atherosclerotic plaque dimensions during the progression and regression of coronary atherosclerosis. In addition, the potential role of IVUS and the advantages of quantitative 3D IVUS and plaque volume measurements are discussed.

Chapter 13 summarizes the main technical aspects of 3D IVUS and reports on advantages and individual limitations of various 3D IVUS systems. In addition, technique and potential of dynamic 3D imaging are explained. Currently, curved vessel segments are straightened out by most quantitative 3D IVUS systems ("linear 3D systems"), but recent developments permit computerized measurements in real spatial 3D reconstructions.

Chapter 14 demonstrates that quantitative 3D IVUS is in some settings not required or even not useful. In this study, 3D IVUS would indeed not have been helpful, as both left main stems and plaque formations examined were relatively short. Conventional two-dimensional IVUS was used to obtain new insights into vascular remodeling in response to left main atherosclerosis, which was examined in 107 left main coronary arteries. The IVUS data suggest that lumen dimensions may not be preserved, even if plaque occupies no more than 20% to 40% of the vessel area. Thus, there is more variation in the remodeling response during earlier stages of plaque accumulation than is commonly suggested.

In conclusion, quantitative 3D IVUS is a feasible approach that permits a reliable and reproducible analysis of the luminal and vascular dimensions along an entire coronary segment. The studies reported in this thesis clearly indicate that quantitative 3D IVUS can be remarkably helpful to gain further insights into the mechanisms of both coronary atherosclerosis and catheter-based coronary interventions. Particularly in combination with ECG-gated image acquisition, quantitative 3D IVUS also has the potential to gain clinical importance and become a routine technique.

SAMENVATTING EN CONCLUSIES

Samenvatting

Drie-dimensionele intravasculaire ultrageluid systemen verschaffen de techniek voor de geautomatiseerde quantitatieve analyse van relatief lange beeld sequenties. Deze benadering biedt de mogelijkheid om de subjectiviteit bij handmatige contourtekening te reduceren en om de volumetrische IVUS metingen te vergemakkelijken. Bij de meeste studies (zie de hoofdstukken 1-4 en 7-11) werd een 3D *contour detectie* systeem gebruikt, dat zowel de contouren van het lumen als ook de externe vasculaire grenzen vaststelt, gebaseerd op de toepassing van een minimum cost algoritme. In hoofdstuk 5 en 6 werd een *acoustisch quantificatie* systeem gebruikt dat slechts het lumen opspoort, gebaseerd op het gebruik van een algoritme voor statistische patroon herkenning.

De thesis belicht talrijke studies die gebruik maken van quantitatieve 3D IVUS, die uitgevoerd werden in het Thoraxcentrum en in de Erasmus Universiteit te Rotterdam. Het doel van de werkzaamheden was (1) de methode te valideren (deel 1) en (2) om met behulp van deze techniek verdere inzichten te verkrijgen in de mechanismen van atherosclerose in de coronairen en in die van de interventies in de coronairen door middel van percutane catheterisatie zoals stentimplantatie en directionele coronaire atherectomie (deel 2).

Hoofdstuk 1 geeft de in vitro validatie weer van 3D IVUS *contour detectie* in sclerotische menselijke coronairarteriëen. Dwarsdoorsnede metingen op doorsnede plaatjes en volume metingen door middel van 3D IVUS komen goed overeen met de resultaten die verkregen worden bij handmatig contour tekenen en laten daarbij kleine verschillen tussen de methoden onderling zien met kleine standaard afwijkingen (cross-sectional area: ≤6.2%, volumina: ≤ 4.3%) en hoge correlatie coëfficienten (r≥0.97). De 3D IVUS metingen correleren tevens goed met de histomorphometrische data (r≥0.80).

Hoofdstuk 2 geeft een validerende studie weer in een tubulair fantoom met segmenten van verschillende luminaire dimensies. De 3D IVUS *contour detectie* laat duidelijk een goede overeenkomst en een hoge correlatie zien tussen de reëele waarden. Daarnaast wordt in dit hoofdstuk de variabiliteit in de metingen tussen enerzijds de analyse van klinische 3D beeld sequenties en anderzijds de continue gemotoriseerde transducer pullbacks beschreven. Deze variabiliteit is laag (cross-sectional areas: ≤10.8%, volumes <2.8%). In deze studie zijn de IVUS sequenties van de coronaire segmenten met excessieve cyclische bewegingen echter niet geschikt bevonden voor analyse, omdat de in de systolische en diastolische fase ontstane zaagtandachtig uitziende beeldartefacten in de longitudinaal gereconstrueerde secties de automatisch contour detectie bemoeilijkten.

Hoofdstuk 3 beschrijft een nieuwe ECG-getriggerde benadering. Omdat de systolische-diastolische veranderingen in de vasculaire afmetingen enerzijds en de cyclische beweging van de IVUS-catheter anderzijds beeld artefacten kunnen veroorzaken, werd een ECG-getriggerde pullback device ontwikkeld. Bij alle 28 patienten werden met succes ECG-getriggerde beelden verkregen (binnen 3.9±1.5min), zonder dat de patienten klachten kregen. Er was een zeer goede overeenstemming tussen de geautomatiseerde *contour detectie* en de conventionele, manueel verkregen metingen bij 200 gerandomiseerd gekozen IVUS beelden (verschillen ≤1.6% met

SD ≤9.1%). Hoewel de coronaire segmenten in deze studie niet geselecteerd waren en zowel gecalcificeerde delen als ook enkele zijtakken includeerde, lieten de 3D contour analyses met ECG-getriggerde beelden een kleine variabiliteit in de metingen zien (voor cross-sectional area metingen ≤7.2%), die beduidend lager is in vergelijking met de studie met niet-getriggerde 3D IVUS (hoofdstuk 2). Volumetrische metingen lieten een bijzonder lage variabiliteit in de metingen zien (≤3.2%), hetgeen een middeling van de verschillen van de dwarsdoorsneden cross-sectional area metingen weerspiegelt.

Hoofdstuk 4 geeft de impact weer van verschillende sample spacings (afstand tussen twee plaatjes langs de as van het vat) die gebaseerd zijn op de berekening volgens
Simpson's rule. In coronaire segmenten met geringe tot matige atherosclerose had de breedte van de sample spacing een relatief kleine, maar significante impact op de variabiliteit in de volumetrische IVUS metingen. De variabiliteit in de metingen van plaque volume nam bijvoorbeeld met 3% toe, op het moment dat een sample spacing van 0.2mm werd vervangen door een sample spacing van 1mm. Deze bevindingen zouden in aanmerking genomen moeten worden met name als IVUS gebruikt wordt om volumetrische veranderingen op te sporen, waarvan wordt uitgegaan dat ze klein zijn, zoals bijvoorbeeld in studies naar de progressie en regressie van atherosclerose.

In **hoofdstuk 5** worden van de kleinste lumen area van 38 stents de in vivo metingen vergeleken, die vast werden gesteld door middel van 3D IVUS (*acoustisch quantificatie*), twee-dimensionele (2D) IVUS en door geometrische en densitometrische quantitatieve coronair angiografie. Calcificaties belemmerden soms de automatische lumen detectie door 3D IVUS. De resultaten van de metingen met 2D IVUS waren weinig groter dan die verkregen door 3D IVUS, hetgeen voor een deel mogelijk het gevolg was van de misinterpretatie door het computer algoritme van de trage bloedstroom vlak bij de vaatwand. De metingen met 2D en 3D IVUS waren significant groter dan de angiografische data. Niettemin werden significante correlaties gevonden tussen alle vier de technieken (r=0.58–0.87). De hoge correlatie tussen videodensitometrie en de IVUS data suggereren een bijzondere potentieel voor videodensitometrie.

Hoofdstuk 6 doet verslag van een serie on-line observaties met 3D (*acoustisch quantificatie*) en 2D IVUS na de succesvolle implantatie van 20 Wallstents en 20 Palmaz-Schatz stents met behulp van slechts angiografie. Inzichten met IVUS in het acute resultaat van stenting in de coronair getuigden van significante verschillen tussen korte (14.3±3.3mm) balloon expandable Palmaz-Schatz stents en lange (35.1±7.7mm) self-expandable Wallstents. Hoewel angiografische resultaten en visuele inschattingen van het IVUS resultaat wijzen op een goede uitkomst bij beide stenttypen, bereikten maar weinig Wallstents een stent-reference lumen area ratio (= minimal stent area gedeeld door gemiddelde reference area) ≥0.8. De lagere waarden van deze ratio bij de Wallstents worden waarschijnlijk veroorzaakt door vessel tapering, wijzend op het feit dat deze berekende parameter, die verkregen werd uit ervaringen met de Palmaz-Schatz stent, niet geschikt zou zijn om de adequaatheid vast te stellen van relatief lange stents zoals de Wallstents.

Hoofdstuk 7 beschrijft een studie met ECG-getriggerde IVUS beeld opname en on-line 3D *contour detectie* na coronaire stenting (34 stents). De studie werd gedaan om de uitvoerbaarheid en de betrouwbaarheid van deze diagnostische be-

nadering in deze bijzondere klinische setting te onderzoeken. ECG-getriggerde beeld opnamen om on-line 3D analyse binnen 8.7±0.6min mogelijk te maken werden bij alle patienten met succes verkregen. Het analyseren van de lumen dimensies over de lengte van een geheel gestent segment met gebruik van 3D IVUS was niet alleen goed uitvoerbaar, maar het leverde ook meer accurate resultaten op dan bij analyses met gebruik van de conventionele handmatige manier met 2D videobeelden, opgenomen tijdens het continu terugtrekken van de IVUS catheter. Bij de conventionele aanpak werden de minimale stent lumen area's significant overschat in vergelijking met zowel de on-line 3D analyses als ook met de off-line
3D re-analyses ($p<0.005$). Bij zowel de on-line als ook bij de off-line 3D IVUS analyses bereikten bovendien 14 stents (41%) niet een tevoren vastgestelde ratio van stent expansie, echter slechts de helft van dit aantal (n=7) werd aangetoond door de conventionele 2D analyse ($p< 0.02$). De overschatting van de minimal stent area bij de conventionele 2D analyse is waarschijnlijk het gevolg van het iets te proximaal dan wel te distaal meten ten opzichte van de plaats van het echte minimale lumen.

Hoofdstuk 8 doet verslag van 15 "Magic" Wallstents (goede radiografische zichtbaarheid), die geïmplanteerd werden volgens de strategie van stent oversizing gevolgd door ballon inflaties met hoge drukken. Tussen post-interventie en follow-up onderzoek liet quantitatieve coronair angiografie een toename van de gemiddelde stent diameter zien van 3.7±0.4mm tot 4.2±0.4mm ($p<0.0001$). Follow-up onderzoek met 3D IVUS (*contour detectie*) toonde aan dat 52±18% van het stent volume door neointimale groei werd gevuld; het neointimale volume/cm stent bedroeg 64±22 mm^3. Late zelf-expansie van de stent droeg bij aan de accomodatie van neointimale proliferatie, maar toonde ook een significante relatie aan met de mate van neointimale ingroei in de stent. Voor- en nadelige effekten van late stent expansie leken in evenwicht te zijn, aangezien een relatie met het late verlies van lumen of met de lumen dimensies tijdens follow-up niet aangetoond kon worden.

Hoofdstuk 9 beschrijft een intermediaire coronaire laesie, waarin de vessel area ter plaatse van het smalste deel van het lumen (gemeten met 3D IVUS *contour detectie*) kleiner was dan dat ter plaatse van het distale referentiepunt. Angioplastiek was niet van toepassing omdat er een normale distale coronaire flow reserve was, hetgeen gemeten werd met 0.014-inch Doppler guide wire. Dit case report is het eerste ooit gepubliceerd dat met behulp van 3D IVUS een laesie beschrijft met een inadequate compenserende vergroting ("reverse Glagovian modeling").

Hoofdstuk 10 onderzoekt met het gebruik van 3D IVUS (*contour detectie*) de vraag of laesies met en zonder inadequate compenserende vergroting verschillend zijn wat betreft hun volumetrische eigenschappen. De resultaten van deze studie waren met name interessant in het licht van de recente kritieken, die beargumenteren dat de observatie van laesies met inadequate compenserende vergroting met behulp van de conventionele 2D IVUS mogelijk het resultaat zijn van locale vaatspasmen of van
het collaberen van de vaten, veroorzaakt door het inbrengen van de IVUS catheter. In een serie van 35 patienten die behandeld werden door coronaire interventies door middel van percutane angioplastiek, lieten 15 laesies een inadequate compenserende vergroting zien (vessel area ter plaatse van het kleinste lumen < distale referentie). Laesies met een inadequate compenserende vergroting verschilden significant van de overige

laesies, in die zin dat zowel plaque als vaatvolume van de laesies met inadequate compenserende vergroting significant kleiner waren ($p<0.05$).

In **hoofdstuk 11** wordt geëvalueerd of verschillen in de toestand van de vat remodulering voor interventie, bekeken met quantitatieve 3D IVUS (*contour detectie*), van invloed zouden kunnen zijn op de dimensies van het lumen op lange termijn na succesvolle directionele coronaire atherectomie. Bij laesies met (n=16) en zonder (n=30) inadequate vasculaire vergroting werd er geen verschil gevonden in zowel de pre- als ook in de postinterventionele quantitatieve angiografische gegevens en in de IVUS lumen dimensies. Quantitatieve angiografie in de follow-up na 6 maanden toonde echter kleinere minimal lumen diameters ($p<0.03$) en reference lumen diameters ($p<0.02$) in laesies met inadequate compenserende vergroting die vastgesteld werd vóór de interventie. Laesies met inadequate compenserende vergroting blijken dus minder goede lumen dimensies te hebben na procedures met directionele coronaire atherectomie, ondanks aanvankelijk angiografisch succes.

Hoofdstuk 12 geeft de limitaties van quantitatieve angiografie weer met betrekking tot de beoordeling van atherosclerotische plaque dimensies tijdens de progressie en regressie van coronaire atherosclerose. Daarnaast worden de potentiele rol van IVUS, de voordelen van quantitatieve 3D IVUS en de plaque volume metingen besproken.

In **hoofdstuk 13** worden de belangrijkste technische aspekten van 3D IVUS samengevat en wordt er verslag uitgebracht van de voordelen en de individuele beperkingen van verschillende 3D IVUS systemen. Daarnaast worden techniek en mogelijkheden van dynamische 3D IVUS beeldverwerking uitgelegd. Momenteel worden gekronkelde stukken van een vat bij de meeste quantitatieve 3D IVUS systemen uitgerekt ("lineaire 3D systemen"), maar recente ontwikkelingen maken computer metingen mogelijk in reeele ruimtelijke 3D reconstructies.

Hoofdstuk 14 laat zien dat quantitatieve 3D IVUS in sommige settings niet nodig is of zelfs niet nuttig is. In deze studie zou het gebruik van 3D IVUS inderdaad niet geholpen hebben omdat de linker hoofdstam en de plaque formaties die bekeken werden relatief kort waren. Conventionele 2D IVUS werd gebruikt om nieuwe inzichten te krijgen in vasculaire remodeling als reaktie op atherosclerose in de linker hoofdstam, hetgeen werd bekeken in 107 coronairen. De IVUS data suggereren dat lumen dimensies verkleind worden, zelfs als niet meer dan 20-40% van de vessel area door plaque wordt ingenomen. Er is dus meer variatie in de "remodeling response" tijdens vroegere fases van plaque accumulatie dan algemeen wordt aangenomen.

De conclusie is dat quantitatieve 3D IVUS een praktische techniek is, die een betrouwbare en reproduceerbare analyse mogelijk maakt van de luminale en vasculaire dimensies van een geheel coronair segment. De studies die in deze thesis aangehaald zijn geven duidelijk aan dat quantitatieve 3D IVUS opmerkelijk behulpzaam kan zijn bij het verkrijgen van verdere inzichten in de mechanismen van zowel coronaire atherosclerose als ook van coronaire catheter-interventies. Vooral in combinatie met ECG-getriggerde beeld opnamen heeft quantitatieve 3D IVUS ook het potentieel om klinisch aan importantie te winnen en een routinematige techniek te worden.

ACKNOWLEDGEMENTS

Acknowledgements

The close cooperation with the promotor of this thesis, *Professor Dr. Patrick W. Serruys*, who was my teacher and mentor throughout a period of more than three years, has been a privilege and a continuous stimulation of my research activities. He anticipated the potential of computerized measurements in three-dimensional intravascular ultrasound image sets and continuously supported the research work performed in this field. I am deeply grateful to him for providing me the facilities and substantial freedom that allowed developing, coordinating, and performing the research projects presented in this thesis. In clinical training, it was a pleasure to watch him and to assist his skillful work. Retrospectively, it emerges to be most significant to have learned how he approaches different clinical challenges and how he solves individual problems. After almost one and a half year of interventional work outside the Thoraxcenter, I assert that considering "how Patrick would approach a particular problem" frequently guides my work and clinical decision-making, particularly in complex coronary interventions.

I have thoroughly enjoyed and will certainly miss the expert (often humorous) comments, the constructive criticism and suggestions, and the company of *Dr. Pim J. de Feyter*, who is the co-promotor of this thesis. He taught me to keep things simple and understandable. I agree with his view that one should think straight ahead and remain self-critical in both, research and clinical work. I am very grateful for putting the imaging-oriented studies into clinical perspective. In addition, it is thanks to him that my research activities expanded from the evaluation of the results of catheter-based coronary interventions to assessing the distribution of atherosclerosis and the mechanisms of plaque accumulation. Thanks for training me in coronary interventions, helping me to gradually improve my operative skill, and teaching me to distinguish between clinically important and unimportant issues. I am very grateful for our friendship, which arose during the years of cooperation.

I am grateful to *Professor Dr. Jos R.T.C. Roelandt* for continuously supporting my research and clinical activities. His infectious enthusiasm for technical progress and three-dimensional ultrasound imaging in particular was remarkably stimulating. I enjoyed to work under his directorship at the Thoraxcenter with its high level of expertise and its possibility to cooperate with basic research laboratories and various clinical disciplines.

I am also grateful *to Professor Dr. Nicolaas Bom*, who invented a first real-time intravascular ultrasound catheter tip, for giving me the possibility to cooperate with him and his excellent team of the Laboratory of Experimental Echocardiography at the Erasmus University Rotterdam. Thanks for encouraging me to defend a thesis at the Erasmus University.

The stimulation and continued support of my mentor *Professor Dr. Raimund Erbel*, Director of the Department of Cardiology in the University Hospital Essen, should be particularly emphasized. He encouraged my interest in intravascular ultrasound imaging and established the base for research and clinical work. I am grateful to him for encouraging and supporting my application for a fellowship of the German Research Society (DFG), which meritoriously provided financial support. I enjoyed his kindness and warm-hear-

ted "welcome" when returning to Essen, and I am proud to work in his group. Thanks for everything.

I would like to thank *Professor Dr. J.R.T.C. Roelandt, Professor Dr. N. Bom,* and *Professor Dr. R. Erbel* for critically reviewing this thesis.

I would like to express gratitude to *Dr. Carlo Di Mario* for guiding me through my first year at the Thoraxcenter, giving me inspiration for my research activities, and teaching me both the advanced interpretation of IVUS images and the basics of how to prepare manuscripts and illustrations. At the time he left the Thoraxcenter and returned to Italy, I missed him not only as a colleague but also as a dear friend. He is certainly the most atypical Italian whom I ever met. I doubt that I may reach his "German-like" precision in planning his presentations. Thanks for teaching me.

It was a pleasure to work with *Dr. Wenguang Li,* a talented biomedical engineer and a great expert in field of computer-based image analysis. He gave me the chance to be the first user of his novel computerized system for the analysis of three-dimensional IVUS image sets and to provide my experience and reflections as contribution to its refinement.

I had the honor and privilege to work with *Dr. Gary S. Mintz* from the Washington Cardiology Center. It was certainly not a typical connection with a native English speaker to improve the style of some manuscript, but a true scientific cooperation with one of the most excellent experts of clinical research in cardiology. I am very grateful to him for teaching me how to thoroughly interpret the IVUS data and how to condense a manuscript in order to emphasize its most prominent messages.

It was a result of Gary's initiative that *Dr. Martin B. Leon* and *Dr. Jeffrey J. Popma* from Washington, as well as *Dr. Masakiyo Nobuyoshi* and *Dr. Takeshi Kimura* from the Kokura Memorial Hospital in Kitakyushu, Japan, shared their clinical data with me. I am extremely grateful to these colleagues for continuously supporting this project.

I am very grateful to *Nico Bruining* with whom I worked for several years. He dedicated huge effort into the development of a custom-designed ECG-triggered pullback device that permitted ECG-gated acquisition of IVUS images. His expert knowledge of the technical details and his experience with three-dimensional cardiac ultrasound imaging were greatly helpful, when applying ECG-gated IVUS in the clinical arena. In addition, it was a privilege and honor to assist Nico in his own projects, using the ECG-gated approach.

The support of *Evelyn A. de Vrey,* who analyzed a large series of IVUS runs with the automated three-dimensional contour detection system, was remarkable and should be underlined. Her infectious enthusiasm was like a fresh wind that gave a significant push to the project, which addressed atherosclerotic remodeling with the three-dimensional analysis system.

Dr. Sergei G. Airtian and *Dr. Robert Gil* performed most accurate quantitative angiographic and conventional IVUS analyses. I am very grateful to both of them.

I am grateful for the company and help of *Dr. Michael J.B. Kutryk,* who for some time shared an office with me and checked the style of many manuscripts prior to submission.

I am very grateful to *Dr. David P. Foley* and

Dr. Wim J. van der Giessen, who both were very collegial and gave much support to the IVUS projects. Many thanks also for teaching me in the laboratory.

The expert technical understanding and knowledge of *Dr. Cornelis J. Slager* is exceptional (Cees is able to solve almost any technical problem). I am extremely grateful to him and *Hans C.H. Schuurbiers,* who helped me when performing the in-vitro validation of the three-dimensional contour analysis system. It was a real pleasure to work with both of them. Thanks for our nice discussions.

I am indebted to both *Dr. Elma J. Gussenhoven* and *Dr. Aad van der Lugt,* who supported the histological validation of the three-dimensional contour detection system with their great experience of in-vitro IVUS and anatomical examinations. It was a privilege and a pleasure to assist them in some of their own projects. I really enjoyed our cooperation and our conversations (and coffee breaks).

I also would like to thank all *technicians, nurses, and secretaries of the catheterization laboratory* for their friendship and their patience during the IVUS runs, and *the crew of the computer group* for their technical support. I would like to emphasize the particular input of *Jurgen Ligthart* and his continued support in the catheterization lab. Many IVUS-projects of this thesis would have failed without his enthusiasm and help. He is certainly the most expert clinical IVUS technician, whom I ever met. I am very grateful to *Els Schoenmaker,* the manager of the cath lab, and to *Claudia Sprenger-de Rover, Trude Matlar, Laetitia Bautz,* and *Anja van Huuksloot* for many pleasant conversations and for frequently helping me in the "jungle of bureaucracy". The experience of *Jan Tuin* and *Maud van Nierop* was extremely helpful to obtain high-quality illustrations and slides. I would like to thank them for many years of continuous support.

The tutorship of *Marianne Eichholtz* in the process of this promotion was invaluable. I would like to express my gratitude for her friendly support.

I am grateful for the friendship, support, and collaboration of all *Dutch and international colleagues and researchers,* whom I met at the Thoraxcenter. Although I am not able to line-up all, I would like to mention *Dr. A.H.M.M. Balk (always a friendly word), Dr. A. Bianchi, Dr. A. den Boer (Mr. X-ray), Dr. E. Boursma, Dr. M. van den Brand, Dr. E. Camenzind, Dr. S. Carlier, Dr. F.J. ten Cate, Dr. E.I. Cespedes, F.C. von Egmond, Dr. A.A. Elhendy, Dr. J.N. Hamburger, A. Hartlooper, J. Honkoop, Dr. P. de Jaegere, Dr. N. de Jong, Dr. I. Kantzis, Dr. D. Keane (thanks for reviewing my first manuscript), Dr. M.J.M. Kofflard, Dr. R. Krams, Dr. C.T. Lancée (thanks for your key), Dr. K. Lehmann, E. van de Leur (thanks for your help with the validation work), Dr. M.T. Mallus, F. Mastik, M.-A. Morel, Dr. H. Mudra, Dr. A. Nicosia, Dr. Y. Ozaki, Dr. G. Pasquetto, Dr. F. Prati, Dr. N. van der Putten, Dr. B. Reimers, Dr. P. Ruygrok (thanks for your advice), Dr. A.F.W. van der Steen, E.J.M. van Swijndregt, Dr. S.H.K. The, Dr. V.A.W.M. Umans (thanks for supporting my first paper), Dr. T. Violaris, and J.J. Wentzel.*

I apologize for being unable to recall *all people who supported me and my work.* Many thanks to all of them.

Last but not least, I would like to express my gratitude to my precious wife *Gabriëlle* and my dear *parents* for their great support and encouragement.

CURRICULUM VITAE

Curriculum Vitae

	09.03.1965	born in Aachen, Germany
School Education	1971 – 1984	in Heinsberg, Germany
	1984	Abitur (qualifying for University)
Medical School	1985 – 1992	Heinrich Heine Universität Düsseldorf, Germany; completed with the German Medical Licensure Examination
Medical Doctorate Thesis (Dr. med.)	1993	"Angiographic findings after invasive therapy of myocardial infarction"; thesis defended at the University Düsseldorf, Germany
Clinical Training	1992 – 1994	University Hospital Essen, Germany, Medical Clinic, Department of Cardiology (Director: Professor R. Erbel, MD)
	1994 – 1997	University Hospital Rotterdam-Dijkzigt, The Netherlands, Thoraxcenter, Department of Cardiology (Director: Professor J.R.T.C. Roelandt, MD, PhD)
	1997 –	University Hospital Essen, Germany, Medical Clinic, Department of Cardiology (Director: Professor R. Erbel, MD)
Fellowships and Grants	1989 – 1992	Grant of the National Study Donation (Studienstiftung des Deutschen Volkes), Bonn, Germany
	1994 – 1996	Fellowship of the German Research Society (Deutsche Forschugsgemeinschaft), Bonn, Germany

LIST OF PUBLICATIONS

Publications

Original Articles

1. Li W, **von Birgelen C**, Di Mario C, Boersma E, Gussenhoven WJ, van der Putten N, Bom N. Semi-automated contour detection for volumetric quantification of intracoronary ultrasound. *Computers in Cardiology* 1994; 277-280.

2. Ge J, Koch T, Görge G, Kearney P, Haude M, Baumgart D, **von Birgelen C**, Brennecke R, Meyer J, Erbel R. Reconstruction methods for 3D imaging and quantification of intracoronary ultrasound cross-sectional images using biplanar fluoroscopy. Initial experiences in vitro and in vivo. *Herz* 1995; 20:263-276.

3. Daul A, Hermes U, Schäfers RF, Wenzel R, **von Birgelen C**, Brodde OE. The beta-adrenoceptor subtypes mediating adrenaline- and dobutamine-induced blood pressure and heart rate changes in healthy volunteers. *Int J Clin Pharmacol Ther* 1995; 33:140-148.

4. Di Mario C, Gil R, Camenzind E, Ozaki Y, **von Birgelen C**, Umans V, de Jaegere P, de Feyter PJ, Roelandt JRTC, Serruys PW. Quantitative assessment with intracoronary ultrasound of the mechanisms of restenosis after percutaneous transluminal coronary angioplasty and directional coronary atherectomy. *Am J Cardiol* 1995; 75:772-777.

5. Umans VA, Baptista J, Di Mario C, **von Birgelen C**, de Jaegere P, de Feyter PJ, Serruys PW. Angiographic, ultrasonic and angioscopic assessment of the coronary artery wall and lumen area configuration after directional atherectomy: the mechanism revisited. *Am Heart J* 1995; 130:217-227.

6. **von Birgelen C**, Umans VA, Di Mario C, Keane D, Gil R, Prati F, de Feyter P, Serruys PW. Mechanism of high-speed rotational atherectomy and adjunctive balloon angioplasty revisited by quantitative coronary angiography: edge detection versus videodensitometry. *Am Heart J* 1995; 130:405-412.

7. Bruining N, **von Birgelen C**, Di Mario C, Prati F, Li W, Den Hood W, Patijn M, de Feyter PJ, Serruys PW, Roelandt JRTC. Dynamic three-dimensional reconstruction of ICUS images based on an ECG gated pull-back device. *Computers in Cardiology* 1995; 633-636.

8. Laban M, Oomen JA, Slager CJ, Wentzel JJ, Krams R, Schuurbiers JCH, den Boer A, **von Birgelen C**, Serruys PW, de Feyter PJ. ANGUS: A new approach to three-dimensional reconstruction of coronary vessels by combined use of angiography and intravascular ultrasound. *Computers in Cardiology* 1995; 325-328.

9. Prati F, Di Mario C, Gil R, **von Birgelen C**, Camenzind E, van Swijndregt WJM, de Feyter PJ, Serruys PW, Roelandt JRTC. Usefulness of on-line three-dimensional reconstruction of intracoronary ultrasound for guidance of stent deployment. *Am J Cardiol* 1996; 77:455-461.

10. Gil R, **von Birgelen C**, Prati F, Di Mario C, Ligthart J, Serruys PW. Usefulness of three-dimensional reconstruction for interpretation and quantitative analysis of intracoronary ultrasound during stent deployment. *Am J Cardiol* 1996; 77:761-764.

11. **von Birgelen C**, Gil R, Ruygrok P, Prati F, Di Mario C, van der Giessen WJ, de Feyter PJ, Serruys PW. Optimized expansion of the Wallstent compared to the Palmaz-Schatz stent: on-line observations with two- and three-dimensional intracoronary ultrasound after angiographic guidance. *Am Heart J* 1996; 131:1067-1075

12. **von Birgelen C**, Kutryk MJB, Gil R, Ozaki Y, Di Mario C, Roelandt JRTC, de Feyter PJ, Serruys PW. Quantification of the minimal luminal cross-sectional area after coronary stenting by two-dimensional and three-dimensional intravascular ultrasound versus edge detection and videodensitometry. *Am J Cardiol* 1996; 78:520-525.

13. Gil R, Di Mario C, Prati F, **von Birgelen C**, Ruygrok P, Roelandt JRTC, Serruys PW. Influence of plaque composition on mechnisms of percutaneous transluminal coronary balloon angioplasty

assessed by ultrasound imaging.
Am Heart J 1996; 131:591-597.

14. **von Birgelen C**, Di Mario C, Li W, Schuurbiers JHC, Slager CJ, de Feyter PJ, Roelandt JRTC, Serruys PW. Morphometric analysis in three-dimensional intracoronary ultrasound: an in-vitro and in-vivo study using a novel system for the contour detection of lumen and plaque.
Am Heart J 1996; 132:516-527.

15. **von Birgelen C**, van der Lugt A, Nicosia A, Mintz GS, Gussenhoven EJ, de Vrey E, Mallus MT, Roelandt JRTC, Serruys PW, de Feyter PJ. Computerized assessment of coronary lumen and atherosclerotic plaque dimensions in three-dimensional intravascular ultrasound correlated with histomorphometry.
Am J Cardiol 1996; 78:1202-1209.

16. Bruining N, **von Birgelen C**, Mallus M, de Feyter PJ, de Vrey E, Li W, Prati F, Serruys PW, Roelandt JRTC. ECG-gated ICUS image acquisition combined with a semi-automated contour detection provides accurate analysis of vessel dimensions.
Computers in Cardiology 1996; 53-56.

17. **von Birgelen C**, de Feyter PJ, de Vrey EA, Li W, Bruining N, Nicosia A, Roelandt JRTC, Serruys PW. Simpson's rule for the volumetric ultrasound assessment of atherosclerotic coronary arteries: a study with ECG-gated three-dimensional intravascular ultrasound.
Coron Artery Dis 1997; 8:363-369.

18. **von Birgelen C**, Mintz GS, Nicosia A, Foley DP, van der Giessen WJ, Bruining N, Airiian SG, Roelandt JRTC, de Feyter PJ, Serruys PW. Electrocardiogram-gated intravascular ultrasound image acquisition after coronary stent deployment facilitates on-line three-dimensional reconstruction and automated lumen quantification.
J Am Coll Cardiol 1997; 30:436-443.

19. Reimers B, Di Mario C, Pasquetto G, **von Birgelen C**, Gil R, van den Brand M, van der Giessen W, Foley D, Serruys PW. Long-term restenosis after multiple stent implantation: a quantitative angiographic study.
J Interven Cardiol 1997; 10:287-293.

20. **von Birgelen C**, de Vrey EA, Mintz GS, Nicosia A, Bruining N, Li W, Slager CJ, Roelandt JRTC, Serruys PW, de Feyter PJ. ECG-gated three-dimensional intravascular ultrasound: feasibility and reproducibility of an automated analysis of coronary lumen and atherosclerotic plaque dimensions in humans.
Circulation 1997; 96:2944-2952.

21. **von Birgelen C**, Airiian SG, Mintz GS, van der Giessen WJ, Foley DP, Roelandt JRTC, Serruys PW, de Feyter PJ. Variations of remodeling in response to left main atherosclerosis assessed with intravascular ultrasound in vivo.
Am J Cardiol 1997; 80:1408-1413.

22. van der Lugt A, Gussenhoven EJ, **von Birgelen C**, Tai JA, Pieterman H. Failure of intravascular ultrasound to predict dissection after balloon angioplasty by using plaque characteristics.
Am Heart J 1997; 134:1075-1081.

23. **von Birgelen C**, Mintz GS, de Vrey EA, de Feyter PJ, Kimura T, Popma JJ, Nobuyoshi M, Serruys PW, Leon MB. Successful directional atherectomy of de novo coronary lesions assessed with three-dimensional intravascular ultrasound and angiographic follow-up.
Am J Cardiol 1997; 80:1540-1545.

24. Nicosia A, **von Birgelen C**, Serruys PW, Roelandt JR, Giuffrida G. Three-dimensional reconstruction in intracoronary echography: a new system with automatic contour definition of ECG-gated image acquisition.
Cardiologia 1997; 42:1159-1164.

25. van der Lugt A, Hartlooper A, van Essen JA, Li W, **von Birgelen C**, Reiber JHC, Gussenhoven EJ. Reliability and reproducibility of automated contour analysis in intravascular ultrasound images of femoropopliteal arteries.
Ultrasound Med Biol 1998; 24:43-50.

26. Krams R, Kofflard MJM, Duncker DJ, **von Birgelen C**, Carlier S, Kliffen M, ten Cate FJ, Serruys PW. Decreased coronary flow reserve in hypertrophic cardiomyopathy is related to remodeling of the coronary microcirculation.
Circulation 1998; 97:230-233.

27. **von Birgelen C**, Mintz GS, de Vrey EA, Kimura T, Popma JJ, Airiian SG, Leon MB, Nobuyoshi M, Serruys PW, de Feyter PJ. Atherosclerotic coro-

nary lesions with inadequate compensatory enlargement have smaller plaque and vessel volumes: observations with three-dimensional intravascular ultrasound in vivo.
Heart 1998; 79:137-143.

28. Bruining N, **von Birgelen C**, de Feyter PJ, Ligthart J, Li W, de Vrey EA, Serruys PW, Roelandt JRTC. ECG-gated versus non-gated three-dimensional intracoronary ultrasound analysis: implications for volumetric measurements.
Cathet Cardiovasc Diagn 1998; 43: 254-260.

29. Bruining N, **von Birgelen C**, de Feyter PJ, Ligthart J, Serruys PW, Roelandt JRTC. Dynamic imaging of coronary stent structures: an ECG-gated three-dimensional intracoronary ultrasound study in humans.
Ultrasound Med Biol 1998; 24:631-637.

30. **von Birgelen C**, Airiian SG, de Feyter PJ, Foley DP, van der Giessen WJ, Serruys PW. Coronary Wallstents show significant late, post-procedural expansion despite implantation with adjunct high-pressure balloon inflations.
Am J Cardiol 1998; 82:129-134.

31. Bruining N, **von Birgelen C**, de Feyter PJ, Roelandt JRTC, Serruys PW. Ultrasound appearances of coronary stents as obtained by three-dimensional intracoronary ultrasound imaging in vitro.
J Invas Cardiol 1998; 10:332-338.

Review Articles and Editorials

32. Erbel R, Schön F, Leischik R, **von Birgelen C**, Zeppelini R. Atrial fibrillation: the value of transesophageal echocardiography.
Z Kardiol 1994; 83(Suppl 5):41-47.

33. Görge G, Haude M, **von Birgelen C**, Caspari G, Erbel R. Reperfusion therapy in acute myocardial infarction?
Dtsch med Wschr 1995; 120:375-82.

34. Erbel R, Ge J, Görge G, Kearney P, **von Birgelen C**, Schmermund A, Baumgart D, Brennecke R, Rupprecht HJ, Meyer J. Intravascular ultrasonography in coronary heart disease. Current aspects in the pathogenesis.
Dtsch med Wschr 1995; 120:847-54.

35. **von Birgelen C**, Erbel R, Di Mario C, Li W, Prati F, Ge J, Bruining N, Görge G, Slager CJ, Serruys PW, Roelandt JRTC. Three-dimensional reconstruction of coronary arteries with intravascular ultrasound.
Herz 1995; 20:277-289.

36. **von Birgelen C**, Di Mario C., van der Putten N., Li W., Gil R., Prati F., Ligthart J, Camenzind E, Ozaki Y, Serruys PW, Roelandt JRTC. Quantification in three-dimensional intracoronary ultrasound: importance of image acquisition and segmentation.
Cardiologie 1995; 2:67-72.

37. **von Birgelen C**, Slager CJ, Di Mario C, de Feyter PJ, Serruys PW. Volumetric intracoronary ultrasound: a new maximum confidence approach for the quantitative assessment of progression-regression of atherosclerosis?
Atherosclerosis 1995; 118 (Suppl.): S103-S113.

38. Di Mario, **von Birgelen C**, Prati F, Soni B, Li W, Bruining N, de Feyter PJ, Serruys PW, Roelandt JRTC. Three-dimensional reconstruction of two-dimensional intracoronary ultrasound: clinical or research tool?
Br Heart J 1995; 73(Suppl.2):26-32.

39. **von Birgelen C**, Di Mario C, Reimers B, Prati F, Bruining N, Gil R, Serruys PW, Roelandt JRTC. Three-dimensional intracoronary ultrasound imaging: methodology and clinical relevance for the assessment of coronary arteries and bypass grafts.
J Cardiovasc Surg 1996; 37:129-139.

40. Nicosia A, **von Birgelen C**, Di Mario C, Prati F, Mallus MT, Bruining N, de Feyter PJ, Serruys PW, Giuffrida G, Roelandt JRTC. Three-dimensional reconstruction in intracoronary echocardiography: the advantages, limits and future prospects.
Cardiologia 1996; 41:1165-1174.

41. **von Birgelen C**, Mintz GS, de Feyter PJ, Bruining N, Nicosia A, Di Mario C, Serruys PW, Roelandt JRTC. Reconstruction and quantification with three-dimensional intracoronary ultrasound: an update on techniques, challenges, and future directions.
Eur Heart J 1997; 18:1056-1067.

42. Prati F, Di Mario C, Gil R, Bruining N, Camenzind E, **von Birgelen C**, Serruys PW, Roelandt JRTC.

On-line three-dimensional intracoronary ultrasound for guidance of catheter based interventions.
G Ital Cardiol 1997; 27:123-132.

43. Di Mario C, Görge G, Peters R, Kearney P, Pinto F, Hausmann D, **von Birgelen C**, Columbo A, Erbel R, Mudra H, Roelandt J, Erbel R on behalf of the Study Group on Intracoronary Imaging of the Working Group of Coronary Circulation and of the Subgroup on Intravascular Ultrasound of the Working Group of Echocardiography of the European Society of Cardiology. Clinical application and image interpretation in intracoronary ultrasound.
Eur Heart J 1998; 19:207-229.

44. **von Birgelen C**, Kutryk MJB, Serruys PW. Three-dimensional intravascular ultrasound analysis of coronary stent deployment and in-stent neointimal volume: current clinical practice and the concepts of *TRAPIST, ERASER*, and *ITALICS*.
J Invas Cardiol 1998; 10:17-26.

Case Reports

45. **von Birgelen C**, Bug R, Drochner K, Görge G, Erbel R. Crushing retrosternal pain after physical exertion in a 33-year-old patient. True aneurysm of the ascending aorta with intramural hemorrhage: early stage of dissection with threatened rupture.
Med Klinik 1994; 89:81-85.

46. **von Birgelen C**, von Schönfeld J, Görge G, Fabry W, Layer P. Amebic liver abscess with hepatobronchial fistula.
Dtsch med Wschr 1994; 30:1034-1038.

47. Schappert T, Sadony V, Schön F, **von Birgelen C**, Zerkowski H-R, Erbel R. Diagnosis and therapeutic consequences of intramural aortic hematoma.
J Card Surg 1994; 9:508-515.

48. Prati F, Di Mario C, Hamburger JN, Gil R, **von Birgelen C**, Serruys PW. Perforation of a chronic total occlusion with a laser guidewire followed by multiple stent deployment: usefulness of three-dimensional intracoronary ultrasound guidance.
Am Heart J 1995; 130:1285-1289.

49. Reimers B, **von Birgelen C**, van der Giessen WJ, Serruys PW. A word of caution on optimizing stent deployment in calcified lesions: a case of acute coronary rupture with cardiac tamponade.
Am Heart J 1996; 131:192-194.

50. **von Birgelen C**, Di Mario C, Serruys PW. Structural and functional characterization of an intermediate stenosis with intracoronary ultrasound and Doppler: A case of "reverse Glagovian modeling".
Am Heart J 1996; 132:694-696.

51. Pasquetto G, Di Mario C, Bianchi A, **von Birgelen C**, Reimers B, Gil R, Serruys PW. Ultrasound-guided treatment of acute coronary stent thrombosis.
Am Heart J 1996; 132:1081-1084.

52. Nicosia A, van der Giessen WJ, Airiian SG, **von Birgelen C**, de Feyter PJ, Serruys PW. Is intravascular ultrasound after coronary stenting a safe procedure? Three cases of stent damage attributable to ICUS in a tantalum coil stent.
Cathet Cardiovasc Diagn 1997; 40: 265-270.

53. **von Birgelen C**, Haude M, Liu F, Ge J, Görge G, Welge D, Wieneke H, Baumgart D, Opherk D, Erbel R. Treatment of a coronary pseudoaneurysm by stent-graft implantation.
Dtsch med Wschr 1998; 123:418-422.

Bookchapters and Invited Reviews

54. **von Birgelen C**, Di Mario C, Li W, Prati F, Bom N, Roelandt JRTC, Serruy PW. Three-dimensional reconstruction of intracoronary ultrasound images: technical approaches, clinical applications, and current limitations in the assessment of vessel dimensions. In: Gotto AMJr, Lenfant C, Catapano AL, Paoletti R (eds.): *Multiple Risk Factors in Cardiovascular Disease: Vascular and Organ Protection*. Dordrecht: Kluwer Academic Publishers. 1995: 267-287.

55. **von Birgelen C**, Di Mario C, Ruygrok PN, Prati F, Li W, Ligthart J, Gil R, de Feyter PJ, Serruys PW, Roelandt JRTC. Assessment of atherosclerotic plaques and coronary interventions by intracoronary ultrasound.

Thoraxcenter Journal 1995; 7:19-26.

56. Di Mario C, Gil R, **von Birgelen C**, Piraino R, de Feyter PJ, Roelandt JRTC, Serruys PW. Intracoronary ultrasound and quantitative angiography - a combined approach. In: PJ de Feyter, C Di Mario and PW Serruys (eds.): *Quantitative Coronary Imaging*. Rotterdam: Barjesteh, Meeuwes & Co and Thoraxcentre, Erasmus University. 1995: 28-56.

57. Bom N, Li W, van der Steen AFW, de Korte CL, Gussenhoven EJ, **von Birgelen C**, Lancee CT, Roelandt. Intravascular ultrasound: technical update 1995. In: PJ de Feyter, C Di Mario and PW Serruys (eds.): *Quantitative Coronary Imaging*. Rotterdam: Barjesteh, Meeuwes & Co and Thoraxcentre, Erasmus University. 1995: 89-106.

58. Gil R, Di Mario C, Prati F, **von Birgelen C**, Ruygrok P, Roelandt JRTC, Serruys PW. Influence of plaque composition on mechanisms of percutaneous transluminal coronary balloon angioplasty assessed by ultrasound imaging. In: PJ de Feyter, C Di Mario and PW Serruys (eds.): *Quantitative Coronary Imaging*. Rotterdam: Barjesteh, Meeuwes & Co and Thoraxcentre, Erasmus University. 1995: 141-157.

59. **von Birgelen C**, Di Mario C, Prati F, Bruining N, Li Wenguang, de Feyter PJ, Roelandt JRTC. Intracoronary ultrasound: three-dimensional reconstruction techniques. In: PJ de Feyter, C Di Mario and PW Serruys (eds.): *Quantitative Coronary Imaging*. Rotterdam: Barjesteh, Meeuwes & Co and Thoraxcentre, Erasmus University. 1995: 181-197.

60. Prati F, Di Mario C, Gil R, **von Birgelen C**, Camenzind E, Ligthart J, Montauban van Swijndregt EWJ, Roelandt JRTC, Serruys PW. Usefulness of on-line three-dimensional reconstruction of intracoronary ultrasound for guidance of stent deployment. In: PJ de Feyter, C Di Mario and PW Serruys (eds.): *Quantitative Coronary Imaging*. Rotterdam: Barjesteh, Meeuwes & Co and Thoraxcentre, Erasmus University. 1995: 198-210.

61. **von Birgelen C**, Di Mario C, Li W, Slager C, de Feyter PJ, Roelandt JRTC, Serruys PW. Volumetric quantification by intracoronary ultrasound. In: PJ de Feyter, C Di Mario and PW Serruys (eds.): *Quantitative Coronary Imaging*. Rotterdam: Barjesteh, Meeuwes & Co and Thoraxcentre, Erasmus University. 1995: 211-226.

62. Bom N, Li W, van der Steen AFW, de Korte CL, Gussenhoven EJ, **von Birgelen C**, Lancee C. Intravascular ultrasound: possibilities of image enhancement by signal processing. In: E. van der Wall, T.H. Marwick and J.H.C. Reiber (eds). *Advances in Imaging Techniques in Ischemic Heart Disease*. Dordrecht: Kluwer Academic Publishers. 1995: 113-125.

63. Slager CJ, Laban M, Oomen JA, **von Birgelen C**, Li W, Krams R, Schuurbiers JCH, den Boer A, Serruys PW, Roelandt JRTC, de Feyter PJ. Three-dimensional geometry and orientation of coronary lumen and plaque: reconstruction from angiography and ICUS (ANGUS).
Thoraxcenter Journal 1995; 7:36-37.

64. Li W, Bom N, **von Birgelen C**, van der Steen TFW, de Korte CL, Gussenhoven EJ, Lancee CT. *State of the art in ICUS quantitation*. In: JHC Reiber, EE van der Wall (eds.): Cardiovascular Imaging. Dordrecht: Kluwer Academic Publishers. 1996: 79-92.

65. **von Birgelen C**, Serruys PW. Three-dimensional intravascular ultrasound in interventional cardiology. In: Beyar R, Keren G, Leon MB, and Serruys PW (eds.): *Frontiers in Interventional Cardiology*. London: Martin Dunitz Publishers. 1997: 269-279.

66. **von Birgelen C**, Serruys PW. Three-dimensional intravascular ultrasound assessment of coronary stent deployment.
Thoraxcenter Journal 1997; 8:29-31.

67. Sonka M, McKay CR, **von Birgelen C**. Computer analysis of intravascular ultrasound images. In: C.T. Leondes (ed.): *Medical Imaging Systems Techniques and Applications: Cardiovascular System*. Gordon and Breach Publishers, Newark, N.J. 1997: 183-226

68. Cespedes EI, de Korte CL, van der Steen AFW, **von Birgelen C**, Lancee CT. Intravascular elastography: principles and potentials.
Semin Intervent Cardiol 1997; 2:55-62.

69. Slager CJ, Wentzel JJ, Oomen JAF, Schuurbiers

JCH, Krams R, **von Birgelen C**, Tjon A, Serruys PW, de Feyter PJ. True reconstruction of vessel geometry from combined X-ray angiographic and intracoronary ultrasound data.
Semin Intervent Cardiol 1997; 2:43-47.

70. **von Birgelen C**, Li W, Bom N, Serruys PW. Quantitative three-dimensional intravascular ultrasound.
Semin Intervent Cardiol 1997; 2:25-32.

71. **von Birgelen C**, de Feyter PJ, Roelandt JRTC. Three-dimensional reconstruction of intracoronary ultrasound. In: Erbel R, Roelandt JRTC, Ge J, Görge G (eds.): *Intravascular Ultrasound.* London: Martin Dunitz Publishers. 1998: 51-60.

72. **von Birgelen C**, Nicosia A, Serruys PW, Roelandt JRTC. Assessment of balloon angioplasty and directional atherectomy with three-dimensional intracoronary ultrasound. In: Erbel R, Roelandt JRTC, Ge J, Görge G (eds.): *Intravascular Ultrasound.* London: Martin Dunitz Publishers. 1998: 183-189.

73. **von Birgelen C**, Mallus T, Serruys PW. Three-dimensional intravascular ultrasound reconstruction and quantification: a valuable approach for clinical decision making. In: RJ Siegel (ed.): *Intravascular Ultrasound Imaging in Coronary Artery Disease.* New York: Marcel Dekker, Inc. 1998: 177-203.

Met dank aan

Boston Scientific

Cardialysis

Cordis / Johnson & Johnson

Endosonics

Guidant / ACS

Schwarz Pharma

Tomtec

UCB Pharma